Universität Stuttgart

Baustatik und Baudynamik

# Statical Analysis of Network Arch Bridges

## Master Thesis

submitted by

Alejandro Niklison

in

April 2010

Institut für Baustatik und Baudynamik
Prof. Dr.-Ing. habil. Manfred Bischoff

# Statical Analysis of Network Arch Bridges

October 7th, 2009 – April 7th 2010


| | |
|---|---|
| Author | **Alejandro Jose Niklison**<br>Matr.-Nr.:2542427 |
| 1st Supervisor | Prof. Dr.-Ing. habil. Manfred Bischoff<br>Institute of Structural Mechanics<br>Universität Stuttgart<br>Pfaffenwaldring 7, 70550 Stuttgart<br>Germany |
| 2nd Supervisor | Dipl. -Ing. (FH) Annika Sorg, M. Sc.<br>Institute of Structural Mechanics<br>Universität Stuttgart<br>Pfaffenwaldring 7, 70550 Stuttgart<br>Germany |

# Abstract

The primary topic of this dissertation is the study of different parameters that influence the structural behavior of network arch bridges. As a particular example the bridge over the river Lužnice in the Czech Republic is examined.
First, a simplified static computation of the Lužnice bridge is presented, along with different assumptions regarding the elements, materials and loading of the bridge. The worst loading conditions are determined.
Considering this, four different parameters are studied: the hanger arrangement, the form of the arch, the rise of the arch and the number of hangers.
As the hanger arrangement constitutes the main characteristic of network arch bridges, special emphasis is placed on this parameter. In particular, two hanger arrangements are analyzed: A configuration based on the linear variation of the slopes and a radial arrangement, proposed by Brunn and Schanack in their diploma thesis [BSC].
Different shapes of the arch are proposed and studied, as well as modifications in the rise of the arch and the number of hangers.
Finally, different alternatives are proposed and compared with the original configurations of the bridge over the river Lužnice.

## Declaration

I, Mr. Alejandro José Niklison, declare that this master´s thesis is written independently and no sources have been used other than the stated referenced.

…..... …..
*Place/Date* *Signature*

# Contents

# List of Figures

# List of Tables

# Nomenclature

| | |
|---|---|
| $\varphi_0$ | Initial Angle |
| $\Delta\varphi$ | Angle increment |
| M | Bending Moments |
| N | Axial Forces |
| S | Stress |
| Coord | Coordinates |
| $R_{rel}$ | Radio of the circular part of the arch |
| *long1* | Distance from where the parabolic shape begins |

# Chapter 1

# Introduction

## 1.1 Network Arch Bridges

Developed by the norwegian engineer Per Tveit in the end of the 1950s, the network arch bridges are considered as the most slender and lightest arch bridges in the world.

Network arch bridges are arch bridges in which some of the hangers intersect others hangers at least twice. With an optimal design, the hangers act like a web of a simply supported beam in which the tie and the arch are the tensile and the compresive flanges respectively. Most of the shear force is carried to the supports by the vertical components of the forces in the arch, and the variation in the shear force is taken by variations in the forces in the hangers. Because of this, the arch and the tie are mainly subjected to axial forces with reduced bending moments. This results in very small sections and a slender and atractive bridge.

In order to achive an optimal design several consideration should be taken into account [TNA]:

- It is recommendable for the arch to be part of a circle, as this contributes to even bending moments along the tie and to a more constant axial force in a longer portion of the arch. However, in this thesis other forms are investigated in Section 3.2.
- The upper nodes of the hangers should be equidistantly spaced along the arch.
- The lower nodes of the hangers should be placed in a way that the variation of the maximum forces in the hangers is minimum, and the relaxation of the hangers is avoided.
- The tie should be a concrete slab between concrete edge beams. As the bending moment in the middle of the span in usually bigger than the longitudinal bending, there is no need for steel beams.
- The axial forces between the ends of the arches should be taken by longitudinal prestressing. Transversal prestressing is only necessary if the distance between edge beams is more than 10.00 meters.
- All hangers should have the same cross section.
- Special attention should be dedicated to the choice of the hanger arrangement. Different hanger arrangements are examinated in Section 3.1.

Regarding the method of erection of network arch bridges, it is recommendable to use a temporary lower chord, whenever is possible. A steel skeleton can be built combining the lower chord with the arches and the hangers in a suitable location. The skeleton can be moved to the final position with cranes [TNA].

The advantages of the Network arch bridges over the arches with vertical hangers are exposed next.

For evenly distributed loads an arch with vertical hangers could be a good solution, as all elements are mainly subjected to axial forces (Fig. 1). However, a partial load of the span will lead to a deflection of the arch and tie, increasing significantly the bending moments (Fig.2).

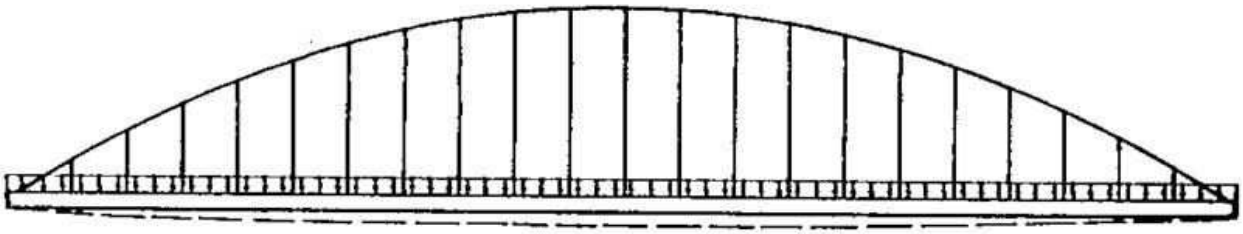

**Figure 1.** Arch bridge with vertical hangers – Even Load [TNA]

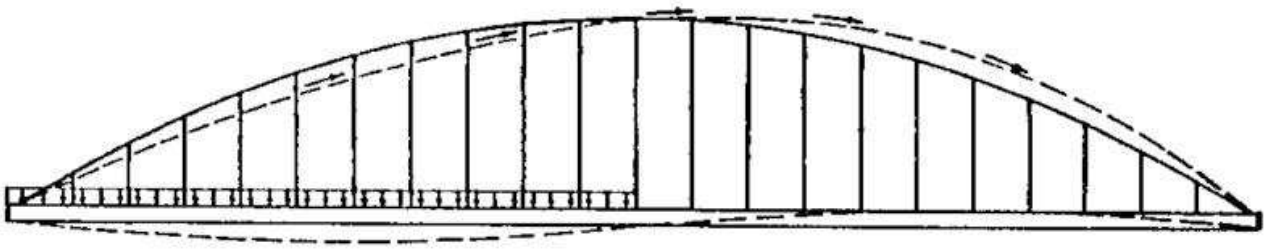

**Figure 2.** Arch bridge with vertical hangers – Partial Load [TNA]

For the case of partial loading, the network arch bridge has a better structural response. For an optimal hanger arrangement, the loads are led to the arches such that there is little bending in the chords. A high stiffness is attained and the deflections of the arch and tie are restricted by the inclined hangers. The stiffness in the arch planes cause the deck to span between them, without taking much longitudinal bending. In consequence it can be slender.

Figure 3 shows influence lines for bending moments between a bridge with vertical hangers and a network arch bridge [TNA]. The first bridge was built at Straubing in 1977. The network arch bridge was design by Per Tveit for the IABSE Congress in Vienna in 1980. In [TNA] Per Teat note that the maximum influence ordinate for the tie in the network arch is the same as for a simply supported beam of 5.60 m of span. As the distance between the arches of the bridge is 15.00 m, the bending moment in the tie is much smaller than the maximum bending moment in the slab.

Observing the influence lines for the arches and the lower chords in Figure 3, it can be notice that the values for the network arch bridges are much smaller than the values for the bridge with vertical hangers. It can also be notice that the form of the influence lines for the arch is quite similar to the form of the influence lines for the tie.

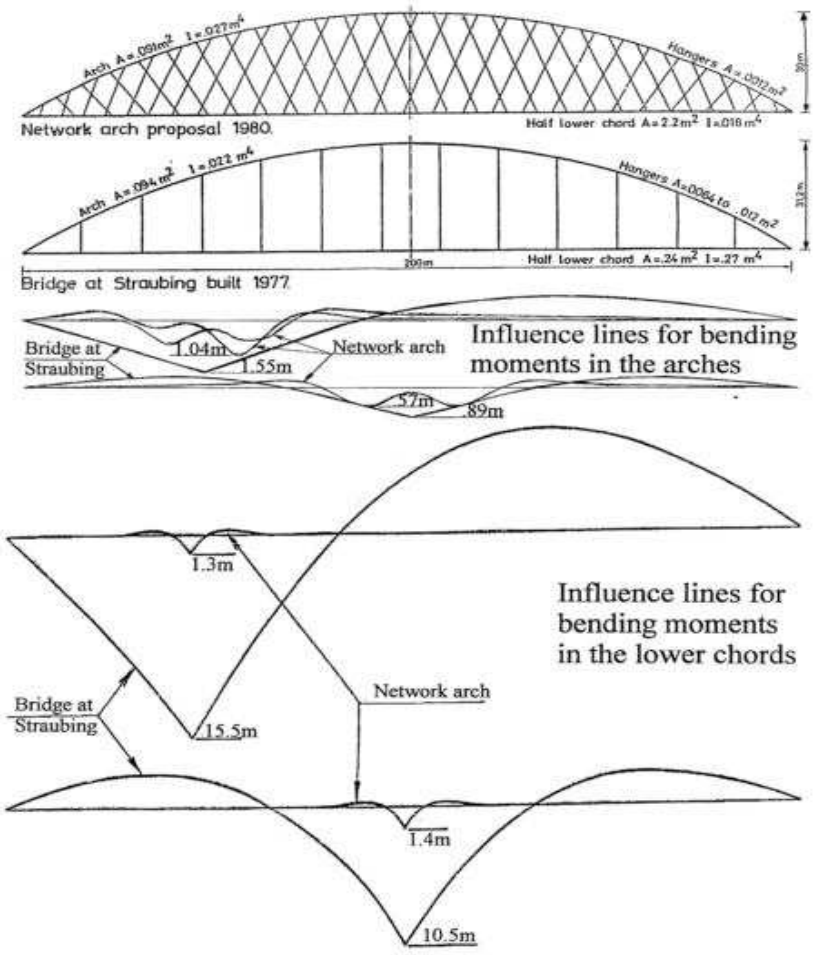


**Figure 3.** Areas, stiffnesses and influence lines for the lower and upper chord of two tied arches [TNA]

As a particular example for this thesis, the bridge over the river Lužnice, close to Bechyně in the Czech Republic is used (Fig. 4). This is the third network arch bridge in the world with steel arches and a prestressed concrete deck.

**Figure 4.** Bridge over the river Lužnice close to Bechyně in the Czech Republic [LIM]

The 41.00 m, single-lane bridge replaced an old steel lattice bridge. As the setting called for a slender structure with an attractive appearance, the network arch was a good choice.

The bridge has two parabolic shaped steel arches, with an inverted U cross section, and a maximum height of 6.05 m. The cross sections are open to allow access for inspection and maintenance. The arches are reinforced with transverse welded steel U beams in the end of the arches and in the one quarter and three quarters points.

The C35/C45 concrete deck is 7.95 m wide and with a thickness of 18 cm under the sidewalks, and 25 to 30 cm under the roadway. It is supported by 38 hangers distributed evenly alongside each arch. It is prestressed by four steel cables embedded in the concrete slab. The cables are anchored in vertical steel face plates at the end of each arch. As the wide of the deck is less than 10.00 m, it is not necessary transversal prestressing and the slab acts like reinforced concrete.

The hangers are stainless steel rods with an outside diameter of 40 mm. The hangers close to the end of the arches need to be prestressed. The other hangers are prestressed by the weight of the deck.

The single traffic lane is 3.60 m, with sidewalks in both sides. Each sidewalk is 1.30 m wide and it is separated from the traffic lane by a steel guardrail that protects the hangers.

The pavement of the road consist of a medium-grained mastic asphalt carpet made of modified asphalt, poured asphalt and waterproofing, with a total thickness of 85 mm.

Before the erection of the bridge, the original bridge had to be moved to another location, placing it on a temporary support to allow the traffic to continue. The steel structure was assembled on-site. It was erected without welding using a steel support scaffolding that was placed on temporary supports (Figure 5). Later, the steel skeleton was placed in the abutments using hydraulic jacks. Once the deck was casted and cured, the hangers were adjusted. After prestressing the slab, the scaffolding was removed.

The Appendix A presents a cross section and a longitudinal section of the Lužnice bridge.

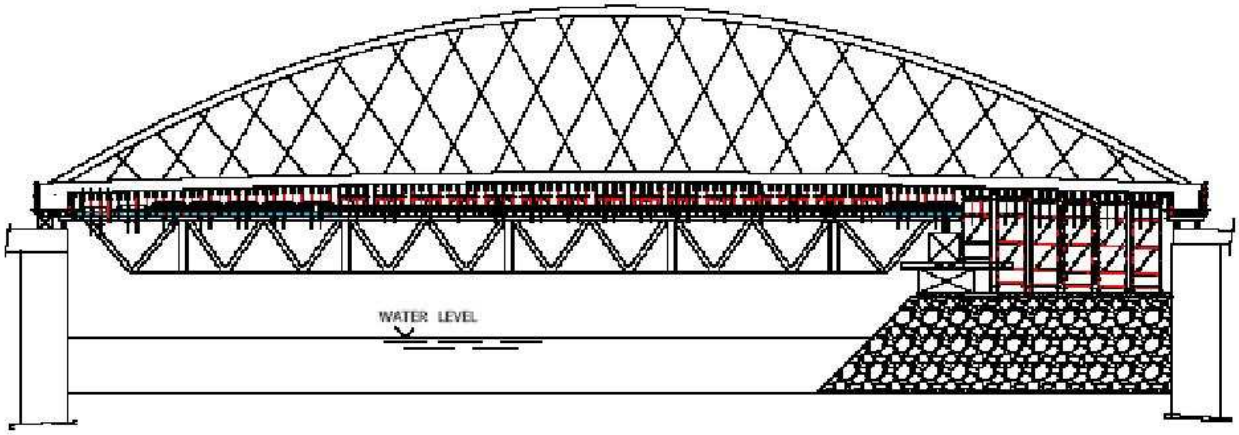


**Figure 5.** Erection of the Lužnice network arch bridge [TNA]

## 1.2. Structural Outline

This dissertation is organized in five parts:

- A simplified statical computation of the Lužnice bridge is presented in Chapter 2. The different assumptions referring the elements, material and actions in the bridge are described extensively. Finally, an analysis of the results is exposed in order to find the worst load cases.
- Chapter 3 concentrates in the study of different parameters in order to determine their influence in the structural behavior of the bridge. The parameters to study are the hanger arrangement, the form of the arch, the rise of the arch and the number of hangers.
- In the Chapter 4 different alternatives to the original configuration are proposed and analyzed.
- The Chapter 5 provides a brief summary of the whole work.

# Chapter 2

# Computation of the bridge over the river Lužnice

In order to study the statical properties of network arch bridges, the bridge over the river Lužnice is chosen as an example. In this chapter a simplified 2D model of the bridge is calculated. As a special emphasis is placed on the difficulty with hangers that do not carry under compressive forces, it is compulsive to do geometrically non-linear computations. For that it is necessary to use elements that do not carry under compressive forces.

For this reason, the finite element software ANSYS, in its version 12.0.1, is used, as it is able to model elements that do not contribute to carry the load when exposed to compressive forces.

The bridge is modeled with beam elements, distinguishing between elements that only carry axial forces (hangers) and elements that carry also shear forces and bending moments (deck and arch).

The units used are meters (m), kilonewtons (KN), second (s) and tons (t).

The Chapter 2 is divided in seven sections:

- The general configuration of the bridge is exposed in Section 2.1 with a detail of the hanger arrangement.
- The Sections 2.2 and 2.3 present the elements and type of material used for the deck, the arch and the hangers, along with its characteristics.
- The Section 2.4. presents the load analysis. In this section the different actions are described, presenting the load models, the combination of actions and the load cases.
- The prestressing of the cables is described in the Section 2.5.
- In the Section 2.6. the results obtained from the models are analyzed. In order to find the worst loading assumptions the maximum values for stress, bending moments and axial forces are presented for each element, along with the corresponding load cases. This is done separately for the elements of hangers, deck and arch, and for an even and a partial loading of the deck.
- Finally, the conclusions are exposed in the Section 2.7.

## 2.1 General Configuration

The arch has a parabolic shape. It begins in the origin of coordinates and it ends in the coordinate (41.00 ; 0.00), as the span of the bridge is 41.00 m. It has its maximum ordinate in the center, with a value of 6.05 m.

For the left margin hinged supports are adopted. The hinged supports allow the rotation, while the translational displacement is not possible. In the right margin, it is considered roller supports. In this case both rotation and translational displacement are allowed.

The Table 1 shows the angles and distances to the origin of one set of hangers. The other set of hangers is the mirrored equivalent.

| x [m] | α [°] |
|---|---|
| 3.12 | 46.33 |
| 5.10 | 50.01 |
| 7.10 | 50.99 |
| 9.10 | 51.02 |
| 11.10 | 53.59 |
| 13.00 | 55.18 |
| 15.08 | 58.13 |
| 17.07 | 60.49 |
| 19.06 | 61.92 |
| 21.07 | 62.78 |
| 23.07 | 63.16 |
| 25.07 | 63.10 |
| 27.07 | 62.58 |
| 29.07 | 61.58 |
| 31.08 | 59.95 |
| 33.08 | 59.64 |
| 35.07 | 60.54 |
| 37.09 | 56.43 |
| 39.11 | 51.54 |

**Table 1.** Values for a set of hangers of the Lužnice network arch bridge

## 2.2 Elements

### 2.2.1 Arch

The arch is modeled with BEAM3 elements [AHlp]. These are uniaxial 2D elements with tension, compression and bending capabilities. The elements have three degrees of freedom at each node: rotation about the nodal Z axis, and translation in the directions of the X and Y axis. Figure 6 shows the geometry and the coordinate system of the element.

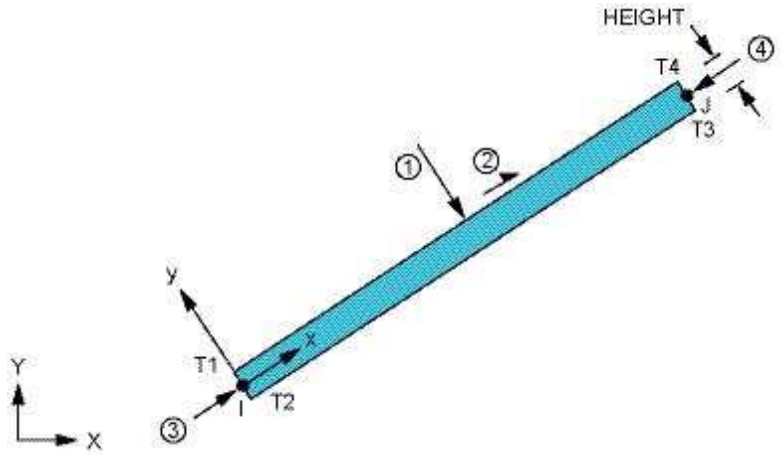


**Figure 6.** Element BEAM3 [Hlp]

Input data [AHlp]:

The BEAM3 element is defined by two nodes, the cross sectional area, the inertia moment, the height and the material properties. The cross section of the arch is illustrated in the Figure 7. The characteristics of the section are:

- Area: 0.3115 e-01 $m^2$
- Inertia Moment: 0.3688 e-03 $m^3$
- Height: 0.32 m

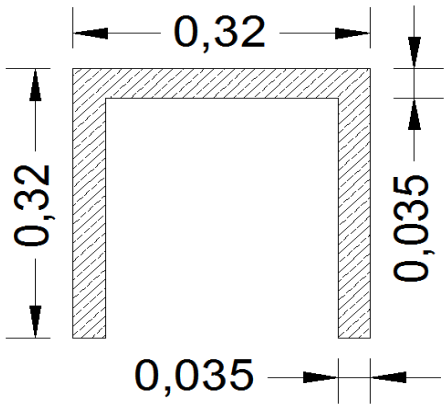


**Figure 7.** Cross Section of the arch

Output data [AHlp]:

The following results are extracted in order to study the structural behavior of the system:

| | |
|---|---|
| SDIR-I | Axial direct stress in node i |
| SDIR-J | Axial direct stress in node j |
| SBYT-I | Bending stress on the element +Y side of the beam, in node i |
| SBYT-J | Bending stress on the element +Y side of the beam, in node j |
| SBYB-I | Bending stress on the element -Y side of the beam, in node i |
| SBYB-J | Bending stress on the element -Y side of the beam, in node j |
| MFORX-I | Member force in the element coordinate system X direction, in node i |
| MFORX-J | Member force in the element coordinate system X direction, in node j |
| MFORMZ-I | Member moment in the element coordinate system Z direction, in node i |
| MFORMZ-J | Member moment in the element coordinate system Z direction, in node j |

The axial direct stress (SDIR) and the bending stresses (SBYT and SBYB) are combined in order to obtain the maximum stress in each node.

### 2.2.2 Deck

The Deck is also modeled with BEAM3 elements (Figure 6) [AHlp].

Input data [AHlp]:

The BEAM3 element is defined by two nodes, the cross sectional area, the inertia moment, the height and the material properties.

In the deck a reduced cross section is adopted. This is due to the fact that point loads are applied where the hangers meet the deck. This loads spread into the deck with a certain angle not taking all the cross section. For this reason the cross section is reduced and the area and moment inertia are calculated for it. In this way the bridge obtained is weaker than the actual bridge, but remaining in the safe side.

Due to the fact that there is not a general method to reduce the cross section, the formula for T-beams is used.

Considering an effective wide [DIN]:

$$b_{eff,i} = 0.2 \cdot b_i + 0.1 \cdot l_0 \qquad \text{(Fig. 8)}$$

with,

$b_{eff,i}$ = effective wide

$b_i$ = real wide.

$l_0$ = effective span according to Figure 9.

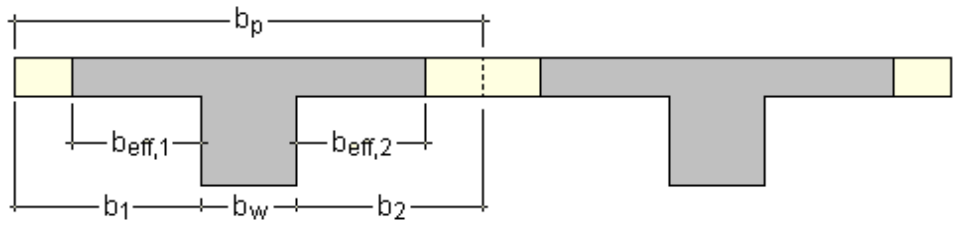


**Figure 8.** Effective wide [DIN]

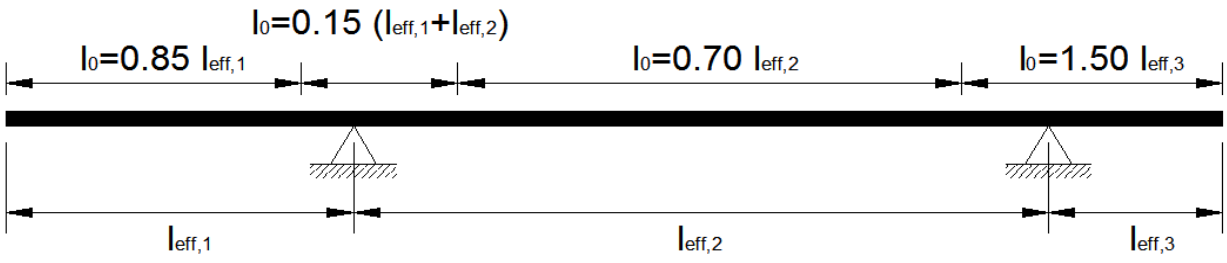


**Figure 9.** Effective span [DIN]

The effective section is shadowed in the Figure 10. The characteristics of the effective section are:

- Area: 0.8471 $m^2$
- Inertia Moment: 0.2183 E-01 $m^3$
- Height: 0.56 m

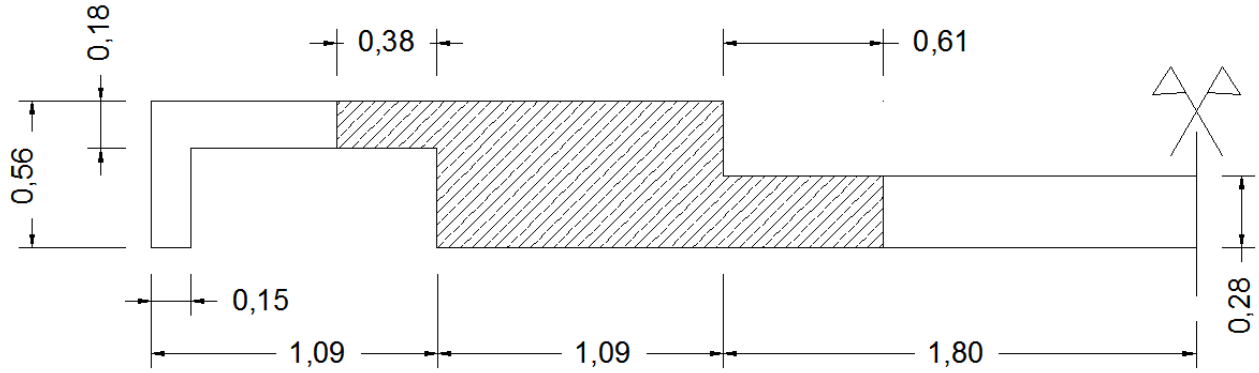


**Figure 10.** Cross Section of deck

Output data [AHlp]:

The following results are extracted in order to study the structural behavior of the system:

| | |
|---|---|
| SDIR-I | Axial direct stress in node i |
| SDIR-J | Axial direct stress in node j |
| SBYT-I | Bending stress on the element +Y side of the beam, in node i |
| SBYT-J | Bending stress on the element +Y side of the beam, in node j |
| SBYB-I | Bending stress on the element -Y side of the beam, in node i |
| SBYB-J | Bending stress on the element -Y side of the beam, in node j |
| MFORX-I | Member force in the element coordinate system X direction, in node i |
| MFORX-J | Member force in the element coordinate system X direction, in node j |
| MFORMZ-I | Member moment in the element coordinate system Z direction, in node i |
| MFORMZ-J | Member moment in the element coordinate system Z direction, in node j |

The axial direct stress (SDIR) and the bending stresses (SBYT and SBYB) are combined to obtain the maximum stress in each node.

### 2.2.3 Hangers

The hangers are modeled considering their impossibility to carry under compressive forces. For this reason the element LINK10 is used [AHlp]. This element has a bilinear stiffness matrix resulting in a uniaxial tension-only element. Under compression the stiffness in the element is removed.

LINK10 has three degrees of freedom at each node: translation in the X, Y and Z nodal directions. No bending stiffness is included. The Figure 11 shows the geometry and the coordinate system of the LINK10 elements.

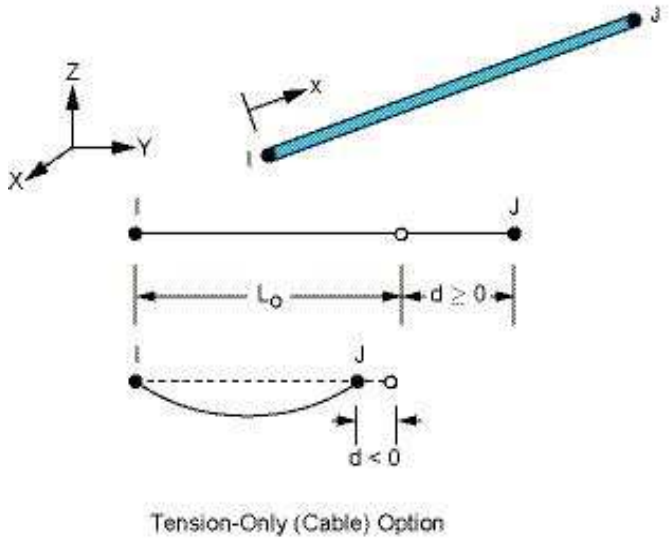


**Figure 11.** Element LINK10

Input data:

The LINK10 element is defined by two nodes, the cross sectional area, an initial strain and the isotropic material properties. The section for the hangers is illustrated in the Figure 12. The characteristics of the section are:

- Area: 0.1257 e-02 $m^2$
- Initial strain = 0.00

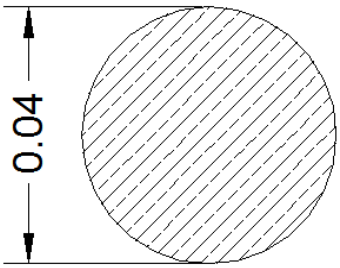


**Figure 12.** Cross Section Hangers

In a first stage, the initial strain is not considered. The structural response of the hangers is study with a special emphasis in the possible relaxation of the hangers. After this study, a new initial strain is assigned. This process is explained in detail in the Section 2.5.

Output data:

The following results are extracted in order to study the structural behavior of the system:

| | |
|---|---|
| SAXL | Axial stress |
| EPELAXL | Axial elastic strain |
| MFORX | Member force in the element coordinate system |

## 2.3 Type of Materials

### 2.3.1 Arch

The following properties are adopted for the steel in the arch:

- Elastic Modulus: 2.1 E-08 KN/m$^2$
- Density: 7.8 t/m$^3$
- Characteristic resistance : 235000 KN/m$^2$ (Bending Stress)

### 2.3.2 Deck

A C35/45 concrete is adopted, with the following properties:

- Elastic Modulus: 2.99 E-07 KN/m$^2$
- Density: 2.5 t/m$^3$
- Characteristic resistance : 3200 KN/m$^2$ (Bending Stress)

### 2.3.3 Hangers

The following properties are adopted for the steel in the hangers:

- Elastic Modulus: 2.1 E-08 KN/m$^2$
- Density: 7.8 t/m$^3$
- Characteristic resistance : 500000 KN/m$^2$ (Axial Stress)

## 2.4 Load Analysis

The actions to be applied to the bridge are determined according with the Eurocode [E1-2]. The verification is done for Ultimate Limit State (ULS).

### 2.4.1 Verification at Ultimate Limit States [E2-1]

At ULS it must be verified that:

$E_d \leq R_d$

Where $E_d$ is the design value of the effects of action and $R_d$ is the design value of the corresponding resistance.

- Effect of actions:

$$E_d = \sum \gamma_{G,j} G_{k,j} + \gamma_P P + \gamma_{Q,1} Q_{k,1} + \sum \gamma_{Q,i} \Psi_{0,i} Q_{k,i}$$

$G_{k,j}$ = characteristic value of the j-th action.

P = permanent action caused by controlled forces or deformation (Prestressing)

$Q_{k,1}$ = characteristic value of the leading variable action.

$Q_{k,i}$ = characteristic value of the accompanying variable actions.

From the Table 4.5.1 of [E1-3], the values of the partial factors are:

Permanent actions (unfavorable): $\gamma_G$ = 1.35 (Concrete)

$\gamma_G$ = 1.20 (Steel)

Permanent actions (favorable): $\gamma_G$ = 1.00

Prestress: $\gamma_P$ = 1.00

Traffic actions: $\gamma_Q$ = 1.50

- Design value of resistance:

The design value of resistance is determined from the characteristic resistance of the material divided by the partial safety factor for material properties $\gamma_M$.

From the table 2.3 of [E2-1], the value of $\gamma_M$ for concrete is:

$\gamma_M = 1.50$ (Concrete)

From the Section 6.1 of [E3-1.1], the value of $\gamma_M$ for steel is:

$\gamma_M = 1.10$ (Steel)

## 2.4.2. Actions

### 2.4.2.1. Permanent Actions

*Self weight of structural elements*

The software ANSYS calculates the self weight of every element from the cross sections and materials properties assigned to them. However, this only applies for the structural elements defined in the model. Additional permanent actions like guardrails, steel railings or pavement on the roadway should be analyzed separately, and it should be defined as distributed or punctual loads.

The self weight of the structural components of the bridge has been already specified in the Section 2.3. However, different values are adopted for the model:

Self weight steel: 7.8 t/m$^2$ . $\gamma_G$ = 7.8 t/m$^2$ . 1.20 = 9.36 t/m$^2$

Self weight concrete: 0 t/m$^2$

The self weight of the steel is multiplied by the partial factor $\gamma_G$ [E1-3] for unfavorable actions, as the weight of the arch and the hangers is considered always unfavorable.

On the other hand, the self weight of the deck is not always considered unfavorable. In the case of a partial loading of the deck, the self weight of the concrete in the loaded area is considered unfavorable, while the self weight in the unloaded area is considered favorable. For this reason it is decided to represent the weight of the deck as an additional permanent load, applying a distributed load and assigning zero density to the elements in the deck.

The additional permanent actions in the deck are represented in the Figure 13.

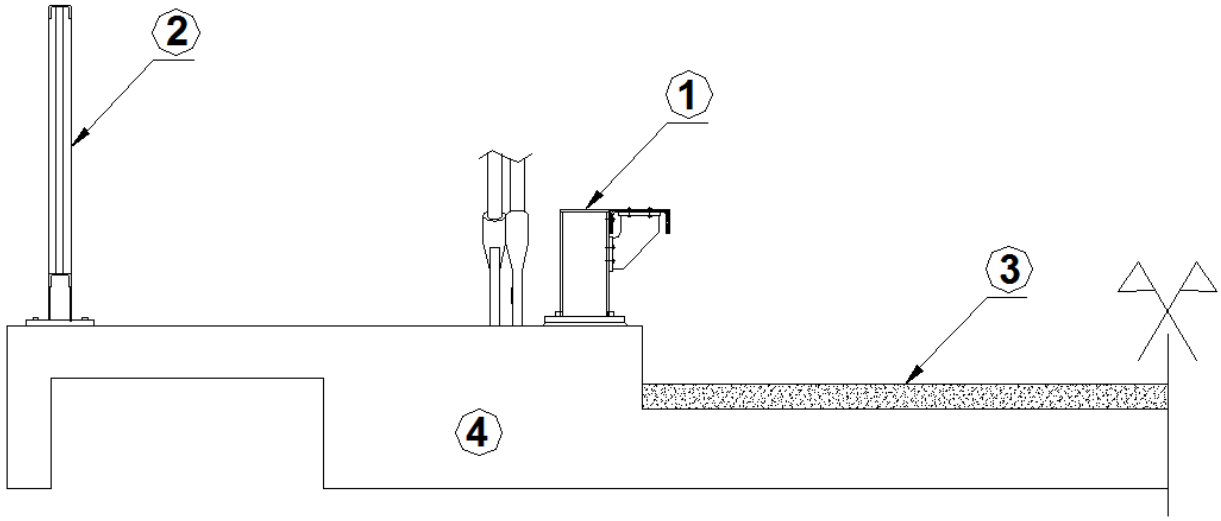


**Figure 13.** Additional permanent actions

1) Steel guardrails: 1 KN/m
2) Steel railings: 1 KN/m
3) Asphalt carpet: 20 KN/m$^3$ . 0.085 m . 1.8 m = 3.06 KN/m
4) Self weight of concrete: $S_d$ . 2.5 t/m$^3$ . g = 1.3 m$^2$ . 2.5 t/m$^3$ . 9.81 m/s$^2$ = 31.88 KN/m

The real cross section of the deck is used to calculate the self weight, instead of using the effective area calculated in the Section 2.2.2.

Finally a distributed load qDL is applied to the deck, with:

qDL = 36.94 KN/m

### 2.4.2.2. Prestressing

As the information about the prestressing is insufficient, this action is not considered.

### 2.4.2.3. Traffic loads

The Eurocode gives several traffic models. For this work the models 1, 2 and 4 are considered.

Traffic lanes should be defined for the application of the traffic loads, assigning a wide of 3.00 m to the traffic lane. As the Lužnice Bridge has a carriage width of 3.60 m, only one traffic lane is defined, with a remaining width of 0.60 m.

**Load Model 1 [E1-2]**

The Load Model 1 consists of two systems.

- A pair of axles, separated by 1.20 m, applied in the most unfavorable longitudinal position. Each one comprising two concentrated loads (positioned in the center of the lane) and having the weight:

  $\alpha_Q \, Q_k = 174.7$ kN.

with:

- $\alpha_Q$ : Adjustment factor, equal to 0.844. $\alpha_{SL}$ ( $\alpha_{SL} = 0.69$ for single lanes carriageways, Table 4.5.5 of [E1-3]).
- $Q_k$ : Axle load with a value of 300 KN for Lane Number 1, Table 4.2 of [E1-2].

- Uniformly distributed load over the width of the traffic lane, having the weight per square meters of notional lane:

  $\alpha_q \, q_k = 5.2$ kN/m$^2$

with:

- $\alpha_Q$ : Adjustment factor, equal to $0.40/\alpha_{SL}$ ( $\alpha_{SL} = 0.69$ for single lanes carriageways, Table 4.5.6 of [E1-3].
- $q_k$ : Distributed load with a value of 9 kN/m$^2$ for Lane Number 1, Table 4.2 of [E1-2].

The Load Model 1 should be applied in the notional lane. In the remaining areas the load magnitude should be:

$$\alpha_{qr}\, q_{rk} = 3.6 \text{ kN/m}^2$$

with:

- $\alpha_{qr}$ : Adjustment factor, equal to 1.44, Table 4.5.6 of [E1-3].
- $q_{rk}$ : Distributed load with a value of 2.5 kN/m$^2$ for the remaining area, Table 4.2 of [E1-2].

The details of the Load Model 1 are presented in Figure 14.

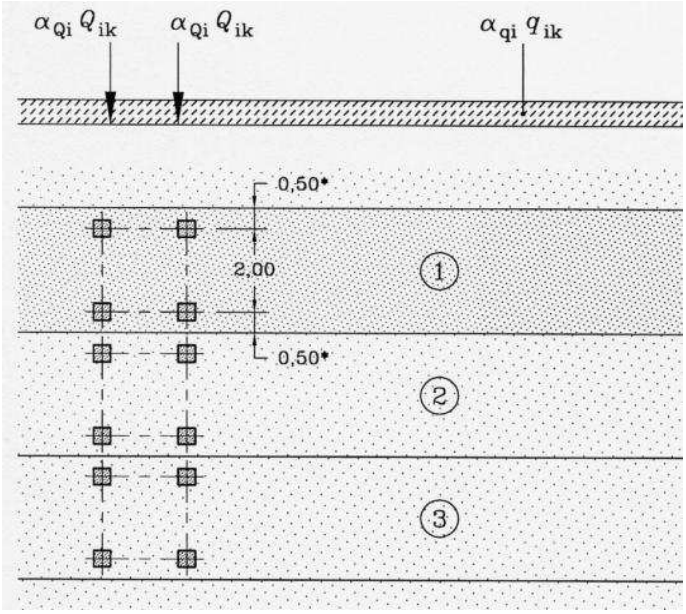


**Figure 14.** Load Model 1 [E1-2]

**Load Model 2 [E1-2]**

The Load Model 2 consists of a single axel load applied in the most unfavorable position, with a value of:

$$\beta_Q\, Q_{ak} = 232 \text{ kN}$$

with:

- $\beta_Q = \alpha_Q$ : Adjustment factor, equal to 0.844. $\alpha_{SL}$ ( $\alpha_{SL}$ = 0.69 for single lanes carriageways, Table 4.5.5 of [E1-3]).
- $Q_{ak}$ = 400kN

The details of the Load Model 2 are presented in the Figure 15.

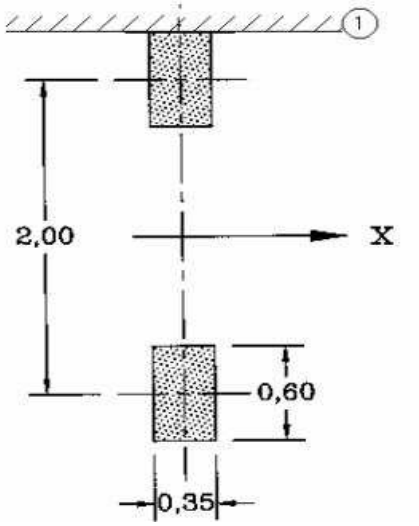


**Figure 15.** Load Model 2 [E1-2]

**Load Model 4**

The Load Model 4 represents the crowd loading, consisting on a uniform distributed load equal to 5.0 kN/m$^2$ [E1-2].

**Loads on footpaths**

For road bridges, an uniformly distributed load equal to 5kN/m$^2$ should be applied in the footpaths (Figure16) [E1-2].

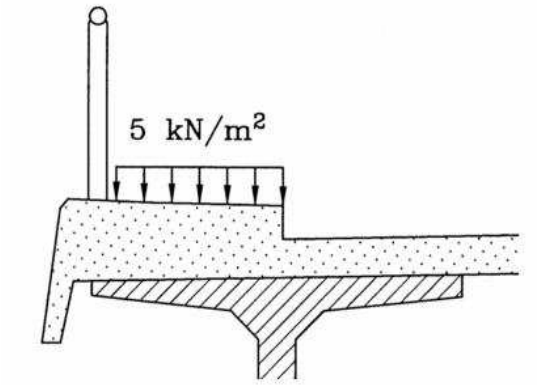


**Figure 16.** Loads on footpaths [E1-2]

### 2.4.2.4. Combination of Actions

Combining each Load Model (LM1, LM2 and LM4) with the loads on the footpaths, and considering the remaining areas, the following load configurations are obtained. As the analysis in this thesis is made in 2D, only one arch will be analyzed. Hence, the loads that correspond to half the width of the bridge will be considered.

*Load combination 1: LM1*

The load combination that includes the Load Model 1 is called LM1. The details are showed in the Figure 17.

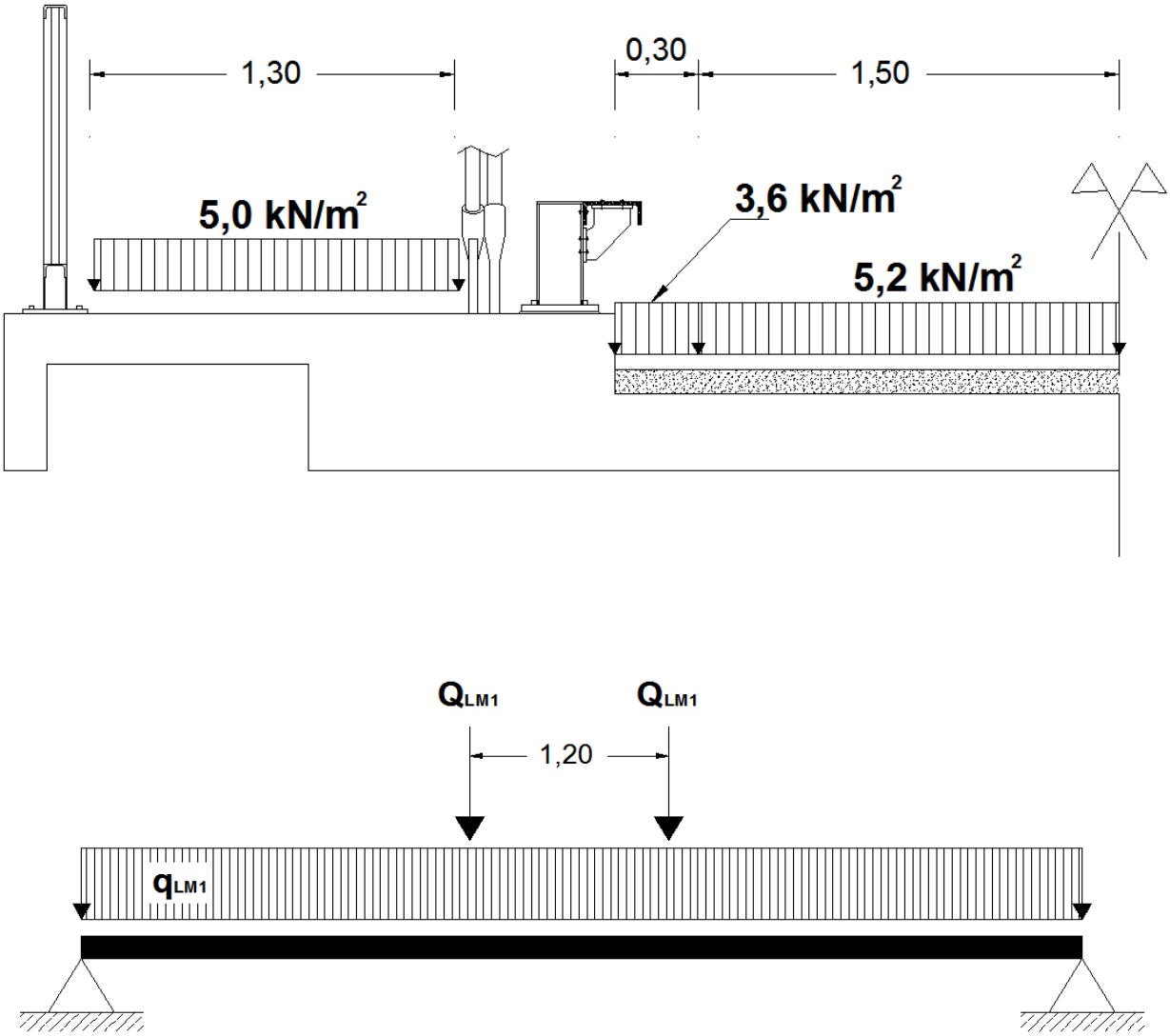


**Figure 17.** Details of LM1 (Transversal and longitudinal)

Uniformly distributed loads:

$q_{LM1}$ = 5.00 kN/m$^2$ . 1.30 m + 3.60 kN/m$^2$ 0.30 m + 5.20 kN/m$^2$ . 1.50 m

$q_{LM1}$ = 15.38 kN/m

Punctual Loads:

$Q_{LM1}$ = 174.7 kN . 0.50 = 87.35 kN

*Load combination 2: LM2*

The load combination that includes the Load Model 2 is called LM2. The details are showed in the Figure 18.

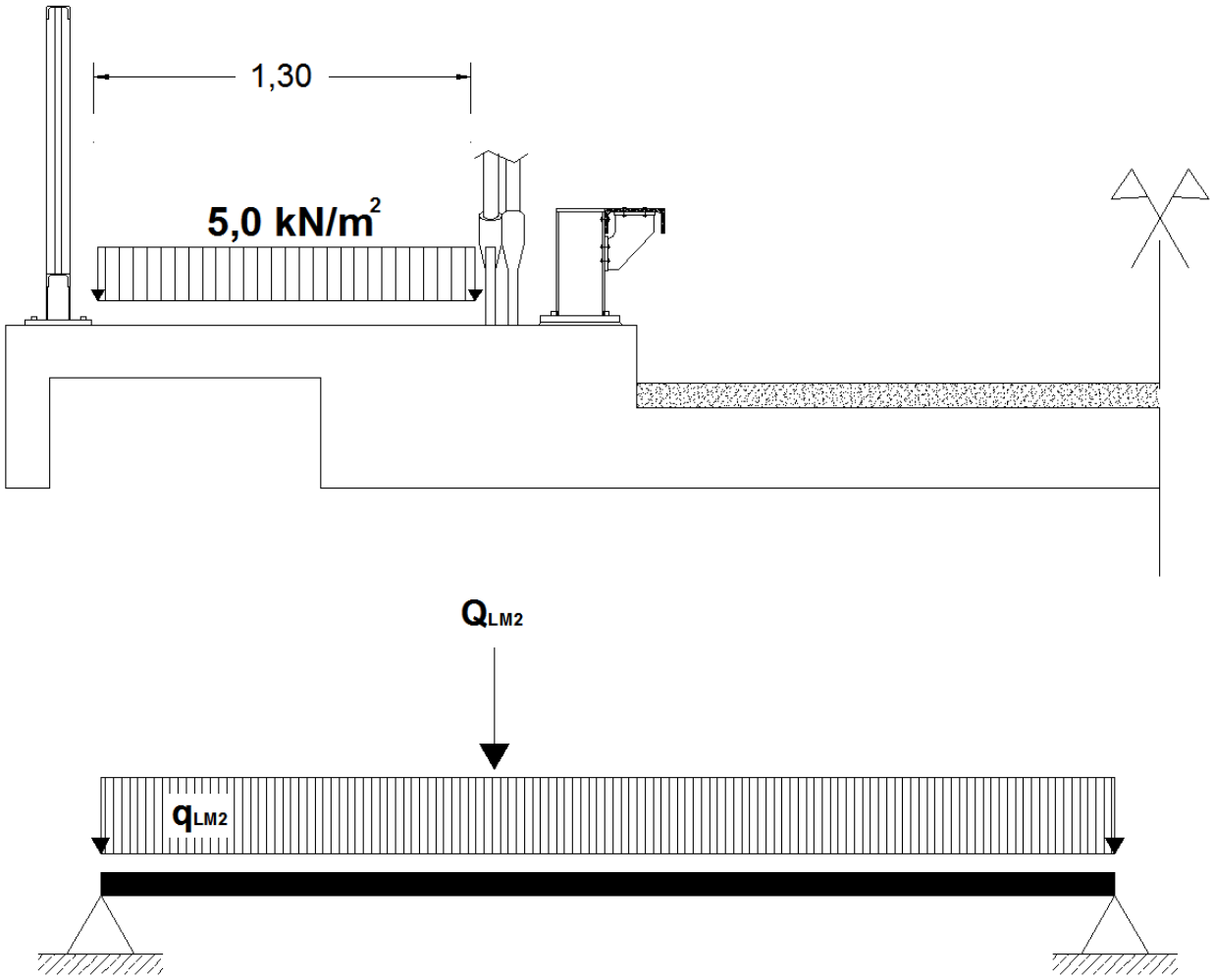


**Figure 18.** Details of LM2 (Transversal and longitudinal)

Uniformly distributed loads:

$q_{LM2}$ = 5.00 kN/m$^2$ . 1.30 m

$q_{LM2}$ = 6.50 kN/m

Punctual Loads:

$Q_{LM2}$ = 232 kN . 0.50 = 116 kN

*Load combination 4: LM4*

The load combination that includes the Load Model 4 is called LM4. The details are showed in the Figure 19.

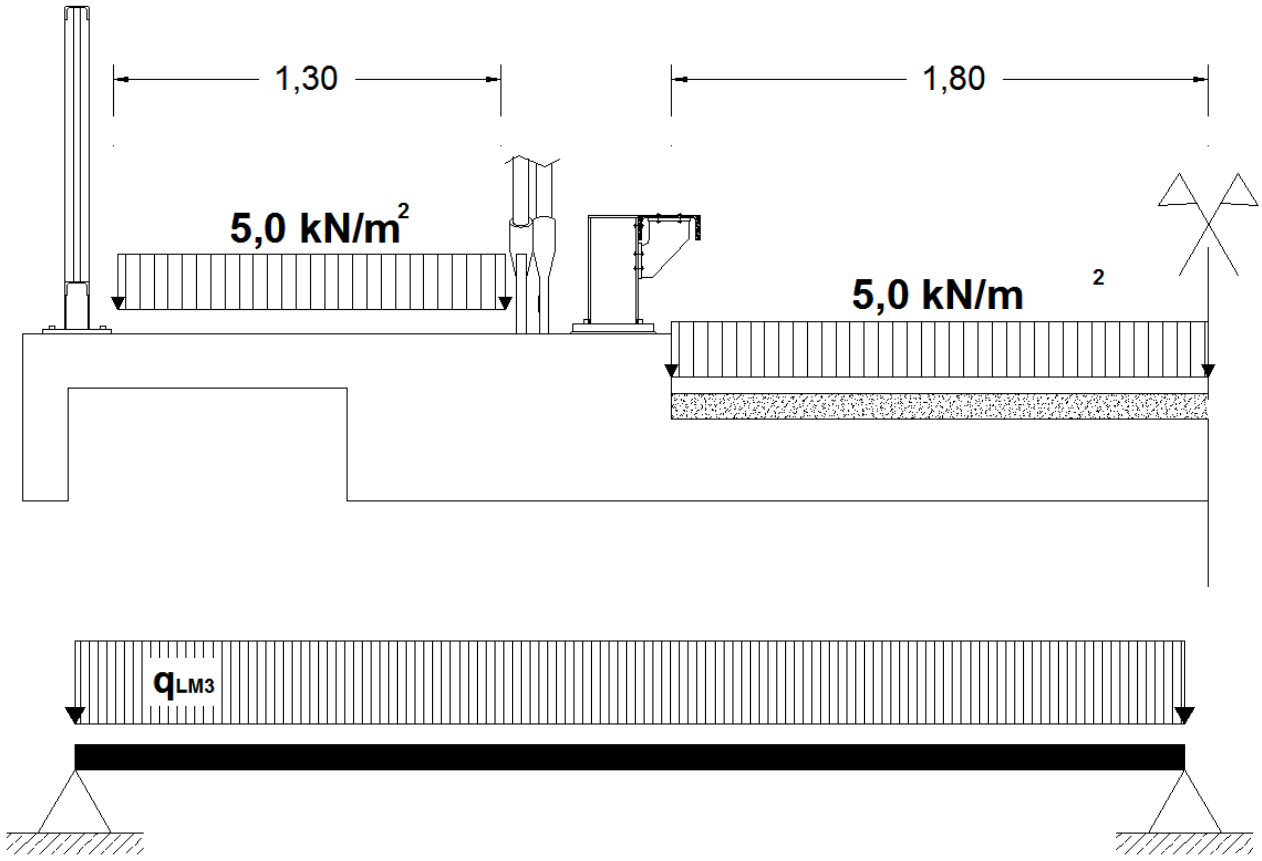


**Figure19.** Details of LM4 (Transversal and longitudinal)

Uniformly distributed loads:

$q_{LM2}$ = 5.00 kN/m$^2$ . 3.10 m

$q_{LM2}$ = 15.50 kN/m

### 2.4.2.5. Load Cases

The different load cases are obtained combining the permanent loads and the traffic loads according to the load combinations exposed in the Section 2.4.1. This is done for different positions of the punctual loads, in order to find the most unfavorable case.

For each position of the punctual loads, the load cases are:

**$E_d = 1.00 \cdot G_{fav} + 1.35 \cdot G_{unfav} + 1.50 \cdot LM1$**
**$E_d = 1.00 \cdot G_{fav} + 1.35 \cdot G_{unfav} + 1.50 \cdot LM2$**
**$E_d = 1.00 \cdot G_{fav} + 1.35 \cdot G_{unfav} + 1.50 \cdot LM4$**

For every load case and each element, it must be verified that:

$E_d \leq R_d$ [E2-1]

The design value of resistance $R_d$ is determined from the characteristic resistance of the material divided by the partial factor on material strength $\gamma_M$:

Arch: $R_d = 235000$ KN/m$^2$ / $\gamma_M = 235000$ KN/m$^2$ / 1.10 = 213636 KN/m$^2$ [E3-1.1]

Deck: $R_d = 3200$ KN/m$^2$ / $\gamma_M = 3200$ KN/m$^2$ / 1.50 = 2133 KN/m$^2$ [E2-1]

Hangers: $R_d = 500000$ KN/m$^2$ / $\gamma_M = 500000$ KN/m$^2$ / 1.10 = 454545 KN/m$^2$ [E3-1.1]

## 2.5 Prestressing of the cables

The prestress force on the hangers is calculated in order to avoid the hangers to relax. As a first step, the code was run with no consideration for the prestressing of the cables, considering only permanent loads.

It is found that under this conditions four hangers relaxed. As the element LINK10 do not work under compression forces, the axial forces in the elements are equal to zero when the hangers have a negative axial deformation. Hence, the c force in each hanger is chosen multiplying the value of the axial elastic strain by the elastic modulus.

The axial elastic strains for the relaxed hangers are:

Hanger 18: 7.9e-5
Hanger 19: 3.8e-4
Hanger 37: 9.09e-5
Hanger 38: 3.4e-4

The resulting stresses are:

Hanger 18: 16590 kN/m$^2$
Hanger 19: 79800 kN/m$^2$
Hanger 37: 19089 kN/m$^2$
Hanger 38: 71400 kN/m$^2$

The stresses are applied as initial strains for the elements. The code is run one more time under this conditions. No hangers relax.

The code is also run for the case of partial load that is applying the traffic actions only in half of the span of the bridge. In this case also no hangers relax.

## 2.6 Results

The Lužnice Bridge is analyzed under two conditions: live load over the whole span and live load over the right half of the span.

The tables with the results are included in Appendix B. The tables show next to each value the corresponding load case. For the case of LC1 and LC2, the punctual loads are applied in different positions along the span. The position of the punctual load is indicated by a number after the name of the load case. For example, LC1.12 means load case LC1, with the first punctual load at 12.00 m from the left support in the case of even load, or 12.00 m from the center of the bridge in the case of partial load.

### 2.6.1. Deck

#### 2.6.1.1. Even load

The Table B.1 shows the maximum and minimum values for the bending moments (M) and axial forces (N) for the deck elements.

The first two pair of columns after the column “Element” show the values of the axial forces with the corresponding load cases. As the axial forces in the deck are always positive, the column of minimum should be ignored. The Figure 20 shows in a graphical format the maximum forces for each element. The maximum value is 3543.5 kN and correspond to the element 2036, in the center of the span, and the load case 1.23, that is, the puntual load in the center of the span. The maximum forces for all elements occur for the load case LC1. The axial forces are higher in the center of the span, decreasing as the element is closer to the supports. However, the values of the maximum axial forces are also important in the elements next to the supports. There are jumps between consecutive values, but they are in the order of 61 kN, that is less than the 2% of the average values.

The third pair of columns shows the maximum moments with the corresponding load cases. The Figure 21 shows in a graphical format the maximum and minimum moments for each element. The maximum value is 872.00 kNm and corresponds to the element 2056, in the right extreme of the deck, and the load case LC1.35 that is, the puntual load near the end of the span. The maximum bending moments in every element occur for LC1. The maximum moments are lower in the supports and in the center of the deck, and it have the highest value in the 1/5 and 4/5 of the span.

The last pair of columns shows the minimum moments with the corresponding load cases. The Figure 21 shows in a graphical format the maximum and minimum moments for each element. The minimum value is -220.66 kNm and correspond to the element 4027, near the center of the deck, and the load case 1.31 that is, the puntual load near the end of the span. The

minimum moments in almost every element occur for LC1. The values that correspond to the load cases LC2 and LC3 are positives and it should be ignored. The highest values are in the ¼ and ¾ of the span.

The Table B.2 shows the maximum and minimum stresses for the deck elements. The Figure 22 shows in a graphical format the maximum and minimum stresses for each element. The minimum value for the stresses is -7288.32 kN/m$^2$ and corresponds to the element 2056, in the right extreme of the deck, and the load case LC1.35 that is, the puntual load near the end of the span. In the same way, the maximum value for the stresses is 15073.77 kN/m$^2$ and corresponds to the element 2056 and the load case LC1.35. The minimum and maximum stresses for all elements occur for the load case LC1. The element next to the right support have a minimum stress for LC2, but its value is less than 0.1% of the highest value. The higher and lower value occur in 1/5 and 4/5 of the span respectively.

The maximum stress is higher than the admisible value 2133 KN/m$^2$; the minimum stress is lower than the admisible value -2133 KN/m$^2$.

The fact that the stresses are higher than the admissible values remarks the importance of the prestressing of the deck. As the prestressing was not considered in this thesis, this is expected.

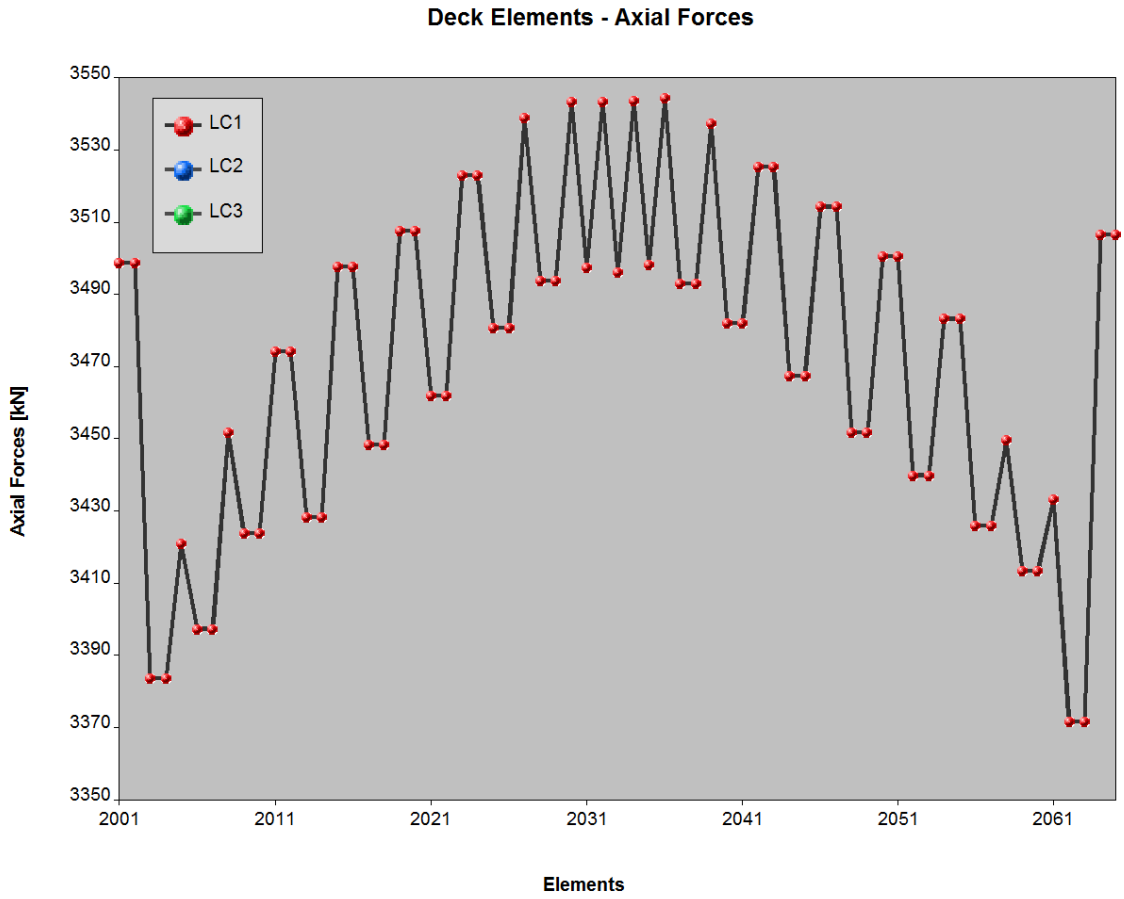


**Figure 20.** Axial forces for the deck elements of the of the Lužnice bridge (Even load)

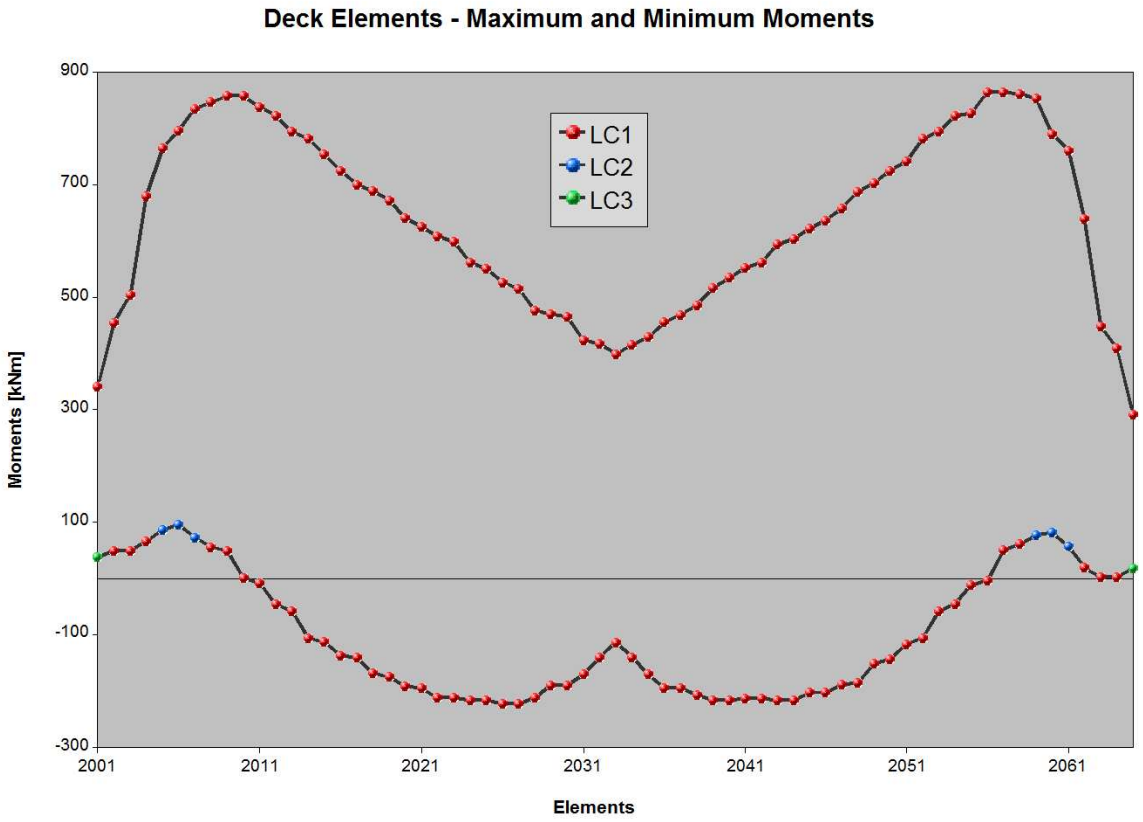


**Figure 21.** Moments for the deck elements of the Lužnice bridge (Even load)

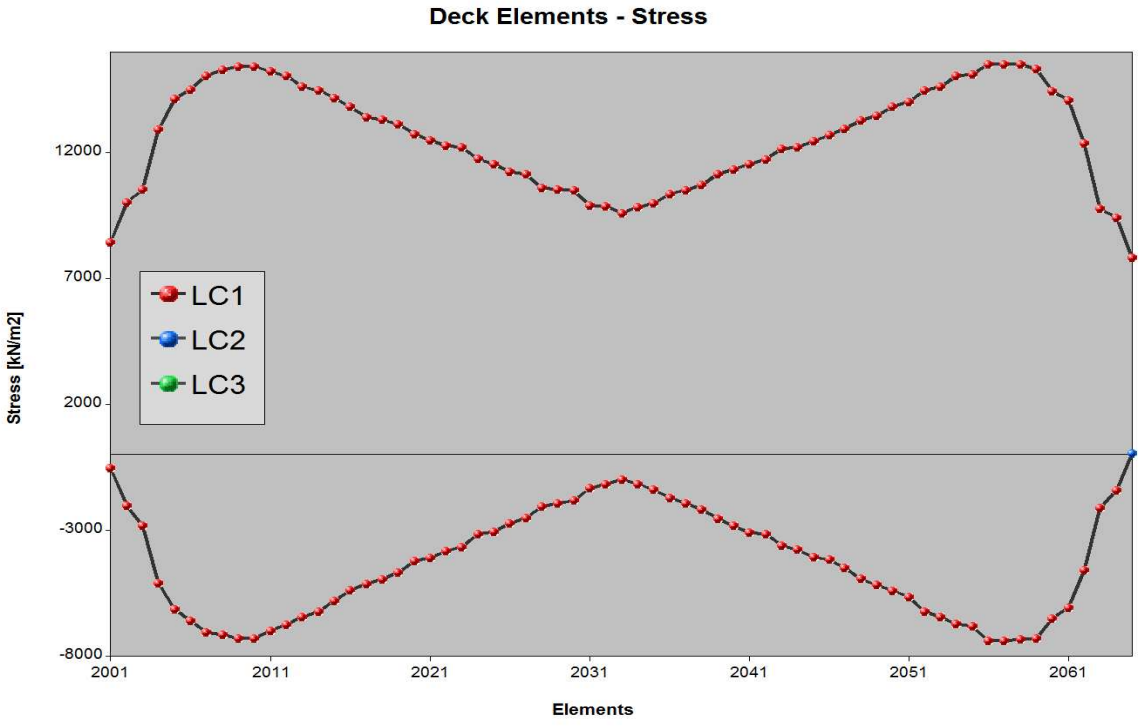


**Figure 22.** Stresses for the deck elements of the Lužnice bridge (Even load)

### 2.6.1.2. Partial Load

The Table B.3 shows the maximum and minimum values for the bending moments (M) and axial forces (N) for the deck elements.

The first two pair of columns after the column “Element” show the values of the axial forces with the corresponding load cases. The Figure 23 shows in a graphical format the maximum forces for each element. As the axial forces in the deck are always positive, the column of minimum should be ignored. The maximum value is 3292.62 kN and correspond to the element 2065, in the right extreme the span, and the load case 1.10 that is, the puntual load in the ¾ of the span. The maximum forces for all elements occur for the load case LC1. The axial forces are higher as the element is closer to the right support, as the right half of the deck is the one loaded with the live load. There are jumps between consecutive values, but their magnitude is of the order of 50 kN, less than the 2% of the average values.

The third pair of columns shows the maximum bending moments with the corresponding load cases. The Figure 24 shows in a graphical format the maximum and minimum bending moments for each element. The maximum value is 1001.45 kNm and corresponds to the element 2048 in the ¾ of the span, and the load case LC1.11, with the puntual load in the ¾ of the span. The maximum moments occur for the load cases LC1 and LC2. However the values for LC2 are negative and should be ignored. The maximum moments have the highest value in the ¾ of the span.

The last pair of columns shows the minimum bending moments with the corresponding load cases. The minimum value is -810.07 kNm and correspond to the element 4023, near the ¼ of the span, and the load case 1.11, with the puntual load in the ¾ of the span. The minimum moments occur for LC1 and LC2. However the values for LC2 are positive and should be ignored. The maximum moments present the highest value in the ¼ of the span.

The Table B.4 shows the maximum and minimum stresses for the deck elements. The Figure 25 shows in a graphical format the maximum and minimum stresses for each element. The minimum value for the stresses is -9606.71 kN/m$^2$ and correspond to the element 2048, in the ¾ of the deck, and the load case LC1.11, with the puntual load in the ¾ of the span. In the same way, the maximum value for the stresses is 16276.01 kN/m$^2$ and corresponds to the element 2048, and the load case LC1.11. The minimum and maximum stresses for all elements occur for the load case LC1. The element next to the left support has a maximum stress for LC2, but its value is less than 15% of the maximum value. The highest and lowest values occur in ¾ of the span, with a minor peak at ¼ of the span.

The maximum stress is higher than the admisible value 2133 KN/m$^2$; the minimum stress is lower than the admisible value -2133 KN/m$^2$.

The fact that the stresses are higher than the admissible values remarks the importance of the prestressing of the deck. As the prestressing was not considered in this thesis, this is expected.

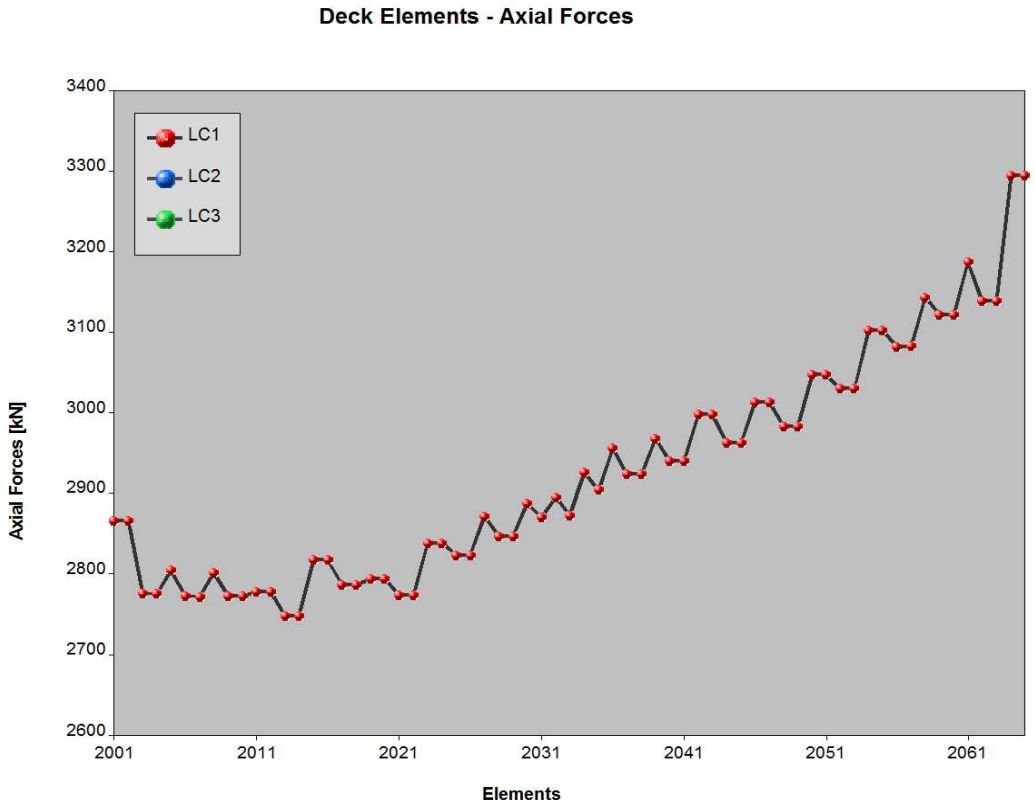


**Figure 23.** Axial forces for the deck elements of the of the Lužnice bridge (Partial Load)

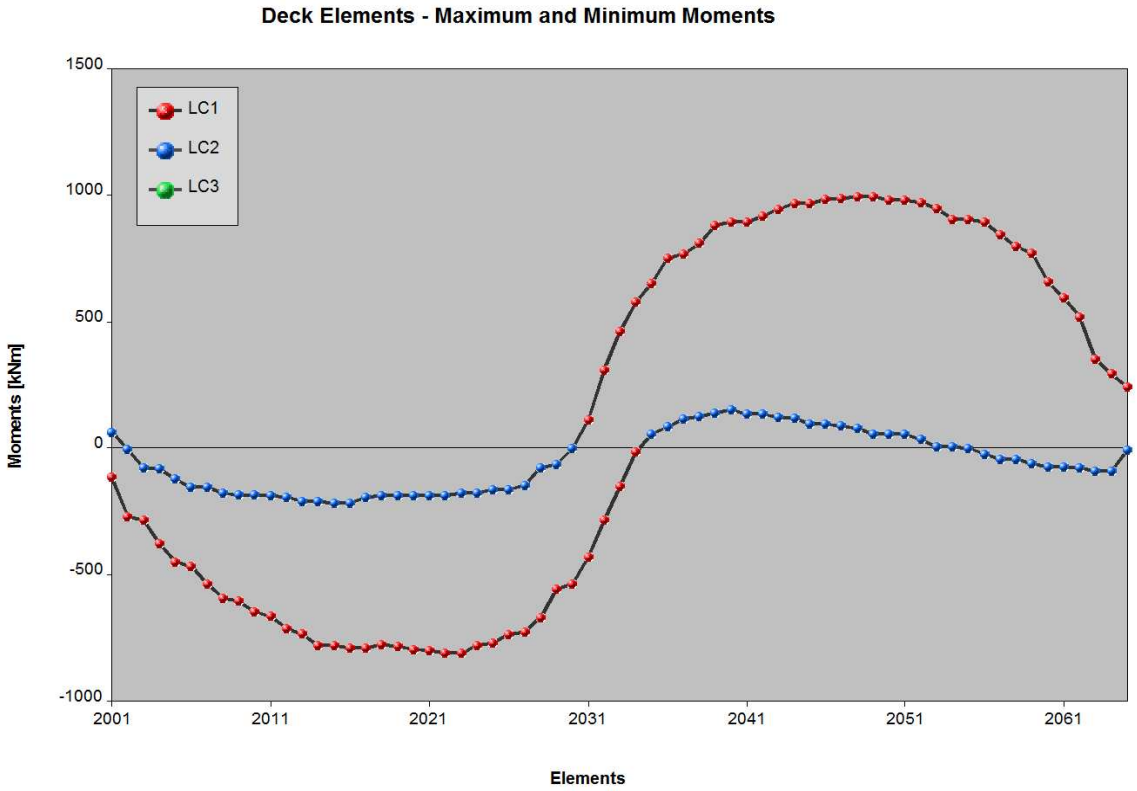


**Figure 24.** Moments for the deck elements of the Lužnice bridge (Partial Load)

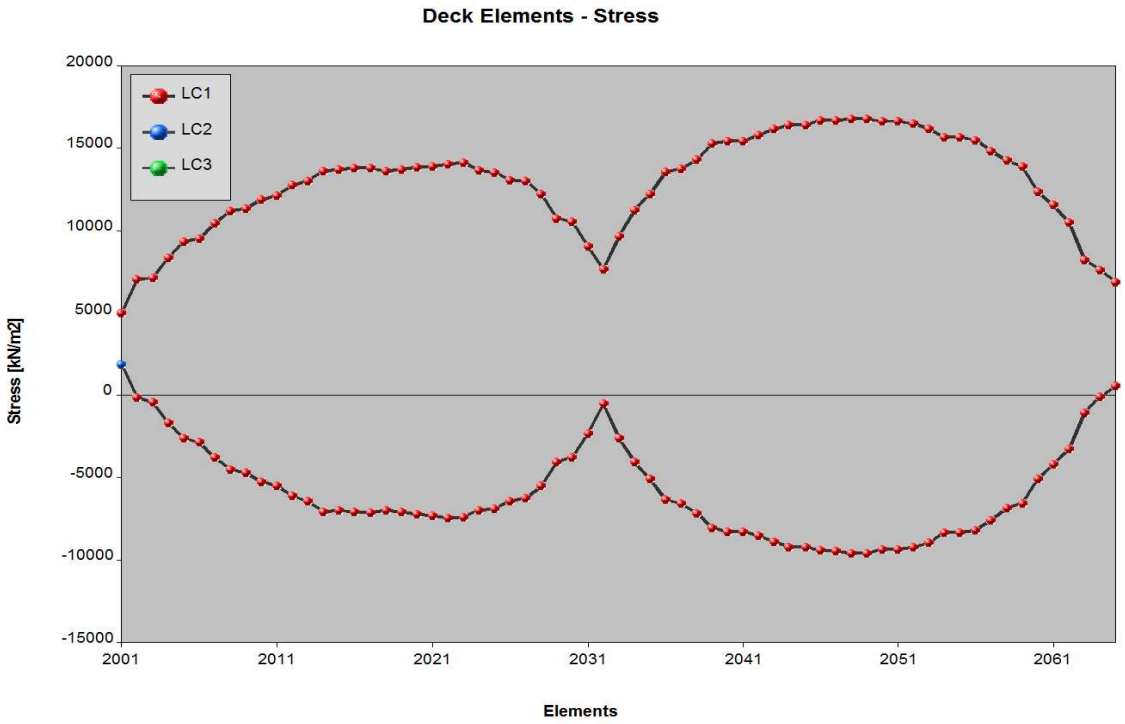


**Figure 25.** Stresses for the deck elements of the Lužnice bridge (Partial Load)

## 2.6.2. Arch

### 2.6.2.1. Even load

The Table B.5 shows the maximum and minimum values for the bending moments (M) and axial forces (N) for the arch elements.

The first two pairs of columns after the column “Element” shows the values of the axial forces with the corresponding load cases. As the axial forces in the archs are always negative, the column of maximum should be ignored. The Figure 26 shows in a graphical format the minimum forces for each element. The minimum value is –4025.23 kN and corresponds to the element 4060, in the right extreme of the arch, and the load case 1.30, with the puntual load in the ¾ of the span. The minimum forces for all elements occur for the load case LC1. The compression forces in the center of the arch are significatly inferior than in the extremes.

The third pair of columns shows the maximum bending moments with the corresponding load cases. The Figure 27 shows in a graphical format the maximum and minimum moments for each element. The maximum value is 136.79 kNm and corresponds to the element 4057 in the right extreme of the arch and the load case LC1.38, with the puntual load near the end of the span. The maximum bending moment in almost every element occurs for LC1. In the last element it occurs for LC3, however the value is less than 5% of the maximum.

The last pair of columns shows the minimum bending moments with the corresponding load cases. The minimum value is -109.35 kNm and corresponds to the element 4048, in the right extreme of the arch, and the load case 1.12, with the puntual load in the ¼ of the span. The minimum moment in almost every element occurs for LC1. However in the extreme the values

correspond to the load case LC2 and are quite important, arriving to a 75% of the minimum. The other minimum values that correspond to the LC2 are mostly positive values, hence should be ignored.

The Table B.6 shows the maximum and minimum stresses for the arch elements. As the stresses are always negative the column of maximum stresses should be ignored. The Figure 28 shows in a graphical format the maximum and minimum stresses for each element. The minimum value for the stresses is -175017.42 kN/m$^2$ and correspond to the element 4057, in the right extreme of the arch, and the load case 1.37, with the puntual load near the end of the span. The minimum stresses for all elements ocur for the load case LC1.
The minimum value is 82% of the minimum admisible stress (-213636 KN/m$^2$ ).

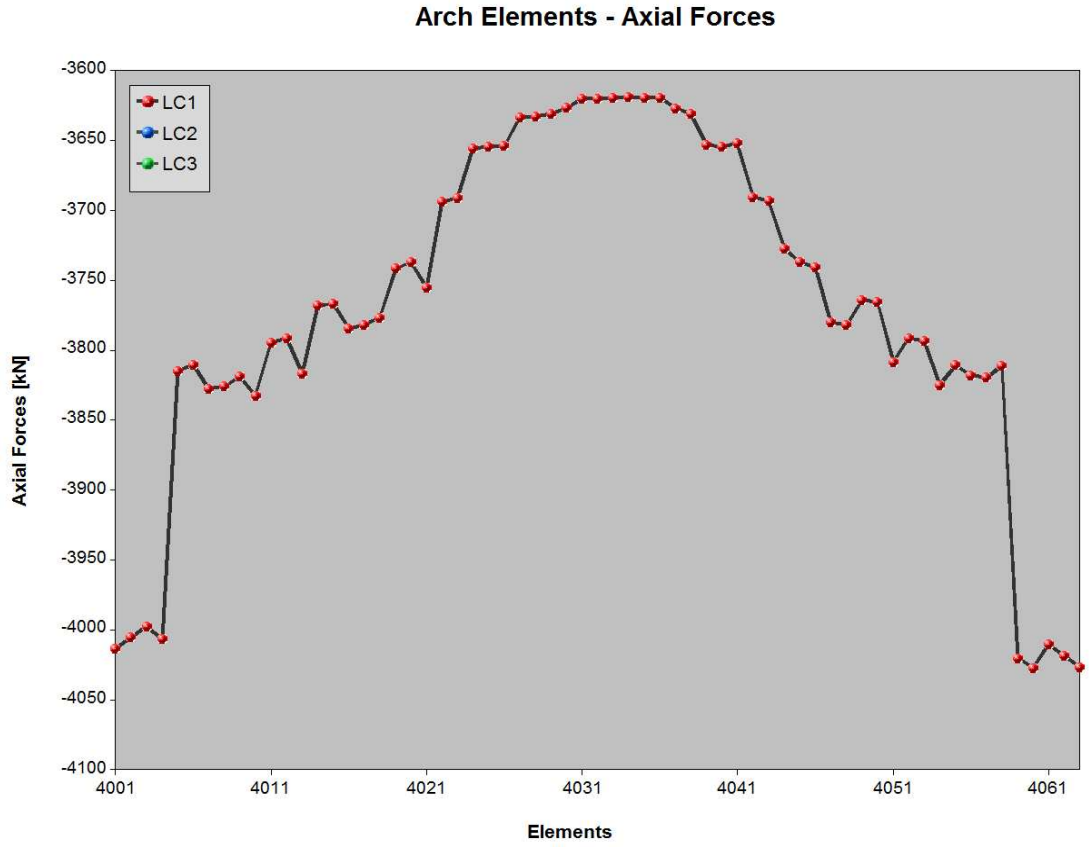


**Figure 26.** Axial forces for the arch elements of the of the Lužnice bridge (Even load)

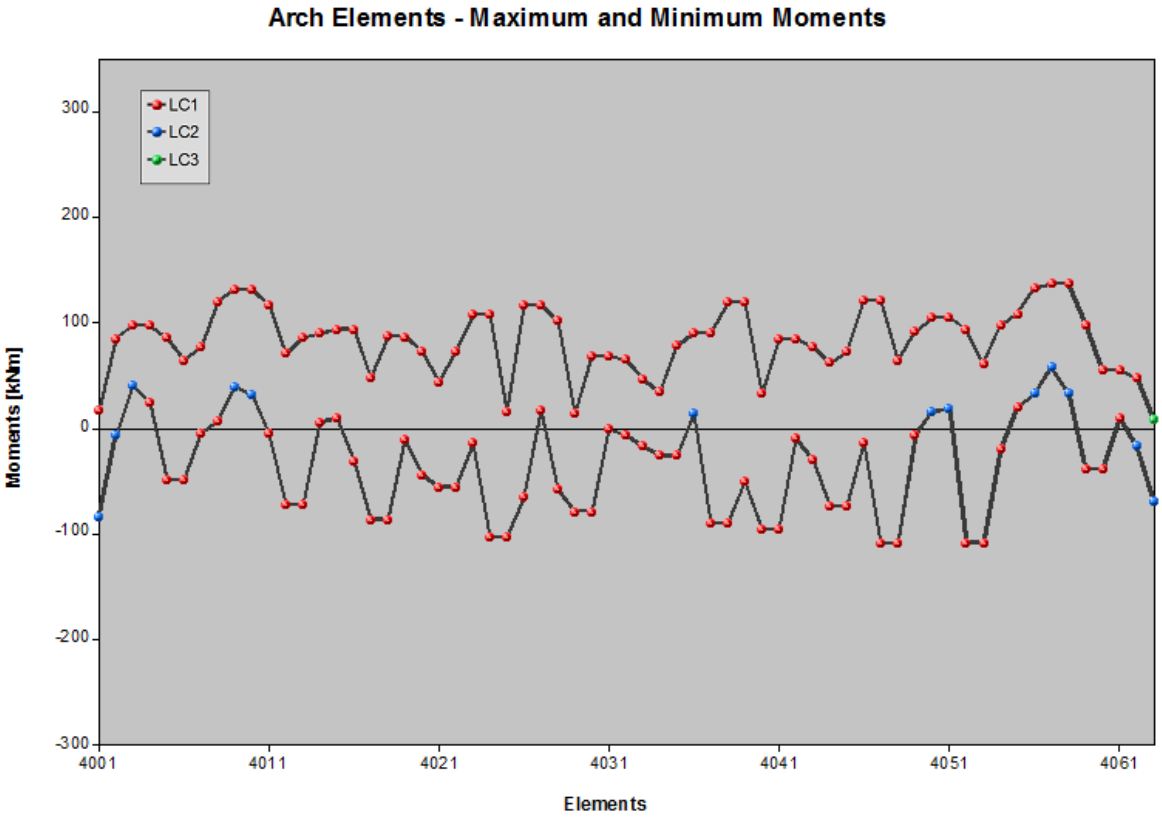


**Figure 27.** Moments for the arch elements of the Lužnice bridge (Even load)

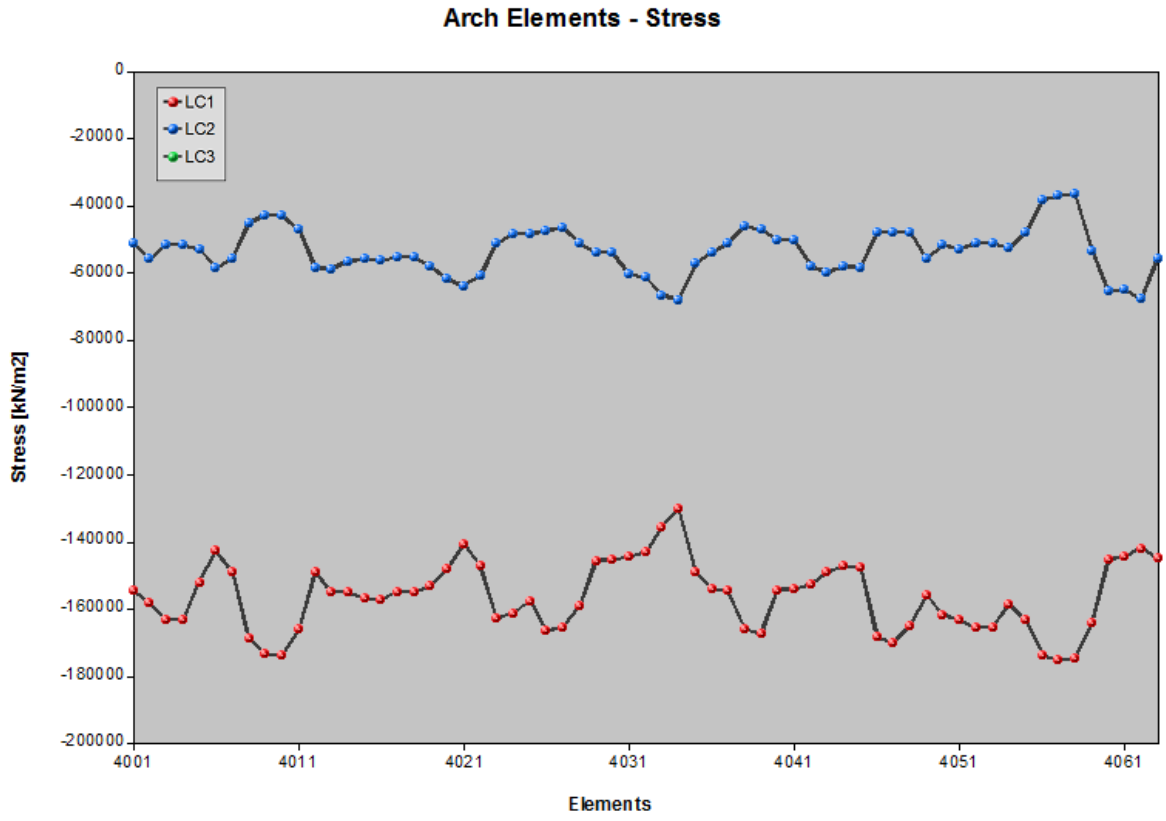


**Figure 28.** Stresses for the arch elements of the Lužnice bridge (Even load)

### 2.6.1.2 Partial Load

The Table B.7 shows the maximum and minimum values for the bending moments (M) and axial forces (N) for the arch elements.

The first two pairs of columns after the column “Element” show the values of the axial forces with the corresponding load cases. As the axial forces in the archs are always negative, the column of maximum should be ignored. The Figure 29 shows in a graphical format the minimum forces for each element. The minimum value is –3772.30 kN and correspond to the element 4063, in the right extreme of the arch, and the load case 1.10, with the puntual load in the ¾ of the span. The minimum forces for all elements occur for the load case LC1. The compression forces in the right side of the arch are significatly higher, as the live load is only applied in the right half of the span.

The third pair of columns shows the maximum bending moments with the corresponding load cases. The Figure 30 shows in a graphical format the maximum and minimum moments for each element. The highest value is 185.72 kNm and correspond to the element 4038 in the 56% of the span, and the load case LC1.08, with the puntual load in the ¾ of the span. The maximum bending moment in the elements of the right half of the arch occurs for LC1. In the left half of the bridge, the maximum moments occurs for LC2. However they are positive or less than 25% of the maximum. In the right extreme the maximum occurs for LC3, but its value is less than 5% of the maximum.

The last pair of columns shows the minimum bending moments with the corresponding load cases. The Figure 30 shows in a graphical format the maximum and minimum moments for each element. The minimum value is -165.05 kNm and correspond to the element 4012, in the left half of the arch, and the load case 1.10, with the puntual load in the ¾ of the span. The minimum moments in the elements of the left side of the arch occurs for LC1. In the left side of the bridge, the minimum moments mostly occur for LC2. However they are positive or less than 40% of the maximum value.

The Table B.8 shows the maximum and minimum stresses for the arch elements. As the stresses are always negative the column of maximum stresses should be ignored. The Figure 31 shows in a graphical format the maximum and minimum stresses for each element. The minimum value for the stresses is -177556.84 kN/m$^2$ and correspond to the element 4039, in the center of the arch, and the load case 1.07, with the puntual load in the ¾ of the span. The minimum stresses for all elements occur for the load case LC1.

The minimum value is 83% of the minimum admisible stress (-213636 KN/m$^2$ ).

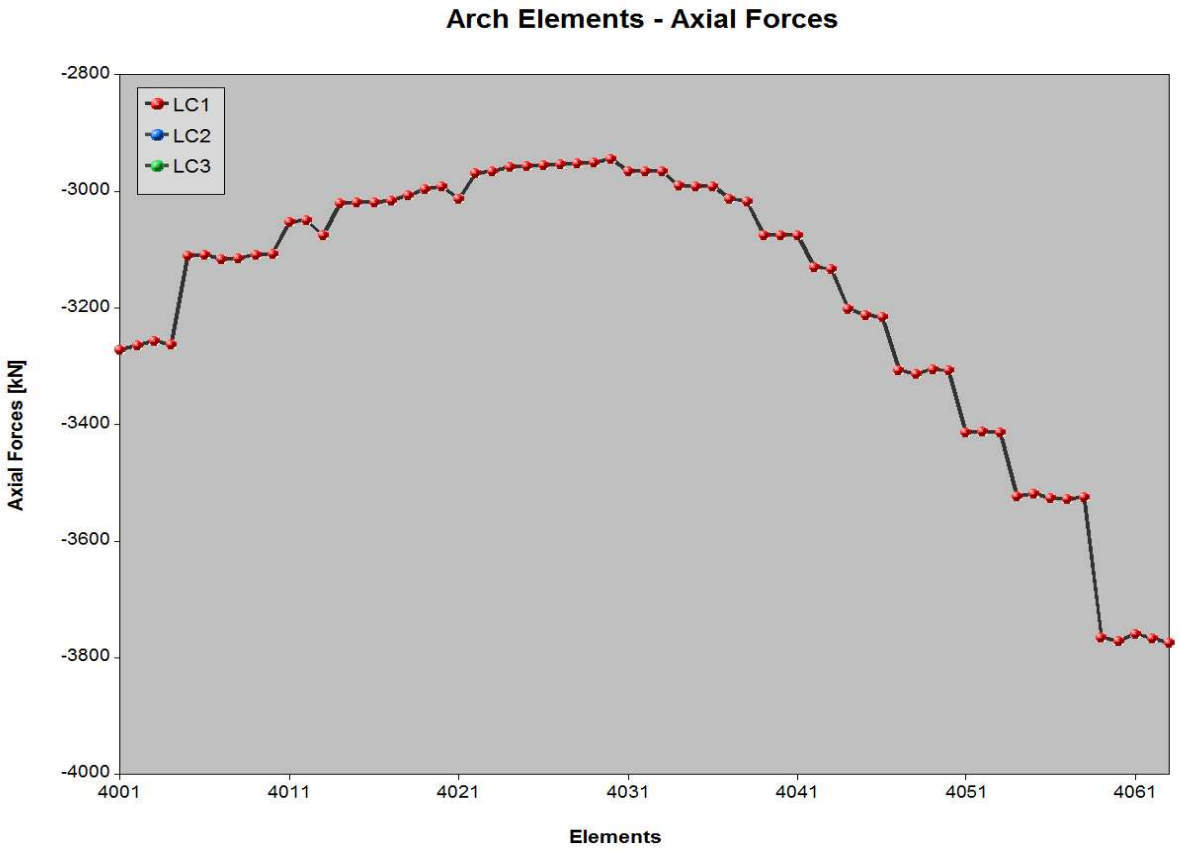


**Figure 29.** Axial forces for the arch elements of the  of the  Lužnice bridge (Partial load)

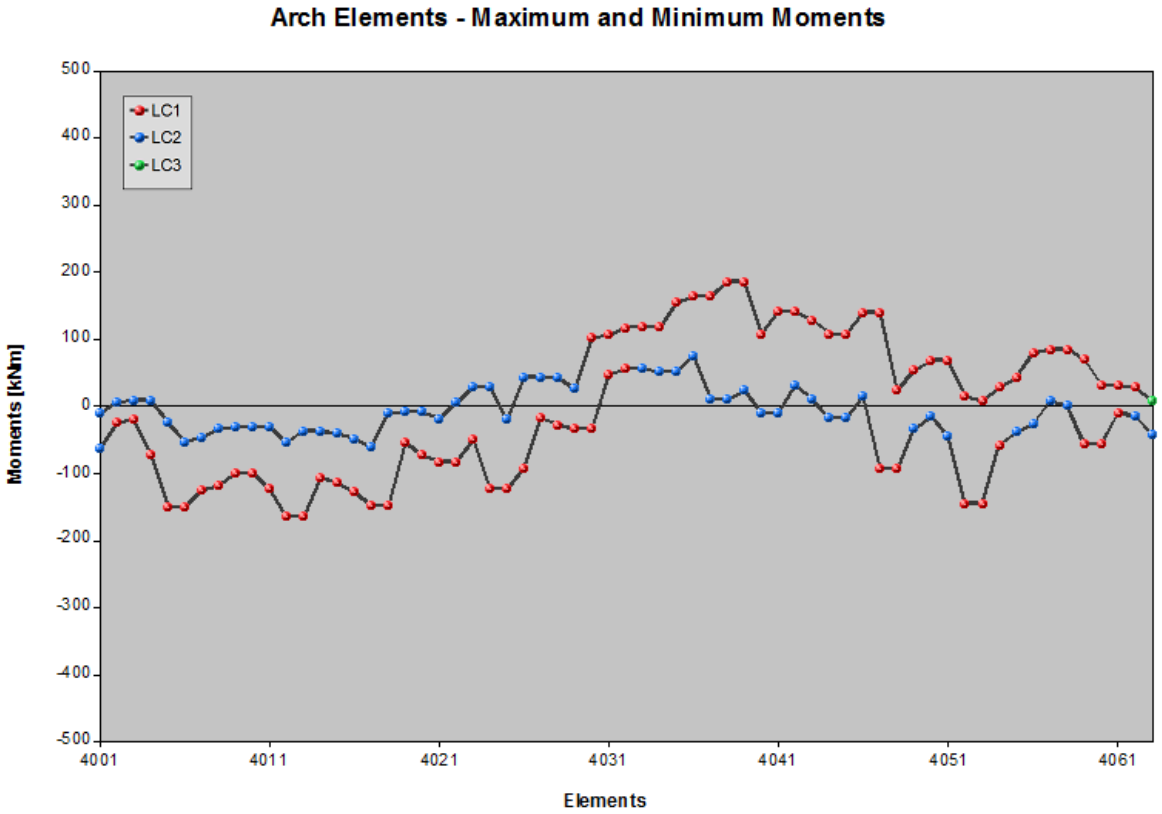


**Figure 30.** Moments for the arch elements of the Lužnice bridge (Partial load)

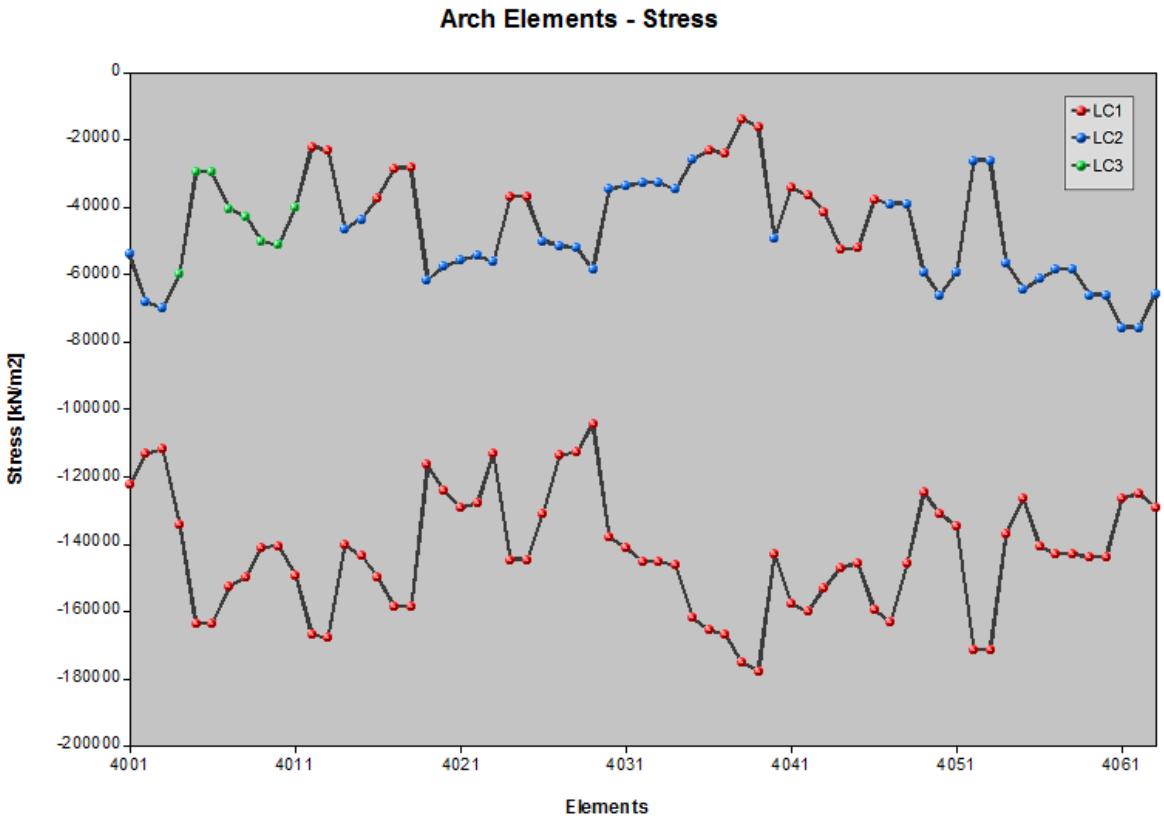


**Figure 31.** Stresses for the arch elements of the Lužnice bridge (Partial load)

### 2.6.3. Hangers

### 2.6.3.1 Even load

The Table B.9 shows the maximum and minimum values for the stresses in the hangers. The hangers are ordered in two sets: one set is the mirrored equivalent of the other. The hangers with a positive slope towards the right extreme of the bridge are referred as Set 1. The hangers with a negative slope away from the right extreme of the bridge are referred as Set 2. The numbers for the hangers are assigned as it is shown in the Figure C.1 in the Appendix C.

In the Table, as the stresses are always positive, the column of minimum should be ignored. The Figure 32 shows in a graphical format the maximum stresses in both sets. The highest value for the stresses is 194047.12 kN/m$^2$ and corresponds to the element 2019, the last hanger of the Set1, and the load case LC1.31, with the puntual load in the ¾ of the span. The maximum stresses for most of the elements occur for the load case LC1. In the first hangers of each set the maximum stresses occur for LC3. However, the values in this hangers are inferior than the average value of the stresses. The highest values correspond to the last hangers of the sets, and they are significatly higher than the stresses in the rest of the hangers.

The maximum value is 42% of the maximum admisible stress (454545 KN/m$^2$ ).

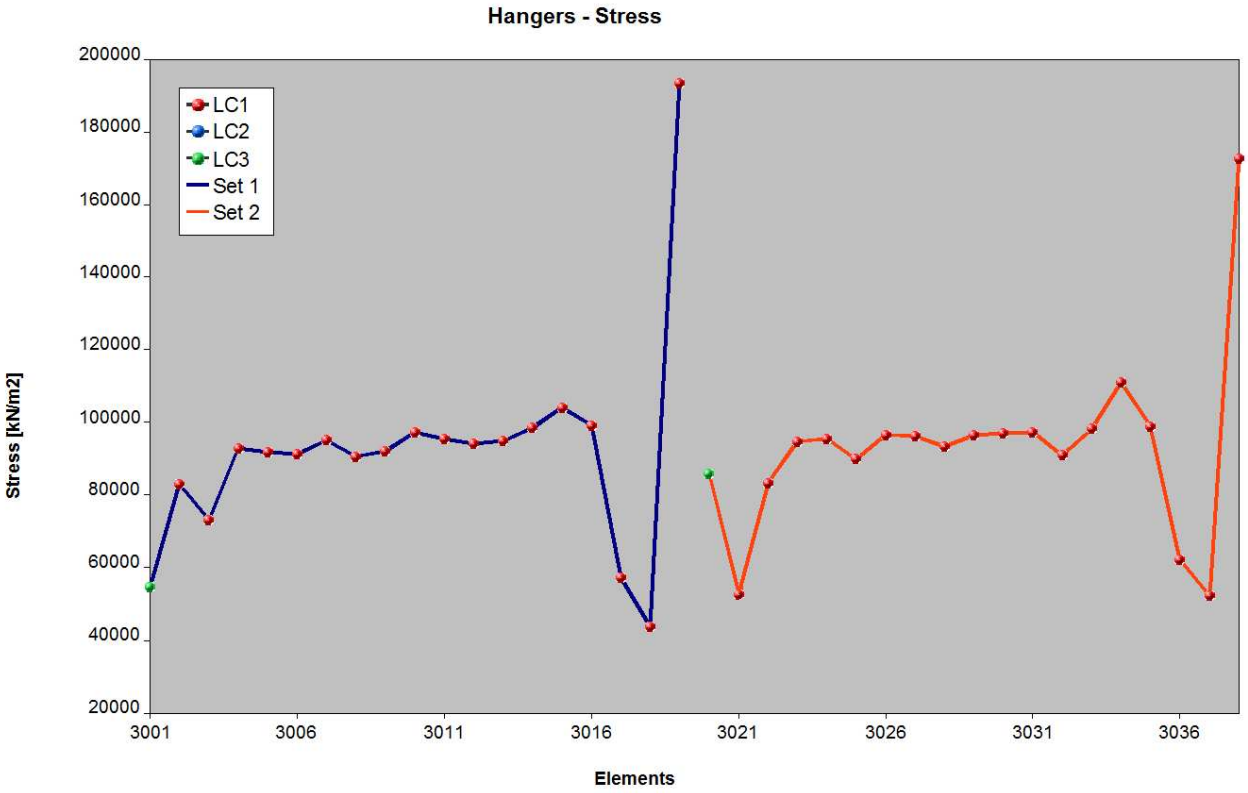


**Figure 32.** Stresses for hangers of the Lužnice bridge (Full Load)

### 2.6.3.2 Partial Load

The Table B.10 shows the maximum and minimum values for the stresses in the hangers. The numbers for the hangers are assigned as it is shown in the Figure C.1 in the Appendix C.

In the Table, as the stresses are always positive, the column of minimum should be ignored.

The Figure 33 shows in a graphical format the maximum stresses in both sets. The highest value for the stresses is 221057.17 kN/m$^2$ and corresponds to the element 2019, the last hanger of the Set1, and the load case LC1.10, with the puntual load in the ¾ of the span. For this load configuration the Set 1 is more solicitated than the Set2.

For the Set1 the maximum stresses for most of the elements occur for the load case LC1. In the first two hangers the maximum stresses occur for LC3. However, the values in this hangers are inferior than the average value of the stresses. For the Set2 the maximum stresses occur for the load cases LC1, LC2 and LC3. The highest value in the last hanger occurs for LC2. This value is 61% of the maximum value of the hangers of Set1.

The highest value is 48% of the maximum admisible stress (454545 KN/m$^2$ ).

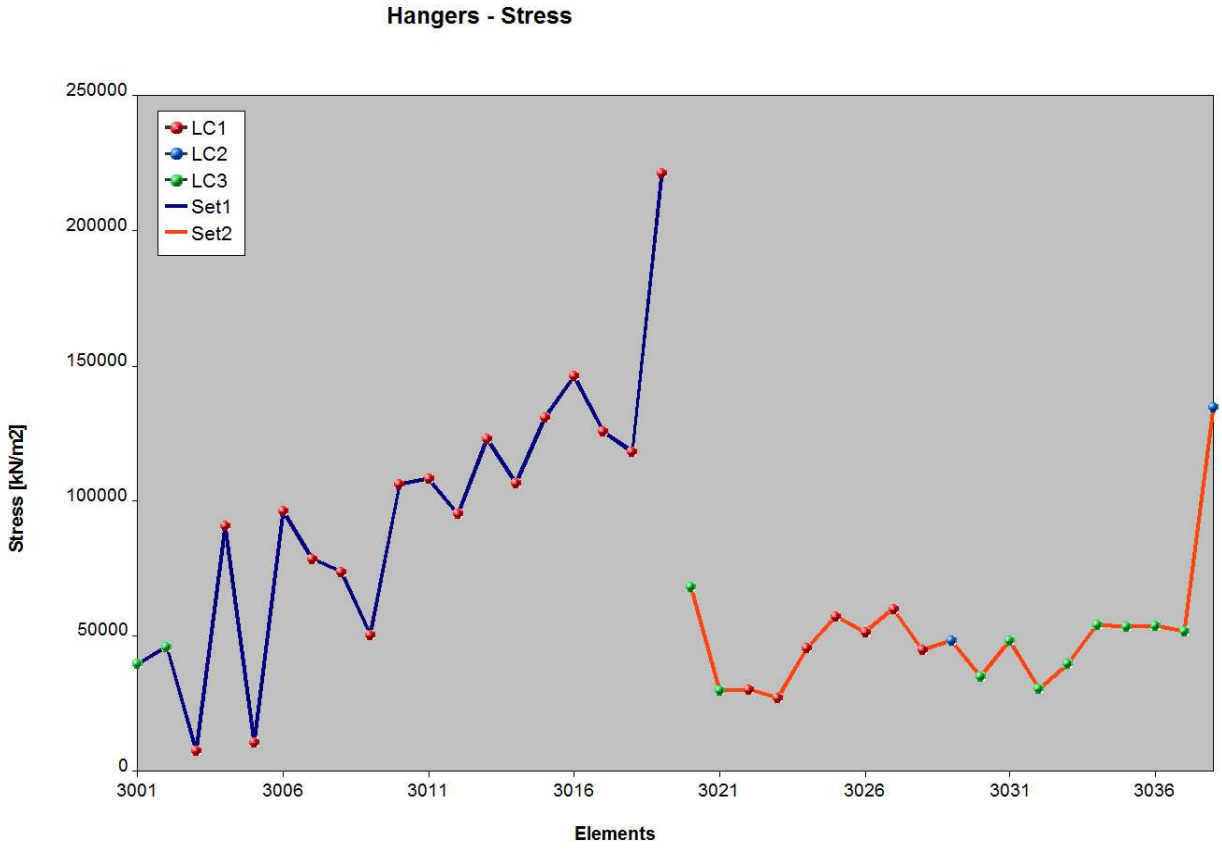


**Figure 33.** Stresses for hangers of the Lužnice bridge (Partial Load)

## 2.7 Conclusions

The maximum and minimum stresses in the elements occur mainly for the load case LC1. Even if for some elements the stresses correspond to another load case, those values are significantly smaller compared with the values of the most loaded elements.

In the case of partial loading of the deck, in the hangers that belong to the Set 2, the maximum stresses occurred for LC2. However for this case the Set1 is significantly more stressed than the Set2. Hence, the highest values correspond to the load case LC1.

For these reason, the study of the bridge will be done only for the load case LC1.

On the other hand, comparing the cases of even and partial loading, the absolute values of the maximum and minimum stresses are quite similar, slightly higher in the second case. But, it has to be considered that under asymmetric loading the benefits of network arch bridges over other types of bridges become more evident. This can be clearly seen in the Figure 22 that shows the stresses in the deck for even loads. While the distributed load in the deck is always even, the punctual load for LC1 change position. In this way, the maximum stress in the center of the deck, that corresponds to a central position of the punctual load (symmetric load), is smaller than the maximum stress at 1/5 of the span, that corresponds to a punctual load at 1/5 of the span (asymmetric load). The stresses in the deck under asymmetric loads are higher than under symmetric loads. Also, under partial loading, the hangers are more susceptible to relax.

Hence, the study will be done for partial loading of the span.

# Chapter 3
# Study of parameters

This Chapter constitutes the main part of this thesis. Different parameters are studied in order to find how they influence the structural behavior and, therefore, the solicitations on the elements of the bridge.

The parameters chosen for this study are:

- Hangers arrangement. *Section 3.1*
- Arch shape. *Section 3.2*
- Number of hangers. *Section 3.3*
- Rise of the arch. *Section 3.4*

An optimal arrangement is characterised by the following attributes [GST]:

- economic/inexpensive.
- fast/easy to build.
- functional,aesthetic,ecological...

This attributes are mainly influenced by the minimum and maximum internal forces. Hence, for this work the following atributes are chosen:

- Maximum and minimum bending moments.
- Maximum and minimum axial forces.
- Maximum and minimum stresses.

The maximum bending moments are not analyzed for the hangers, as this elements are tension-only. For the arch and the deck, the moments with the maximum absolute values are considered.

The minimum axial forces are considered for the hangers, in order to study the posibility of relaxation.

Over 973 bridges are modelled for this study. For each model, the avobe mentioned parameters are stored in matrices for its analysis. Aditional parameters are also analyzed, as the number of relaxed hangers, and the load cases and coordinates or elements corresponding to the maximum solicitations. The values that are considered useful for the interpretations of the structural behavior of the bridge are presented in this work.

## 3.1. Hanger arrangement

Two types of arrangements are considered. In the Section 3.1.1. an arrangement based on the linear variation of the slope of the hangers is presented [TNA]. In the Section 3.1.2. the radial arrangement, proposed by Brunn and Schanack [BSC] is analyzed.

Each hanger arrangement is studied for a circular arch shape, following the recomendations in [TNA]. The radio of the circular arch is adopted in order to mantain the span and the maximum height of the original arch.

### 3.1.1. Linear variation of the slopes

This arrangement is based on a constant angle change between adjacent hangers [TNA]. The upper nodes of the hangers are placed equidistantly along the arch. The slope of each hanger increase lineary from an start angle, according to the function:

$$\varphi = \varphi_0 + \Delta\varphi\,(n-1)$$

Where $\varphi_0$ is the initial angle and $\Delta\varphi$ is the angle increment between hangers. The value *n* is the number of the hanger. Hence the variables used to described this arrangement are the initial angle and the angle increment.

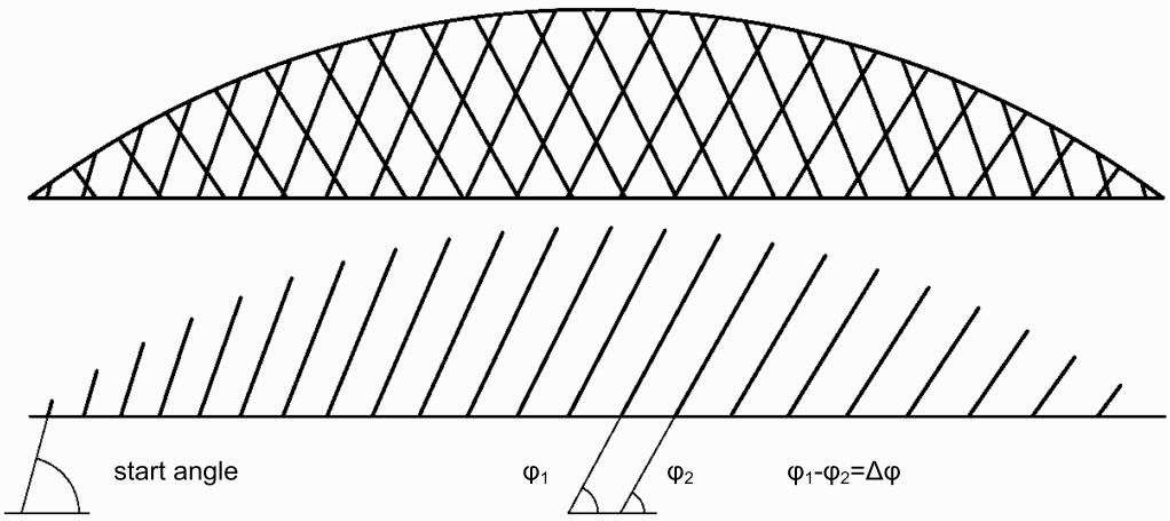


**Figure 34.** Arrangement of the hangers based on the linear variation of the slopes

For the present study 340 bridges are calculated, with a start angle from 65° to 84° and with an angle increment from 0.0° to 3.4°. The study is done for a circular arch shape. The numbers for the hangers are assigned as it is shown in the Figure C.1 in the Appendix C.

### 3.1.1.1. Results

The results are shown in the following diagrams. Every ordinate corresponds to one value of each bridge.

#### 3.1.1.1.1. Bending moments in the deck

The Figure 35 shows the absolute values for maximum bending moments in the deck for each bridge. The highest value presents for a bridge with $\varphi_0$= 84°- $\Delta\varphi$ = 0.0°. This configuration is shown in the Figure 36. The bending moments decrease as the initial angle decreases and as the angle increment increases, until a minimum value for a bridge with $\varphi_0$= 70°- $\Delta\varphi$ = 3.2°. This configuration is shown in the Figure 37.

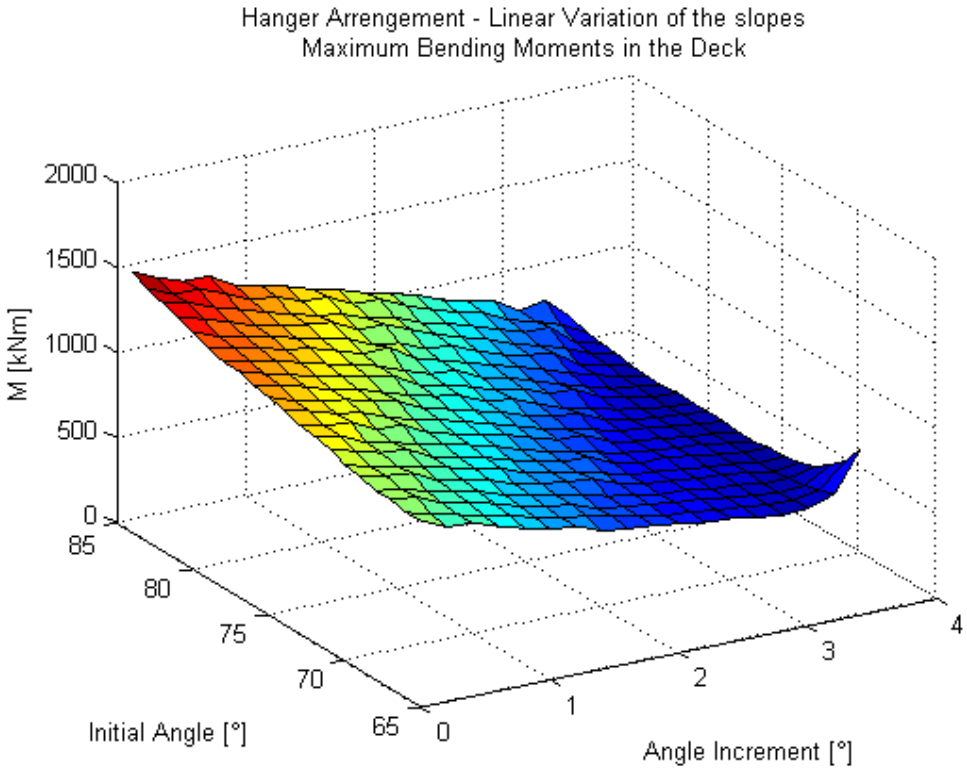


**Figure 35.** Maximum bending moments in the deck (Linear variation of the slopes)

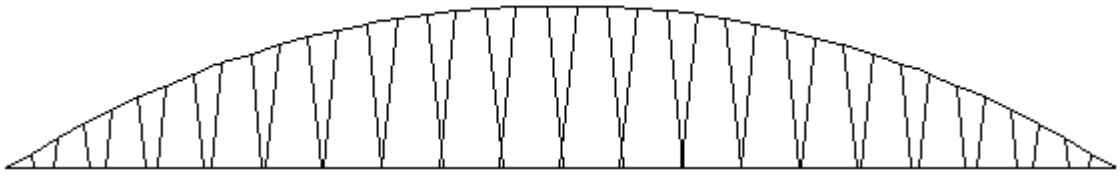

**Figure 36.** Hanger arrangement for $\varphi_0$= 84°- $\Delta\varphi$ = 0.0°

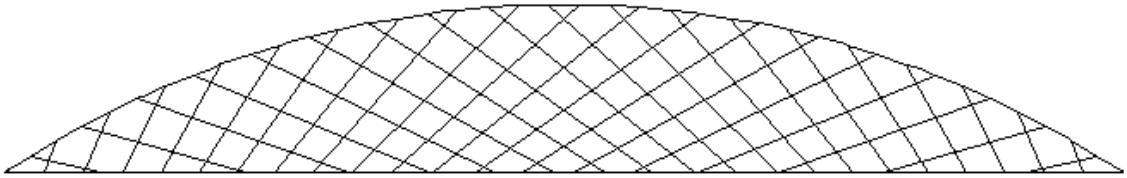

**Figure 37.** Hanger arrangement for $\varphi_0$= 70°- $\Delta\varphi$ = 3.2°

In the bridge of the Figure 36 the hangers intersect each other only once. For this reason the bridge is not a network arch bridge. The value of the maximum bending moment in the deck for this configuration is 1526.61 kNm.

The arrangement of the Figure 37 corresponds to a bridge with $\varphi_0$= 70°- $\Delta\varphi$ = 3.2°. The hangers intersect each other at least two times, fullfilling the condition for the network arch bridges [TNA]. The bridge has the structural behavior of several trusses on top of another. For this reason, the bending in the deck is significatly reduced. The value of the maximum bending moment in the deck for this configuration is 653.70 kNm: 43% of the value for the arrangement of the Figure 36.

The Figure 38 shows in a graphical format the X-coordinate where the maximum value occurs. For high initial angles and small angle increments the maximum value occurs around the 30.0 m from the left support: 73% of the span. As the initial angle decreases and the angle increment increases, the corresponding elements are located closer to the center of the span.

The Figure 39 shows the load cases for which the maximum value occur. For high initial angles and small angle increments the corresponding load case is 1.11, with the puntual load located 31.0 m from the left support: 76% of the span. As the initial angle decreases and the angle increment increases, the load case where the maximum value occur approximates the load case 1.01, with the location of the puntual load approximating the center of the span.

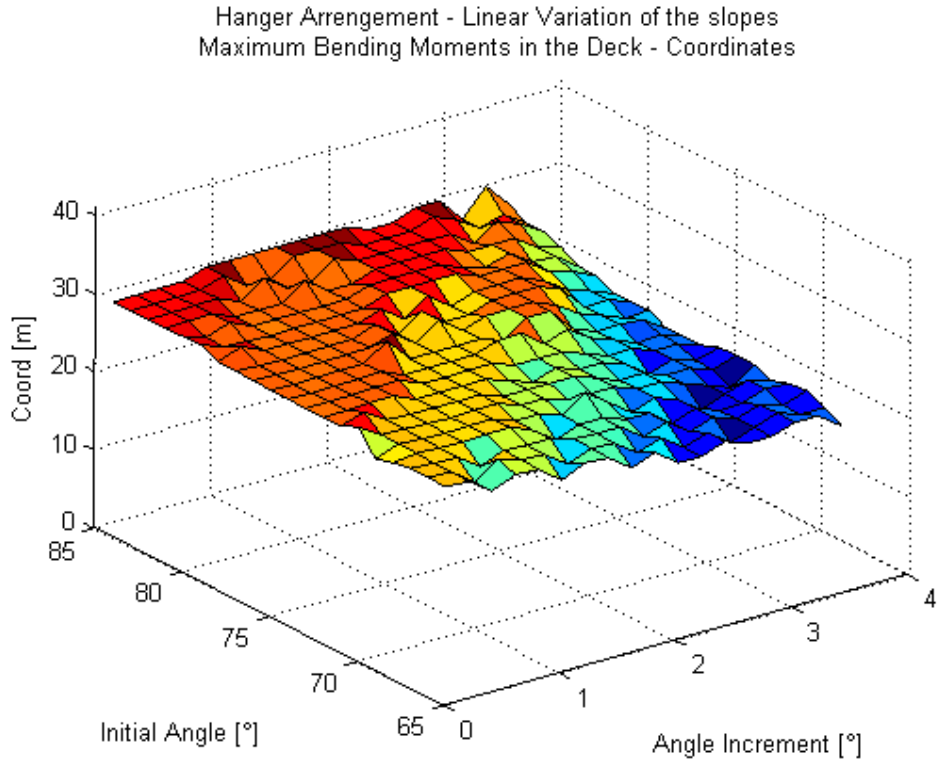


**Figure 38.** Corresponding X-coordinates for the maximum bending moments in the deck (Linear variation of the slopes)

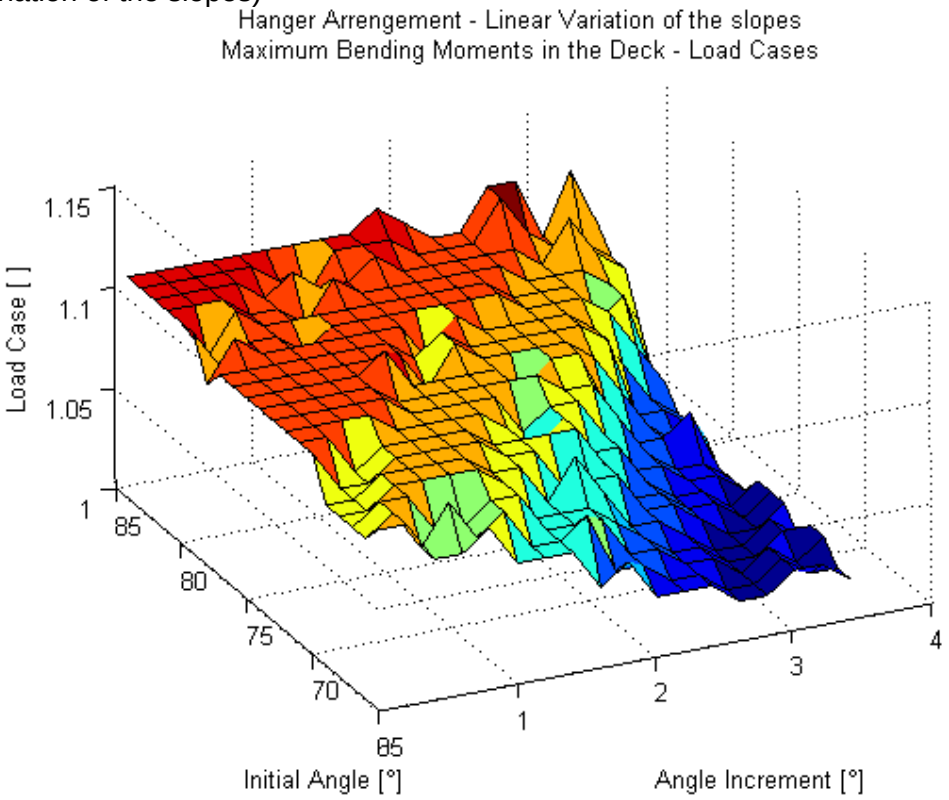


**Figure 39.** Corresponding load cases for the maximum bending moments in the deck (Linear variation of the slopes)

### 3.1.1.1.2. Axial forces in the deck

The Figure 40 shows the values for maximum axial forces in the deck for each bridge. The highest value presents for a bridge with $\varphi_0$= 65° - $\Delta\varphi$ = 3.4°. This configuration is shown in the Figure 41. The axial forces decrease as the initial angle increases and as the angle increment decreases, until a minimum value for a bridge with $\varphi_0$= 84° - $\Delta\varphi$ = 0.0°. This configuration is shown in the Figure 36.

In the arrengement of the Figure 41 the hangers intersect each other at least two times, fullfilling the condition for the network arch bridges [TNA]. The bridge has the structural behavior of several trusses on top of another. The value of the maximum axial force in the deck for this configuration is 3294.64 kN.

The bridge shown on the Figure 36 is not a network arch bridge, as the hangers just intersect each other once. The value of the maximum axial force in the deck for this configuration is 2844.75 kN: 86% of the highest axial force.

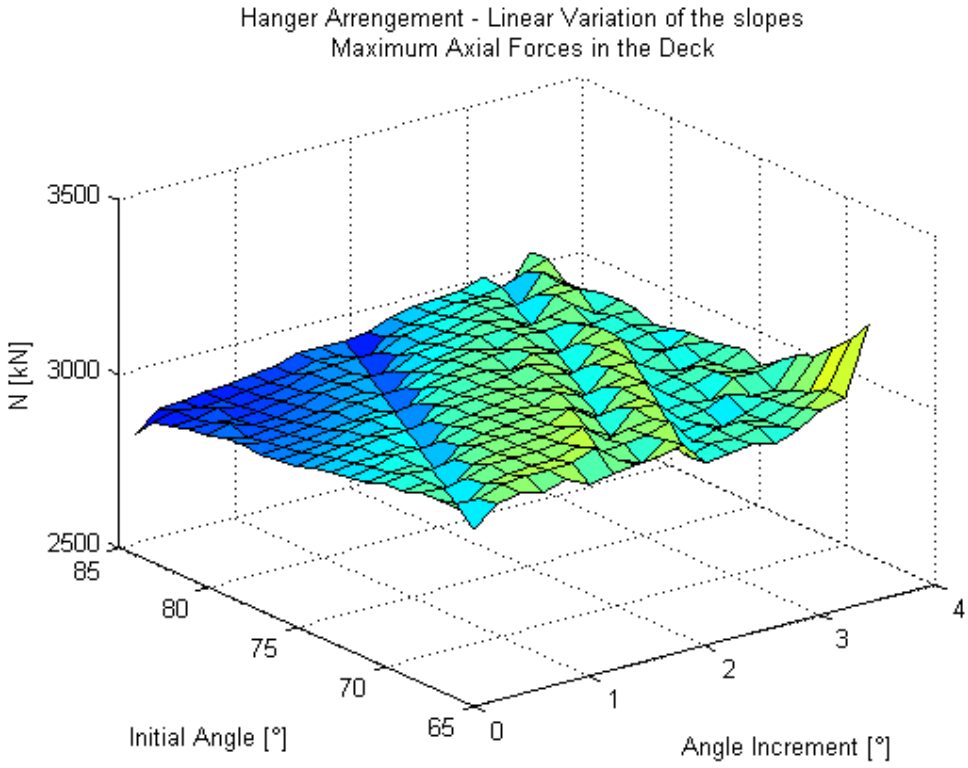


**Figure 40.** Maximum axial forces in the deck (Linear variation of the slopes)

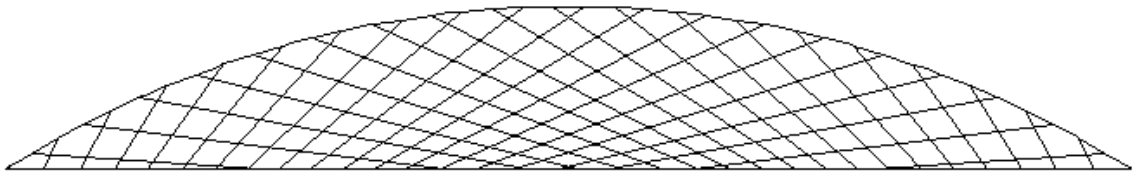

**Figure 41.** Hanger arrangement for $\varphi_0$= 65°- $\Delta\varphi$ = 3.4°

The Figure 42 shows in a graphical format the X-coordinates where the maximum values occur. For all bridges, the maximum value ocurrs mostly near 35.0 m from the left support (85% of the span). However, as the angle increment increases and the initial angle decreases, the corresponding coordinate approaches the right support.

The Figure 43 shows the load cases for which the maximum values occur. For high initial angles and small angle increments the corresponding load case is 1.01, with the puntual load located in the center of the span. As the initial angle decrease and as the angle increment increase, the load case where the maximum value occur approximates the load case 1.12. That is, the location of the puntual load approximates to the 32 m from the left support: the 78% of the span.

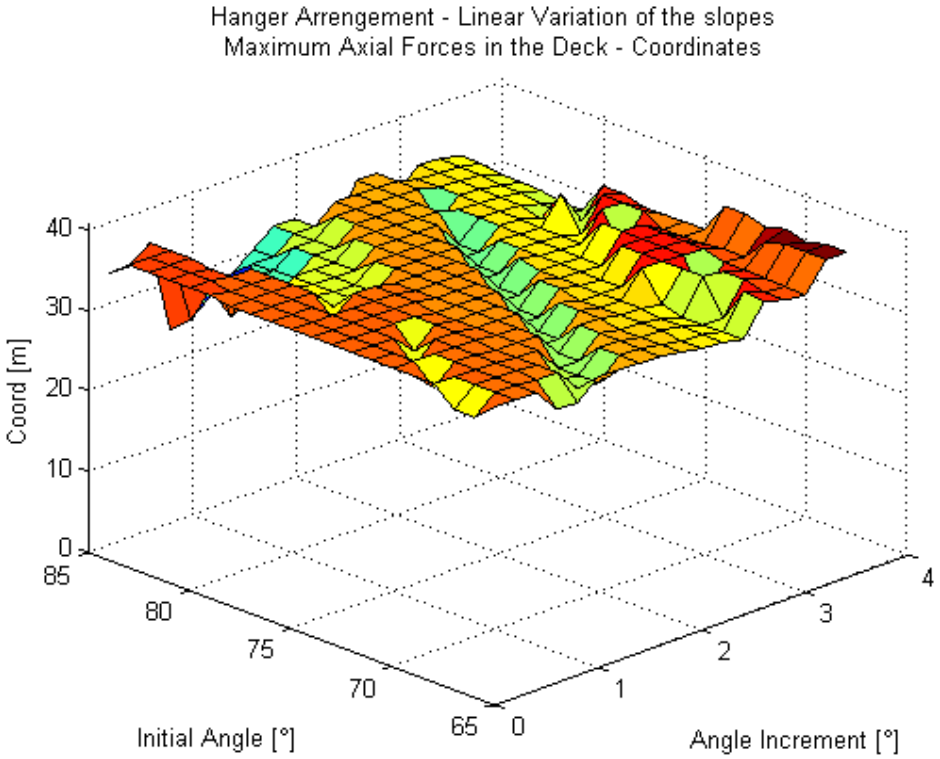


**Figure 42**. Corresponding X-coordinates for the maximum axial forces in the deck (Linear variation of the slopes)

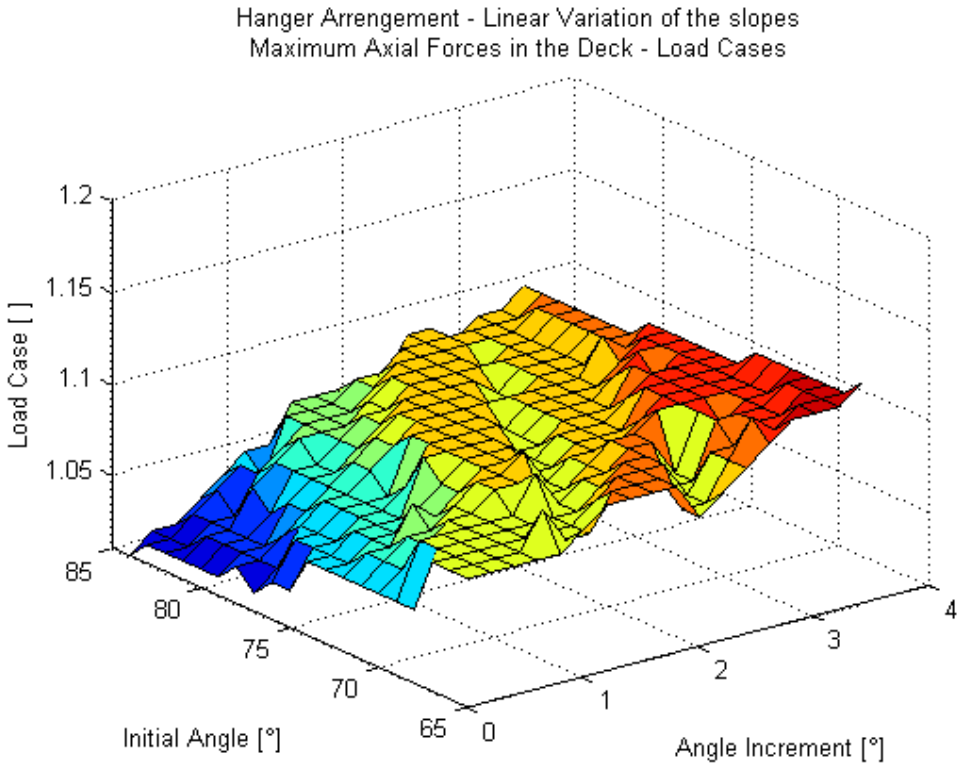


**Figure 43.** Corresponding load cases for the maximum bending moments in the deck (Linear variation of the slopes )

### 3.1.1.1.3. Stresses in the deck

The Figure 44 shows the values for maximum stresses in the deck for each bridge. The highest value presents for a bridge with $\varphi_0$= 84°- $\Delta\varphi$ = 0.0°. This configuration is shown in the Figure 36. The stresses decrease as the initial angle decreases and as the angle increment increases, until a minimum value for a bridge with $\varphi_0$= 70°- $\Delta\varphi$ = 3.2°. This configuration is shown in the Figure 37.

In the bridge of the Figure 36 the hangers intersect each other only once. For this reason the bridge is not a network arch bridge. The value of the maximum stress in the deck for this configuration is 22806.53 kN/m$^2$.

The arrangement of the Figure 37 corresponds to a bridge with $\varphi_0$= 70°- $\Delta\varphi$ = 3.2°. The hangers intersect each other at least two times, fullfilling the condition for the network arch bridges [TNA]. The bridge has the structural behavior of several trusses on top of another. For this reason, the stress in the deck is significatly reduce in comparison with the arrangement of the Figure 36. The value of the maximum stress in the deck for this configuration is 11461.62 kN/m$^2$: a reduction of 50%.

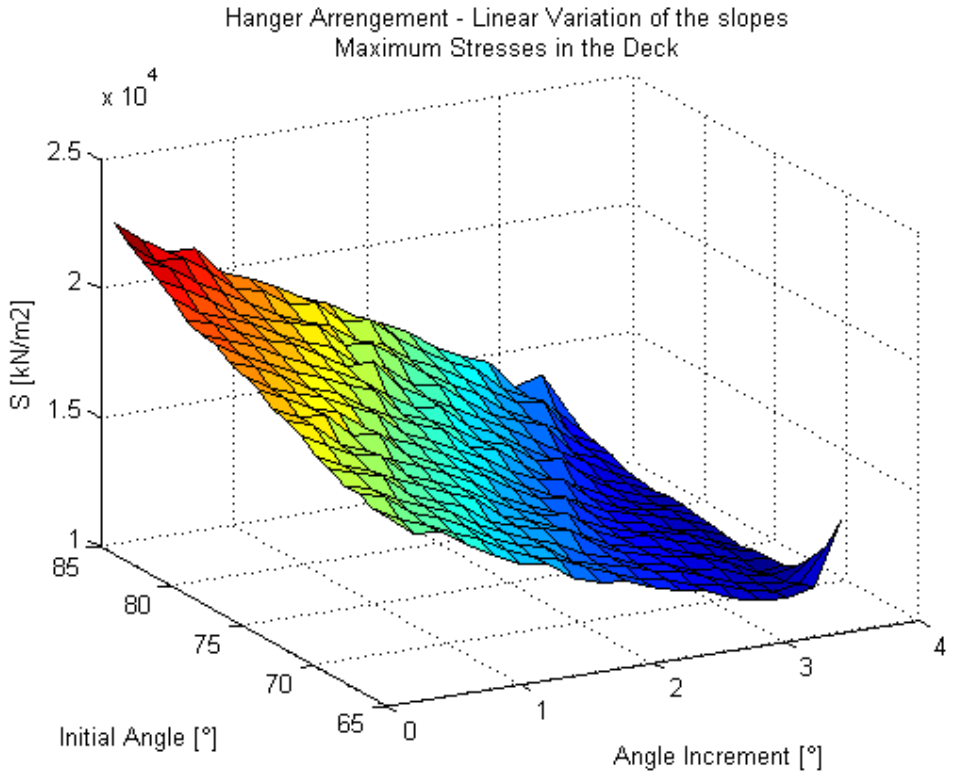


**Figure 44.** Maximum stresses in the deck (Linear variation of the slopes)

The figure 45 shows in a graphical format the X-coordinate where the maximum values occur. For high initial angles and small angle increments the maximum values occur near the 30.0 m from the left support: 75% of the span. As the initial angle decreases and the angle increment increases, the corresponding coordinate is closer to the center of the span.

The Figure 46 shows the load cases for which the maximum values occur. For high initial angles and small angle increments the corresponding load case is 1.11, with the puntual load located 31 m from the left support: 76% of the span. As the initial angle decreases and the angle increment increases, the load case where the maximum value occurs approaches the load case 1.01, with the location of the puntual load approximating the center of the span.

.

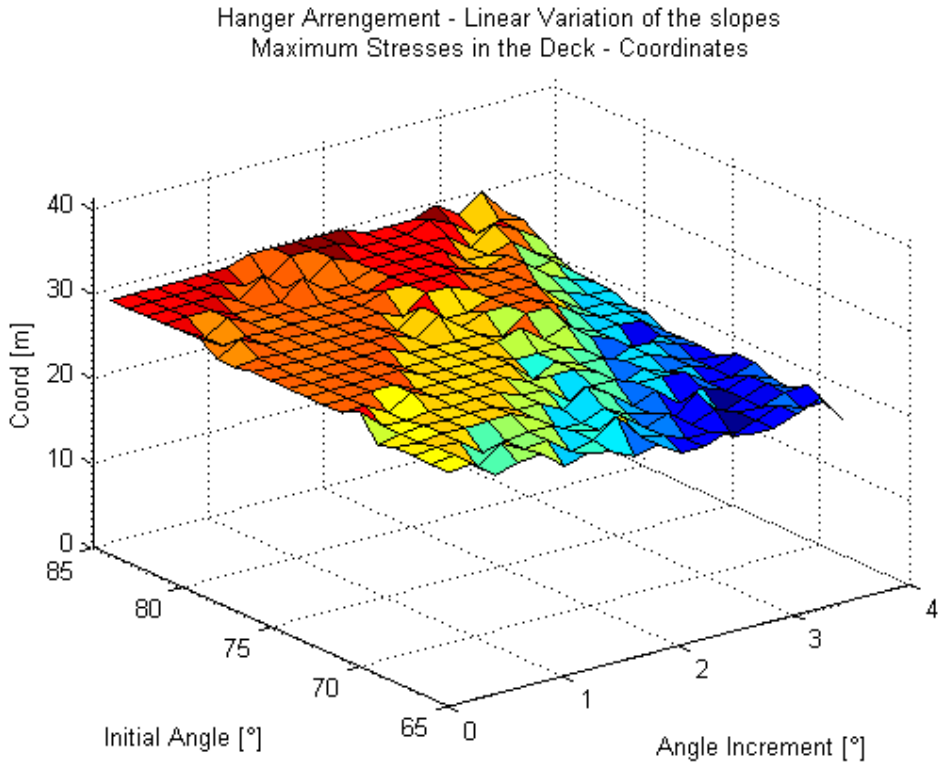


**Figure 45.** Corresponding X-coordinate for the maximum stresses in the deck (Linear variation of the slopes)

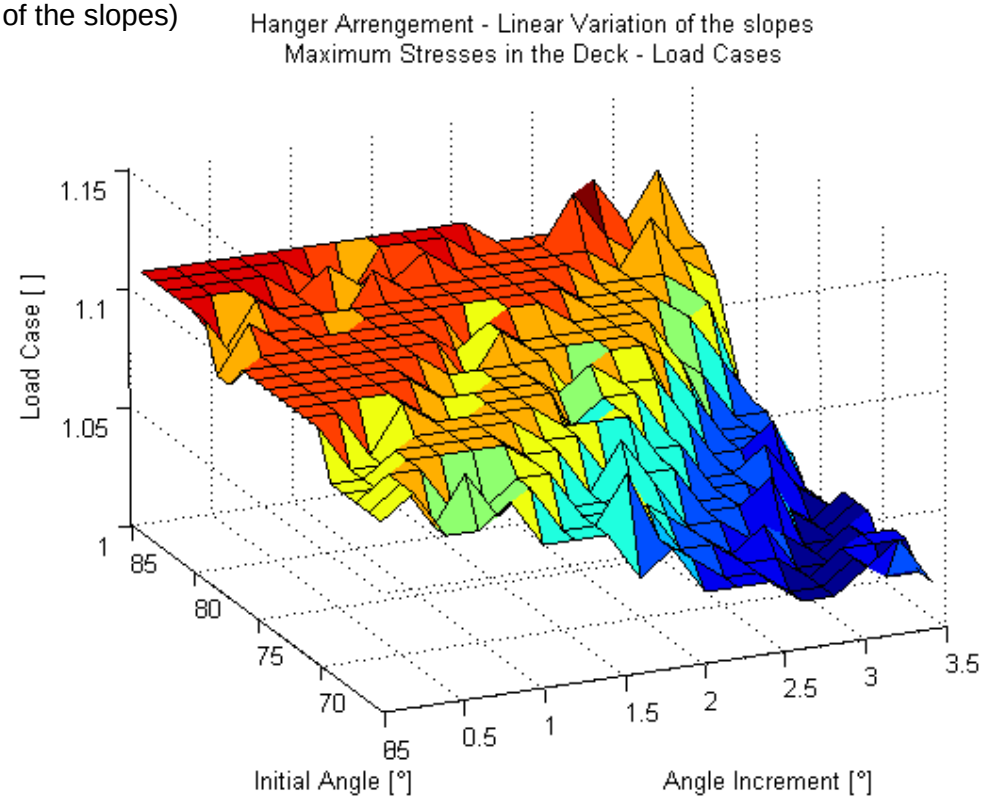


**Figure 46.** Corresponding load cases for the maximum stresses in the deck (Linear variation of the slopes)

### 3.1.1.1.4. Bending moments in the arch

The Figure 44 shows the absolute values for maximum bending moments in the arch for each bridge. The highest value presents for a bridge with $\varphi_0$= 84°- $\Delta\varphi$ = 0.0°. This configuration is shown in the Figure 36. The stresses decrease as the initial angle decreases and as the angle increment increases, until a minimum value for a bridge with $\varphi_0$= 70°- $\Delta\varphi$ = 3.2°.

In the bridge of the Figure 36 the hangers intersect each other only once. For this reason the bridge is not a network arch bridge. The value of the maximum bending moment in the arch for this configuration is 197.89 kNm.

The arrangement of the Figure 37 corresponds to a bridge with $\varphi_0$= 70°- $\Delta\varphi$ = 3.2°. The hangers intersect each other at least two times, fullfilling the condition for the network arch bridges [TNA]. The bridge has the structural behavior of several trusses on top of another. For this reason, the stress in the deck is significatly reduce. The value of the maximum stress in the deck for this configuration is 75.28 kNm: 38% of the value for the arrangement of the Figure 36..

The Figure 48 shows in a graphical format the X-coordinates where the maximum values occur. The maximum bending moments occur mostly 9.0 m from the left support (22% of the span), except for small initial angles and high angle increments, in which the corresponding coordinates approache the right support.

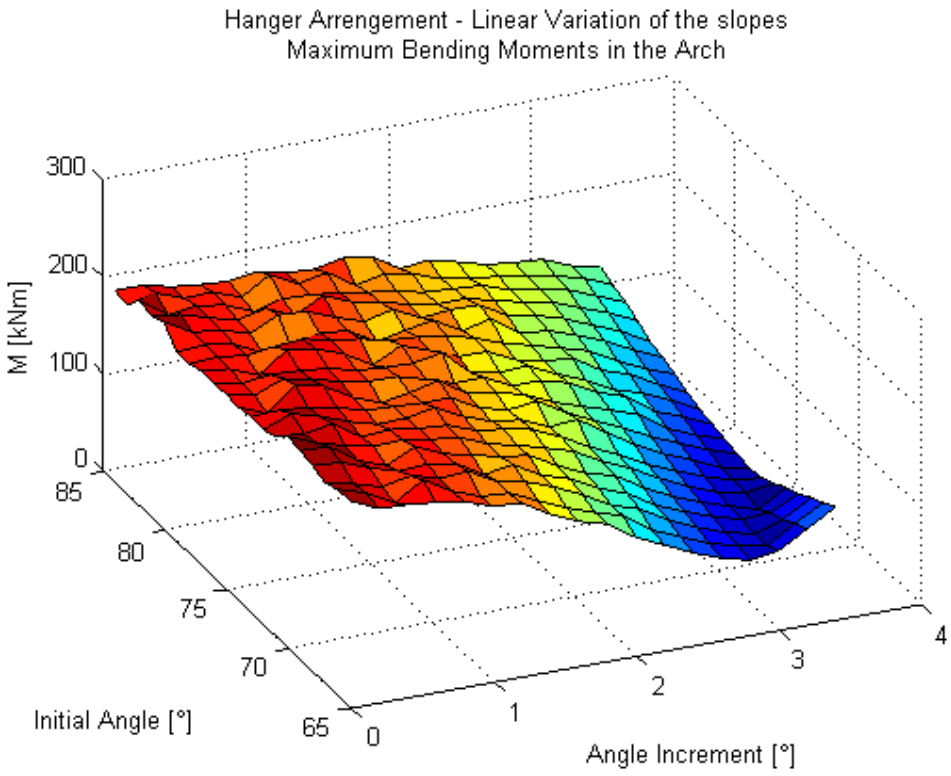


**Figure 47.** Maximum bending moments in the arch (Linear variation of the slopes)

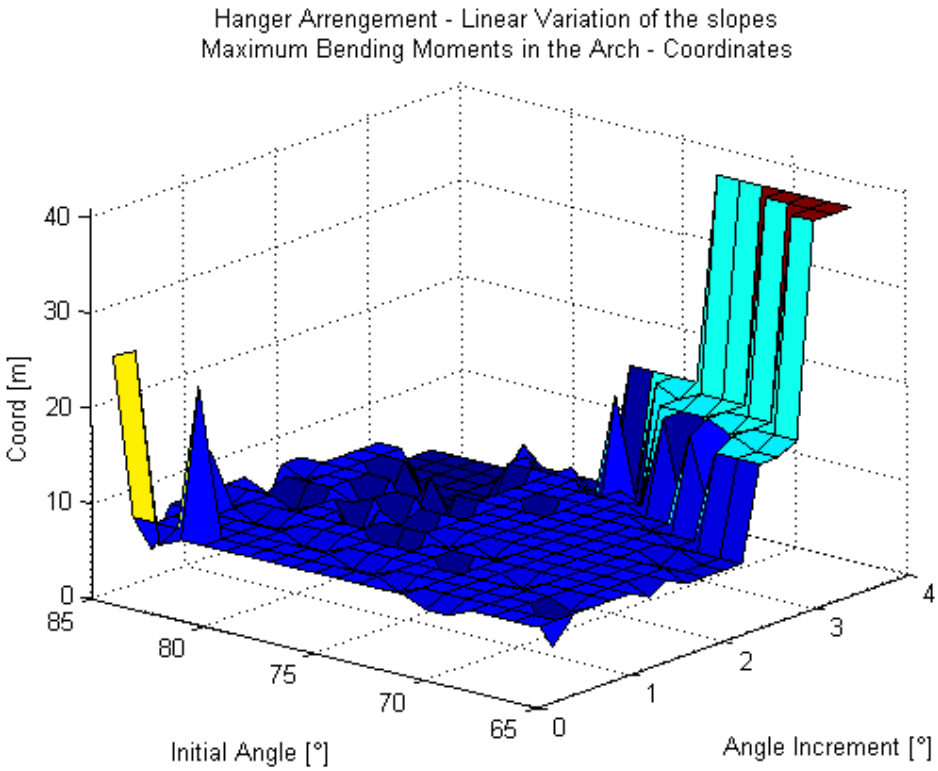


**Figure 48.** Corresponding X-coordinate for the maximum bending moments in the arch (Linear variation of the slopes)

### 3.1.1.1.5. Axial forces in the arch

The Figure 49 shows the values for maximum axial compression forces in the arch for each bridge. The highest compression force presents for a bridge with $\varphi_0$= 65°- $\Delta\varphi$ = 3.4°. This configuration is shown in the Figure 41. The values decrease as the initial angle increases and as the angle increment decreases, until a minimum value for a bridge with $\varphi_0$= 84°- $\Delta\varphi$ = 0.0°. This configuration is shown in the Figure 36.

In the arrengement of the Figure 41 the hangers intersect each other at least two times, fullfilling the condition for the network arch bridges [TNA]. The bridge has the structural behavior of several trusses on top of another. The value of the maximum compression force in the arch for this configuration is -4001.34 kN.

The bridge of the Figure 36 is not a network arch bridge, as the hangers intersect each other only once. The value of the maximum compression force in the arch for this configuration is -3285.81 kN: 82% of the value for the arrengement of the Figure 41.

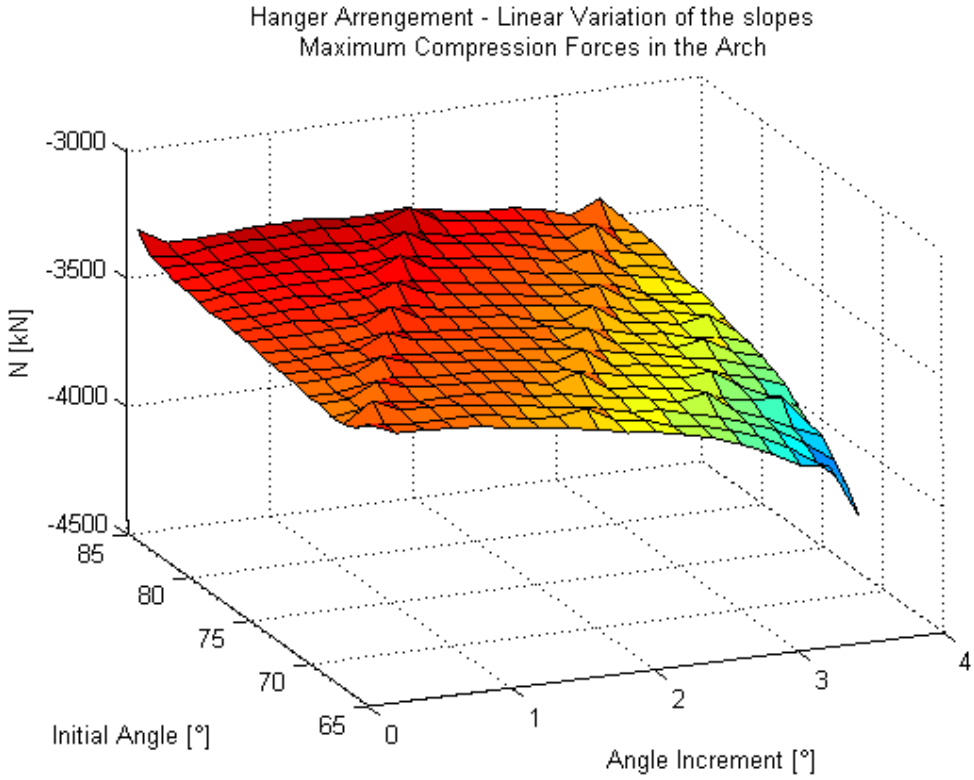


**Figure 49.** Maximum axial compression forces in the arch (Linear variation of the slopes)

The Figure 50 shows in a graphical format the X-coordinate where the maximum values occur. For high initial angles and small angle increments the maximum compression force is located in the right extreme of the arch. As the initial angle decrease and the angle increment increase, the location of the maximum value approximates the center of the span.

The Figure 51 shows the load cases for which the maximum values occur. In the Figure it can be seen a “central peak”. In the points with $\varphi_0$= 84°- $\Delta\varphi$ = 0.0°and $\varphi_0$= 65°- $\Delta\varphi$ = 3.4°the load case where the maximum value occurs is around 1.01, with the puntual load in the center of the span. As the variables approach the “central peak”, the corresponding load case approximates 1.10, with the puntual load located 30.0 m from the left support: 75% of the span.

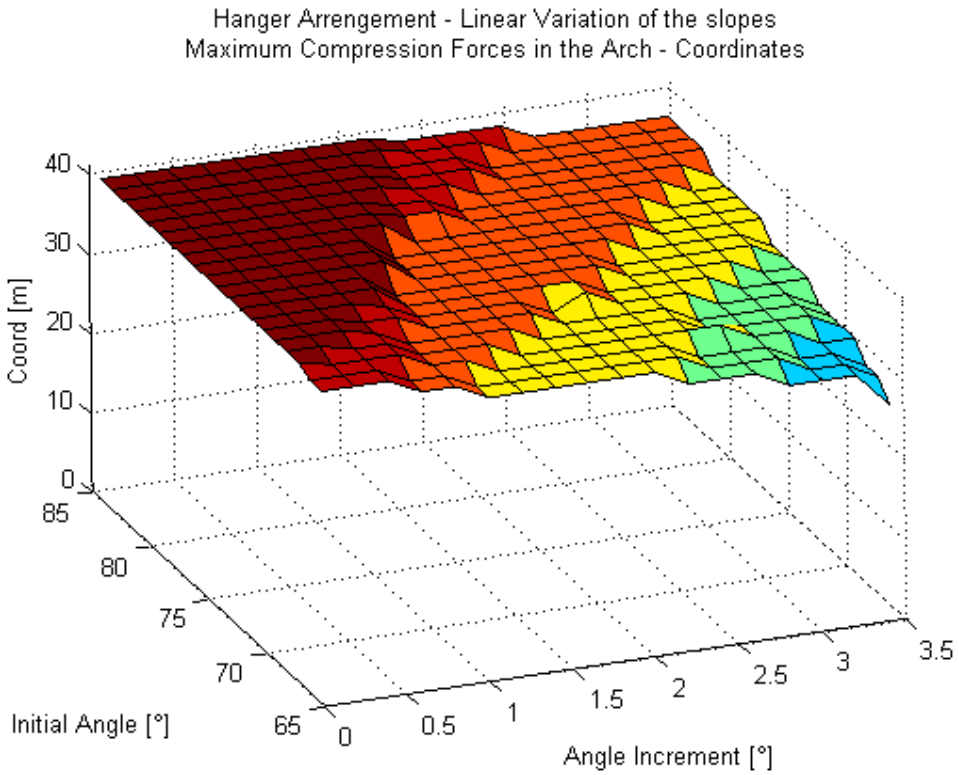


**Figure 50**. Corresponding X-coordinate for the maximum axial compression forces in the arch (Linear variation of the slopes)

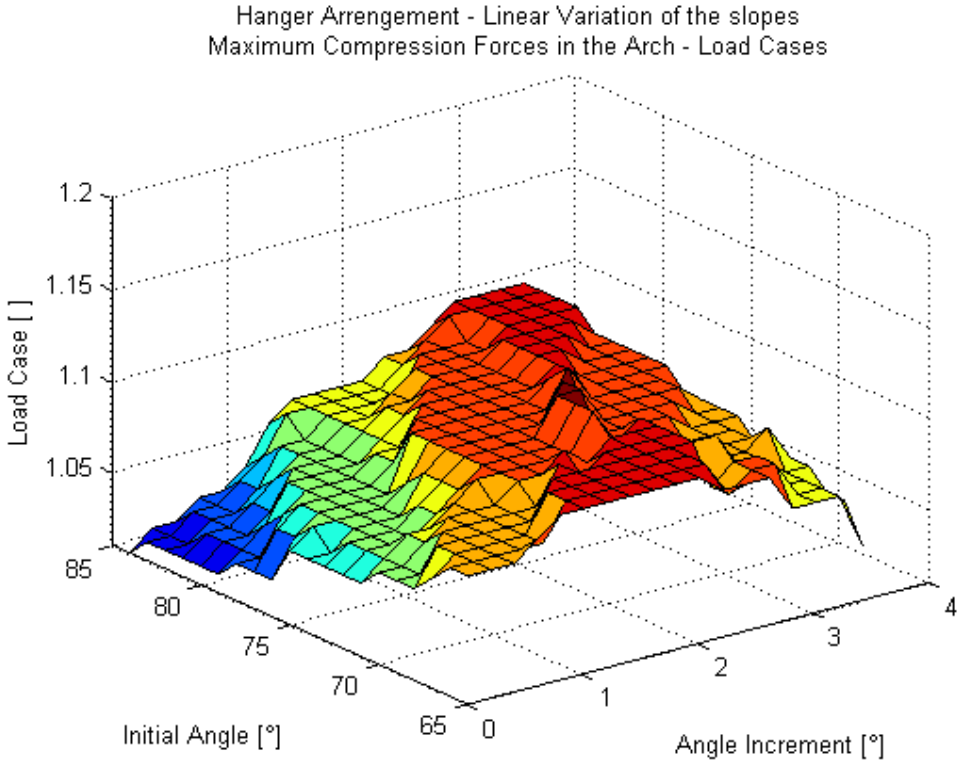


**Figure 51**. Corresponding load cases for the maximum axial compression forces in the arch (Linear variation of the slopes)

### 3.1.1.1.6. Stresses in the arch

The Figure 52 shows the values for maximum negative stresses in the arch for each bridge. The highest value presents for a bridge with $\varphi_0$= 70° - $\Delta\varphi$ = 0.0°. This configuration is shown in the Figure 53. The negative stress decrease as the initial angle decreases and as the angle increment increases, until a minimum value for a bridge with $\varphi_0$= 73° - $\Delta\varphi$ = 3.0°. This configuration is shown in the Figure 54.

In the arrangement of the Figure 53, the hangers intersect each other two times, fullfilling the condition for the network arch bridges [TNA]. The bridge has the structural behavior of two trusses on top of another. The value of the maximum negative stress in the arch for this configuration is -189623.73 kN/m$^2$.

In the arrangement of the Figure 54, the hangers intersect each other more than two times, fullfilling the condition for the network arch bridges [TNA]. The bridge has the structural behavior of six trusses on top of another. The value of the maximum negative stress in the arch for this configuration is -140129.41 kN/m$^2$, of 74% the value for configuration in the Figure 53.

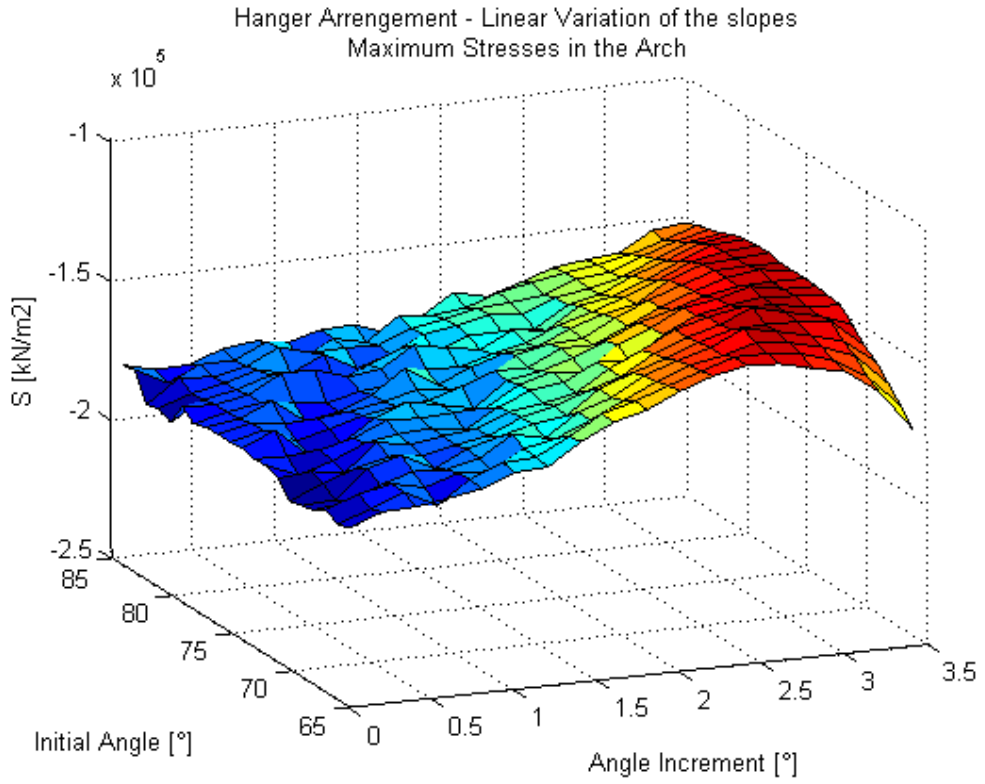


**Figure 52.** Maximum stresses in the arch (Linear variation of the slopes)

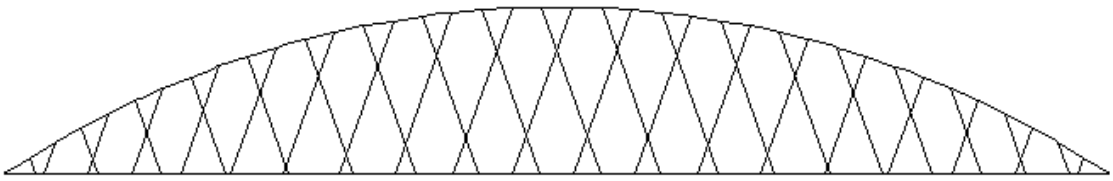

**Figure 53.** Hanger arrangement for $\varphi_0$= 70° - $\Delta\varphi$ = 0.0°

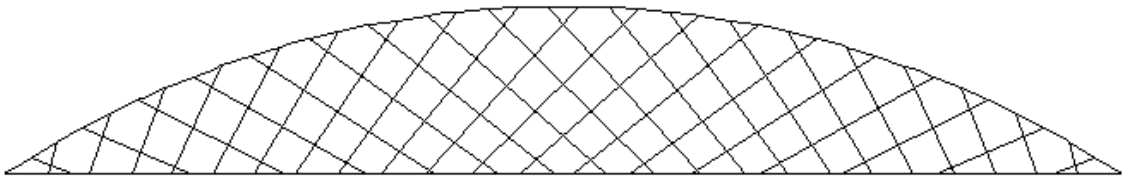

**Figure 54.** Hanger arrangement for $\varphi_0$= 73° - $\Delta\varphi$ = 3.0°

The Figure 55 shows in a graphical format the X-coordinate where the maximum value occur. For values of $\Delta\varphi$ less than 2.8°, the maximum values occur near the left support. For angle increments bigger than 3.0°, the corresponding elements are located next to the right support.

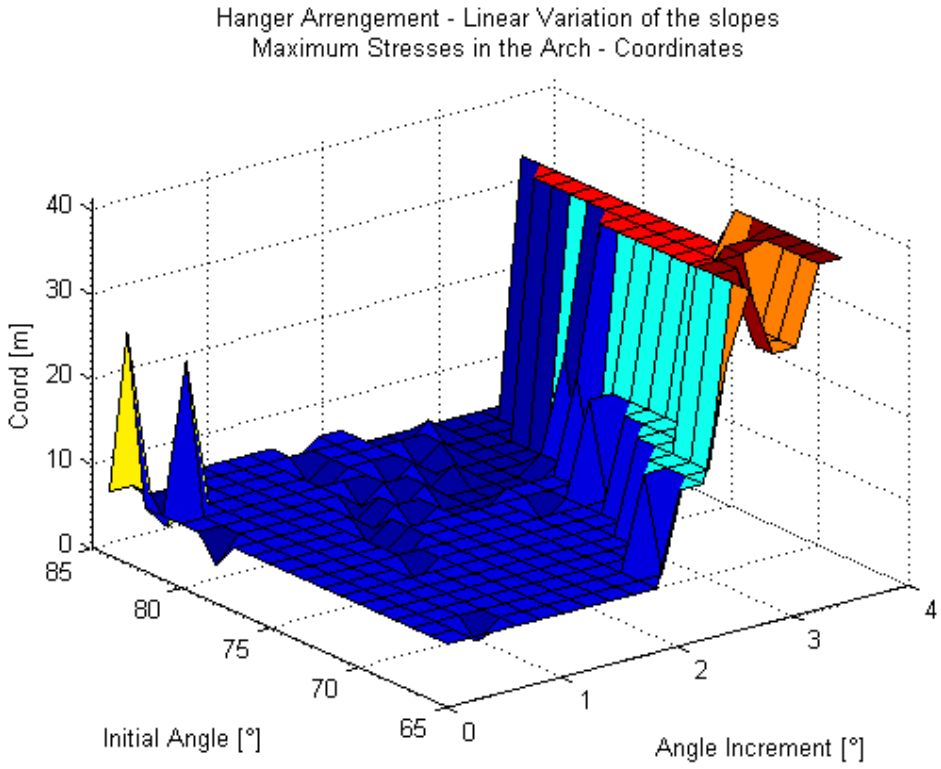


**Figure 55**. Corresponding X-coordinate for the maximum stresses in the arch (Linear variation of the slopes)

### 3.1.1.1.7. Stresses in the hangers

The Figure 56 shows the values for maximum stresses in the hangers for each bridge.The highest value presents for a bridge with $\varphi_0$= 65°- $\Delta\varphi$ = 3.4°. This configuration is shown in the Figure 41. The values decrease as the initial angle increases and as the angle increment decreases, until a minimum value for a bridge with $\varphi_0$= 84°- $\Delta\varphi$ = 0.0°. This configuration is shown in the Figure 36.

In the arrengement of the Figure 41 the hangers intersect each other at least two times, fullfilling the condition for the network arch bridges [TNA]. The bridge has the structural behavior of several trusses on top of another. The value of the maximum stress in the hangers for this configuration is 176697.25 kN/m$^2$.

The bridge of the Figure 36 is not a network arch bridge, as the hangers intersect each other only once. The value of the maximum stress in the hangers for this configuration is 106608.15 kN/m$^2$: 60% of the value for the configuration in the Figure 53.

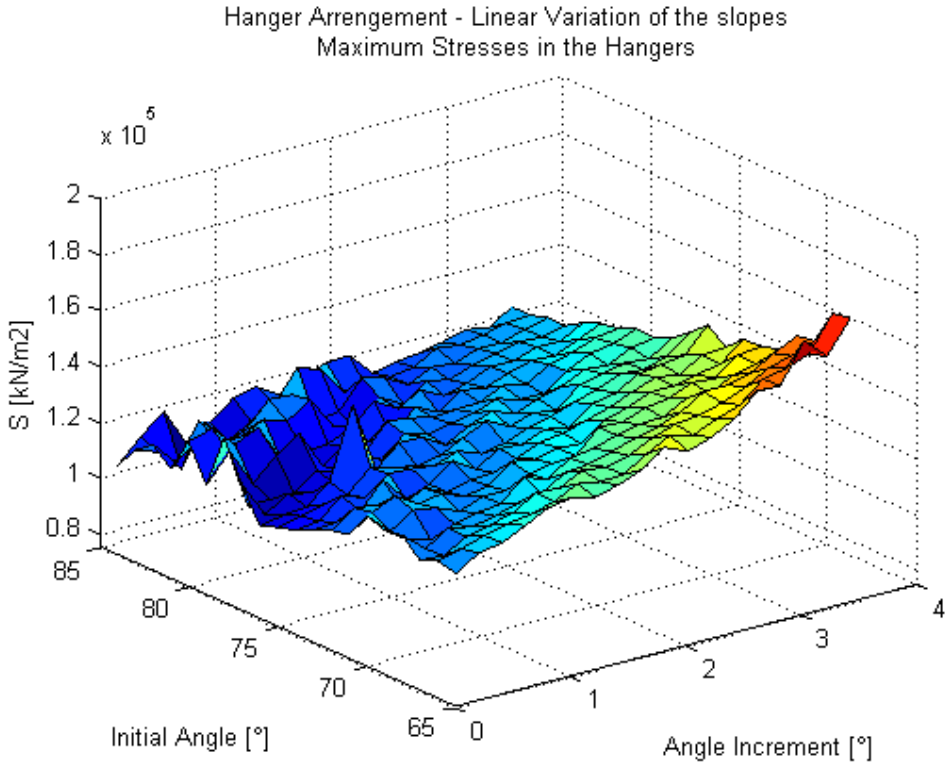


**Figure 56.** Maximum stresses in the hangers (Linear variation of the slopes)

### 3.1.1.1.8. Relaxed hangers

The Figure 57 shows the number of relaxed hangers for each bridge. The prestressing of the hangers was not considered. In the Figure, it can be noticed an area where there are no relaxed hangers. For values of the initial angle smaller than 73° and angle increments smaller than 2.2°, the structure presents relaxed hangers.

The relaxed hangers are located in the extremes of the bridge, next to the supports.

The relaxed hangers are:

- One relaxed hanger: 3001
- Two relaxed hangers: 3001; 3038

The elements 3001 is the first hanger of the Set 1. The element 3038 is the last hanger of the Set 2.

The Figure 58 shows a hanger arrangement with $\varphi_0$= 65° - $\Delta\varphi$ = 0.0°. This configuration presents two relaxed hangers in the extremes. A configuration with no relaxed hangers is shown in the Figure 41, with $\varphi_0$= 65° - $\Delta\varphi$ = 3.4°.

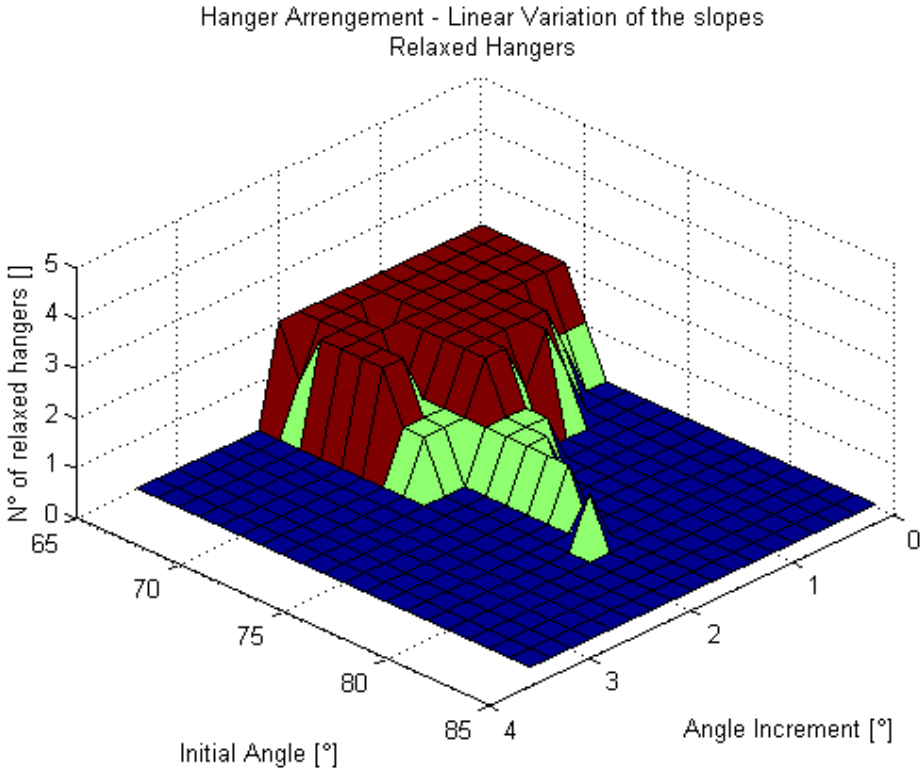


**Figure 57.** Number of relaxed hangers (Linear variation of the slopes)

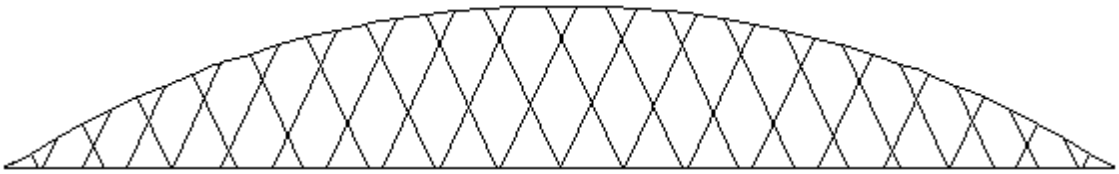

**Figure 58.** Hanger arrangement for $\varphi_0$= 65°- $\Delta\varphi$ = 0.0°

### 3.1.1.2. Conclusions

The Figure 59 shows the number of times the hangers intersect each other in each bridge. The bridge behaves as a network arch bridge if the number of intersections is at least two.

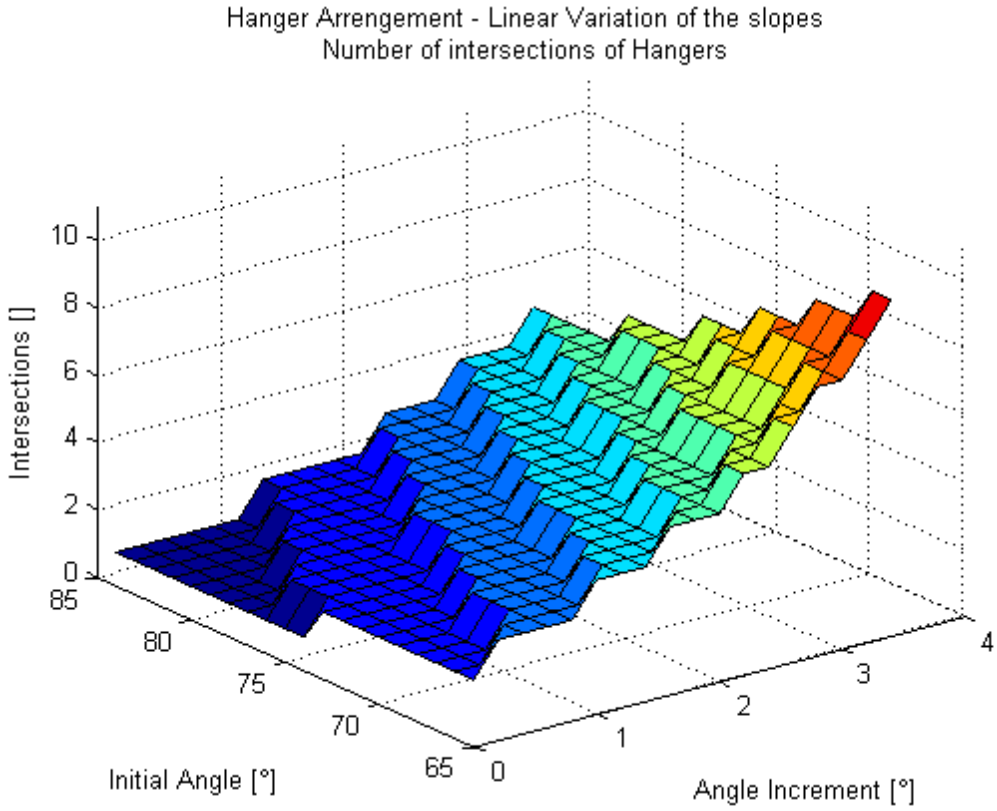


**Figure 59.** Number of times the hangers intersect each other in each bridge

For small angle increments and big initial angles, the numer of intersections is equal to 1, hence the corresponding bridges are not network arch. As the angle increment increases and the initial angle decreases, the number of intersections increase.

If in a structure the hangers intersect each other two times, the bridge have the structural behavior of two trusses on top of another, giving less bending in the arch and the deck. This effect

will be greater if the hangers intersect several times, as the structural behavior corresponds to several trusses on top of another. Hence, as the numer of intersections increases ,the bending moments in the arch and deck decreases.

The bending moments in the deck correspond to those in the arch, and in both cases the highest values occur in the bridges that do not behave like network arch bridges. The lowest values are obtained for small initial angles and big angle increments, which corresponds to the bridges in which the hangers intersect each other several times. The reduction is important: 40% of the highest values in both cases.

The axial forces in the deck also correspond to the axial forces in the arch. In this case the lowest values are obtained for the hanger arrangement with $\varphi_0$= 84° - $\Delta\varphi$ = 0.0°, that do not behaves as network arch bridges. However, in the graphics for the deck and the arch it can be observed that the maximum and the minimum values are only isolated peaks. Outside this two values, the variation of the axial forces is not important. As an example two points are taken. In the deck, for a hanger arrangement with $\varphi_0$= 70 - $\Delta\varphi$ = 2.8°, the axial force is 3015.80 kN. For an hanger arrangement with $\varphi_0$= 80 - $\Delta\varphi$ = 1.0°, the axial force is 2967.14 kN : the reduct ion is of only 2%. The same occur for the arch.

From this we can say that the hanger arrangement has an important influence on the values of the bending moments in the deck and arch, while the variation in the axial forces due to the arrangement it is not significant.

Hence, it is expectable that the form of the graphic for maximum stresses in the arch and in the deck corresponds to the one obtained for the moments. The lowest values are obtained for small initial angles and big increment angles, which corresponds to bridges in which the hangers intersect each other several times.

The maximum stresses in the hangers are obtained for the bridges in which the hangers intersect each other several times. As the number of intersections decreases, the stresses decrease. For a number of intersections inferior to 3 the increment is not significant, less than 5%. However, for a higher number of intersections the stresses in the hangers increase very fast, arriving to an increment of 36% for 6 intersections and 61% for 10 intersections.

In the arch and the hangers the stresses are lower than the admissible values. The fact that the stresses in the deck are higher than the admissible values remarks the importance of the prestressing of the deck. As the prestressing was not considered in this thesis, it was expected than the admissible stress are exceeded.

According to the Figure 57, the relaxation of the hangers occur for small initial angles and small angle increments.

The Figure 41 and 58 show configurations with $\varphi_0$= 65° - $\Delta\varphi$ = 3.4° and $\varphi_0$= 65° - $\Delta\varphi$ = 0.0° respectively. While the first case presents no relaxation, the second case presents two relaxed hangers. The configuration of Figure 58 shows steeper hangers than in the case of Figure 41, which leads to more relaxed hangers. This confirms what can be found in [TNA] : "Too steep hangers lead to too much relaxation of hangers".

Also steeper hangers lead to bigger bending moments and deflections. The Figures 60 and 61 show the deformation for the load case 1.01 with $\varphi_0$= 65° - $\Delta\varphi$ = 0.0° and $\varphi_0$= 65° - $\Delta\varphi$ = 3.4° respectively. In the first Figure the arch move to the left, increasing deflection and bending moments, with the presence of relaxed hangers in the extremes. On the other hand the deformation for the second configuration shows a better distribution of the forces, with smaller deflections and no relaxed hangers.

Therefore, while small initial angles and high angle increments results in low stresses in arch and deck but important stresses in the hangers, high initial angles and small angle increments results in low stresses in the hangers but important stresses in arch and deck. Moreover, small initial angles and small angle increments cause relaxed hangers. Hence, a hanger arrangements with high initial angles and high angle increments provides the best results.

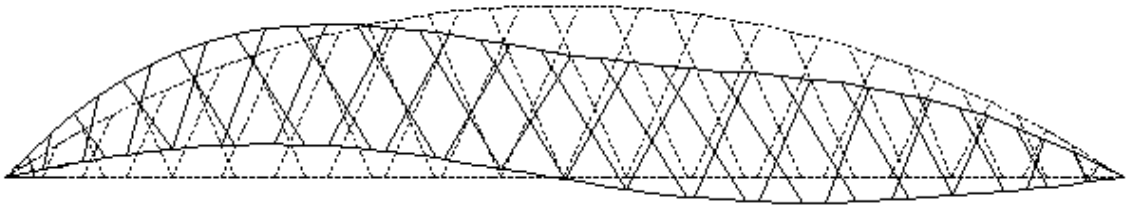

**Figure 60.** Deformations for hanger arrangements with $\varphi_0$= 65° - $\Delta\varphi$ = 0.0°

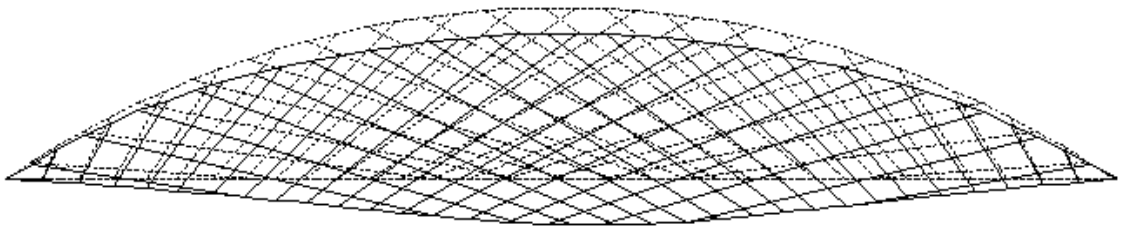

**Figure 61.** Deformations for hanger arrangements with $\varphi_0$= 65° - $\Delta\varphi$ = 3.4°

### 3.1.2. Radial arrangement

Brunn and Schanack proposed this arrangement in their diploma thesis [BSC].

The loads are distributed uniformly acting in the radial direction of the arch. This decreases the bending moments in an arch with circular shape. Also the axial forces in the hangers result smaller.

If all the hangers have the same axial force, it could be considered that the resulting forces of the hangers are directed along the connecting lines of their intersections, as shown in the Figure 62.

However, due to the presence of moving loads, the axial forces in the hangers are not the same. Nonetheless, this still could be considered as a good approximation.

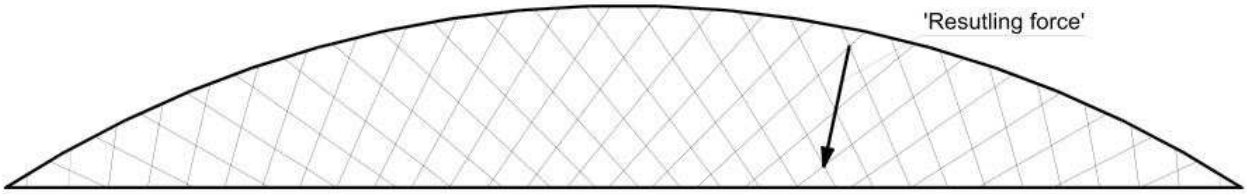


**Figure 62.** Radial arrangement [BSC]

The upper nodes of the hangers are placed equidistantly along the arch [TNA]. The variable for this arrangement is the angle with which the hangers cross each other. For this study, the variable adopted is the angle between radius and hanger at the first crossing of the hangers below the arch, as shown in the Figure 63.

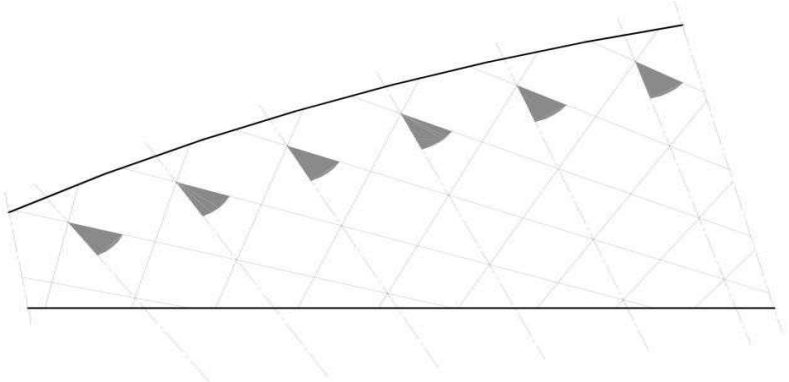

**Figure 63.** Radial arrangement. The adopted variable is the angle marked as grey [BSC]

For the present study 115 bridges are calculated, with a cross angle from 0° to 57°. The study is done for a circular arch shape. The number of element for the hangers is assigned as shown in the Figure C.2 in the Appendix C.

### 3.1.2.1. Results

The results are shown in the following diagrams. Every ordinate corresponds to one value of each bridge.

#### 3.1.2.1.1. Bending moments in the deck

The Figure 64 shows the absolute values for maximum bending moments in the deck for each bridge. If we see the Figure, we notice that the values decrease from a cross angle equal to 0° until a minimum between 40° and 50°. From 50° to 57° the bending moments increase significatly.

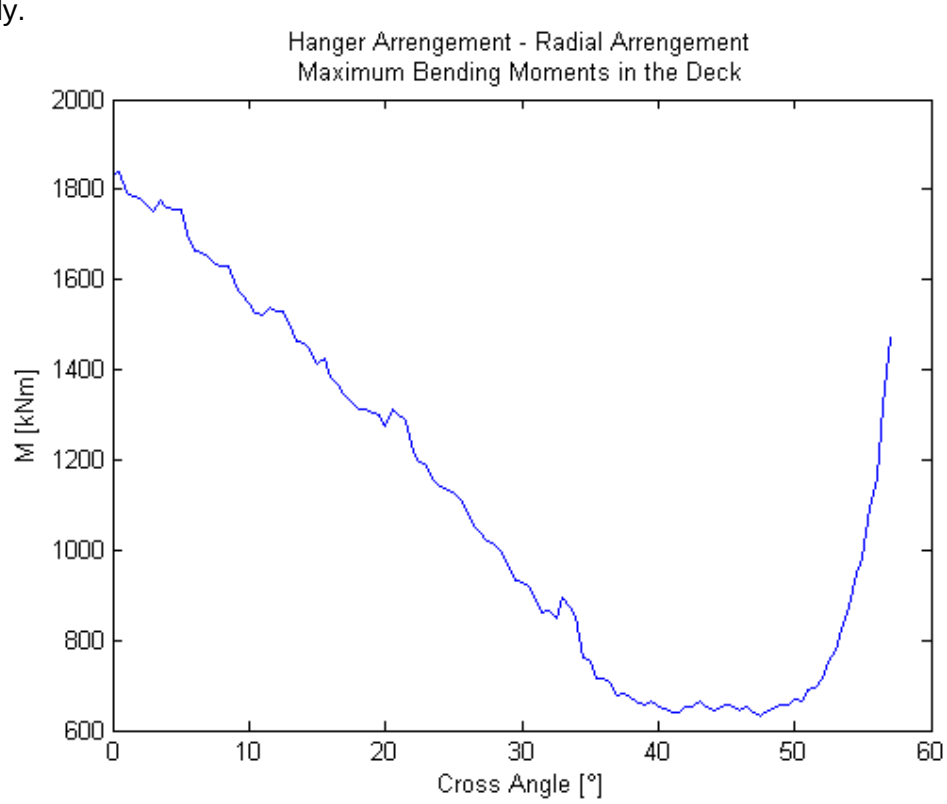


**Figure 64.** Maximum bending moments in the deck (Radial arrangement)

The Figure 65 shows an arrangement with a cross angle equal to 45° that corresponds to the minimum bending moments.

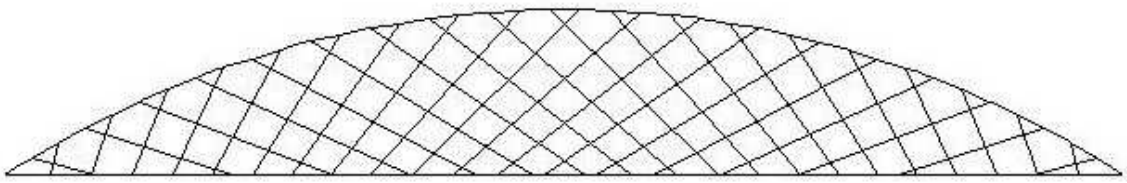

**Figure 65.** Radial arrangement. Cross angle = 45°

In the arrangement of Figure 65 the hangers intersect each other several times. This fulfill the condition for the network arch bridges. For this reason the bending moments in the deck are significantly reduce. The maximum bending moment for this arrangement is 656.50 kNm. That is 36% of the value for the "spoked wheel arrangement" with the cross angle equal to 0°: 1836.17 kNm and in the same order of the best value for the arrangements with linear variation of the slopes: 653.70 kNm.

The Figure 66 shows in a graphical format the X-coordinates where the maximum values occur. For cross angles smaller than 30° the corres ponding element is between 30.0 m and 33.0 m from the left support that is between 73% and 80% of the span. As the cross angle is increased, the maximum value presents closer to the center of the span. For a cross angle equal to 55° the maximum value occurs 21.48 m from the left support (52% of the span).

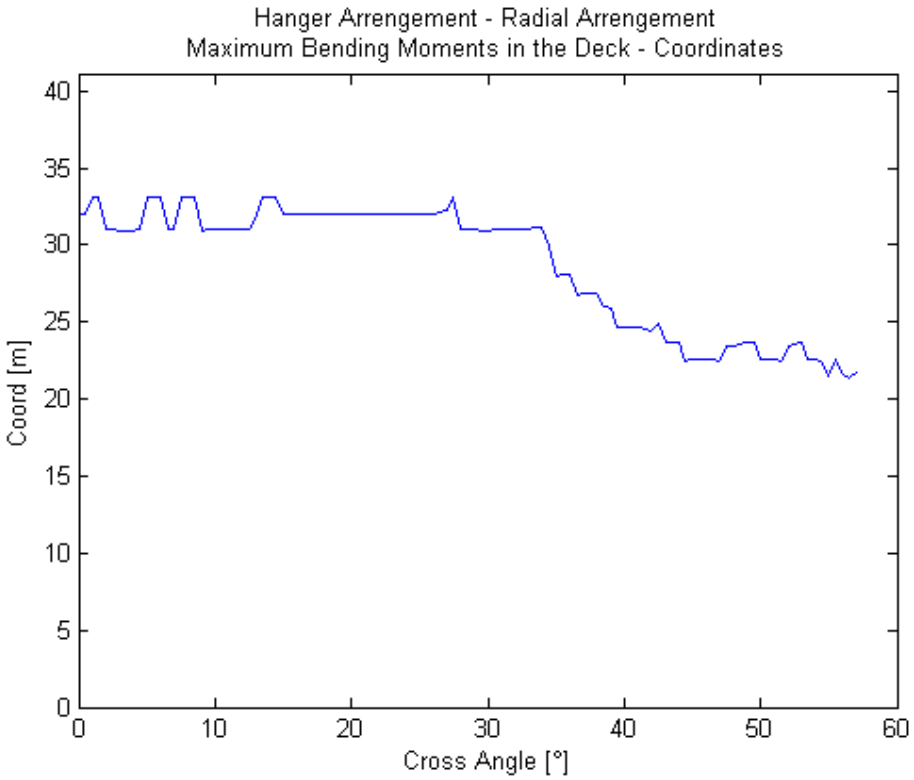


**Figure 66.** Corresponding X-coordinates for the maximum bending moments in the deck (Radial arrangement)

The Figure 67 shows the load cases for which the maximum values occur. If the cross angle is smaller than 34° the corresponding load ca se approaches 1.13, with the punctual load located 34.0 m from the left support: 83% of the span. For cross angles bigger than 45° the corresponding load case approximates 1.02, with the punctual load situated near the center of the span.

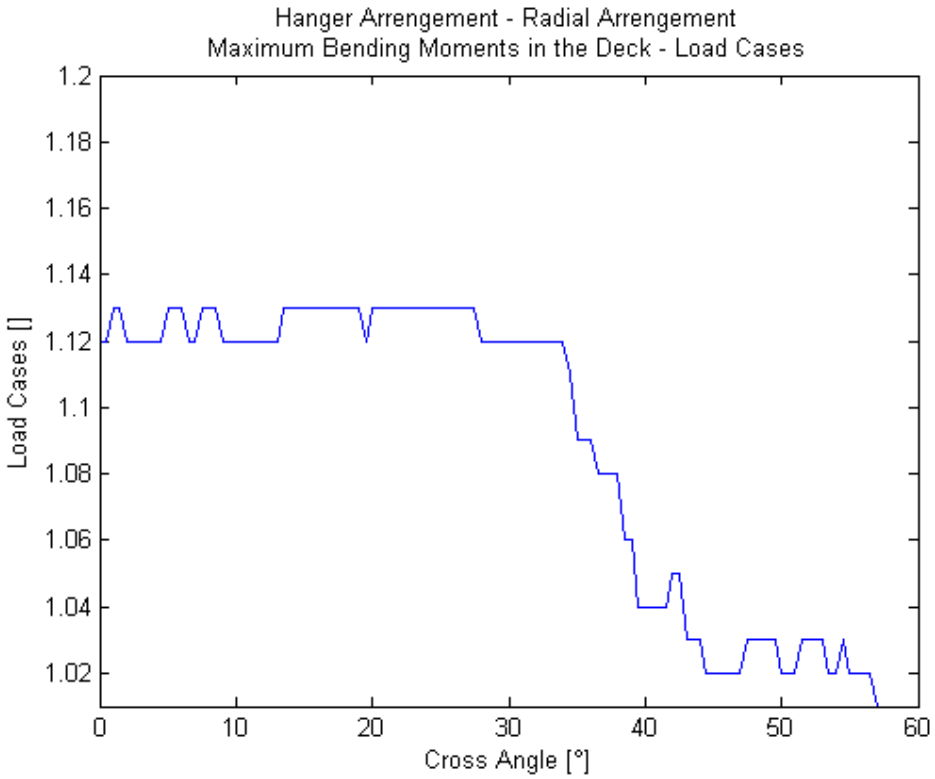


**Figure 67.** Corresponding load cases for the maximum bending moments in the deck (Radial arrangement)

#### 3.1.2.1.2. Axial Forces in the deck

The Figure 68 shows the values for maximum axial forces in the deck for each bridge. The lowest values appear as the arrangement approaches to a “spoked wheel” arrangement, that is when the cross angle is equal to 0°. As the cross a ngle increases, the maximum axial forces are higher. However, the variation is not important for cross angles smaller than 50°. For angles bigger than 50°the axial forces increase significantly.

The axial force for an arrangement with a cross angle equal to 0°is 2925.13 kN. For a cross angle equal to 50°the axial force is 3084.93 kN: 1.05 times the previous value.

For a cross angle equal to 57°the maximum axial fo rce is 3468.89 kN: 1.19 times the value for a cross angle equal to 0°.

The Figure 69 shows in a graphical format the X-coordinate where the maximum values occur. For small values of the cross angle the maximum values occur near the center of the span. As the cross angle is increased, the maximum value presents closer to the right support. For a cross angle equal to 55°the maximum value occurs n ext to the right support.

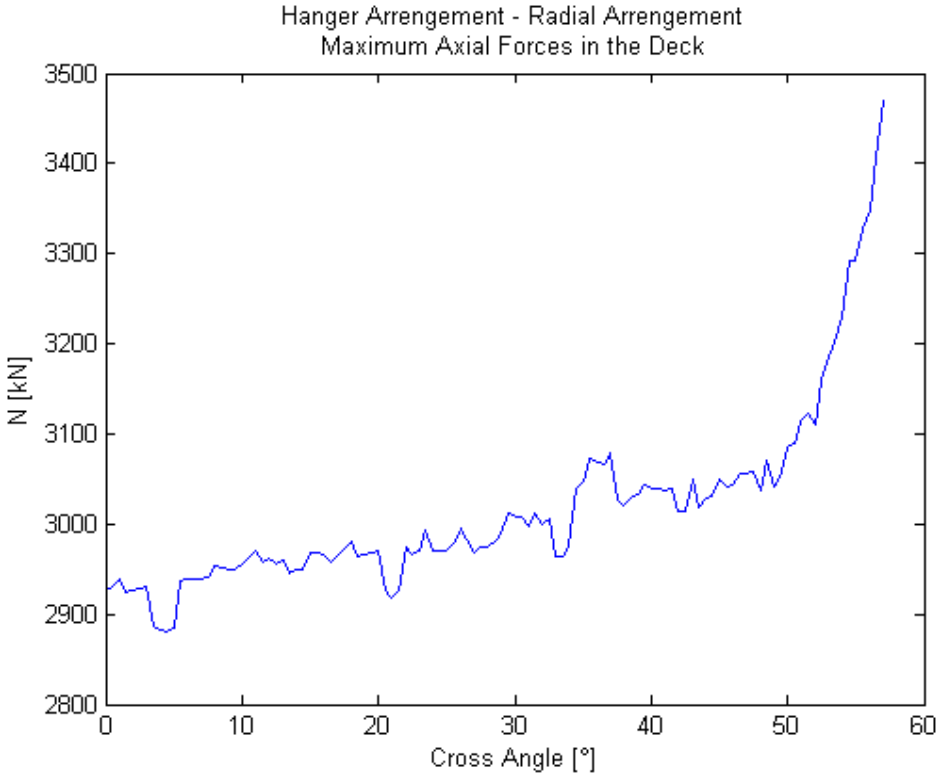


**Figure 68.** Maximum axial forces in the deck (Radial arrangement)

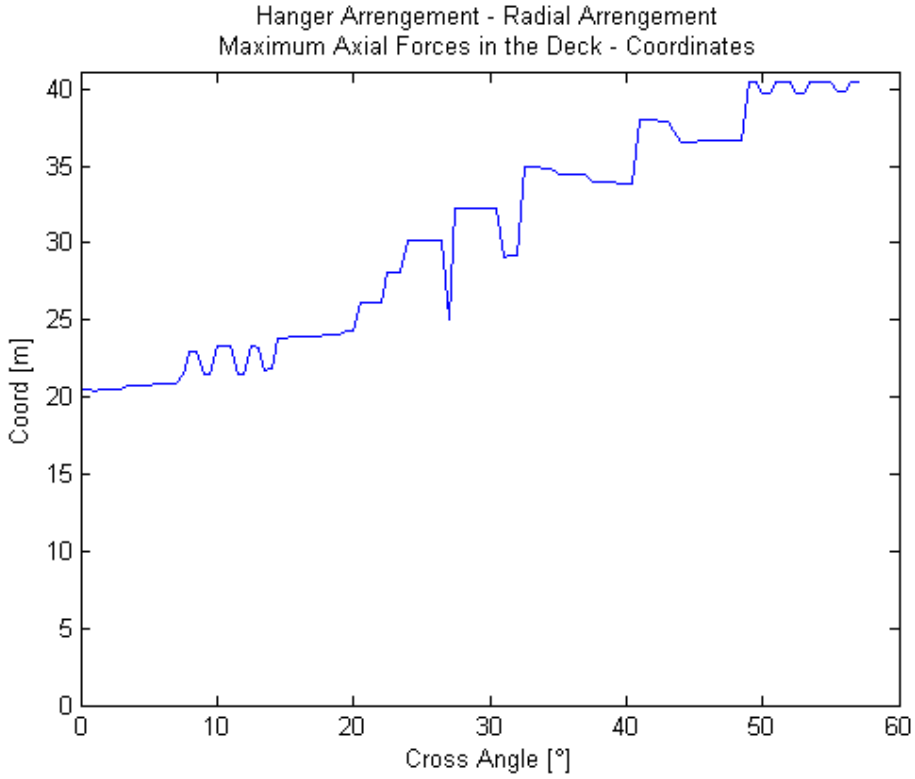


**Figure 69.** Corresponding X-coordinates for the maximum axial forces in the deck (Radial arrangement)

The Figure 70 shows the load cases for which the maximum values occur. When the cross angle is small the corresponding load case is around 1.01, with the punctual load near the center of the span. As the cross angle increases, the position of the punctual load that correspond to the maximum value approaches the right support. For a cross angle equal to 55° the maximum value occurs for the load case 1.13 that corresponds to the punctual load 6.00 m from the right support.

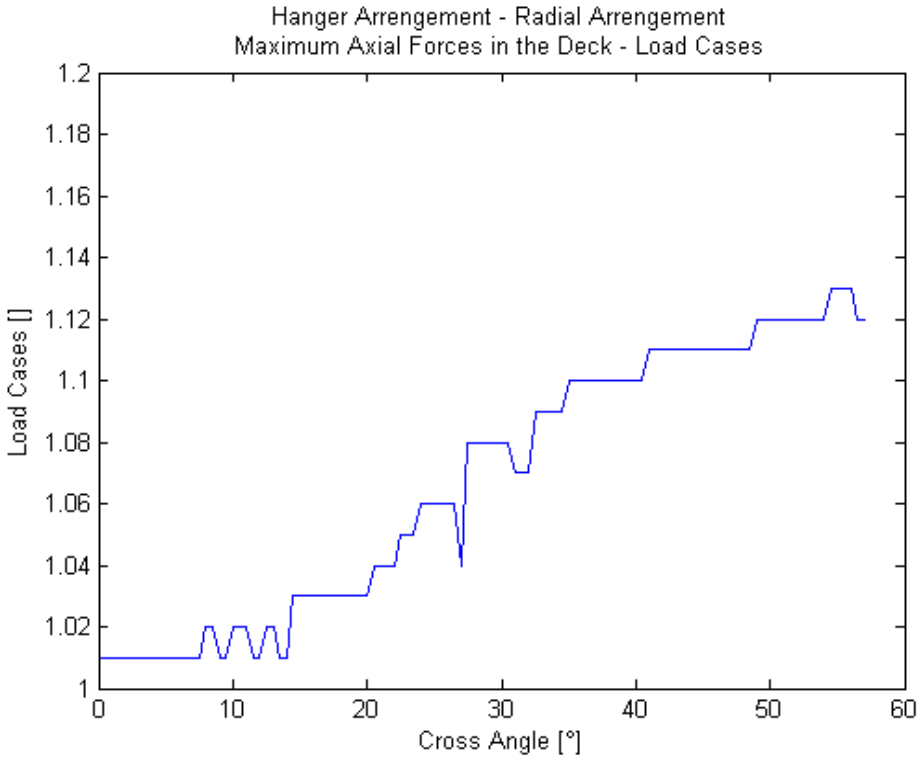


**Figure 70.** Corresponding load cases for the maximum axial forces in the deck (Radial arrangement)

### 3.1.2.1.3. Stresses in the deck

The Figure 71 shows the values for maximum stresses in the deck for each bridge. If we see the figure, we notice that values decrease from a cross angle equal to 0° until a minimum between 40° and 50°. From 50° to 57° the stresses i ncrease significantly.

The figure 65 shows an arrangement with a cross angle equal to 45° that corresponds to the minimum values for the stresses. In this arrangement the hangers intersect each other several times. This fulfill the condition for network arch bridges. For this reason the stress in the deck is significantly reduce. The value of the stress for this arrangement is 11520.15 kN/m$^{2.}$ That is 43% of the value for the "spoked wheel arrangement" with a cross angle equal to 0°: 26714.00 kN/m$^{2.}$ and it is in the same order of the best value for the arrangements with linear variation of the slopes: 11461.62 kN/m$^2$.

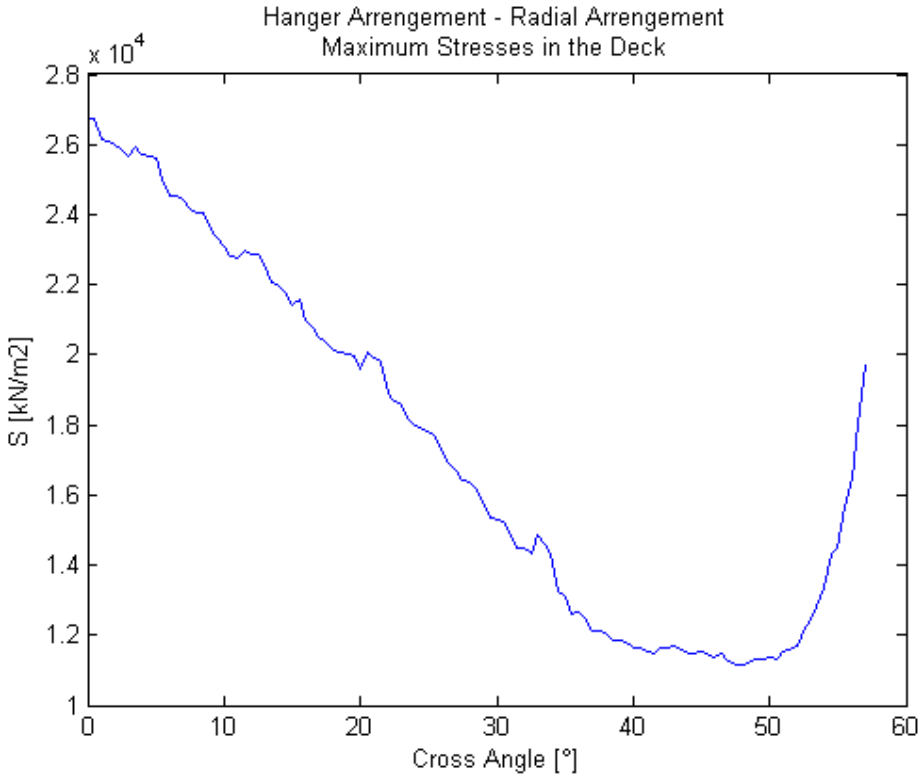


**Figure 71.** Maximum stresses in the deck (Radial arrangement)

The Figure 72 shows in a graphical format X-coordinate where the maximum values occur. For cross angles smaller than 30° the corresponding element is between 30.0 m and 33.0 m from the left support that is between 73% and 80% of the span. As the cross angle is increased, the maximum value presents closer to the center of the span. For a cross angle equal to 55° the maximum value occurs 21.48 m from the left support (52% of the span).

The Figure 73 shows the load cases for which the maximum values occur. If the cross angle is smaller than 34° the corresponding load ca se approximates 1.13, with the punctual load 34.00 m from the left support. For cross angles bigger than 40° the corresponding load case approaches 1.03, with the punctual load situated near the center of the span.

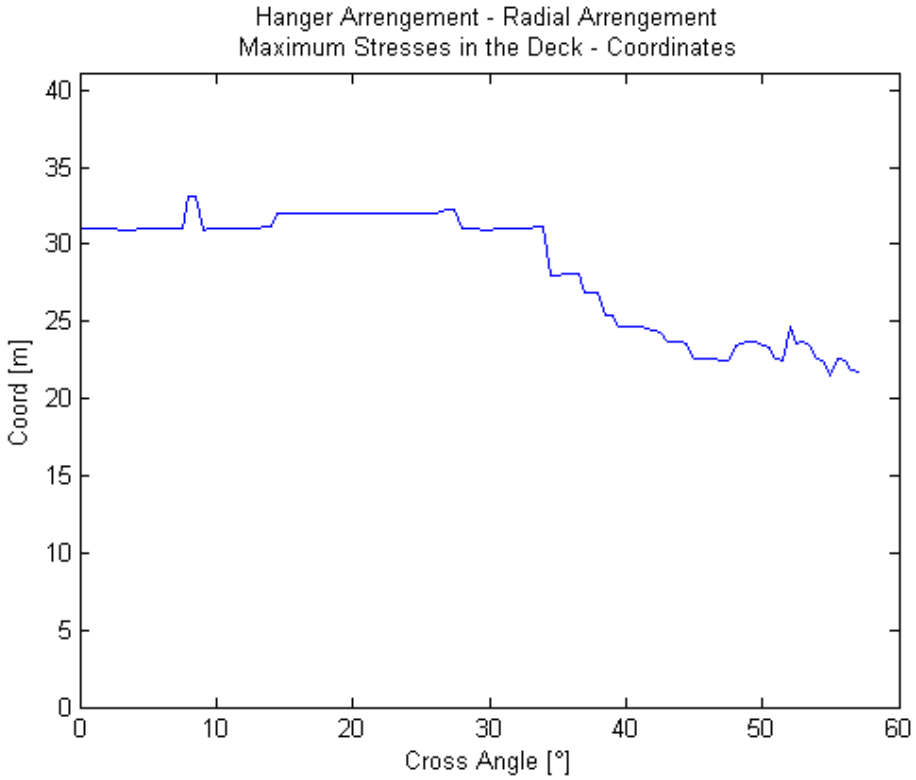


**Figure 72.** Corresponding X-coordinates for the maximum stresses in the deck (Radial arrangement)

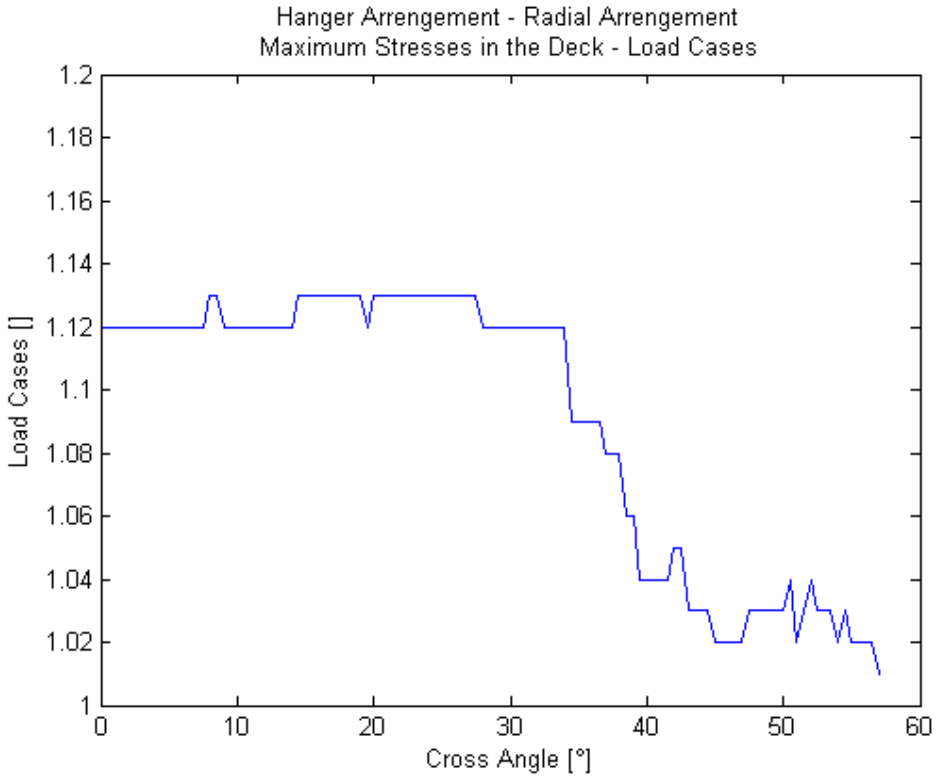


**Figure 73.** Corresponding load cases for the maximum stresses in the deck (Radial arrangement)

### 3.1.2.1.4. Bending moments in the arch

The Figure 74 shows the absolute values for maximum bending moments in the arch for each bridge. If we see the figure, we notice that the values decrease from a cross angle equal to 0° until a minimum between 45° and 50°. From 50° to 57° the bending moments increase.

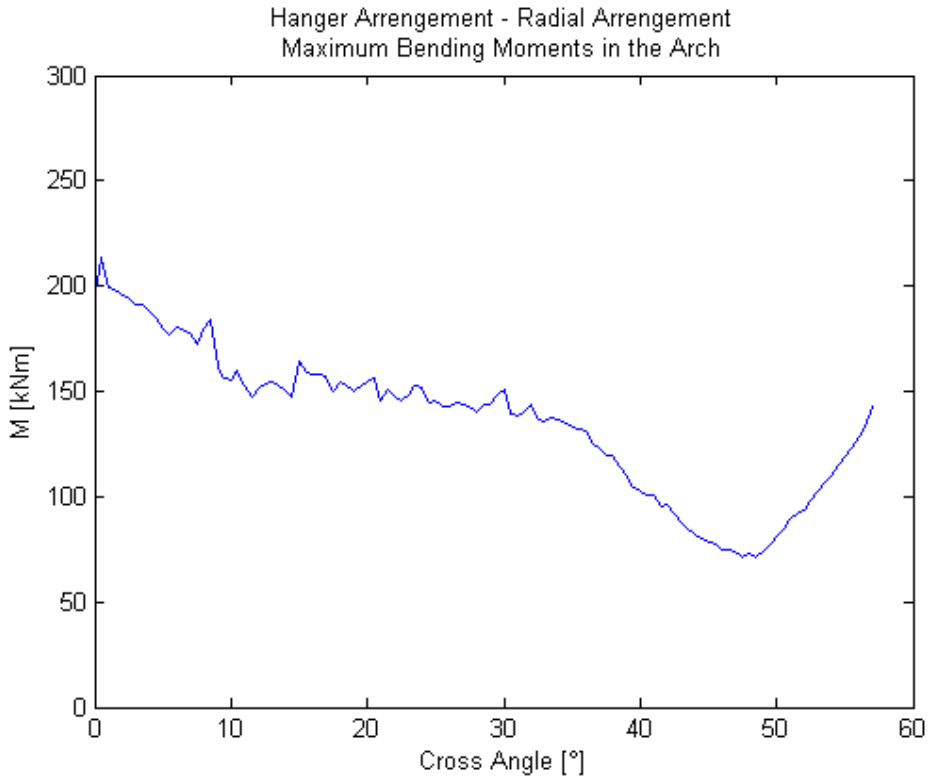


**Figure 74.** Maximum bending moments in the arch (Radial arrangement)

The figure 75 shows an arrangement with a cross angle equal to 47.5° that corresponds to the lowest values for the bending moments in the arch.

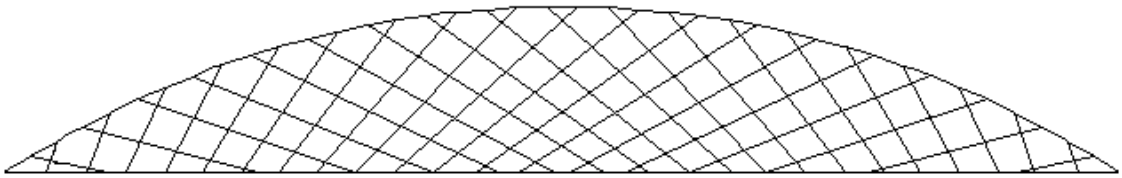

**Figure 75.** Radial arrangement. Cross angle = 47.5°

In the arrangement of Figure 75 the hangers intersect each other several times. This fulfill the condition the network arch bridges. For this reason the bending moments in the arch are significantly reduce. The value of the bending moment for this arrangement is 71.02 kNm. That is 37% of the value for the “spoked wheel arrangement” with the cross angle equal to 0°: 194.48 kNm and 95% of the best value for the arrangements with linear variation of the slopes: 75.28 kNm.

The figure 76 shows in a graphical format the X-coordinate where the maximum values occur. The maximum values occur less than 10.00 m from the left or right support. That is, between the 0% and 25% of the span or between the 75% and 100%. Exceptions are the hanger arrangements with cross angles between 42° and 50°.

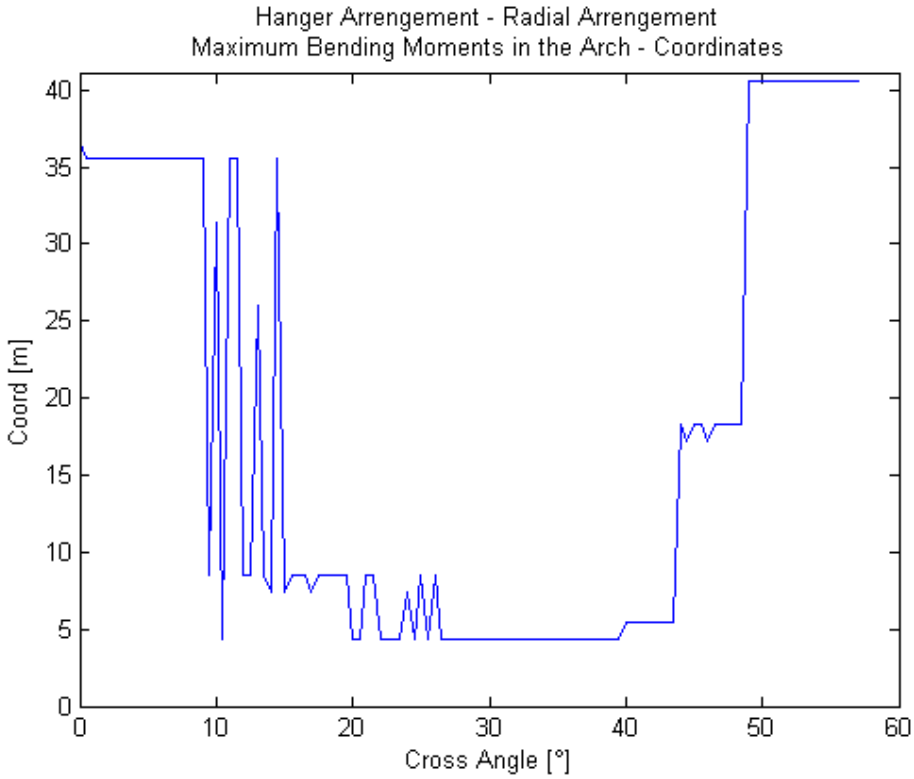


**Figure 76.** Corresponding X-coordinates for the maximum bending moments in the arch (Radial arrangement)

The Figure 77 shows in a graphical format the number of the load cases for which the maximum values occur. The maximum values occur mostly for the load cases between 1.04 and 1.16. This corresponds to a position of the punctual load between 25.00 m and 37.00 m from the left support that is 61% and 90% of the span.

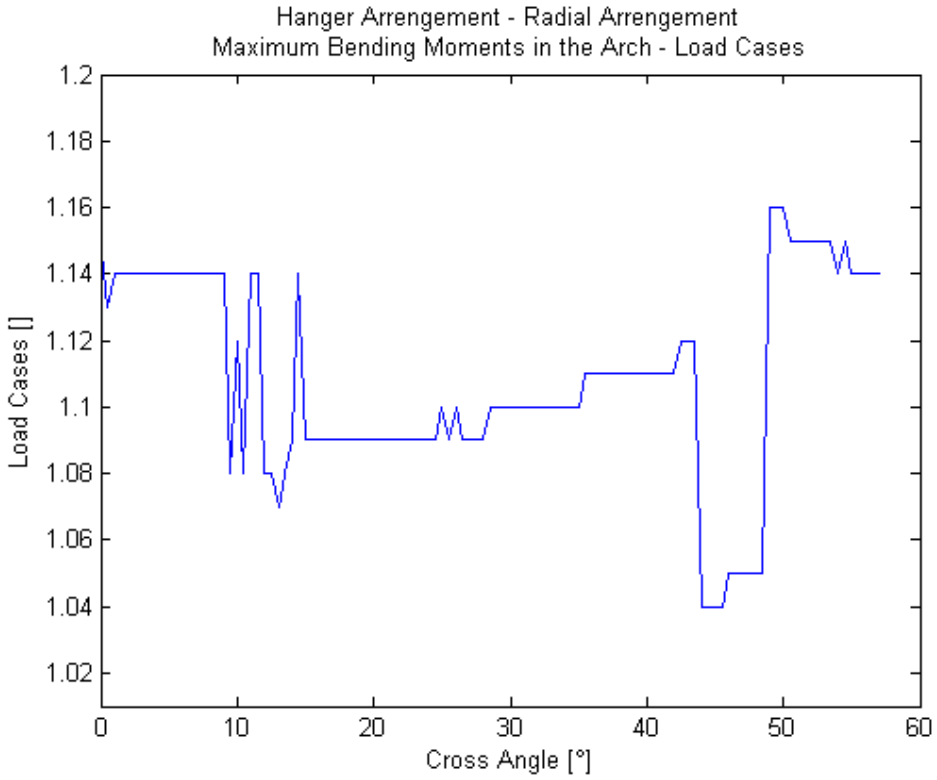


**Figure 77.** Corresponding load cases for the maximum bending moments in the arch (Radial arrangement)

### 3.1.2.1.5. Axial forces in the arch

The Figure 78 shows the values for maximum axial compression forces in the arch for each bridge. If we see the figure, we notice that the lowest values for the compression forces correspond to the “spoked wheel arrangement” shown in the Figure 79. From this point the compression forces increase as the cross angle increases.

For this arrangement the hangers do not intersect each other. For this reason the bridge is not a network arch bridge. The corresponding maximum axial force is -3019.53 kN. That is 71% of the maximum value, that corresponds to a cross angle of 57°: -4236.86 kN; and 92% of the best value for the arrangements with linear variation of the slopes: -3285.81 kN.

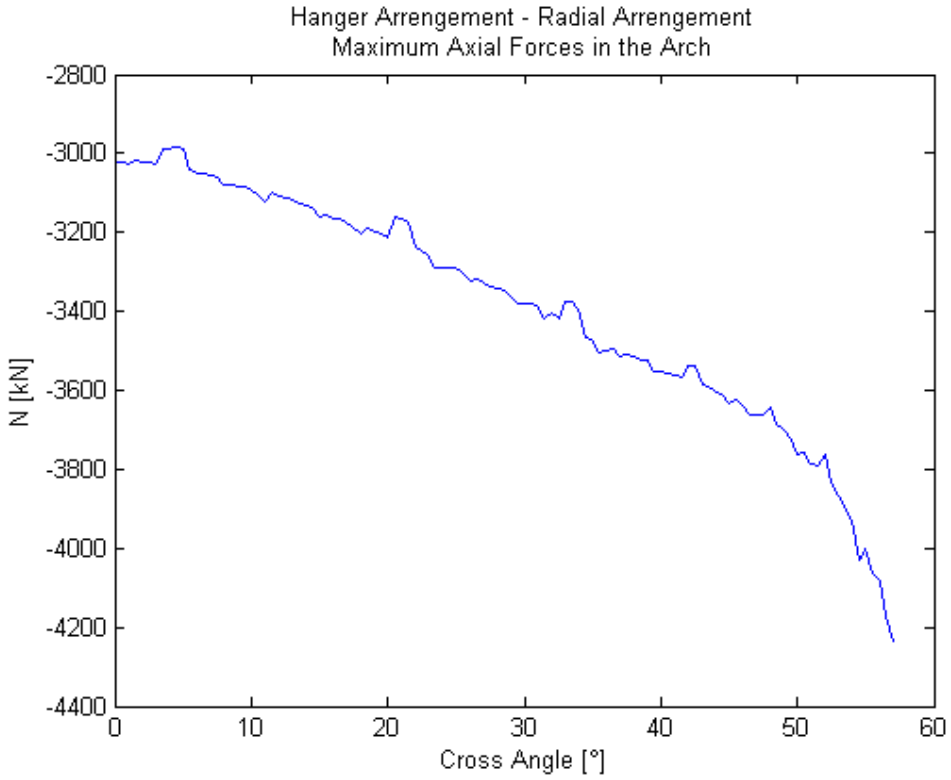


**Figure 78.** Maximum axial compression forces in the arch (Radial arrangement)

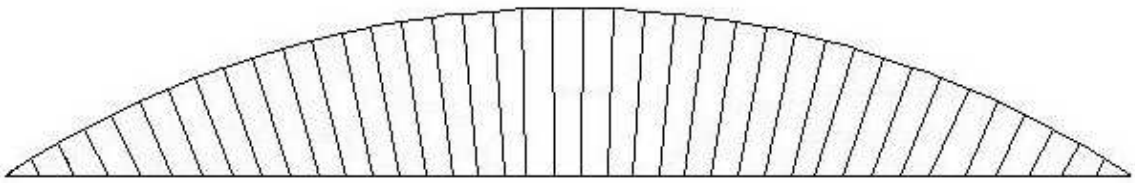

**Figure 79.** Radial arrangement. Cross angle = 0°

The figure 80 shows in a graphical format the X-coordinates where the maximum values occur. For a cross hanger smaller than 40° the maxi mum compression forces occurs in the extremes of the arch. As the cross angle is increased, the maximum value presents closer to the center of the span. For a cross angle of 57° the ma ximum compression force occurs at a distance of 25 m from the left support: 61% of the span.

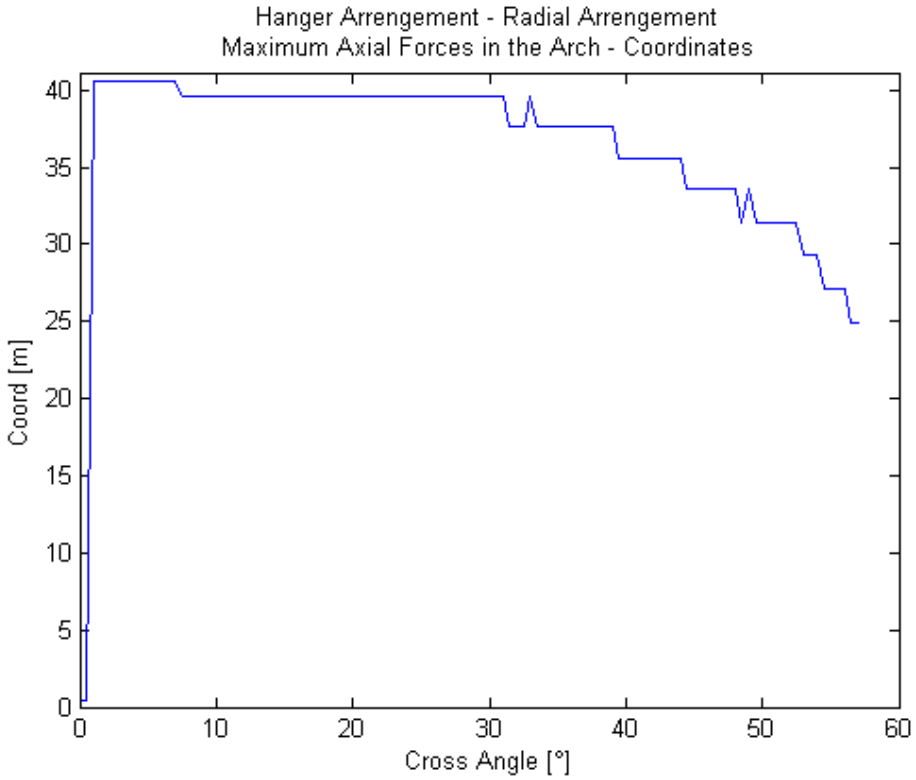


**Figure 80.** Corresponding X-coordinates for the maximum axial compression forces in the arch (Radial arrangement)

The Figure 81 shows the load cases for which the maximum values occur. For cross angles smaller than 35°, the position of the punctu al load that corresponds to the maximum axial compression force approaches the ¾ of the span, as the angle is increase. For a cross angle equal to 0° the load case is 1.01, with the punctua l load in the center of the span. For a cross angle of 35° the corresponding load case is 1.10, w ith the punctual load 30.00 m from the left support: 73% of the span.

For cross angles bigger than 35°, the corresponding position of the punctual load approaches the middle of the span as the angle increases. For a cross angle of 57° the corresponding load case is 1.03, with the punctual load 24.00 m from the left support: 58% of the span.

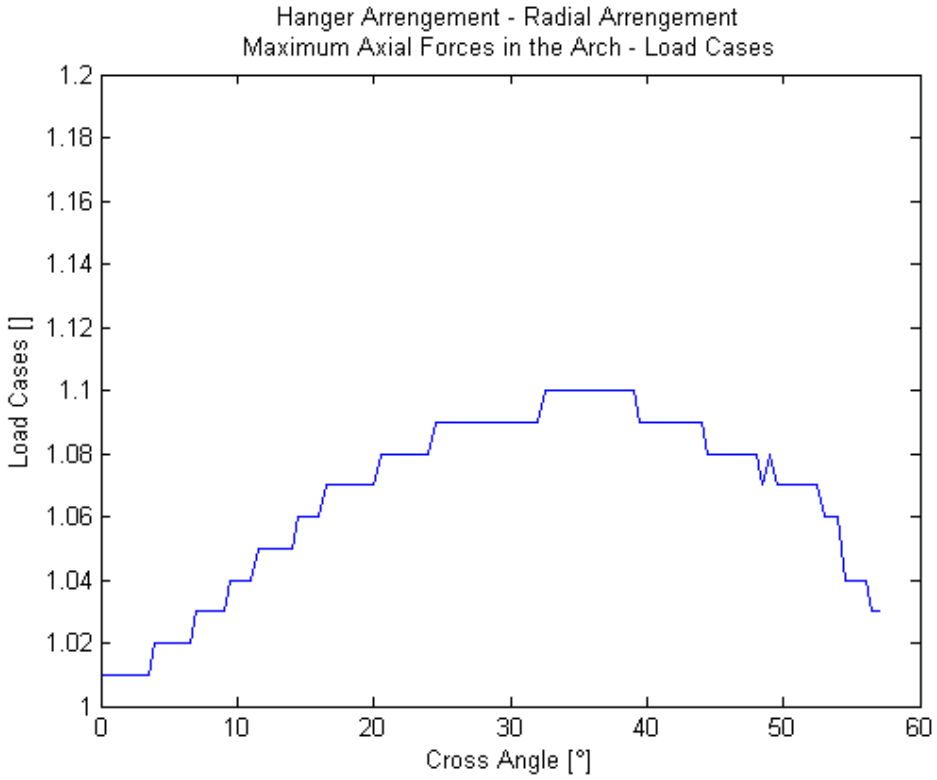


**Figure 81.** Corresponding load cases for the maximum axial compression forces in the arch (Radial arrangement)

### 3.1.2.1.6. Stresses in the arch

The Figure 82 shows the values for maximum negative stresses in the arch for each bridge. If we see the figure, we notice that the values decrease from a cross angle equal to 0° until a minimum between 40° and 50°. From 50° to 57° the stresses increase significantly.

The figure 65 shows an arrangement with a cross angle equal to 45° that corresponds to the lowest values for the stresses.

In the arrangement of Figure 65 the hangers intersect each other several times. Hence, the bridge has the structural behavior of several trusses on top of another. This fulfill the condition for network arch bridges. For this reason the negative stress in the arch is reduced. The value of the maximum negative stress for this arrangement is -142108.92 kN/m$^2$. That is 81% of the value for the "spoked wheel arrangement": -173534.36 kN/m$^2$; and in the same order of the best value for the arrangements with linear variation of the slopes: -140129.41 kN/m$^2$.

The Figure 83 shows in a graphical format the X-coordinates where the maximum values occur. The maximum values occur less than 10.00 m from the left or right support. That is, between the 0% and 25% of the span or between the 75% and 100%.

The Figure 84 shows in a graphical format the number of the load cases for which the maximum values occur. The maximum values occur mostly for the load cases between 1.06 and 1.14. This corresponds to a position of the punctual load between 27.00 m and 35.00 m from the left support that is 66% and 85% of the span.

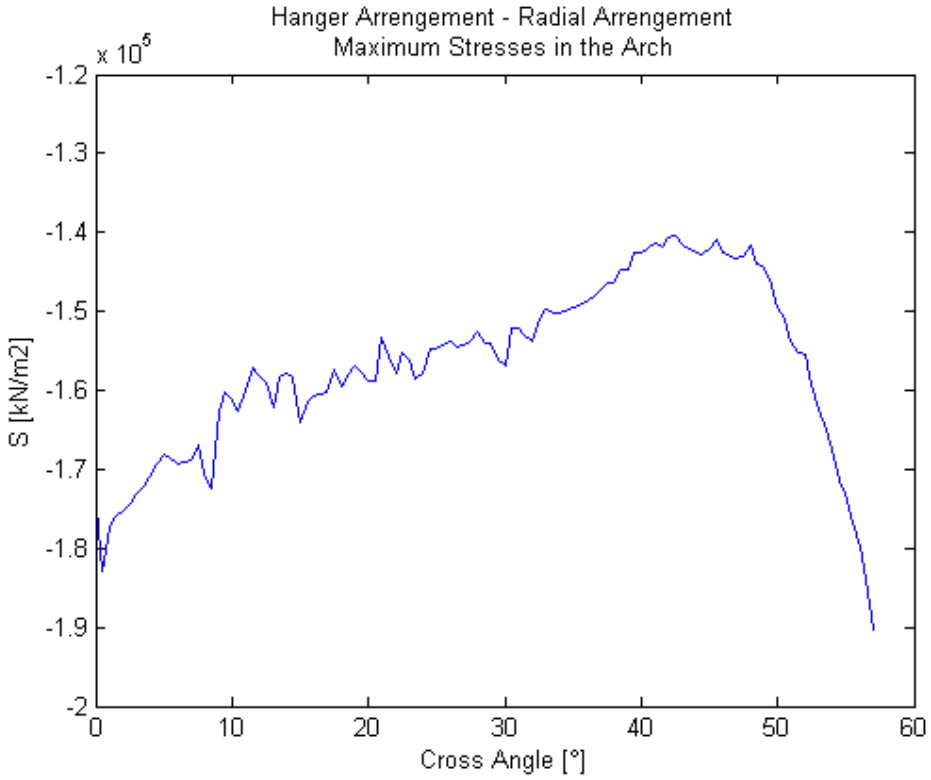


**Figure 82.** Maximum stresses in the arch (Radial arrangement)

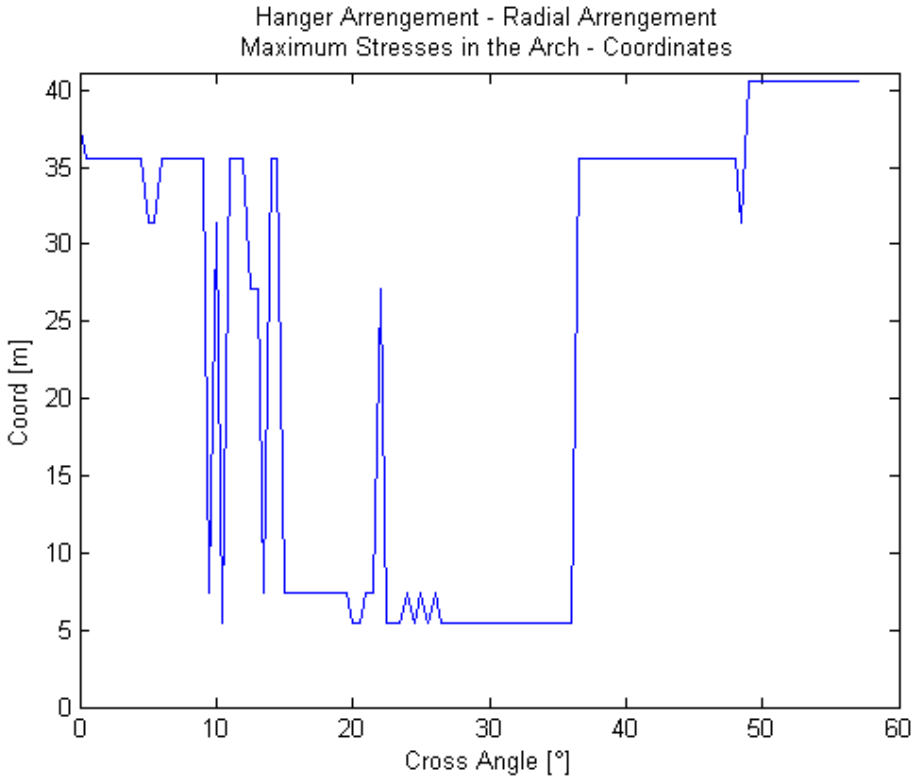


**Figure 83.** Corresponding X-coordinates for the maximum stresses in the arch (Radial arrangement)

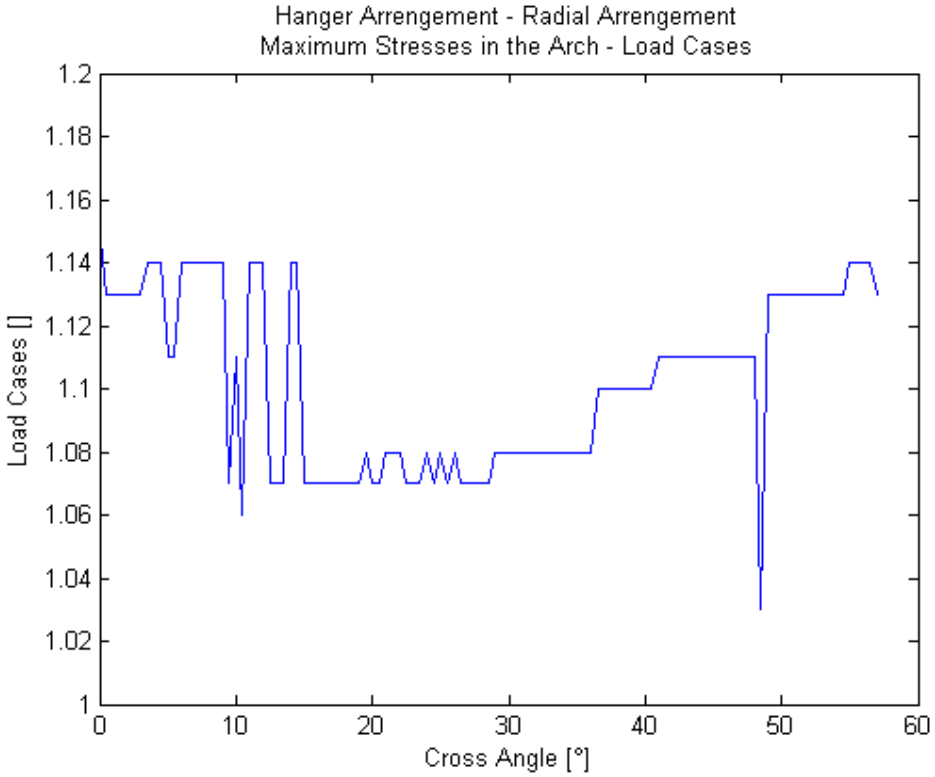


**Figure 84.** Corresponding load cases for the maximum stresses in the arch (Radial arrangement)

### 3.1.2.1.7. Stresses in the hangers

The Figure 85 shows the values for maximum stresses in the hangers for each bridge. The minimum stress corresponds to a cross angle equal to 0°. However, for angle smaller than 25° the stresses do not increase significantly. The maximum stress for an angle of 0° is 87588.89 kN/m$^2$, while for an angle of an angle of 21° is 104875.21 kN/m$^2$: 1.20 times the previous value.

For angles bigger than 25° the increment of the str esses becomes more important. The stress for an angle of 50° is 153067.13 kN/m$^2$: 1.75 times the stress for a cross angle of 0°. Th e stress for an angle of 57° is 212251.66 kN/m$^2$: 2.42 times the stress for a cross angle of 0°.

The values for the arrangements with linear variation of the slopes are bigger than the values for the radial arrangement. The best value for the first case is 106608.15 kN/m$^2$, 1.22 times the best value for radial arrangement.

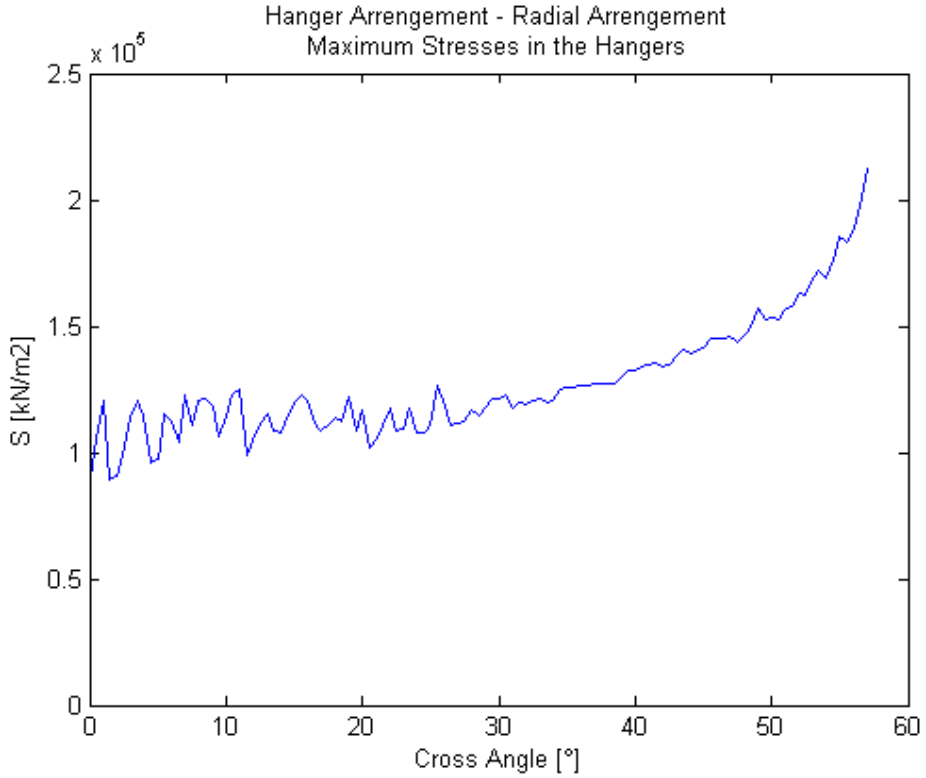


**Figure 85.** Maximum stresses in the hangers (Radial arrangement)

The Figure 86 shows in a graphical format the number of the element where the maximum values occur. The maximum stresses always correspond to an element between 3009 and 3035, that is, the hangers located at a distance bigger than 8 .00 m from the supports: between the 20% and 80% of the span. For cross angles bigger than 35°, as the angle increase the hanger with the maximum stress approaches the center of the span.

The Figure 87 shows the load cases for which the maximum values occur. The load cases that correspond to the maximum stress are between 1.01 and 1.16. The position of the punctual load is between 21.00 m and 37 m of the left support: between the 50% and 90% of the span. For a cross angle bigger than 35°, as the angle increas es the location of the load case that causes the maximum stress approaches the center of the span.

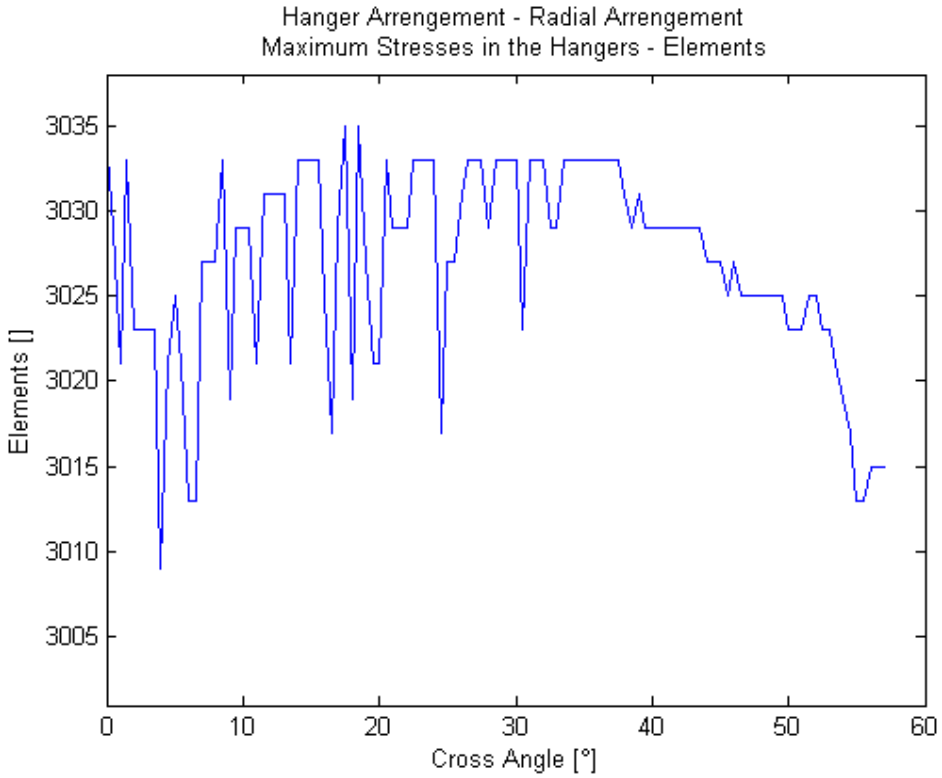


**Figure 86.** Corresponding elements for the maximum stresses in the hangers (Radial arrangement)

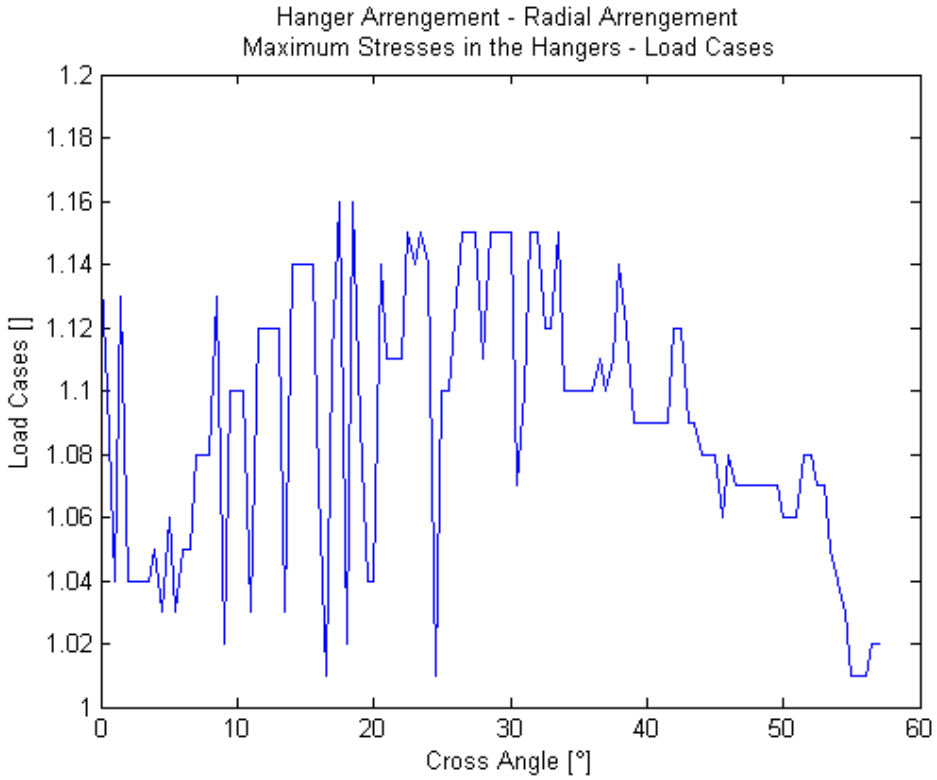


**Figure 87.** Corresponding load cases for the maximum stresses in the hangers (Radial arrangement)

### 3.1.2.1.8. Relaxed hangers

The Figure 88 shows the number of relaxed hangers for each bridge. There are no relaxed hangers for most of the hanger arrangements. The exceptions are the configurations that correspond to cross angles equal to 1° and 9°, with one relaxed hanger, and to an angle equal to 3.5°, with three relaxed hangers.

For the radial arrangement, the relaxed hangers are located in the center of the bridge. None of this configurations corresponds to network arch bridges.

The relaxed hangers are:

- Cross angle = 1°: 3019
- Cross angle = 3.5°: 3018, 3021, 3022.
- Cross angle = 9°: 3017.

The maximum number of relaxed hangers correspond to the load case 1.06. The position of the punctual load is 27.00 m from the left support that is 66% of the span.

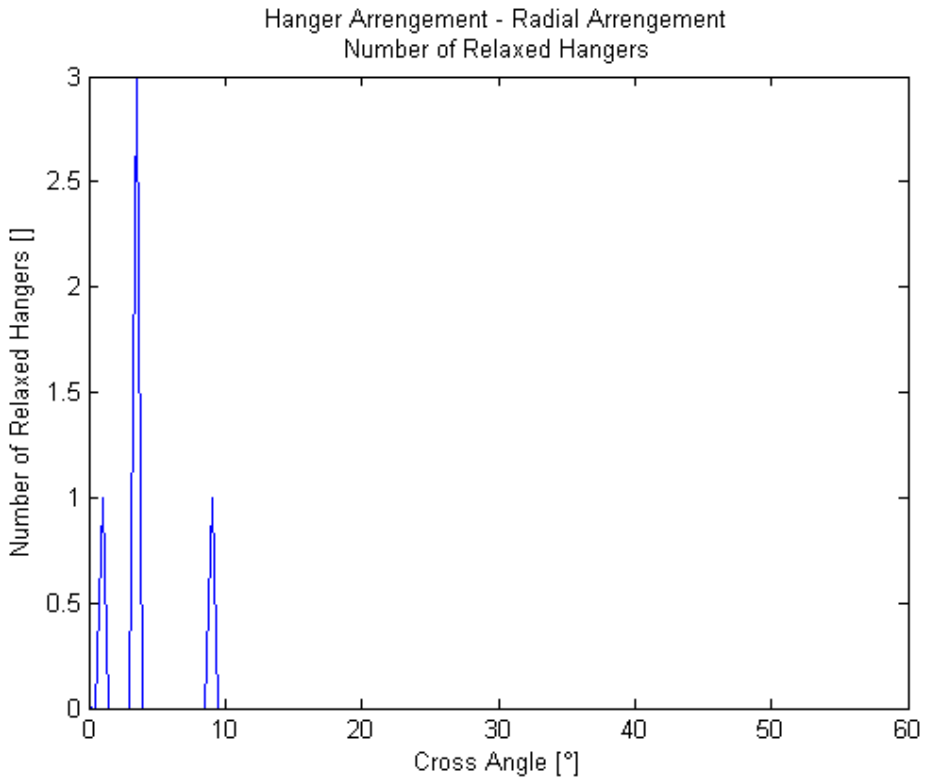


**Figure 88.** Number of relaxed hangers (Radial arrangement)

### 3.1.2.2. Conclusions

A network arch bridge configuration is obtained when the hangers intersect each other at least two times. This is achieved when the cross angle is higher than 15°.

The minimum bending moments in the deck are obtained for cross angles between 40° and 50°. For angles bigger than 50° or smaller than 40° the increment of the moments is important.

On the other hand, for angles smaller than 50° the influence of the cross angle over the axial forces is the deck is very small, around 5%. Even for angles bigger than 50° the influence is not significant: less than 15%.

For this reason the form of the graphic obtained for the stresses in deck is quite similar to the one obtained for the bending moments. As in the case of the hanger arrangement based in the linear variation of the slopes, the configuration of the hangers has important an influence on the values of the bending moments in the deck, while the variation of the axial forces due to the arrangement is not significant.

Comparing the results for this arrangement with the results for the hanger arrangement based in the linear variation of the slopes we find similar results, with slightly higher values for the second case. While for the radial arrangement the stresses in the deck are between 11520.15 kN/m$^2$ and 26714.00 kN/m$^2$ , for the arrangement based in the linear variation of the slopes the values are between 11461.62 kN/m$^2$ and 22806.53 kN/m$^2$.

The minimum bending moments in the arch are obtained for cross angles between 45° and 50°. For angles bigger than 50° or smaller than 45° the increase of the moments is important. The influence of the cross angle over the axial forces in the arch is more significant than in the deck.

Comparing the results in the arch for this arrangement with the results for the hanger arrangement based in the linear variation of the slopes we do not find any improvement. The stresses are of the same order in both cases.

In the deck the elements where the maximum stress occur are in the center of the span, while in the arch the elements located in the extremes quarters are the ones that support the highest stresses. The hangers near the center of the span present the higher stresses.

In the arch and hangers the stresses are lower than the admissible values. The fact that the stresses in the deck are higher than the admissible values remarks the importance of the prestressing of the deck. As the prestressing was not considered in this thesis, it is expected than the admissible stresses are exceeded.

The smallest stresses in the hangers are obtained for small cross angles, approaching the “spoked wheel configuration”. For bigger angles the values increase significantly. Here we find an improvement: the values for the radial arrangement are 82% smaller than the results for the hanger arrangement based in the linear variation of the slopes:

Only three configurations show relaxed hangers. This hanger arrangements do not correspond to network arch bridges, as the hangers do not intersect each other at least two times. The bridges that fulfill this condition have no relaxed hangers.

## 3.2. Shape of the arch

In order to examine the influence of the shape of the arch over the structural behavior of the bridge two principal arch shapes are chosen: the parabolic arch, and the circular arch.

In addition, it is considered the possibility of the combination of this two shapes. A parabolic shape is adopted in the extremes of the arch, and a circular shape in the center. The circular part of the arch in this case has a radius bigger than the one obtained for a fully circular arch. In the point where the circular arch meets the parabolic arch, the tangent line has the same slope.

The variables use to describe this configuration are the radio of the circular part of the arch $R_{Rel}$, and the distance from where the parabolic shape begins, *long1*. The radio $R_{rel}$ is expressed as a percentage of the radius for a fully circular arch, with $R_{rel} > 1.0$. The distance *long1* is expressed as a percentage of the span, with *long1* ≤ 0.5. This variables are shown in the Figure 89.

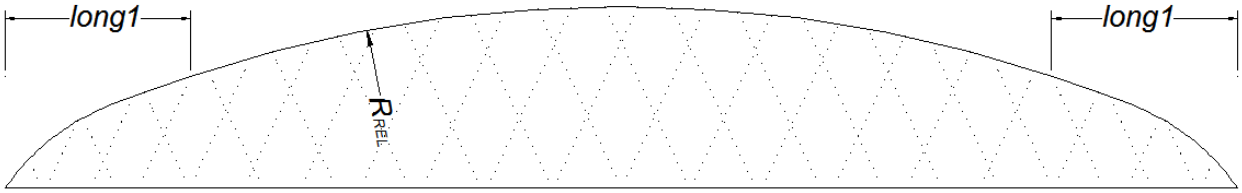


**Figure 89.** Variables used to described the shape of the arch

A hanger arrangement that corresponds to a linear variation of the slopes is used for this examination, with an initial angle of 70° and an an gle increment of 1.0°. The bridge configuration is shown in figure 90.

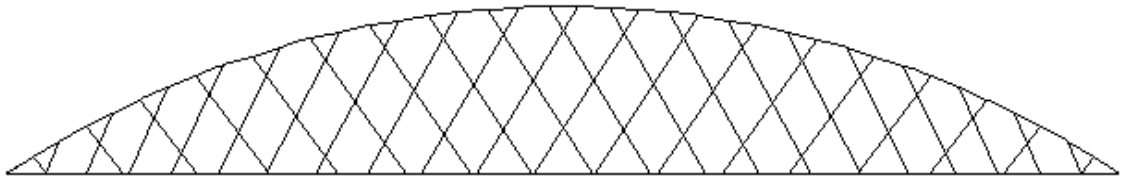

**Figure 90.** Hanger arrangement for $\varphi_0 = 70° - \Delta\varphi = 1.0°$

The results obtained for this bridge are:

- Maximum bending moment in the deck: 971.30 kNm
- Maximum axial force in the deck: 3068.27 kN
- Maximum Stress in the deck: 15884.76 kN/m$^2$
- Maximum bending moment in the arch: -188.50 kNm
- Maximum axial force in the arch: -3448.22 kN
- Maximum stress in the arch: -176040.98 kN/m$^2$
- Maximum stress in the hangers: 124854.89 kN/m$^2$
- Number of relaxed hangers: 2

For the present study 400 bridges are calculated, with a radius $R_{rel}$ from 1.1 to 3.0, and a distance *long1* from 0.05 to 0.5. The numbers assigned to the hanger elements are the same as for the hanger arrangement based on the linear variation of the slope, as shown in the Figure C.1 in the Appendix C.

### 3.2.1. Results

The results are shown in the following diagrams. Every ordinate corresponds to one value of each bridge.

#### 3.2.1.1. Bending moments in the deck

The Figure 91 shows the absolute values for maximum bending moments in the deck for each bridge. The maximum stress increase as $R_{rel}$ increases and *long1* decreases until a maximum value at $R_{rel}$ = 3 and *long1* = 0.05. This configuration is shown in the Figure 92.

For the bridge shown in the Figure 92 the maximum axial force is 4025.09 kNm , 4.10 times the value obtain for a circular arch shape.

The stress for a parabolic arch is represented in the graphic for the points with distance *long1* = 0.5. The Figure 93 shows an example for this configuration. The maximum bending moment for a parabolic arch is 971.81 kNm, approximately the same value as for a circular arch shape.

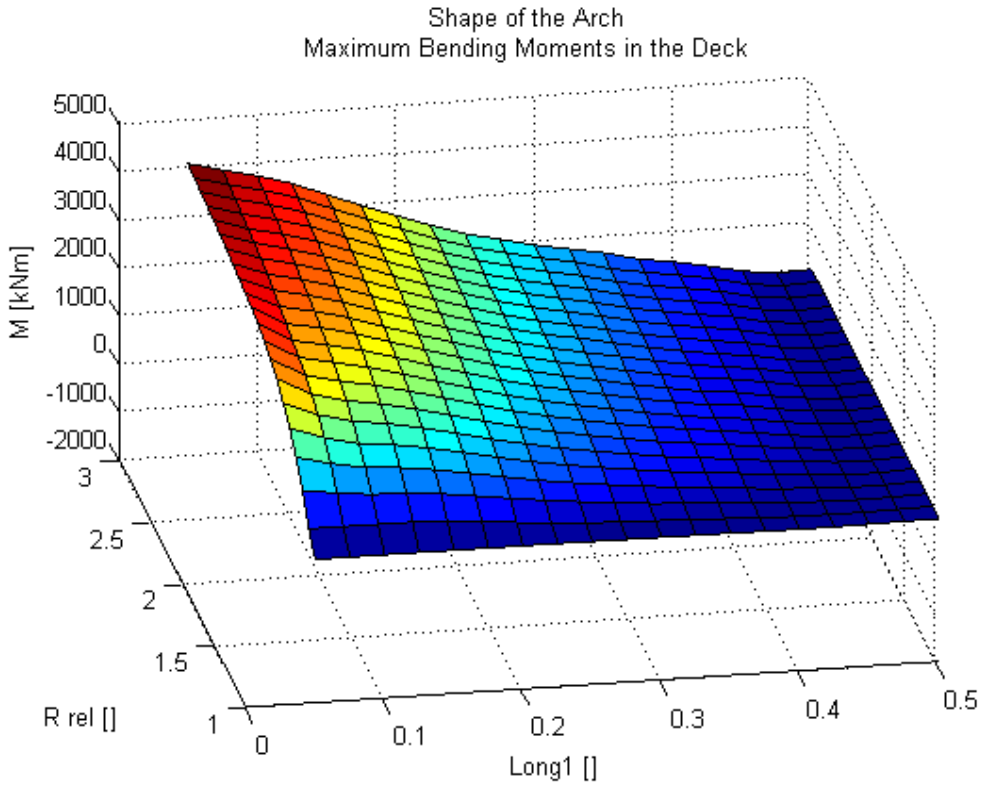


**Figure 91.** Maximum bending moments in the deck (Shape of the arch)

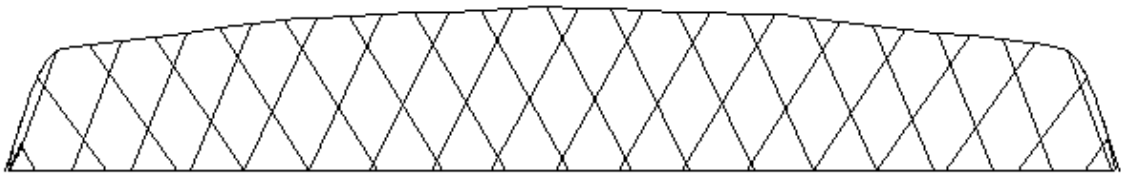

**Figure 92.** Arch shape: $R_{rel}$=3.0 ; *long1* = 0.05

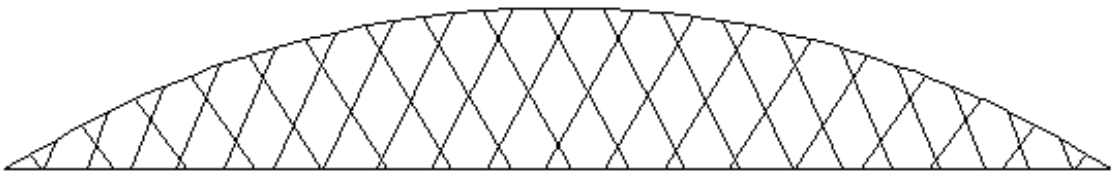

**Figure 93.** Arch shape: $R_{rel}$=1.0 ; *long1* = 0.50

The Figure 94 shows the X-coordinates where maximum values occur. For *long1* smaller than 0.35, the maximum bending moment presents 4.00 m from the left support (10% of the span). For *long1* bigger than 0.35, it occurs around the 25.00 m from the left support, that is 61% of the span. For circular arches the corresponding coordinate is 27.80 m from the left support (70% of the span).

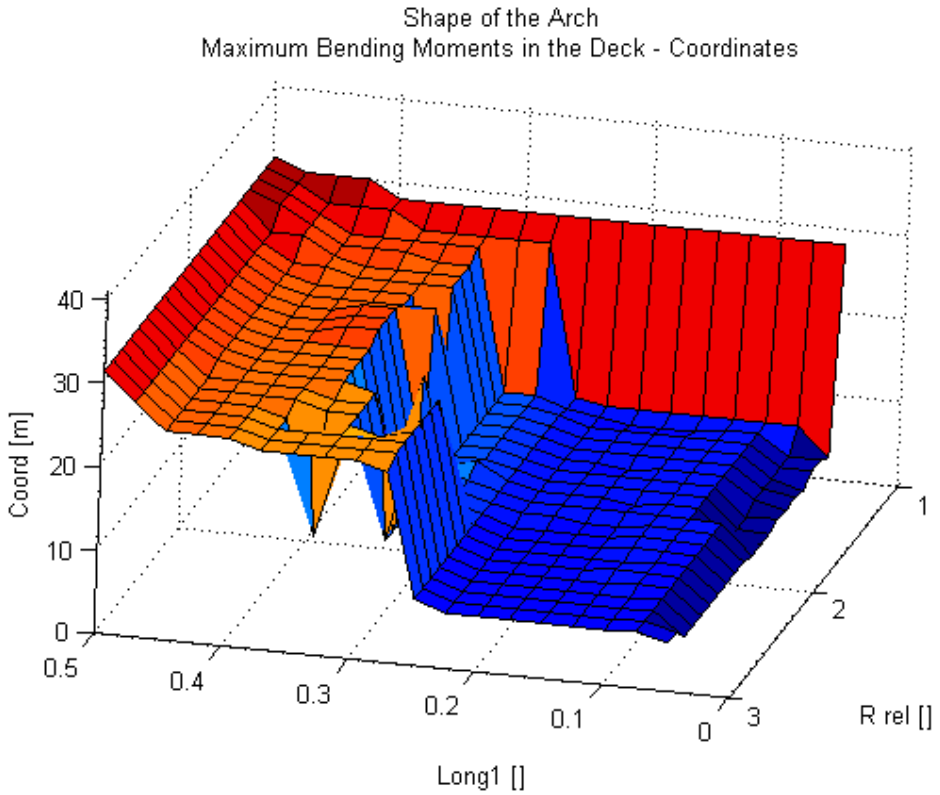


**Figure 94.** Corresponding X-coordinates for the maximum bending moments in the deck (Shape of the arch)

The Figure 95 shows the load cases for which the maximum values occur. For *long1* smaller than 0.30, the position of the punctual load is around 28.00 m form the left support (load case 1.07), that is 68% of the span. For values of *long1* between 0.30 and 0.45 the position of the punctual load that causes the maximum bending moment is near the center of the span.

For parabolic (*long1*=0.5) and circular arches the corresponding load cases are around 1.10, with the punctual load 31.00 m from the left support (76% of the span).

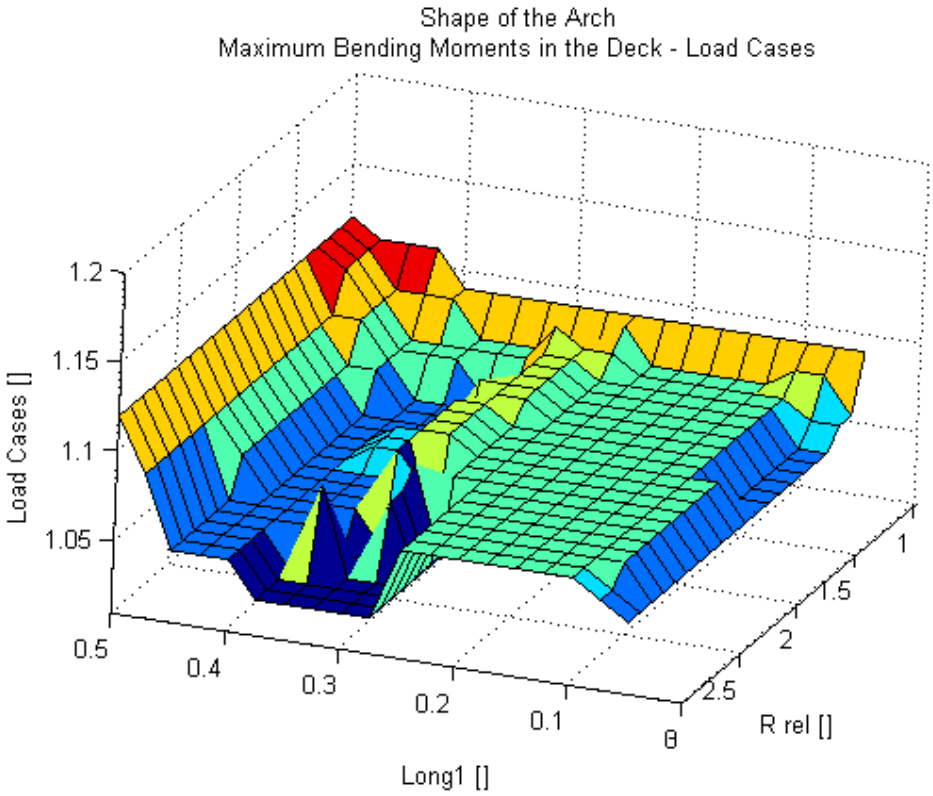


**Figure 95.** Corresponding load cases for the maximum bending moments in the deck (Shape of the arch)

### 3.2.1.2. Axial forces in the deck

The Figure 96 shows the values for maximum axial forces in the deck for each bridge. Axial forces decrease as $R_{rel}$ increases and *long1* decreases, until a minimum value at $R_{rel}$ = 3 and *long1* = 0.05. This configuration is shown in the Figure 92.

The bending moment for a parabolic arch is represented in the graphic by the points with distance *long1* = 0.5. The Figure 93 shows this configuration. The maximum axial force for a parabolic arch is 3141.16 kNm, 1.02 times the value for a circular arch shape.

For the bridge with $R_{rel}$ = 3 and *long1* = 0.05 the maximum axial force is 2452,48 kN, 80% of the value obtained for a circular arch shape.

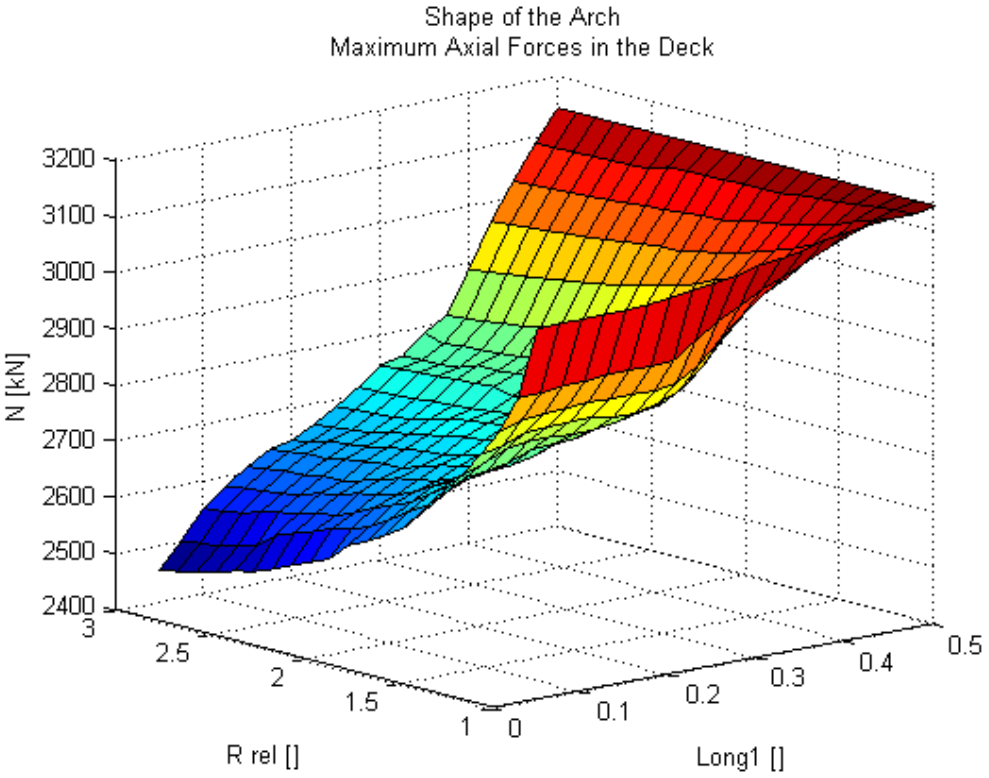


**Figure 96.** Maximum axial forces in the deck (Shape of the arch)

The figure 97 shows in a graphical format the X-coordinates where the maximum values occur. For *long1* between 0.15 and 0.35 and $R_{rel}$ higher than 1.4 the maximum axial forces occur approximately in the middle of the span. In the rest of the graphic the maximum values present 35.00 m from the left support: 85% of the span.

The Figure 98 shows the load cases for which the maximum values occur. For *long1* smaller than 0.35, the corresponding load case is around 1.02: the location of the punctual load is in the center of the span. For *long1* bigger than 0.35, the position of the punctual load is around 30.00 m form the left support (load case 1.09): 73% of the span. For small values of $R_{rel}$ the position of the punctual load that causes the maximum axial force is less centered in the span, approaching the right support.

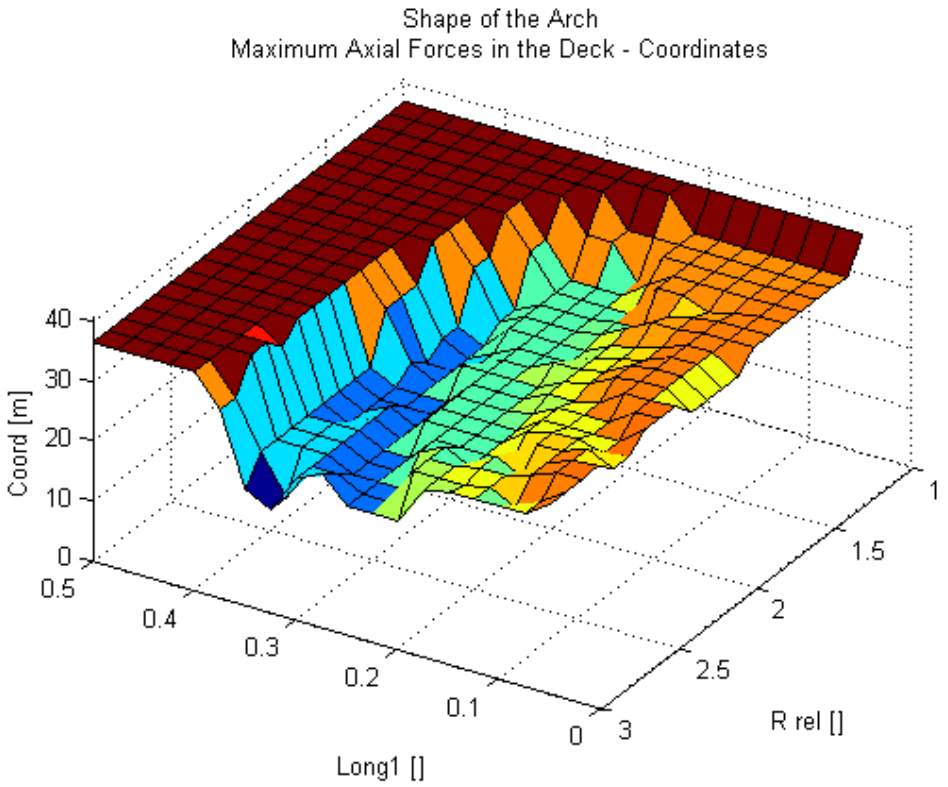


**Figure 97.** Corresponding X-coordinates for the maximum axial forces in the deck (Shape of the arch)

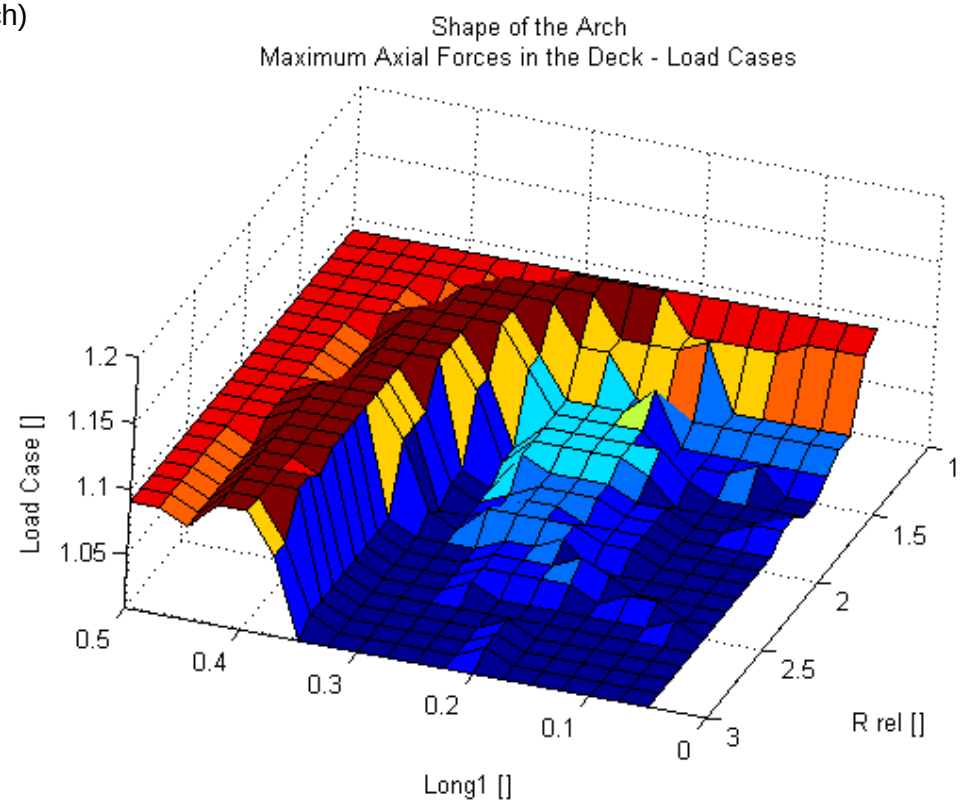


**Figure 98.** Corresponding load cases for the maximum axial forces in the deck (Shape of the arch)

### 3.2.1.3. Stresses in the deck

The Figure 99 shows the values for maximum stresses in the deck for each bridge. The maximum stress increase as $R_{rel}$ increases and *long1* decreases until a maximum value at $R_{rel}$ = 3 and *long1* = 0.05. This configuration is shown in the Figure 92. For this bridge the maximum axial force is 54397,71 kN/m$^2$ , 3.41 times the value obtained for a circular arch shape.

The stress for a parabolic arch is represented in the graphic for the points with distance *long1* = 0.5. The Figure 93 shows this configuration. The maximum stress for a parabolic arch is 15963,19 kN/m$^2$, approximately the same value that for a circular arch shape.

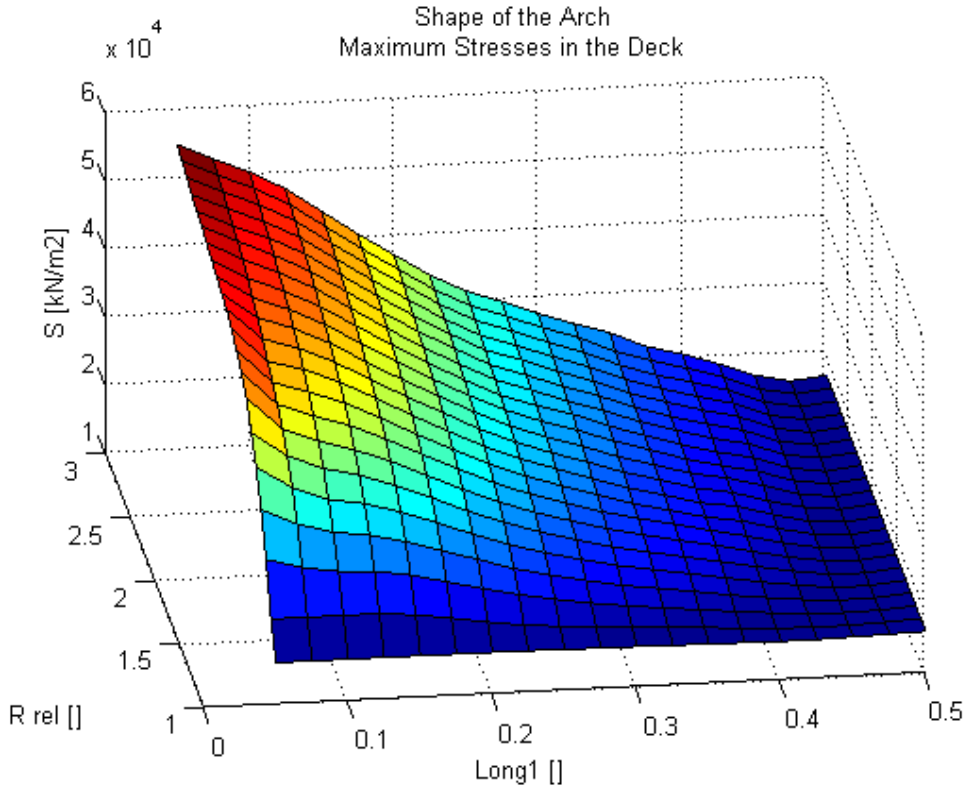


**Figure 99.** Maximum stresses in the deck (Shape of the arch)

The Figure 100 shows the X-coordinates where maximum values occur. For *long1* smaller than 0.25, the maximum stress presents 7.00 m from the left support (10% of the span). For *long1* bigger than 0.25, it occurs around 25.00 m from the left support: 61% of the span. For circular arches the corresponding coordinate is 27.80 m from the left support (70% of the span).

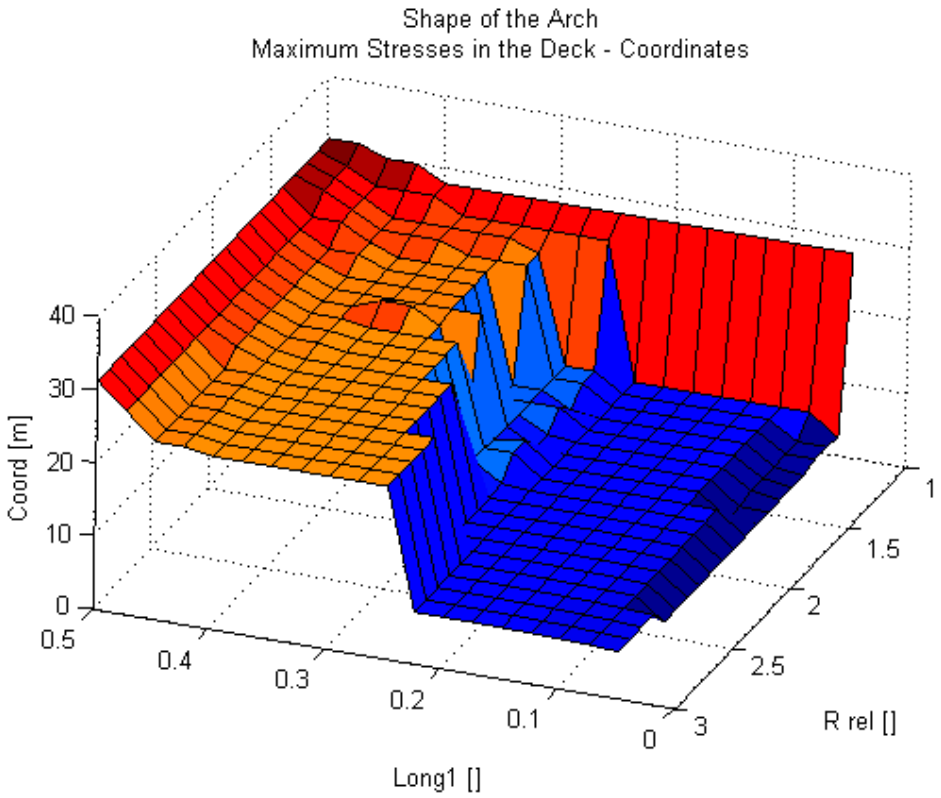


**Figure 100.** Corresponding X-coordinates for the maximum stresses in the deck (Shape of the arch)

The Figure 101 shows the load cases for which the maximum values occur. For *long1* smaller than 0.25, the position of the punctual load is around 28.00 m form the left support (load case 1.07): 68% of the span. For values of *long1* between 0.25 and 0.45 the position of the punctual load that causes the maximum axial force is near the center of the span.

For parabolic (*long1*=0.5) and circular arches the corresponding load cases are around 1.12, with the punctual load 33.00 m from the left support (80% of the span).

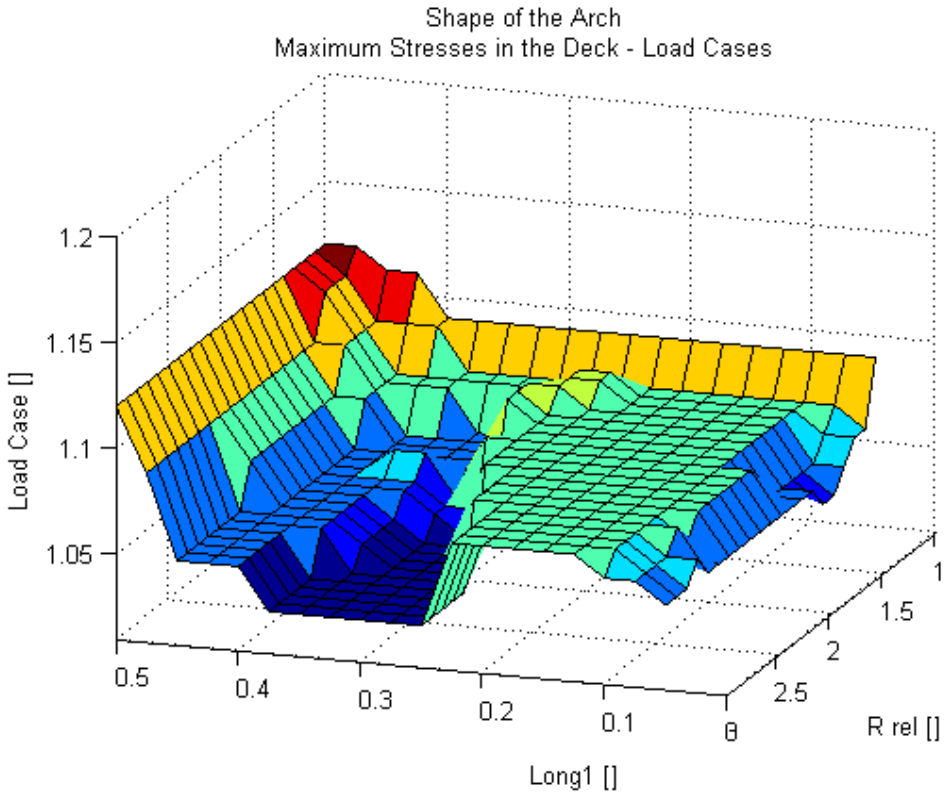


**Figure 101.** Corresponding load cases for the maximum stresses in the deck (Shape of the arch)

### 3.2.1.4. Bending moments in the arch

The Figure 102 shows the absolute values for maximum bending moments in the arch for each bridge. The maximum stress increase as $R_{rel}$ increases and as *long1* decreases, until a maximum value at $R_{rel}$ = 3 and *long1* = 0.05. For this bridge the maximum bending moment is -1584.85 kNm, 8.43 times the value obtained for a circular arch shape. This configuration is shown in the Figure 92.

The maximum bending moment for a parabolic arch is 156.15 kNm, 83% of the value for a circular arch shape.

The figure 103 shows the X-coordinate where the maximum values occur. For *long1* higher than 0.3 the maximum bending moment presents the center of the span. Outside this range the maximum values occur less than 10 m from the left support..

The figure 104 shows in a graphical format the load cases where the maximum values occur. For $R_{rel}$ bigger than 1.7 and *long1* smaller than 0.35 the corresponding load case is 1.20, with the location of the punctual load near the right support. Outside this range the position of the punctual load is near the center of the span.

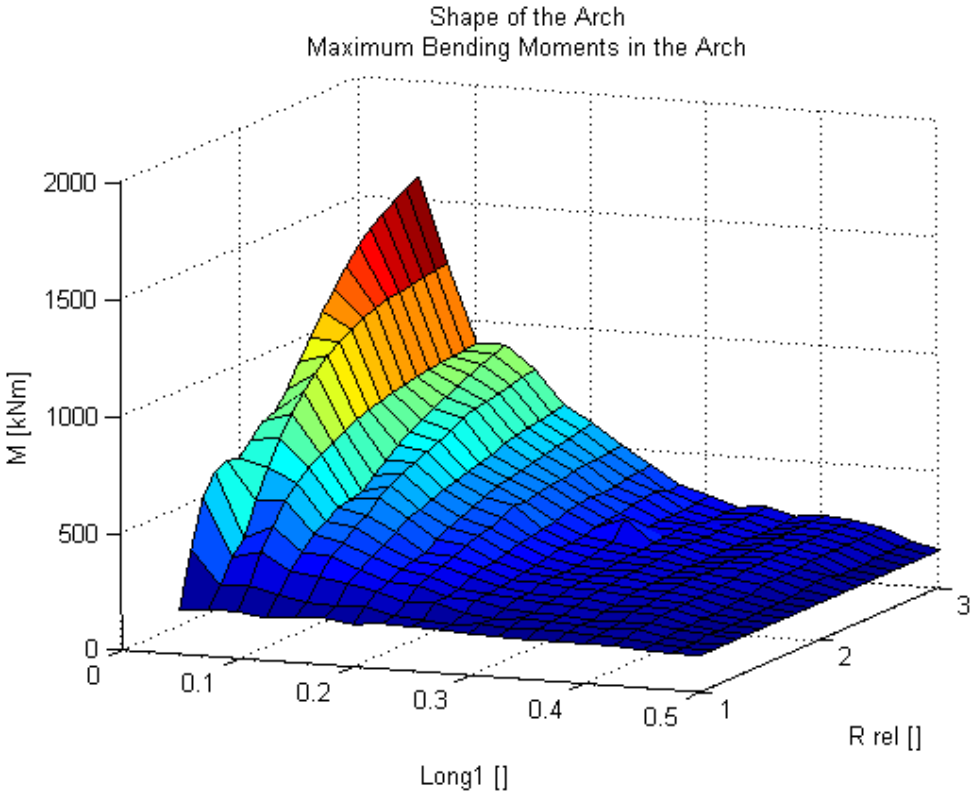


**Figure 102.** Maximum bending moments in the arch (Shape of the arch)

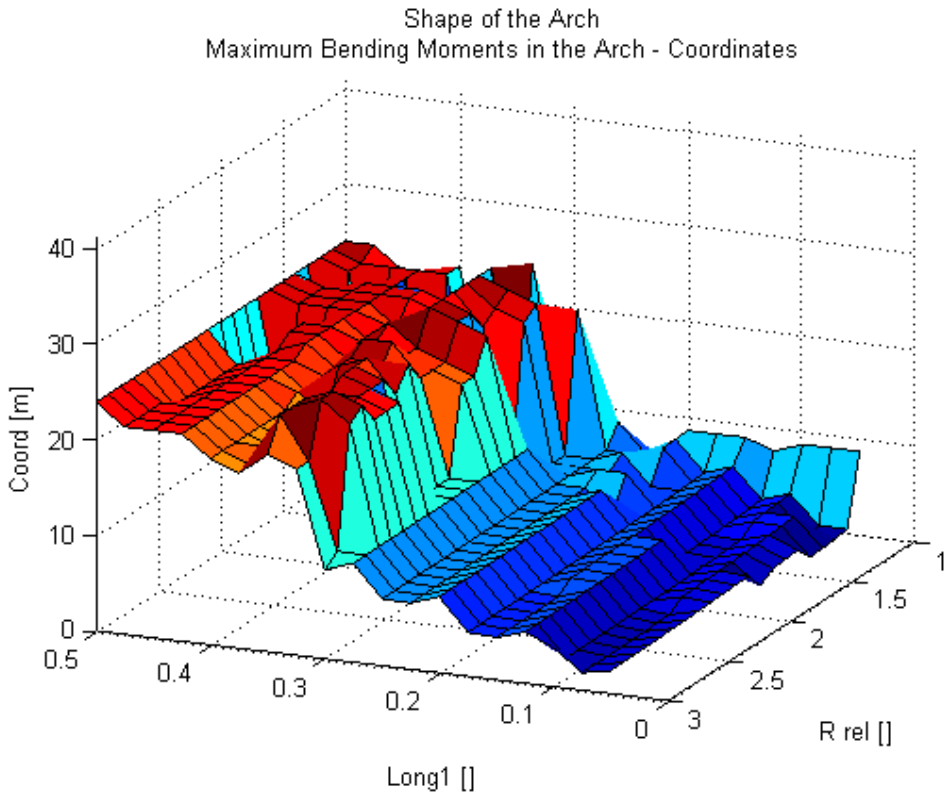


**Figure 103.** Corresponding X-coordinates for the maximum bending moments in the arch (Shape of the arch)

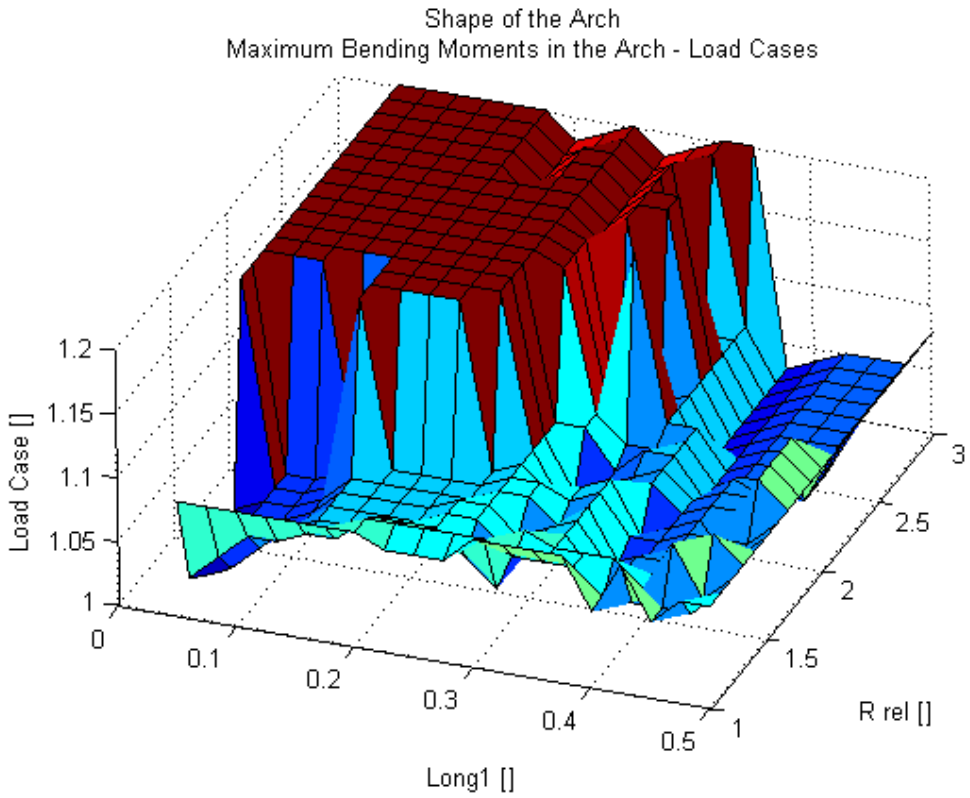


**Figure 104.** Corresponding load cases for the maximum bending moments in the arch (Shape of the arch)

### 3.2.1.5. Axial forces in the arch

The Figure 105 shows the values for maximum axial compression forces in the arch for each bridge. In the figure we can see that the minimum compression forces are in a "peak". The Figure 106 shows the configuration for a bridge in this "peak", with $R_{rel}$ = 3.0 and *long1*=0.125. The corresponding maximum axial force is -2647.45 kN, 77% of the value for a circular arch shape.

The maximum axial force for a parabolic arch is -3504.71 kN, 1.02 times the value for a circular arch shape.

The Figure 107 shows in a graphical format the X-coordinates where the maximum values present. The maximum axial forces occur in the extremes of the arch.

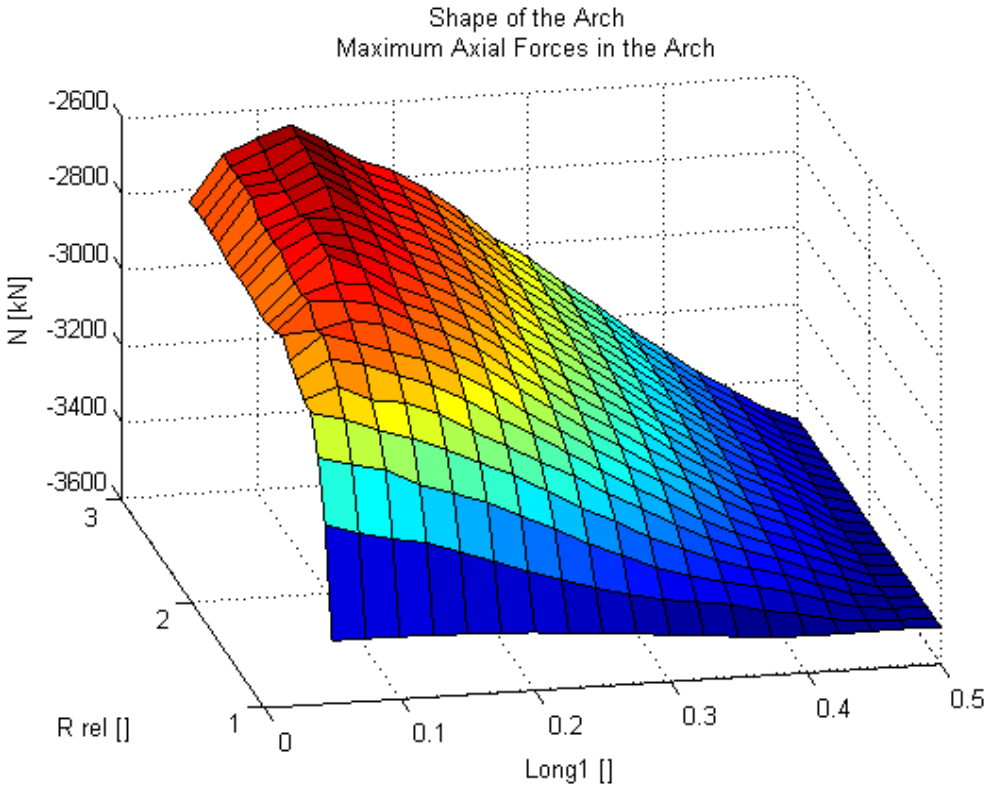


**Figure 105.** Maximum axial compression forces in the arch (Shape of the arch)

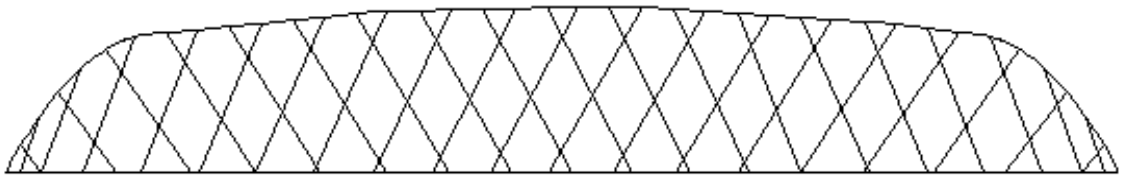

**Figure 106.** Arch shape: $R_{rel}$=3.0 ; *long1* = 0.125

The Figure 108 shows the load cases for which the maximum values occur. For *long1* smaller than 0.20, the corresponding load case is around 1.03, with the location of the punctual load near the center of the span. For values of *long1* higher than 0.20, and for $R_{Rel}$ =1, the position of the punctual load that causes the maximum axial force is around 31.00 m, that is 77% of the span (load case 1.10).

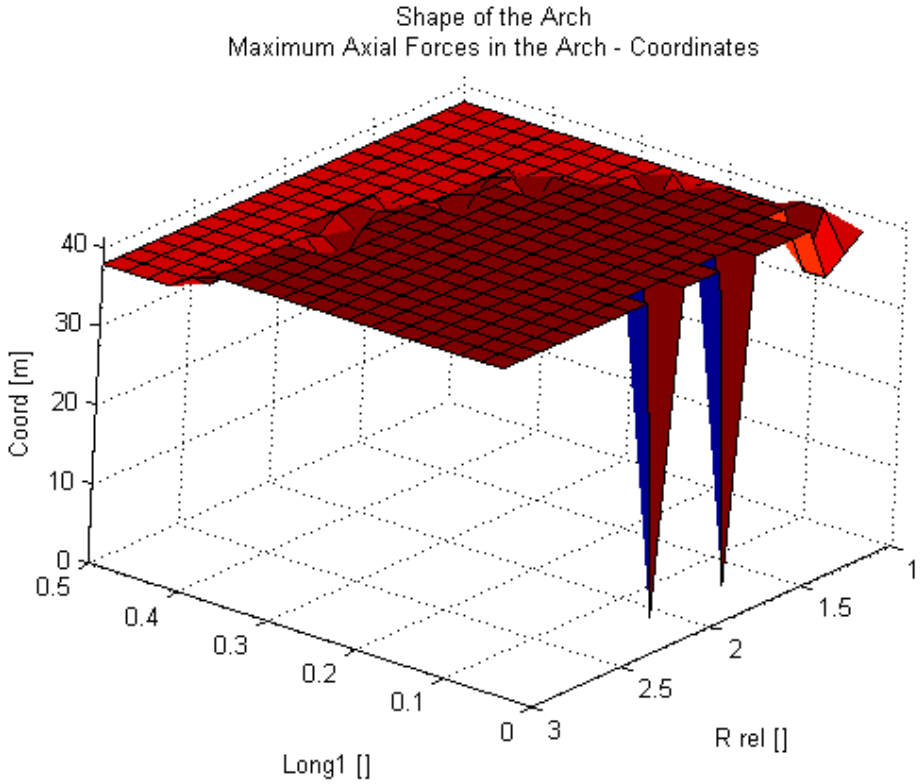


**Figure 107.** Corresponding X-coordinates for the maximum axial compression forces in the arch (Shape of the arch)

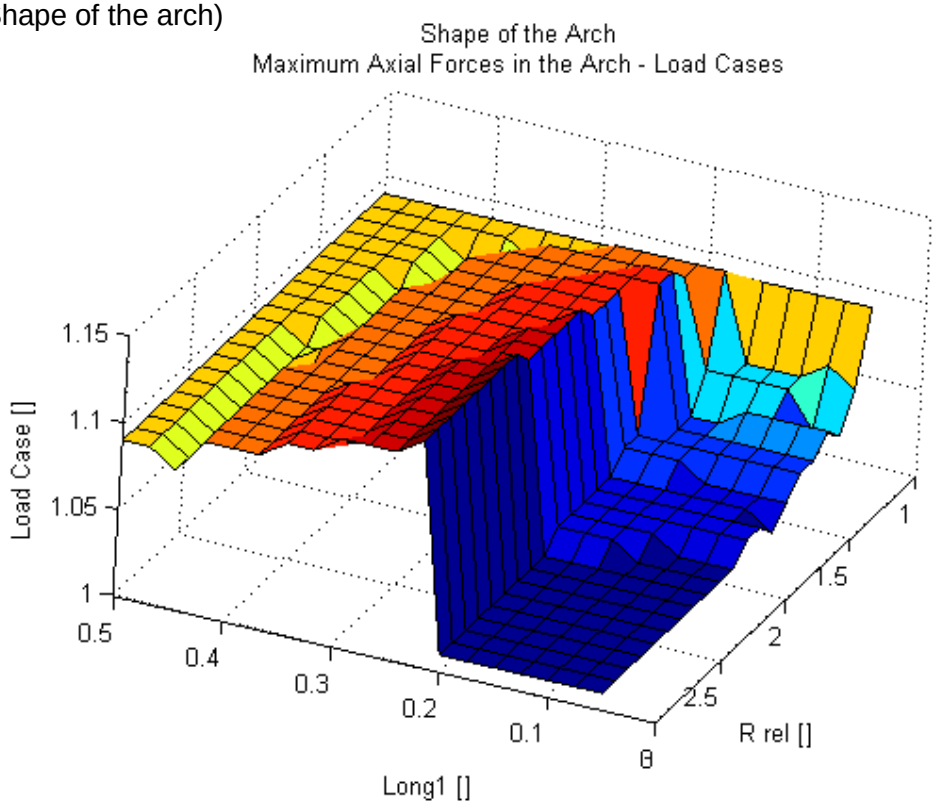


**Figure 108.** Corresponding load cases for the maximum axial compression forces in the arch (Shape of the arch)

### 3.2.1.6. Stresses in the arch

The Figure 109 shows the values for the maximum negative stresses in the arch for each bridge. The maximum stresses increase as $R_{rel}$ increases and as *long1* decreases, until a maximum value at $R_{rel}$ = 3 and *long1* = 0.05. For this bridge the maximum negative stress is -748012.80 kN/m$^2$ , 4.25 times the value obtained for a circular arch shape. This configuration is shown in the Figure 92.

The maximum negative stress for a parabolic arch is -165375.49 kN/m$^2$, 94% the value for a circular arch shape.

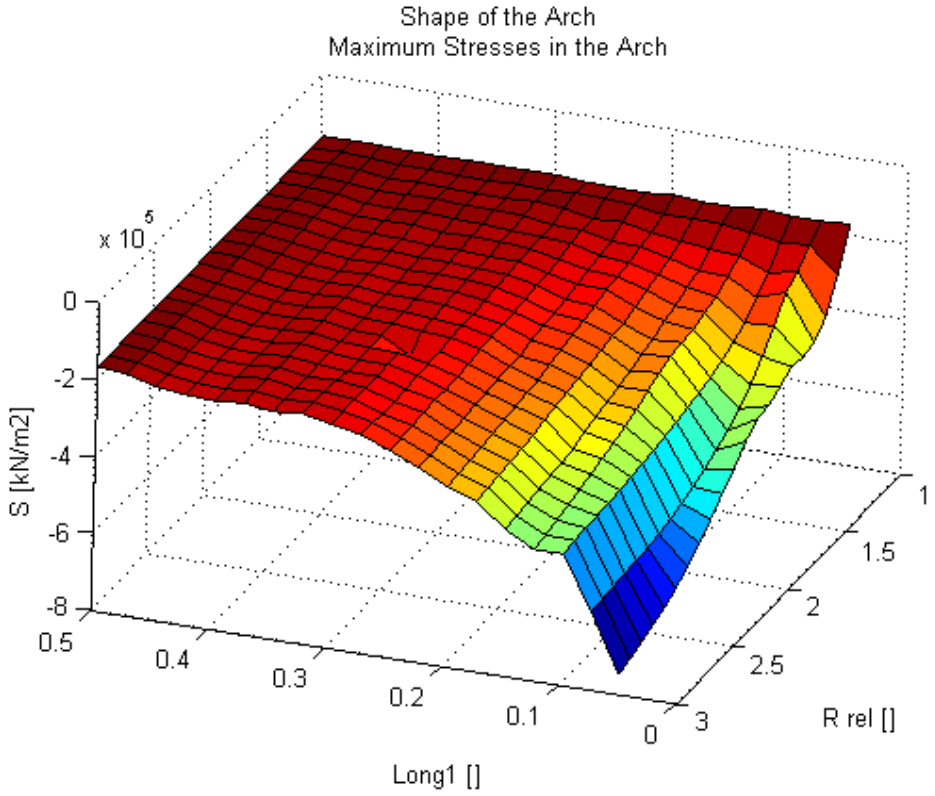


**Figure 109.** Maximum stresses in the arch (Variation of the shape of the arch)

The Figure 110 shows the X-coordinates where the maximum values occur. For *long1* higher than 0.3 the maximum bending moment presents the center of the span. Outside this range the maximum values occur less than 10 m from the left support.

The Figure 111 shows in a graphical format the load cases where the maximum values occur. For $R_{rel}$ bigger than 1.9 and *long1* smaller than 0.25 the corresponding load case is around 1.20, with the location of the punctual load near the left support. Outside this range the position of the punctual load is near the center of the span.

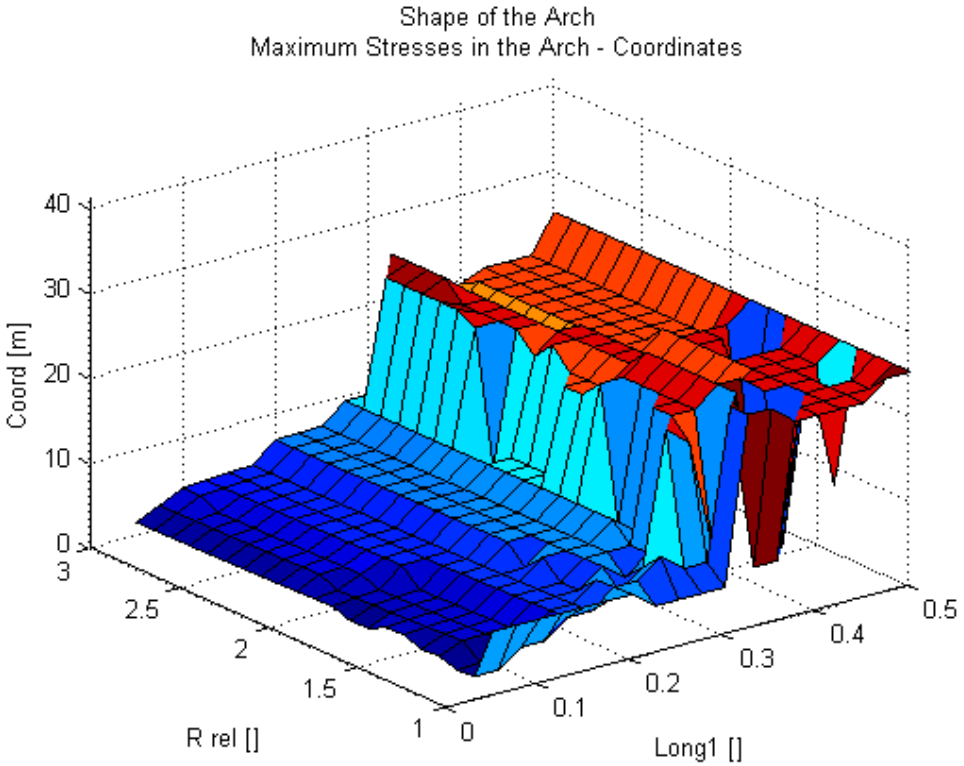


**Figure 110.** Corresponding X-coordinates for the maximum stresses in the arch (Shape of the arch)

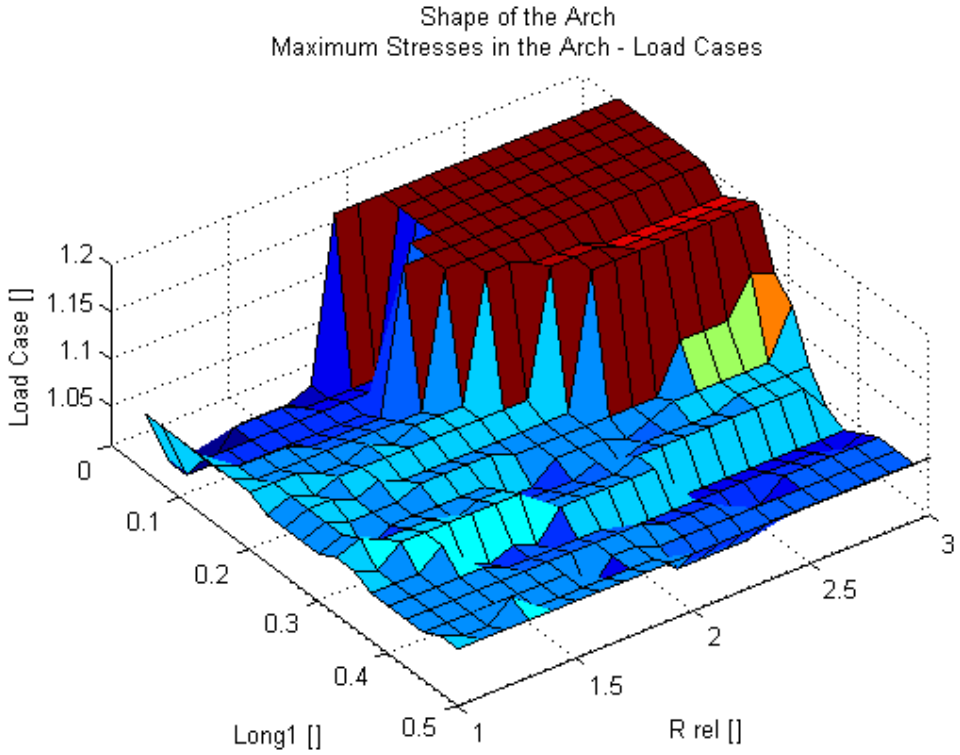


**Figure 111.** Corresponding load cases for the maximum stresses in the arch (Shape of the arch)

### 3.2.1.6. Stresses in the hangers

The Figure 112 shows the values for maximum stresses in the hangers for each bridge. The maximum stresses increase as $R_{rel}$ increases and as *long1* decreases until a maximum value at $R_{rel}$ = 3 and *long1* = 0.05. For this bridge the maximum stress is 988131.87 kN/m$^2$ , 7.91 times the value obtain for a circular arch shape. This configuration is shown in the Figure 92.
The maximum stress for a parabolic arch is 124616.42 kN/m$^2$, a value similar to the one obtained for a circular arch shape.

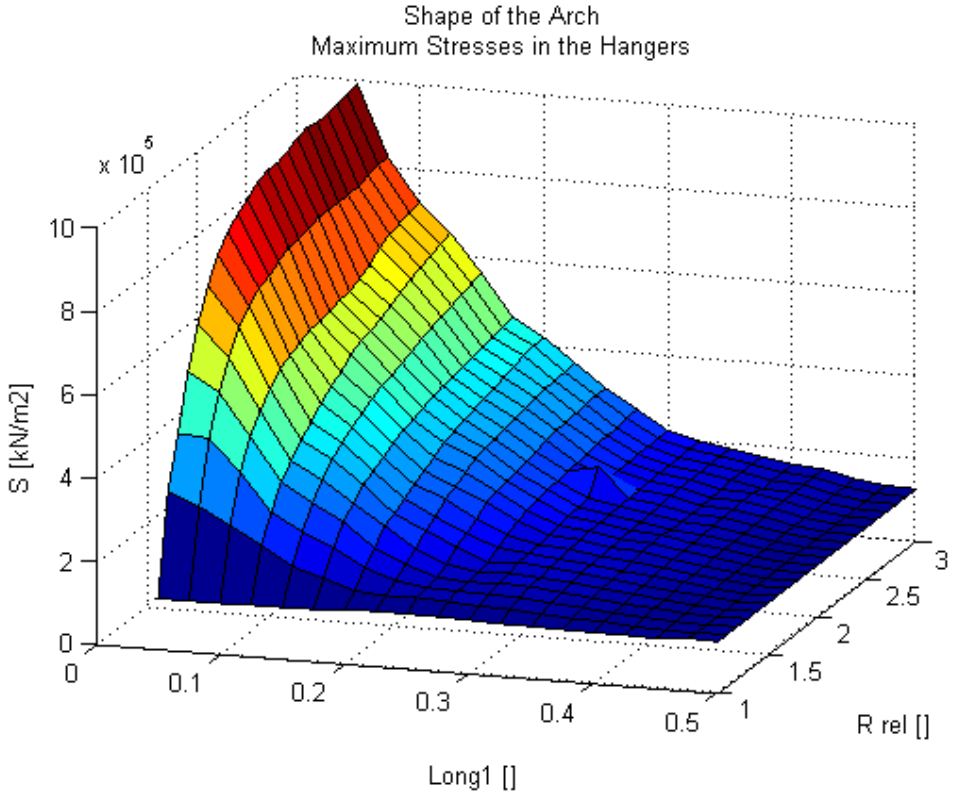


**Figure 112.** Maximum stresses in the hangers (Shape of the arch)

The figure 113 shows in a graphical format the number of the element where the maximum values occur. For *long1* smaller than 0.30, the corresponding elements correspond to the Set 1. For values of *long1* higher than 0.30 the elements where the maximum stress occur correspond to the Set 2. In both cases the hangers with the maximum stresses are in the right extreme of the span.

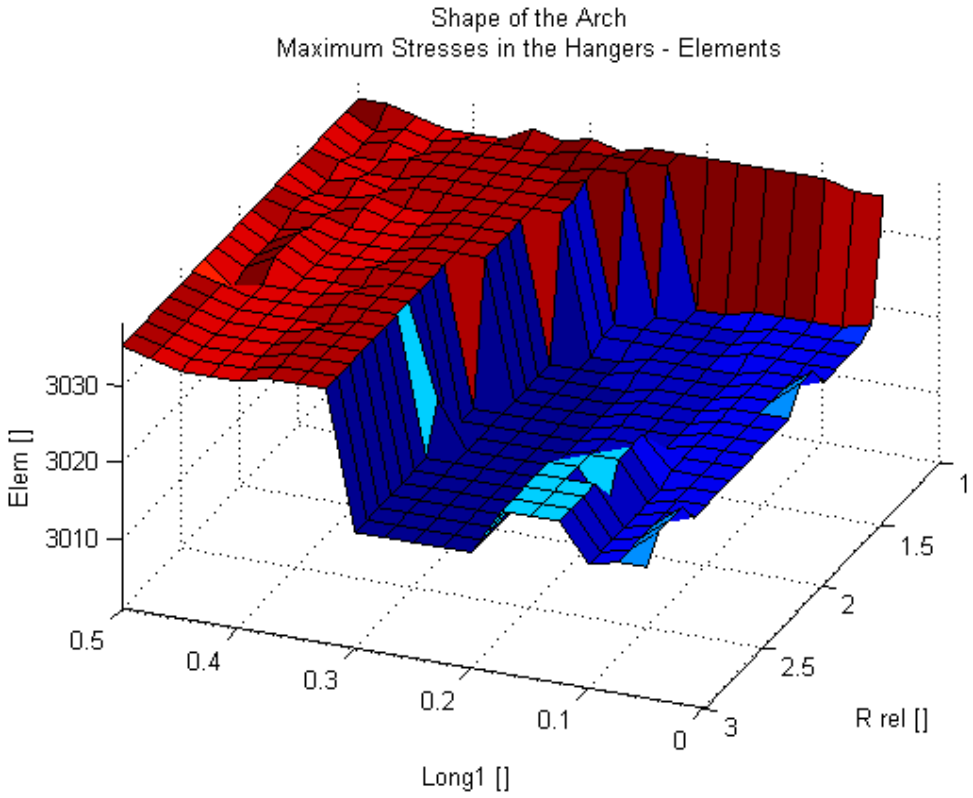


**Figure 113.** Corresponding elements for the maximum stresses in the hangers (Variation of the shape of the arch)

### 3.2.1.8. Relaxed hangers

The Figure 114 shows the number of relaxed hangers for each bridge. The prestressing of the hangers is not considered. The number of relaxed hangers increase as $R_{rel}$ increases and as *long1* decreases, until a maximum value at $R_{rel}$ = 3 and *long1* = 0.05, with 18 relaxed hangers.

The number of relaxed hanger for a circular arch shape is 2. For *long1* higher than 0.2 the number of relaxed hangers does not change significantly. For *long1* smaller than 0.25 and $R_{rel}$ smaller than 2.0 there are some configurations that present zero relaxed hangers. Two of this configurations are shown in the Figures 115 and 116.

The relaxed hangers are located in the extremes of the bridge, next to the supports, and sloping away from the center of the bridge.

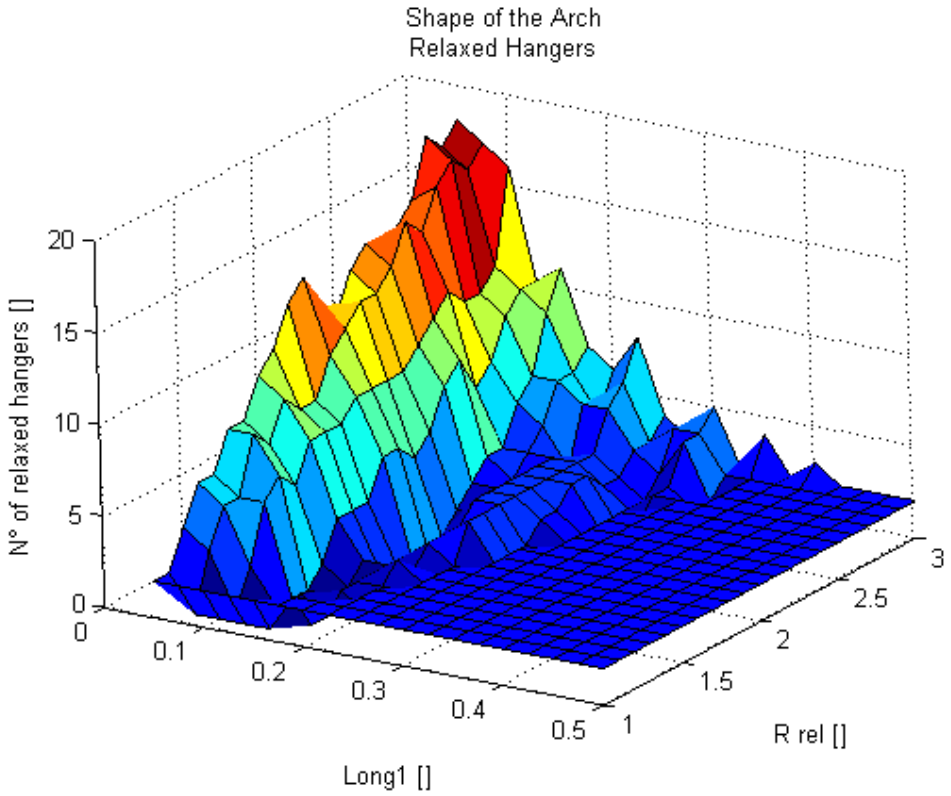


**Figure 114.** Relaxed hangers (Shape of the arch)

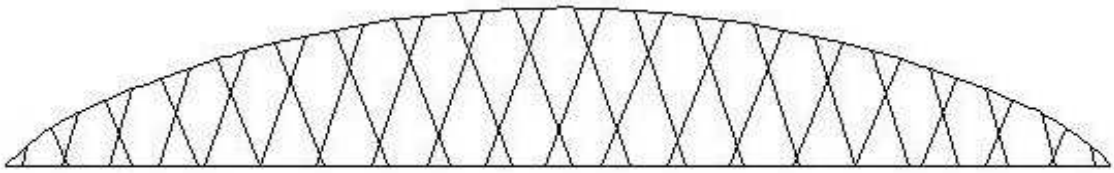

**Figure 115.** Arch shape: $R_{rel}$=1.1 ; *long1* = 0.075

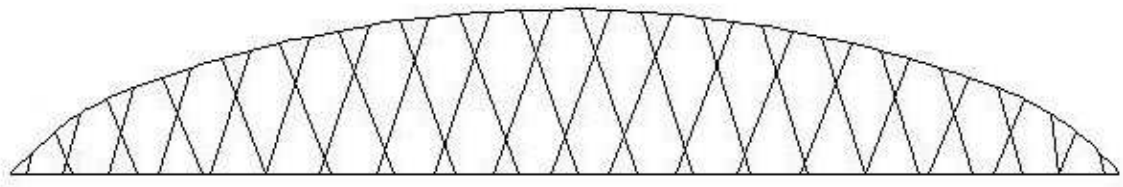

**Figure 116.** Arch shape: $R_{rel}$= 1.2 ; *long1* = 0.10

### 3.2.2. Conclusions

In the deck, the values for bridges with a parabolic arch or a circular arch are quite similar. The values for the bending moments and the stresses are the same in both cases, while the axial forces increase less than 5% for a parabolic arch.

The maximum bending moments in the deck have a minimum when the form of the arch is fully parabolic or fully circular. For *long1* higher than 0.45 the values do not change significantly, as the form of the arch still approaches a parabola. However, for smaller values of *long1*, little increments of $R_{rel}$ cause important increments of the bending moments, arriving to a peak for $R_{rel}$= 3.0 ; *long1* = 0.05. As the configuration approaches this point the behavior of the structure changes from an "arch behavior" to a "portico behavior", with two "columns" and a "beam". While the upper chord presents an "arch behavior" the maximum bending moments in the deck are in its center. When the structure act as a "portico" the maximum bending moments are in the supports.

On the other hand, the axial forces decrease as the structure approaches to a "portico" behavior. While the structure act as an arch, the deck takes the horizontal forces from the upper chord. As the structure approximate a "portico" this horizontal forces decrease.

However, even if for a "portico" configuration the axial forces are inferior, the maximum stresses are almost four times higher.

As in the deck, the stress in the arch for bridges with a parabolic or a circular arch are quite similar, around 6% smaller for the first.

The maximum bending moments in the arch have small values for parabolic of circular arches. As *long1* decreases and $R_{rel}$ increases the structure approaches to a "portico" behavior, and the value of the bending moments increase until a maximum at $R_{rel}$= 3.0 ; *long1* = 0.05. In an inverse way, the graphic for the maximum axial forces in the arch shows that at this points the compression forces arrive to a minimum. These is because while the arch resolved into compressive stress, the "portico" does it into bending stress, hence the axial forces are reduced. However, as the structure approximates a "portico", the stresses increase significantly, arriving in the worst cases to four times the value for circular arches.

The bending moments in the deck correspond to those in the arch, as in both cases the highest values occur for the same configuration, and the lowest values are obtained for fully circular and parabolic arches. The increment is more important in the arch than in the deck. For the arch the maximum values are 13 times higher than the minimum, while for the deck are only 4 times higher.

In the same way, the axial forces in the deck correspond to the axial forces in the arch. In this case the reduction is 20% for the deck and 23% for the arch.

From this we can say that the shape of the arch has an important influence on the values of the bending moments in the deck and arch, while the variation in the axial forces due to this variable it is not significantly. Hence, it is expectable that the form of the graphic for maximum stresses in the arch and the deck corresponds to the one obtained for the bending moments.

The stresses in the hangers also increase as the structures start to behave as a “portico” instead than as an arch. The maximum stresses in the worst cases are 8 times higher than for circular arches.

In the arch and the hangers the stresses are lower than the admissible values. The fact that the stresses in the deck are higher than the admissible values remarks the importance of the prestressing of the deck. As the prestressing is not considered in this thesis, this is expected.

The relaxation of the hangers is not influenced significantly for values of *long1* higher than 0.2. For values smaller than 0.2, the number of relaxed hangers increases as *long1* decreases, until a maximum of 18 in the worst cases.

However for small values of $R_{rel}$ and *long1* good results are achieved for some particular configurations, obtaining in some cases structures with no relaxed hangers. This presents as a possibility for solving the problem of relaxing hangers: prestressing can be avoided by just changing the shape of the arch near the supports.

## 3.3. Rise of the arch

In order to study the influence of different arch rises, 40 bridge are calculated. In most of the existing network arch bridges the rise of the arch is between 14% and 17% of the span [TNA]. This is because of aesthetic reasons, as higher rises do not look good. For this examination bridges with rises between 14% and 18% are calculated.

A radial arrangement is used for this examination, with a cross angle of 45°. The bridge configuration is shown in figure 65. The rise of this bridge is 6.05 m / 41.00 m = 14.8%.

The results obtained for this bridge are:

- Maximum bending moment in the deck: 656.50 kNm
- Maximum axial force in the deck: 3049.99 kN
- Maximum Stress in the deck: 11520.15 kN/m$^2$
- Maximum bending moment in the arch: 78.19 kNm
- Maximum axial force in the arch: -3633.84 kN
- Maximum stress in the arch: -142108.92 kN/m$^2$
- Maximum stress in the hangers: 141278.44 kN/m$^2$
- Number of relaxed hangers: 0

The number of element for the hangers is assigned as shown in the Figure C.2 in the Appendix C.

### 3.3.1. Results

The results are showed in the following diagrams. Every ordinate corresponds to one value of each bridge.

#### 3.3.1.1. Bending moments in the deck

The Figure 117 shows the absolute values for maximum bending moments in the deck for each bridge. The bending moments decrease from a rise of 14.0% to a rise of 17.0%.

The highest bending moment is 675.40 kNm, for a rise of 14.0%. At a rise of 17.0% the bending moment is 600.10 kNm: 89% of the highest value.

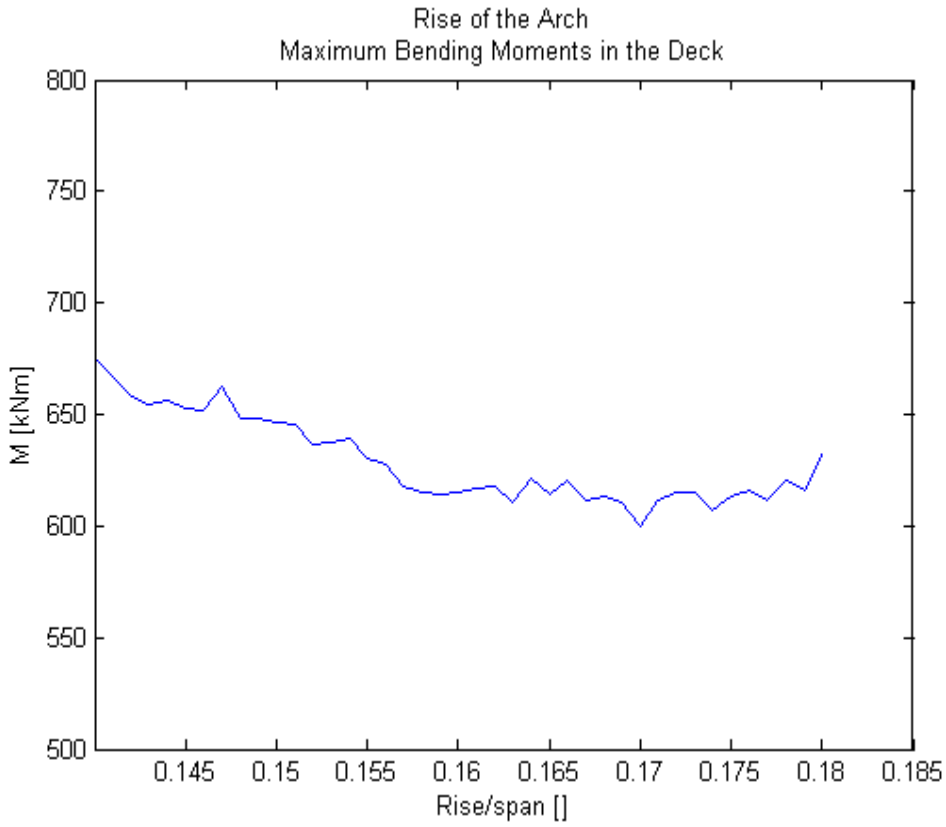


**Figure 117.** Maximum bending moments in the deck (Rise of the Arch)

### 3.3.1.2. Axial Forces in the deck

The Figure 118 shows the values for maximum axial forces in the deck for each bridge. The values decrease linearly from 3225.03 kN for a rise of 14%, to 2466.34 kN for a rise of 18%, 76% of the highest value.

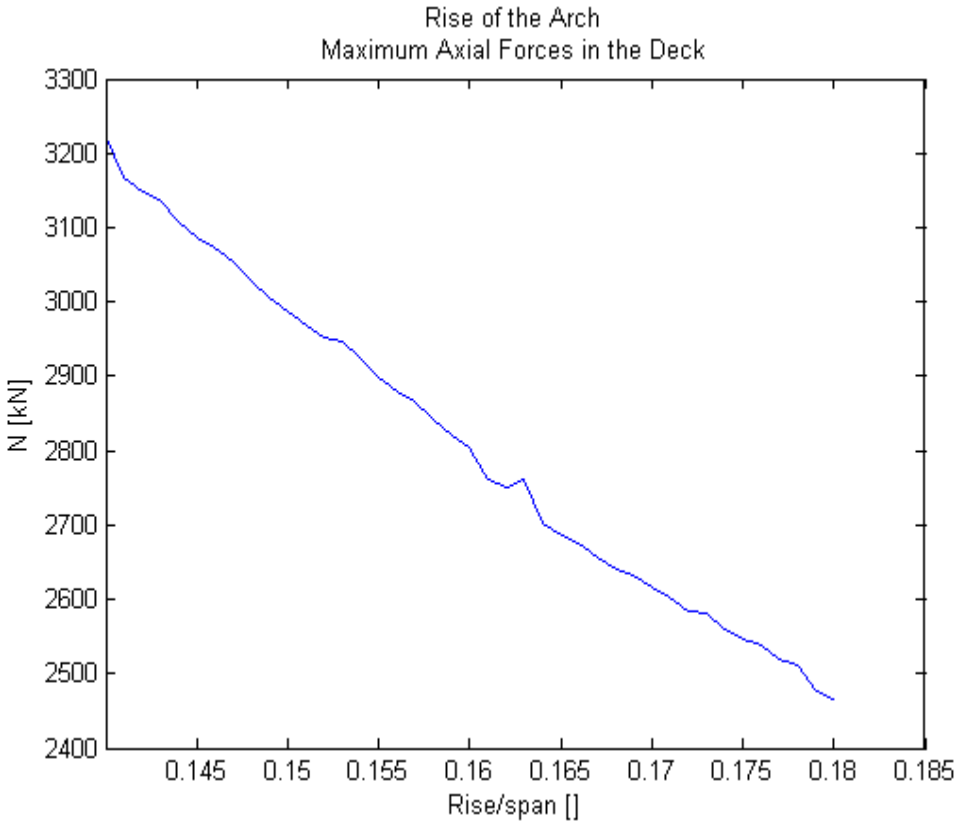


**Figure 118.** Maximum axial forces in the deck (Rise of the Arch)

### 3.3.1.3. Stresses in the deck

The Figure 119 shows the values for maximum stresses in the deck for each bridge. The stresses decrease from a rise of 14% to a rise of 17.9%.

The maximum stress for a rise of 14% is 12023.53 kN/m$^{2.}$. For a rise of 17.9% the stress is 10051.82 kN/m$^2$, 84% of the highest value.

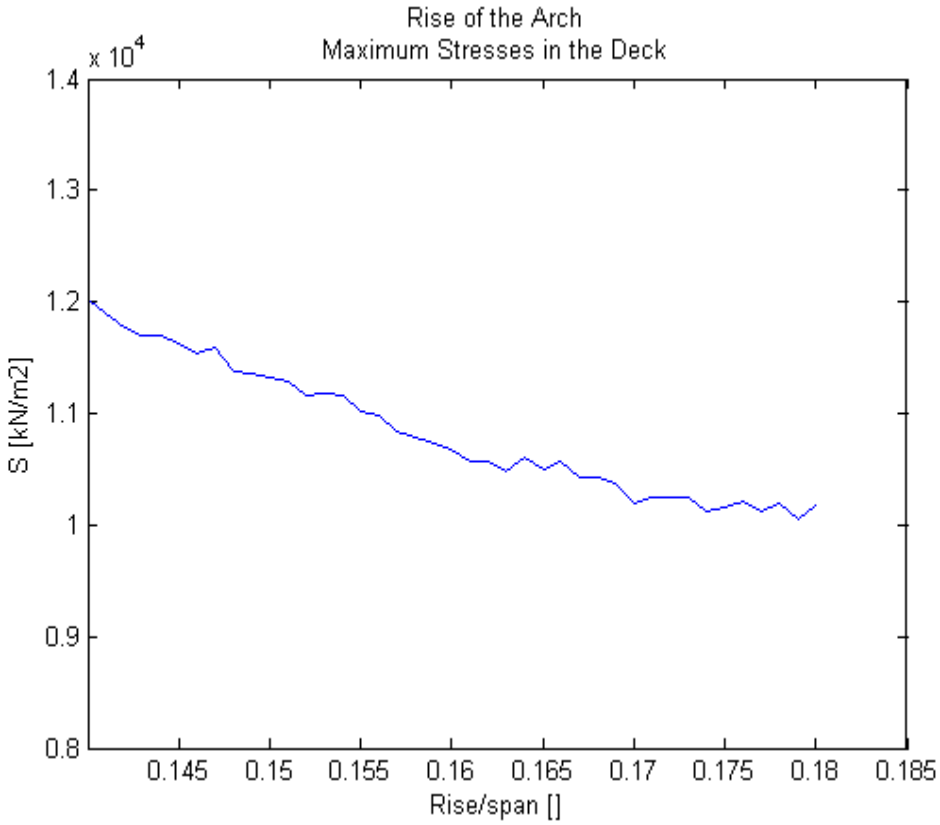


**Figure 119.** Maximum stresses in the deck (Rise of the Arch)

### 3.3.1.4. Bending moments in the arch

The Figure 120 shows the absolute values for maximum bending moments in the arch for each bridge. The curve fluctuates around a value of approximately 84 kNm. The fluctuations have a magnitude of 20 kN, 23% of the previous value. The highest value occurs for a rise of 17.5% and is equal to 104.44 kNm. The lowest value presents for a rise of 15.9% and it has value of 64.73 kNm.

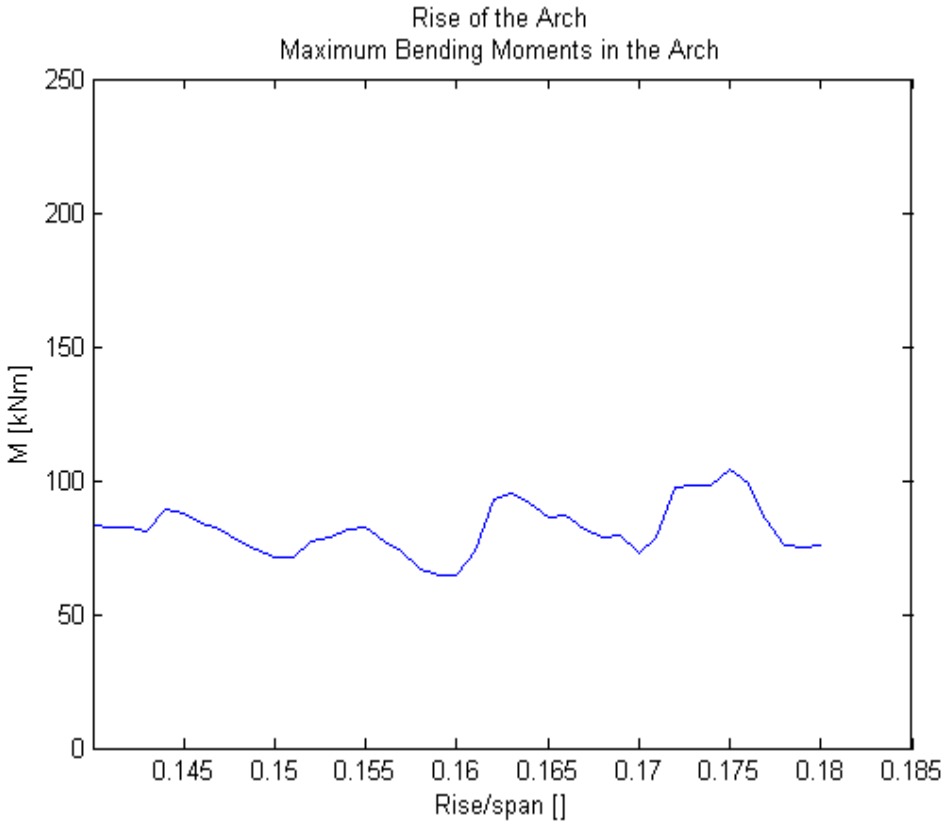


**Figure 120.** Maximum bending moments in the arch (Rise of the Arch)

### 3.3.1.5. Axial forces in the arch

The Figure 121 shows the values for maximum axial compression forces in the arch for each bridge. The compression forces decrease linearly from -3757.05 kN for a rise of 14%, to -3137.57 kN for a rise of 18%: 83% of the highest value.

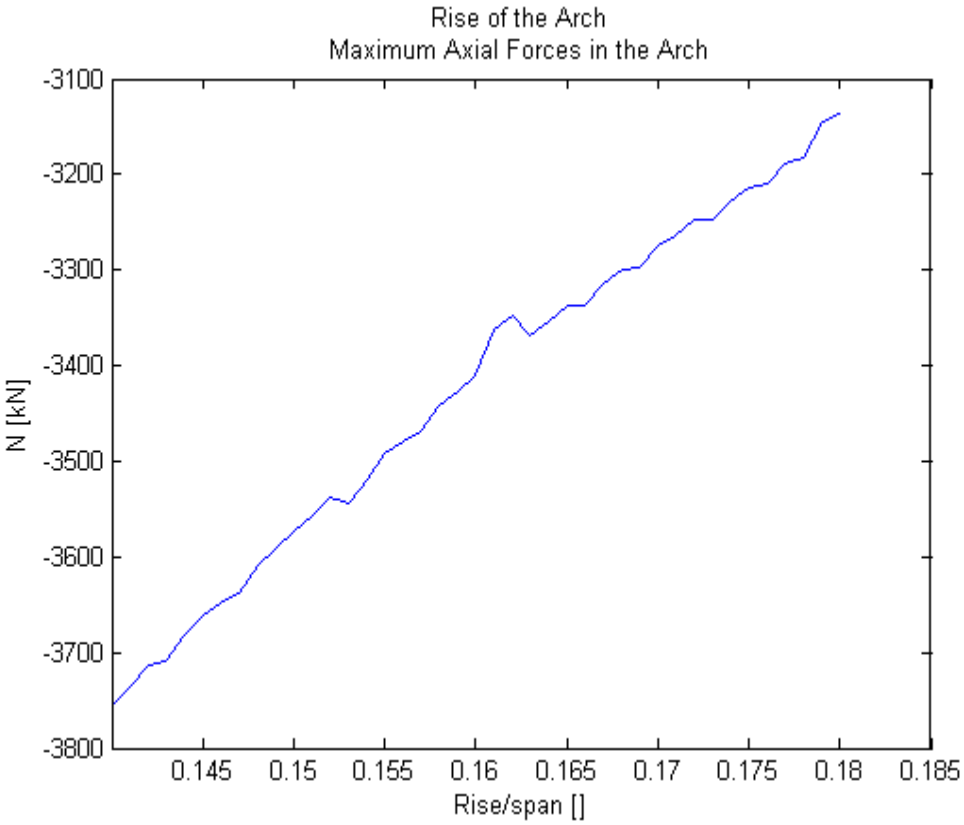


**Figure 121.** Maximum axial compression forces in the arch (Rise of the Arch)

### 3.3.1.6. Stresses in the arch

The Figure 122 shows the values for maximum stresses in the arch for each bridge. The negative stresses decrease from -152557.50 kN/m$^2$ at a rise of 14.2% to a value of -130315.31 kN/m$^2$ at a rise of 17.9%: 85% of the highest value. The fluctuations in the curve have a magnitude of 6000 kN/m$^2$, 4% of the maximum negative stress.

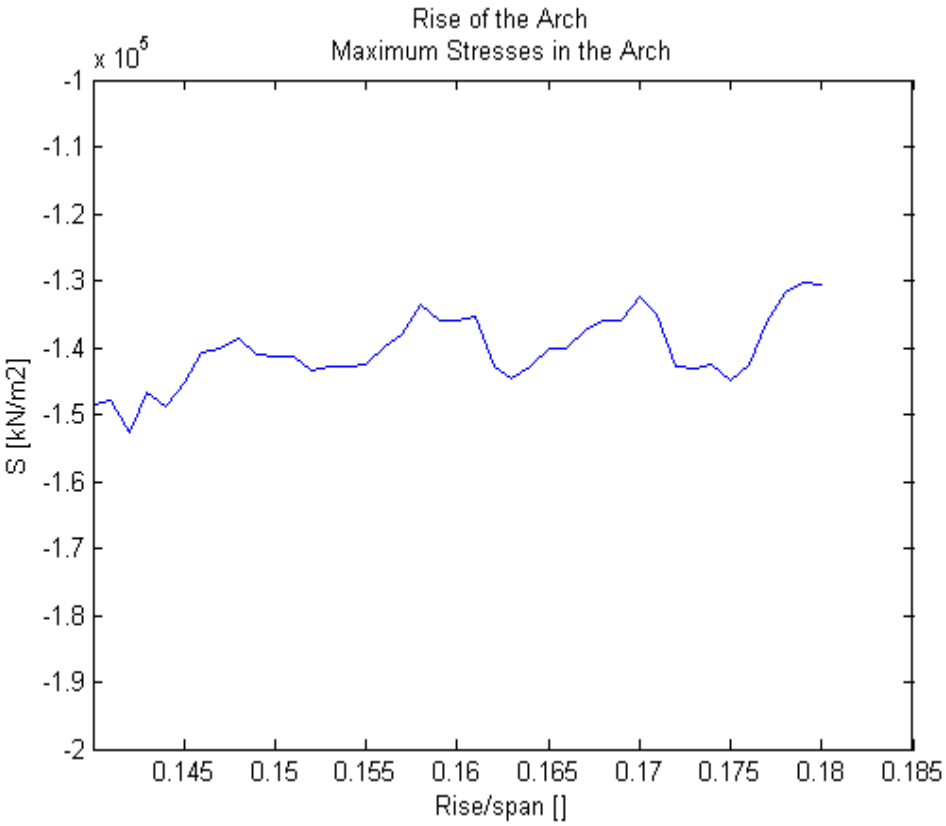


**Figure 122.** Maximum stresses in the arch (Rise of the Arch)

### 3.3.1.7. Stresses in the hangers

The Figure 123 shows the values for maximum stresses in the hangers for each bridge. The stresses decrease from 144566.99 kN/m$^2$ at a rise of 14.4% to a value of 135407.66 kN/m$^2$ at a rise of 18%: 94% of the highest value. The fluctuations in the curve have a magnitude of 1500 kN/m$^2$, 1% of the highest value.

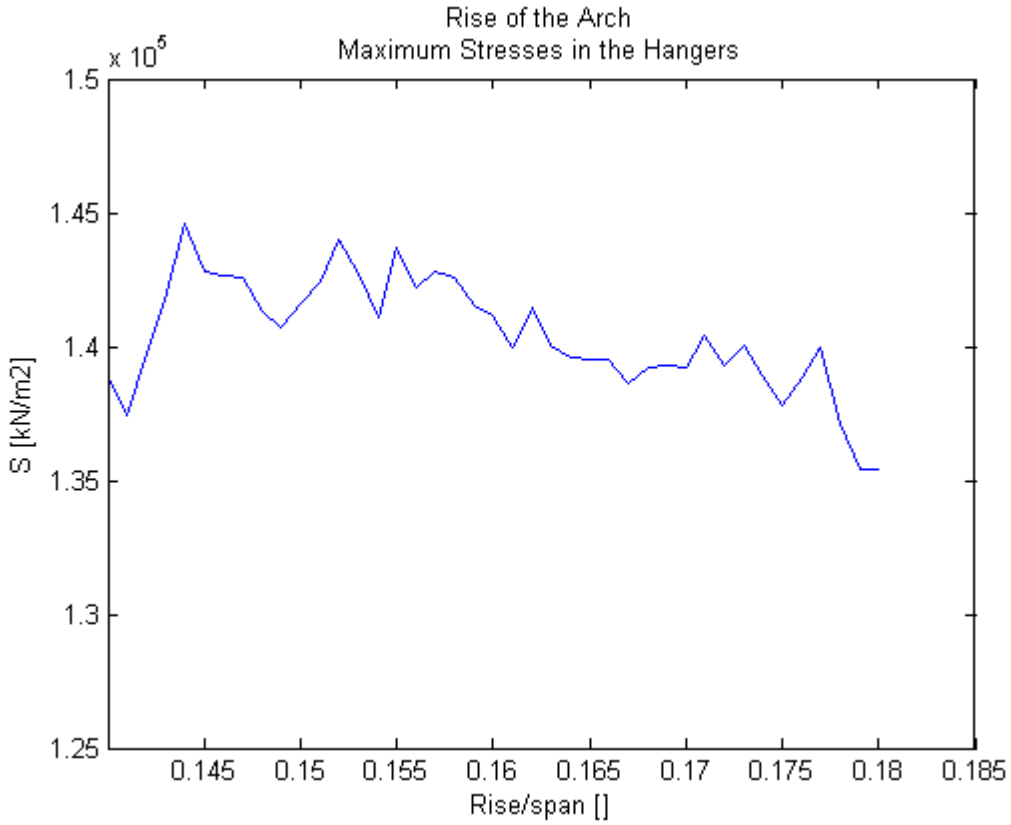


**Figure 123.** Maximum stresses in the hangers (Rise of the Arch)

### 3.3.1.8. Relaxed hangers

There are no relaxed hangers in the bridges calculated.

## 3.3.2. Conclusions

The arch and the deck in the network arch bridges behave as the chords of a simply supported beam: the arch being in compression and the deck being in tension. The axial forces in the chords are inversely proporsional to the rise of the arch. As observed in the graphics for axial forces in the deck and the arch, a higher ratio between the rise and the span reduce the compression and tension forces in the chords.

This also occurs for the bending moments, but the reduction is much smaller.

Finally we can observe that the stresses in the arch, the deck and the hangers are reduce as the ratio between the rise and the span is incremented.

Nevertheless the advantages of higher rises, aesthetic reason should be considered, limiting the rise of the arch to values between 14% and 17%

## 3.4. Number of hangers

In order to study the influence of the number of hangers 58 bridge are calculated. The number of hangers in the models varies from 19 to 76.

A radial arrangement is used for this examination, with a cross angle of 45°. The bridge configuration is shown in the Figure 65. This bridge has 38 hangers.

The results obtained for this bridge are:

- Maximum bending moment in the deck: 650.80 kNm
- Maximum axial force in the deck: 3045.90 kN
- Maximum Stress in the deck: 11507.07 kN/m$^2$
- Maximum bending moment in the arch: -96.27 kNm
- Maximum axial force in the arch: -3642.89 kN
- Maximum stress in the arch: -146467.12 kN/m$^2$
- Maximum stress in the hangers: 123037.74 kN/m$^2$
- Number of relaxed hangers: 0

The number of element for the hangers is assigned as shown in the Figure C.2 in the Appendix C.

### 3.4.1. Results

The results are showed in the following diagrams. Every ordinate corresponds to one value of each bridge.

#### 3.4.1.1. Bending moments in the deck

The Figure 124 shows the absolute values for maximum bending moments in the deck for each bridge. The values become smaller as the number of hangers increase. However, the decrease of the moments is higher for bridges with less than 30 hangers than for bridges with more than 30 hangers. The bending moments decrease from 714.91 kNm for 19 hangers to 646.89 kNm for 31 hangers: a reduction of 10%. On the other hand, the maximum bending moment for a bridge with 43 hangers is 635.89 kNm, a reduction of 2% in comparison with the bending moment obtained for a bridge with 31 hangers.

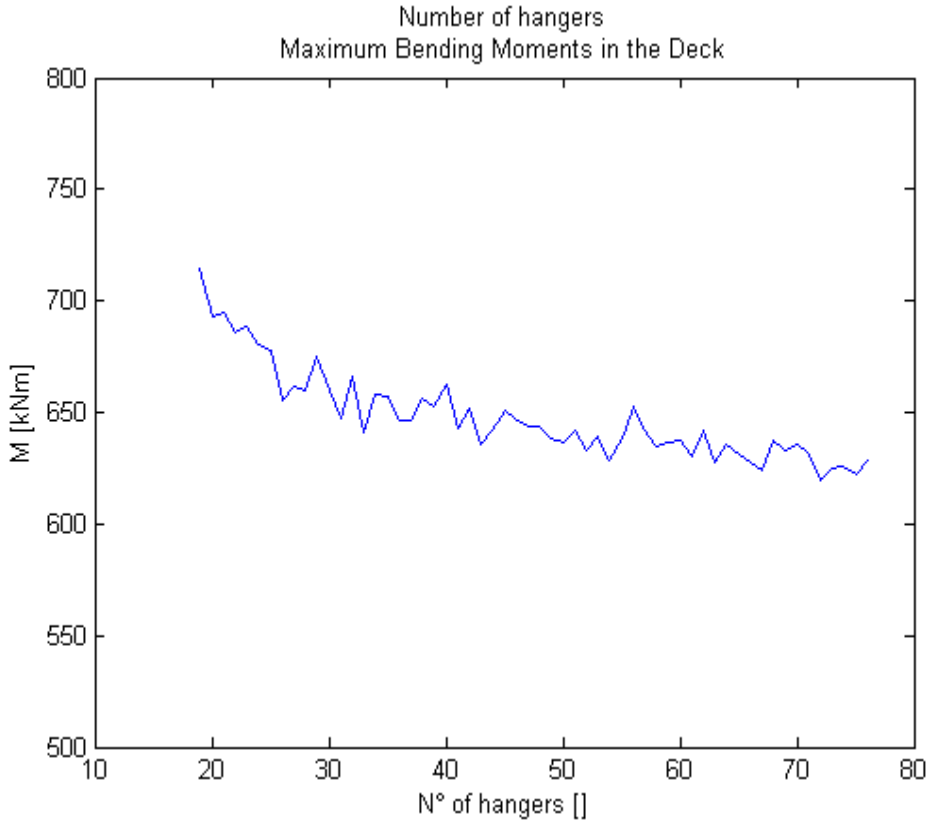


**Figure 124.** Maximum bending moments in the deck (Number of Hangers)

### 3.4.1.2. Axial forces in the deck

The Figure 125 shows the values for maximum axial forces in the deck for each bridge. As the number of hangers is higher, the axial forces increase.

The maximum value for a bridge with 22 hangers is 2986.14 kN. For a bridge with 76 bridge the axial force is equal to 3111.60 kN. This implies an increment of 4%.

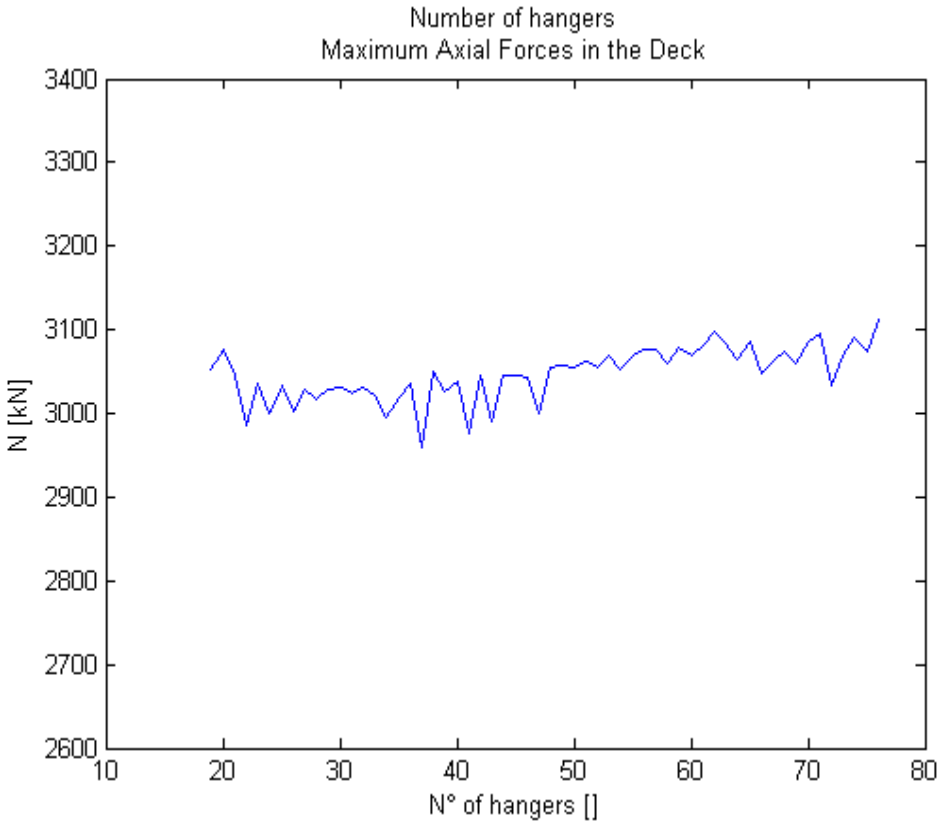


**Figure 125.** Maximum axial forces in the deck (Number of Hangers)

### 3.4.1.3. Stresses in the deck

The Figure 126 shows the values for maximum stresses in the deck for each bridge. The values become smaller as the number of hangers increase. However, the decrease of the stresses is higher for bridges with less than 30 hangers than for bridges with more than 30 hangers. The stresses decrease from 12259.63 kN/m$^2$ for 19 hangers to 11431.33 kN/m$^2$ for 31 hangers, a reduction of 7%. On the other hand, the maximum stress for a bridge with 43 hangers is 11294.00 kN/m$^2$, a reduction of 1% in comparison with the stress obtained for a bridge with 31 hangers.

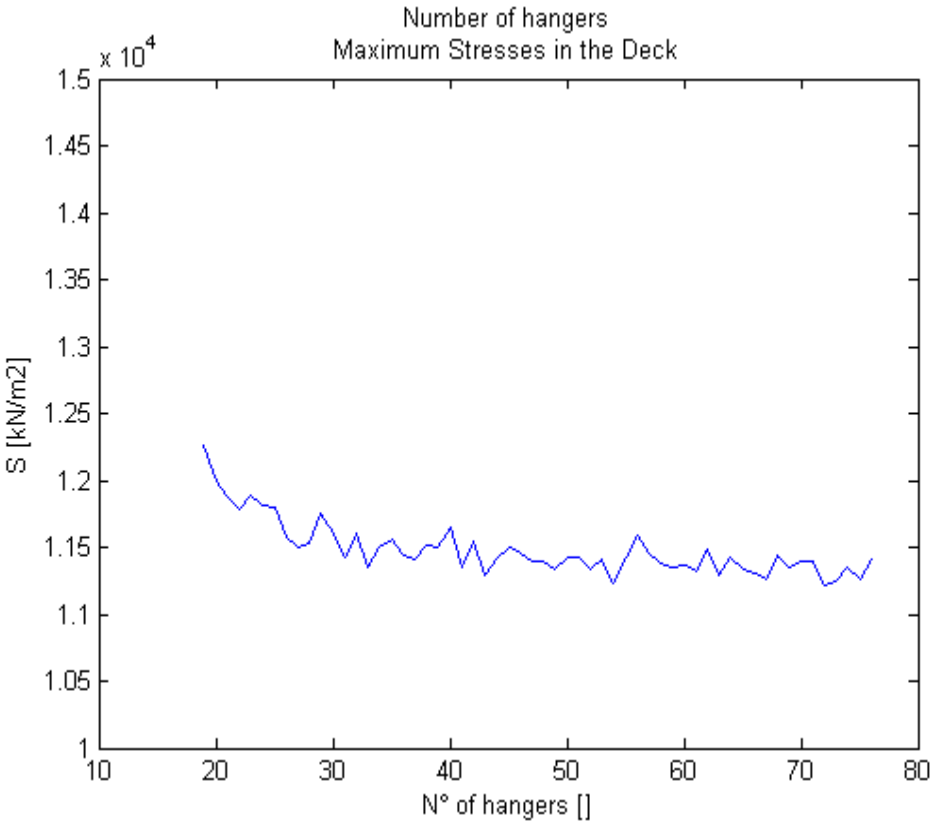


**Figure 126.** Maximum stresses in the deck (Number of Hangers)

### 3.4.1.4. Bending moments in the arch

The Figure 127 shows the absolute values for maximum bending moments in the arch for each bridge. As the number of hangers becomes higher, the bending moments decrease.
The maximum value for a bridge with 19 hangers is 116.19 kN. For a bridge with 76 bridge the bending moment is equal to -86.46 kN. The decrease of the absolute value of the bending moments is of 26%.

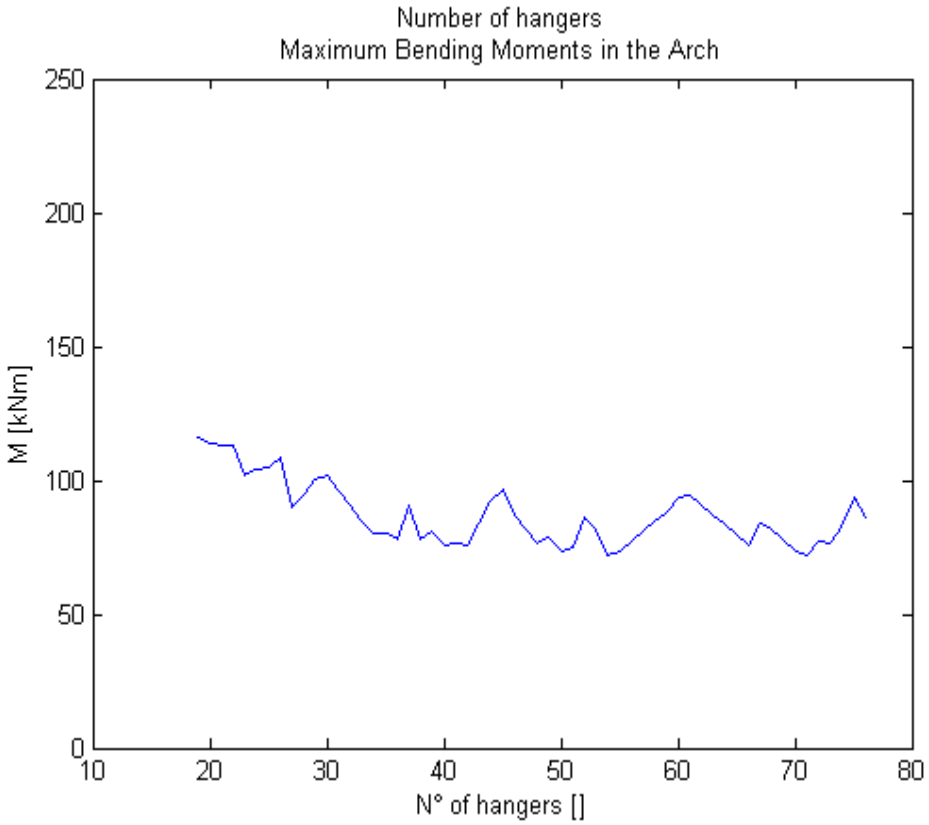


**Figure 127.** Maximum bending moments in the arch (Number of Hangers)

### 3.4.1.5. Axial forces in the arch

The Figure 128 shows the values for maximum axial compression forces in the arch for each bridge. The compression forces become higher as the number of hangers increase.

The maximum compression force in a bridge with 19 hangers is -3574.47 kN, while for a bridge with 76 hangers, it is -3789.41 kN. The increment is of 6%.

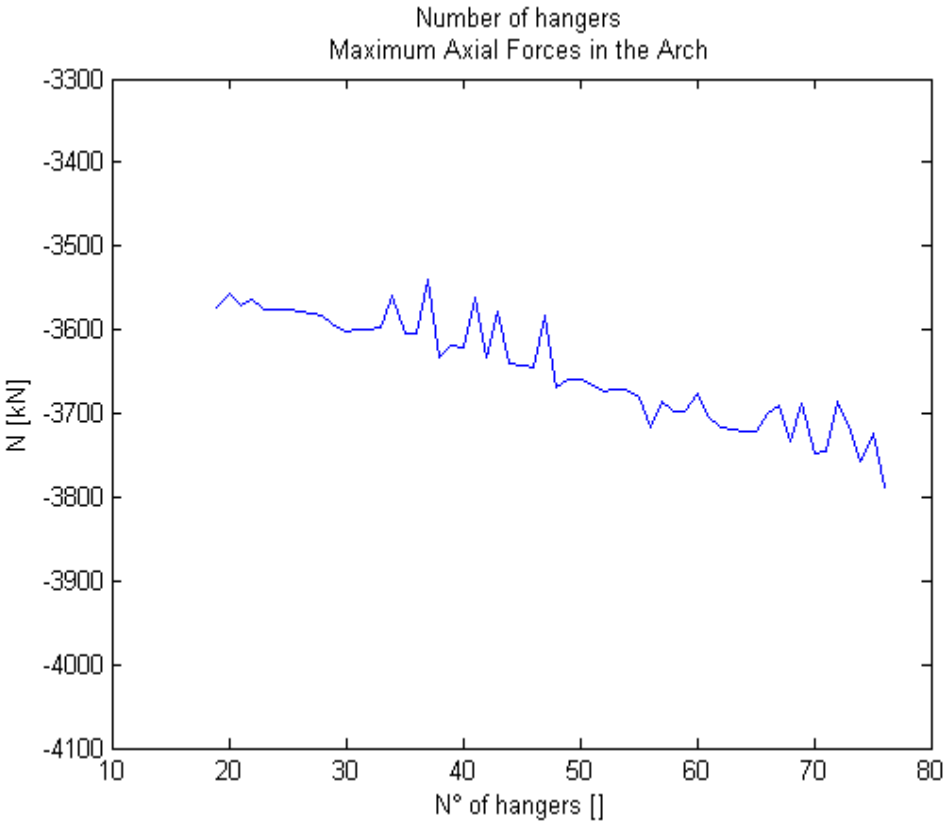


**Figure 128.** Maximum axial compression forces in the arch (Number of Hangers)

### 3.4.1.6. Stresses in the arch

The Figure 129 shows the values for maximum stresses in the arch for each bridge. The values decrease as the number of hangers increases. However, the decrease of the stresses is higher for bridges with less than 35 hangers than for bridges with more than 35 hangers. The values decrease from -157180.26 kN/m$^2$ for 19 hangers to -146273.00 kN/m$^2$ for 35 hangers, a reduction of 7%. On the other hand, the maximum stress for a bridge with 51 hangers is -144843.36 kN/m$^2$, a reduction of 1% in comparison with the stress obtained for a bridge with 35 hangers.

There are fluctuations in the curve with a medium magnitude of 7000 kN/m$^2$, 4% of the highest value.

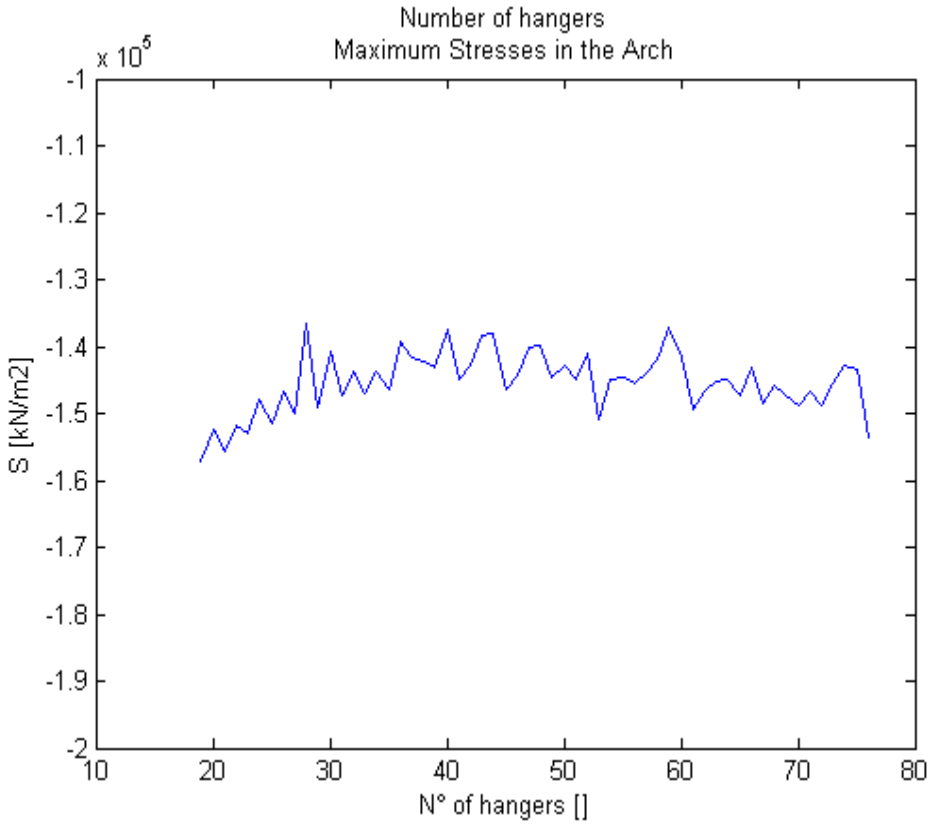


**Figure 129.** Maximum stresses in the arch (Number of Hangers)

### 3.4.1.7. Stresses in the hangers

The Figure 130 shows the values for maximum stresses in the hangers for each bridge. The stresses decrease as the number of hangers increases. However, the decrease of the stresses is higher for bridges with less than 50 hangers than for bridges with more than 50 hangers. The values decrease from 216613.45 kN/m$^2$ for 24 hangers to 114323.32 kN/m$^2$ for 50 hangers, a reduction of 47%. On the other hand, the maximum stress for a bridge with 76 hangers is 80685.07 kN/m$^2$, a reduction of 29% in comparison with the stress obtained for a bridge with 50 hangers.

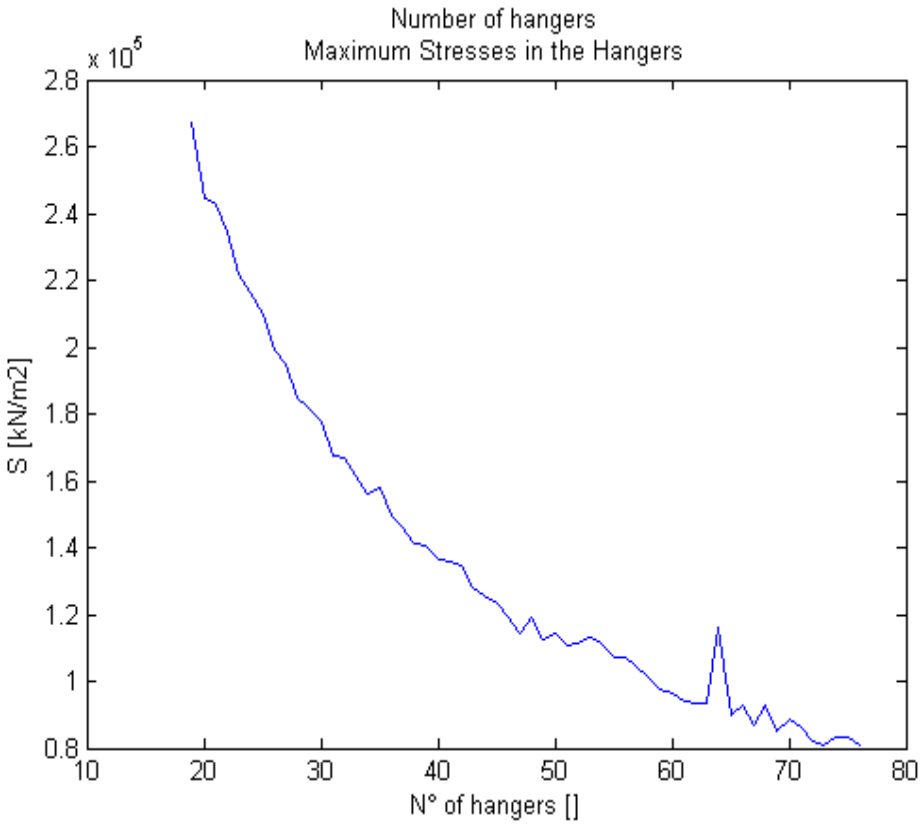


**Figure 130.** Maximum stresses in the hangers (Number of Hangers)

### 3.4.1.8. Relaxed hangers

The Figure 131 shows the number of relaxed hangers for each bridge. As the number of hangers increase, the tendency of the hangers to relax also increase. For bridges with a number of hangers between 20 and 38 there are no relaxed hangers. From 39 to 45, the number of relaxed hangers varies between 1 and 0. Again, between 46 and 55 no relaxation of the hangers is found.

For a number of hangers between 56 and 74 the number of relaxed hangers varies between 1 and 2. A bridge with 75 hangers presents 3 relaxed hangers.

The relaxed elements are located in the extremes of the bridge, next to the supports.

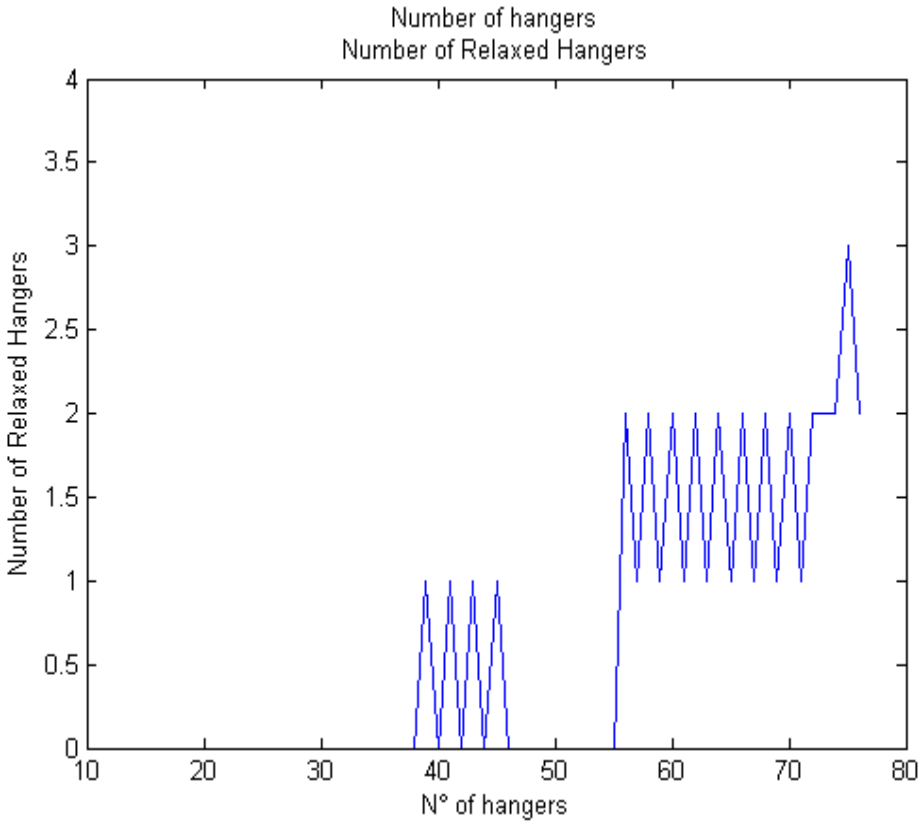


**Figure 131.** Relaxed hangers (Number of Hangers)

### 3.4.2. Conclusions

High number of hangers results in lower values for the stresses in arch, deck and hangers.

However, the influence of the number of hangers over the bending moments in the deck is higher for a small number of hangers: a small variation in the number of hangers will cause a higher variation of the bending moments if the bridge has less than 30 hangers.

As the influence of the number of hangers over the axial forces in the deck and the arch is very small (less than 6%), the variation of the stresses follows the variation of the bending moments. For this reason, the influence of the number of hangers over the stresses is higher when the bridge has a small number of hangers: less than 30 in the case of the deck; less than 35 in the case of the arch.

The same applies for the stresses in the hangers: the influence is higher for bridges with small number of hangers: less than 50.

Always considering aesthetic matters, no more that 40 hangers should be used. After this point the decrease in the stresses as the number of hangers increase is not important, and for more than 40 hanger, relaxation occur.

# Chapter 4
# Study of Alternatives

For this Chapter, three different alternatives to the original configuration are proposed.

Considering the studies from Chapter 3, two parameters are chosen for the comparison: the hanger arrangement and the shape of the arch. In the alternative configurations no changes are made regarding the rise of the arch or the number of hangers. It is considered that this parameters are not important in comparison with the chosen ones. Besides, maintaining the rise of the arch and the number of hangers in the different alternatives provides a better point of comparison between the three systems.

The Section 4.1 presents the three alternatives with a brief description of each one.

In the Section 4.2 the results obtained are analyzed and compared.

Finally, the conclusions and final overlook are exposed in the Section 4.3.

## 4.1. Proposed Configurations

### 4.1.1. Original Configuration

The proposed alternatives are compared with the original configuration of the Lužnice Bridge, described in the Chapter 2. In this case the prestressing of the hangers is considered in order to avoid relaxation.

### 4.1.2. Alternative A

In network arch bridges, a correct choice of the hangers arrangement can improve significantly the stresses in deck, arch and hangers. For the Alternative A, some characteristics of the original bridge are maintained (number of hangers, rise of the arch) and a different configuration of the hangers is proposed.

The alternative A is based in the configuration presented in the Section 3.1.1. : an arrangement based on the linear variation of the slopes. A circular arch shape is used and prestressing of the hangers is not considered.

For this configurations, the lowest stresses in the deck and the arch present for small initial angles and large angle increments. However, this arrangements results in the highest stresses in

the hangers. On the other hand, to obtained small stresses in the hangers large initial angles and small angle increments should be chosen, resulting in high stresses for arch and deck. In addition, small initial angles and small angles increments cause relaxation of the hangers. Hence, hanger arrangements with large initial angles and large angle increments should be used.

An initial angle of 81° and an increment angle of 3 .4° are chosen. The Figure 132 shows a bridge that corresponds to this configuration.

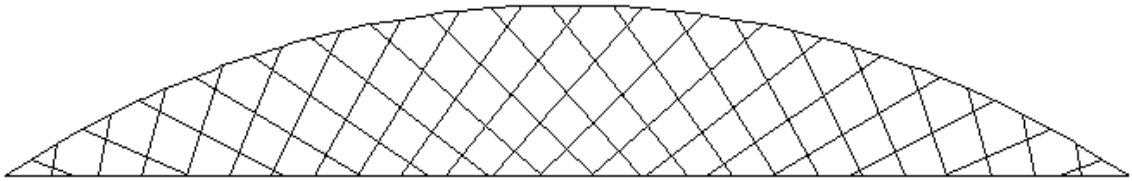

**Figure 132.** Alternative A

### 4.1.3. Alternative B

For the Alternative B, the number of hangers and rise of the arch of the original bridge are maintained and a different configuration of the hangers is proposed.

The alternative B is based in the configuration presented in the Section 3.1.2.: the radial arrangement, proposed by Brunn and Schanack in their diploma thesis [BSC].

In the radial arrangement the lowest stresses for the arch and the deck are obtained for cross angles between 40° and 50°. The lowest stress es in the hangers present for cross angles smaller than 30°. However, the rate of increment fo r angles smaller than 50° is not important.

A cross angle of 41.5° is chosen. The Figure 133 sh ows a bridge that corresponds to this configuration.

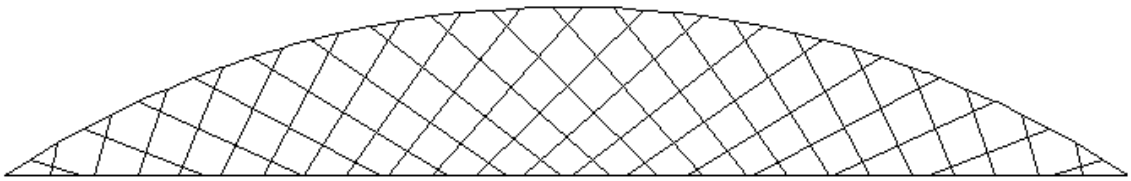

**Figure 133.** Alternative B

### 4.1.4. Alternative C

For the alternative C, all the characteristics of the original configuration are maintained, with the exception of the shape of the arch. While the form of the arch in the Lužnice Bridge is fully parabolic, for this alternative a circular arch shape arch is proposed with a parabolic shape in the extremes.

This configuration is chosen in order to examine the possibility of avoiding the prestressing of the hangers, and to study the shape of the arch as an alternative to prevent relaxation. Hence, the variables are defined in order to obtain no relaxed hangers.

The variables adopted are: a radio $R_{REL}$ 1.2 times the one obtained for a fully circular arch; and the distance *long1,* from where the circular arch begins, equal to 6.15 m: 15% of the span of the bridge. The Figure 89 shows this variables.

The Figure 134 shows a bridge that corresponds to this configuration.

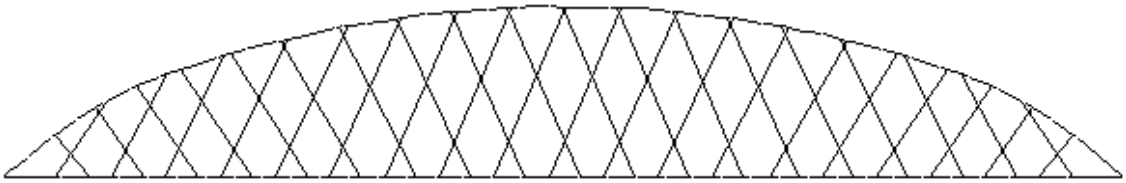

**Figure 134.** Alternative C

## 4.2. Comparison of Alternatives

### 4.2.1. Stresses in the deck

The Figure 135 shows the maximum and minimum stresses in the deck, for each coordinate.The curves correspond to the original configuration, and the three alternatives.

For the original configuration, the highest values for the maximum stresses in the deck occur in two peaks, at 25% and 75% of the span: 13590.88 kN/m$^2$ and 16395.36 kN/m$^2$ respectively.

The Alternatives A and B also present the highest values for the maximum stresses in two peaks. The position of the first peak coincides approximatly with the position for the original configuration, at 25% of the span. For the Alternative A, it has a value of 9317.21 kN/m$^2$ : 69% of the original stress. For the Alternative B, it has a value of 8263.14 kN/m$^2$ : 60% of the original stress.

For the Alternatives A and B the second peak has the form of a “plateau” from 22 m to 33 m from the left support (50% to 80% of the span). For the Alternative A, it has a value of 11983.45 kN/m$^2$ : 73% of the original stress. For the Alternative B, it has a value of 11496.77 kN/m$^2$ : 70% of the original stress.

On the other hand, the Alternative C presents three peaks, at 15%, 60% and 85% of the span. The stresses for the two higher peaks are 24107.60 kN/m$^2$ and 21023.61 kN/m$^2$ , wich are 1.47 and 1.28 times the highest value for the original configuration.

The smaller peak has a stress of 12467.09 kN/m$^2$, 90% of the original stress for this coordinate: 13867.63 kN/m$^2$. From this point to the end of the span, the stresses for the Alternative C are smaller than the stresses for the original configuration, always with a reduction of between 70% and 90%.

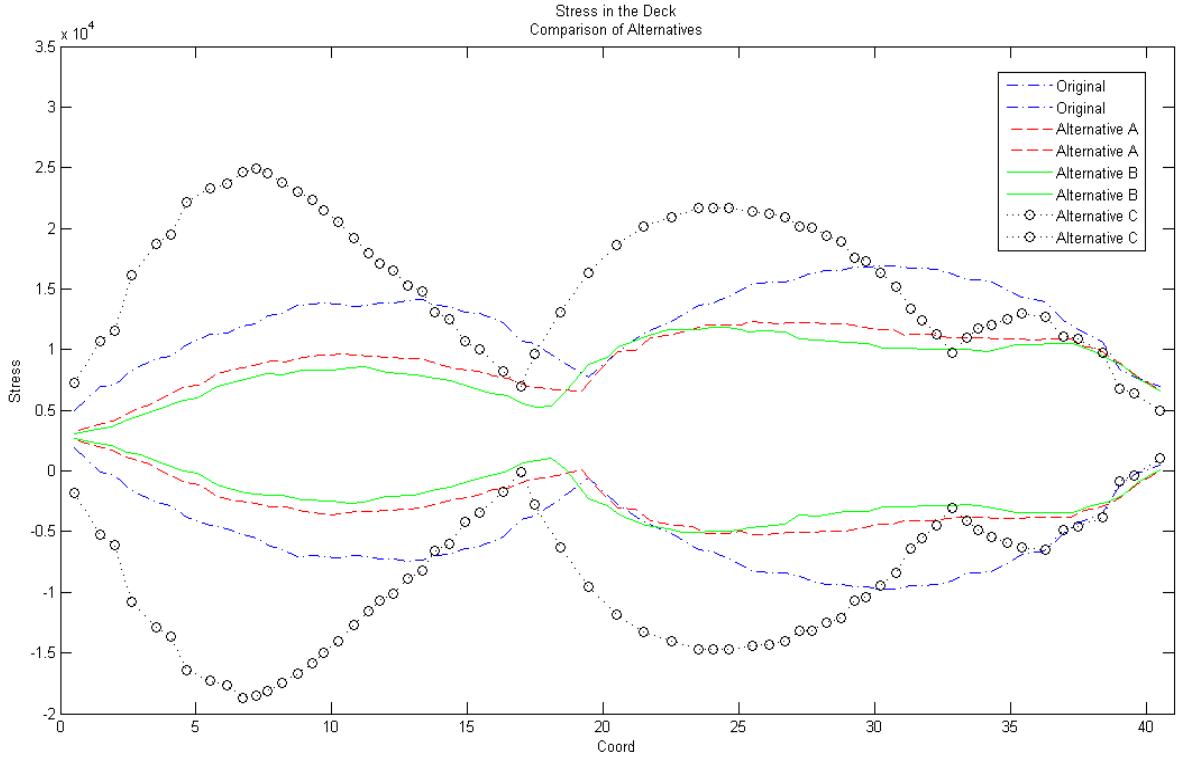


**Figure 135.** Comparison of Alternatives. Stresses in the deck

### 4.2.2. Stresses in the arch

The Figure 136 shows the maximum and minimum stresses in the arch, for each coordinate.The curves correspond to the original configuration, and the three alternatives.

The minimum value for the stresses in the original configuration is -175209.09 kN/m$^2$ and it is located 25 m from the left support, 60% of the span.

The curves that correspond to the Alternatives A and B have similar form and values. The stresses for the Alternative B are slightly smaller.

The minimum stress for the Alternative A is -145173.62 kN/m$^2$, 83% of the original stress. For the Alternative B the minimum stress is -141853.09 kN/m$^2$, 81% of the original value.

The minimum stress for the Alternative C is -224866.74 kN/m$^2$, 1.28 times the original stress.

In all the cases, the highest values for the maximum stresses occur in three peaks, at 10%, 50% and 85%. For the original configuration the highest value occurs in the second peak, while for the alternatives it happens in the first peak.

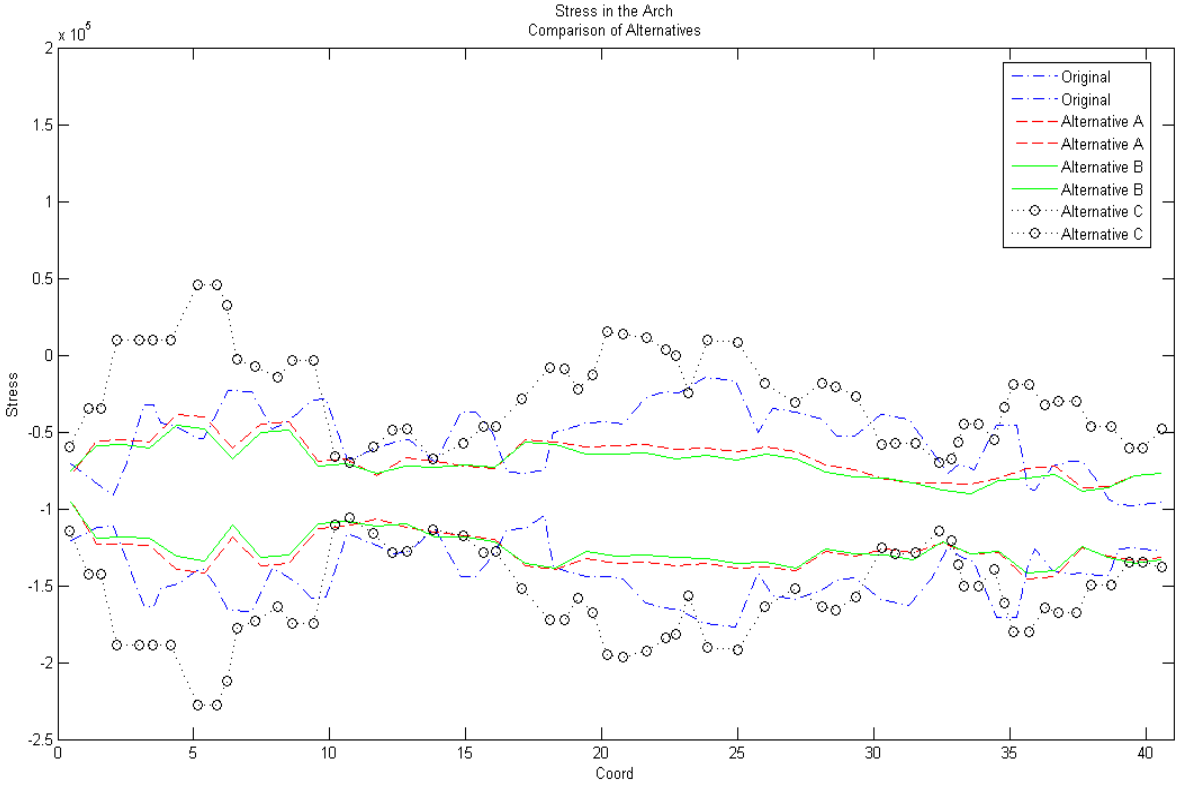


**Figure 136.** Comparison of Alternatives. Stresses in the arch

### 4.2.3. Stresses in the hangers

The Figure 137 shows the maximum stresses for each hanger for the Set 1. The curves correspond to the original configuration, and the three alternatives. The number of elements for the hangers were assigned as is shown in the Figure C.1 of the Appendix C.

All cases present no relaxed hangers. To achieved this it is necessary to prestress the hangers 3019 and 3018 in the original configuration. No prestressing was done for any of the Alternatives.

The maximum stress for the original configuration corresponds to the hanger 3019 and it is equal to 210373.47 kN/m$^2$.

The curves than correspond to the Alternatives A and B are very similar for the hangers 3001 to 3015. There is an increment of the stresses in the Alternative B for the hangers 3016 and 3017. The increment is of less than 35%.

The stresses for the Alternatives A and B are lower than the original stresses for most of the hangers. The exceptions are the hangers 3003 and 3005. As the hanger is closer to the right support, the difference between the curve of the original configuration and the curve of the

alternatives becomes more important, with a significant reduction of the stresses in the Alternatives A and B.

The maximum stress for the Alternative A corresponds to the hanger 3018 and it is equal to 105313.00 kN/m$^2$, 50% of the stress that corresponds to the original configuration.

The maximum stress for the Alternative B corresponds to the hanger 3017 and it is equal to 118269.21 kN/m$^2$, 56% of the stress that corresponds to the original configuration.

The stresses for the Alternative C are inferior than the stresses for the original configuration for the hangers 3005 to 3019, following approximately the same form of the curve . This case present the smallest stress for the hanger 3019, 20% of the original value. However, the stresses for the hangers 3001, 3002 and 3003 are more than four times higher than the original stresses. These hangers are located in the zone where the arch becomes parabolic.

The maximum stress for the Alternative C corresponds to the hanger 3003 and it is equal to 236904.39 kN/m$^2$, 1.13 times the stress that corresponds to the original configuration.

The Figures 138 shows the maximum stresses for each hanger for the Set 2. The curves correspond to the original configuration, and the three alternatives.

Again, all cases present no relaxed hangers. To achieved this it is necessary to prestress the hangers 3037 and 3038 in the original configuration. No prestressing was done for any of the Alternatives.

The maximum stress for the original configuration corresponds to the hanger 3038 and it is equal to 126360.12 kN/m$^2$.

The curves than correspond to the Alternative A and B have similar form and values. The stresses are higher than the original stresses for most of the hangers. The exception is the hanger 3038. The difference is of the order of 65000 kN/m$^2$.

The maximum stress for the Alternative A corresponds to the hanger 3035 and it is equal to 128092.29 kN/m$^2$, 1.01 times the higher value that corresponds to the original configuration.

The maximum stress for the Alternative B corresponds to the hanger 3017 and it is equal to 135372.90 kN/m$^2$, 1.07 times the higher value that corresponds to the original configuration.

The stresses for the Alternative C are inferior than the stresses for the original configuration for the hangers 3024 to 3038, following approximately the same form of the curve. However, the stresses for the hangers 3020 to 3024 are more than seven times higher than the original stresses. These hangers are located in the zone where the arch becomes parabolic.

The maximum stress for the Alternative C corresponds to the hanger 3021 and it is equal to 238099.14 kN/m$^2$, 1.88 times the stress that corresponds to the original configuration.

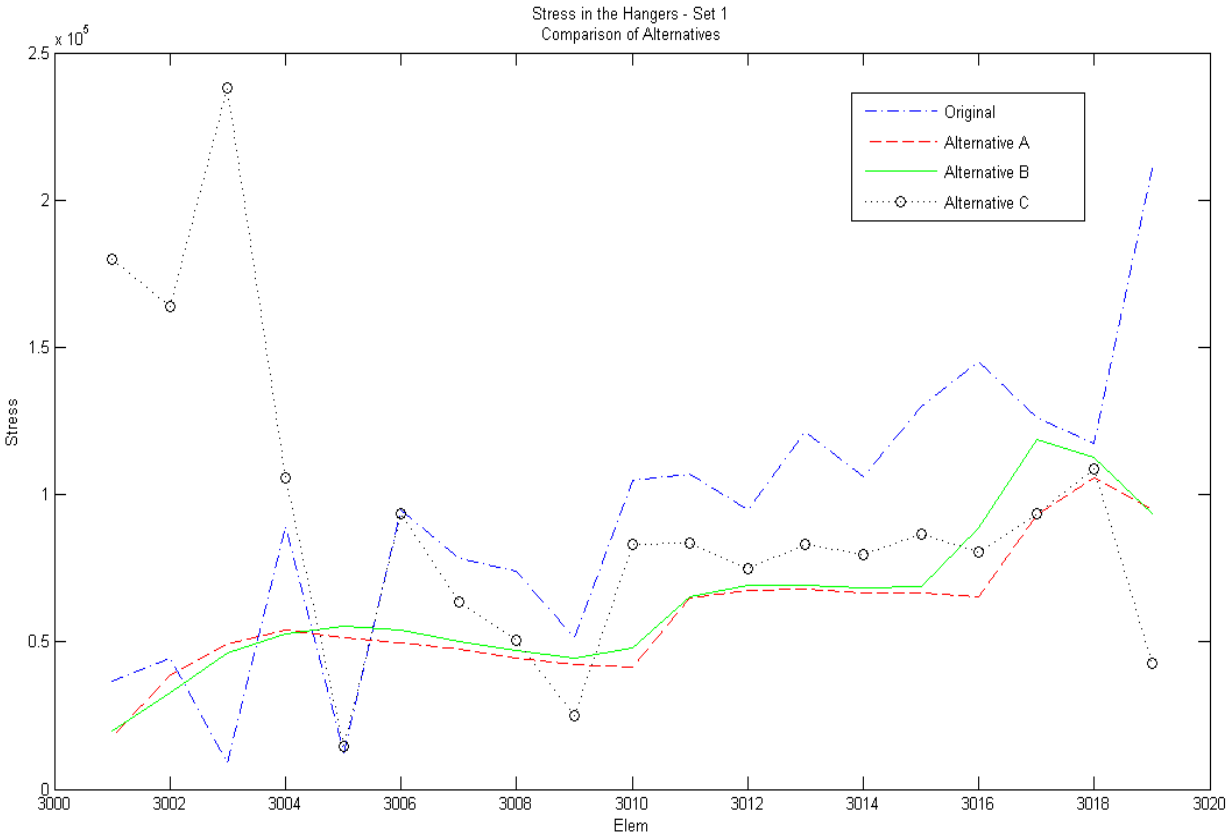


**Figure 137.** Comparison of Alternatives. Stresses in the hangers for the Set 1

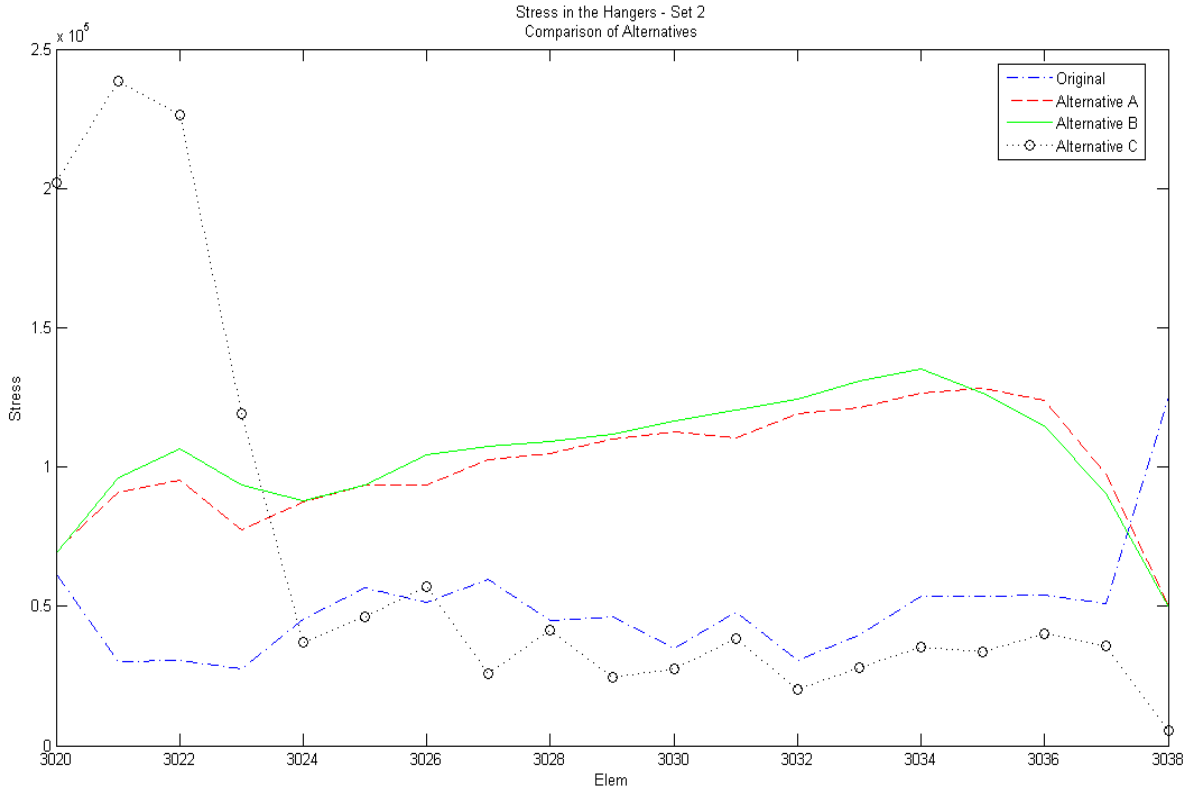


**Figure 138.** Comparison of Alternatives. Stresses in the hangers for the Set 2

## 4.3. Conclusions

From the analysis of the results obtained for the Alternatives A and B in the Figure 135 to 138 of the previous section, it can be noticed how a good choice of the hanger arrangement could improve the stresses in the elements of a bridge.

The results for this two alternatives are surprisingly similar. In the case of the arch and the deck, the form of the curves is similar to the one obtained for the original configuration, with lower values: 70% for the deck and 80% for the arch.

For the stresses in the hangers, however, lower values are only obtained for the Set 1. In this case the form of the curve approximate in a certain way to the one obtained for the original configuration, with an important improvement of the stresses: a reduction of 50%. The decrease of the stresses is specially noticeable for the hanger 3019. In the original configuration this hanger was prestressed, in order to avoid its relaxation. Because of the prestressing force, the stress for this hanger is significantly higher than the others. In the Alternatives A and B the relaxation of the hanger 3019 was avoided without prestressing, hence the maximum stress for this element is drastically reduce.

The Figure 138 shows the maximum stresses in the hangers for the Set 2. In this Figure it can be observed that the form of the curve for the Alternatives A and B differs from the form that correspond to the original configuration, presenting higher values for most of the hangers. However, the highest stress for the Alternatives A and B is of the same order than the highest stress for the original configuration.

The curve for the original configuration shows small stresses for all hangers, except the hanger 3038, that presents a value 2.50 times higher. This occurs because this hanger is prestressed. The stress in the hanger 3019 is 50% smaller for the Alternatives A and B, as these cases present no prestressing.

According to [NAB] all hangers must have the same cross-section. Hence, is desirable to have the smallest possible variation of the maximum stresses in the hangers. This variation is 201630 kN/$m^2$ for the original configuration, 110620 kN/$m^2$ for the Alternative A and 115700 kN/$m^2$ for the Alternative B. This implies a reduction of 50% in the Alternatives A and B.

Besides, as all hangers must have the same cross section, this parameter should be chosen according to the highest maximum stress. Comparing the highest maximum stress for the Alternatives A and B with the maximum stress for the original configuration for all hangers, the values for the alternatives are 60% smaller.

Hence, the improvement obtained with the Alternatives A and B is evident.

The Alternatives A and B presents similar results. Besides, in the Figures 132 and 133 it can be noticed that the configurations are similar. It is curious how using two different methods (Sections 3.1.1 and 3.1.2) similar solutions have been reached.

Regarding the Alternative C, the objective is to propose a different solution for the problem of the relaxation of the hangers. The effect of a change in the form at the ends of the arch is studied. While the original configuration presented four relaxed hangers near the supports, the configuration proposed in the Section 4.1.4. presents none.

However, even if this goal is achieved, the stresses obtained for the Alternative C are significantly higher than in the rest of the cases. The maximum value obtained for this alternative is 1.30 times the maximum value obtained for the original configuration, in both deck and arch.

Regarding the hangers, the stresses for the Alternative C are lower than for the original configuration, except for the hangers near the left support. For this elements the stress increase drastically, arriving to values seven times higher than the original. On the other hand, the stresses for the hangers near the right support are significantly reduced.

Therefore, while the Alternative C gives good results for the hangers in the center and near the right support, decreasing the stresses and avoiding relaxation, it presents an important increment of the stresses in the deck, the arch, and the hangers near the left support. This makes of the Alternative C an unsuitable solution.

Finally, it can be concluded that the Alternatives A and B presents the lowest stresses and the most effective force distribution.

However, more practical issues should be considered. While the total length of the hangers for the original configuration is 182.76 m, it is 217.61 m for the Alternative A and 230.06 for the Alternative B. This means that the length of the hangers is 20% larger for the first alternative and 26% for the second alternative. This implies a higher economical cost, and a larger area exposed to the wind.

Moreover, while in the original configuration the hangers cross each other two times, in the Alternatives A and B the hangers cross each other 6 times. This should be considered as too many intersections of the hangers can complicate replacements in case of breaking.

As it can be seen, even if for Alternatives A and B lower stresses are obtain, a particular study should be done for each bridge, considering constructive and economical aspects, in order to find the most adequate solution.

# Chapter 5
# Summary

The intention of this work is to study the different parameters that influence the structural behavior of network arch bridges. As a particular example, the bridge over the river Lužnice in the Czech Republic is chosen.

After an analysis of the Lužnice bridge in the Chapter 2, the worst loading assumptions for the bridge are determined: the load case LC1 (Load Model 1 [E1-2]), with the live load applied only in the right half of the span.

Considering this, four different parameters are studied in the Chapter 3: hanger arrangement, form of the arch, rise of the arch and number of hangers.

As the hanger arrengement constitutes the main characteristic of the network arch bridge, special emphasis is placed in this parameter. Two arrangements are studied.

The Section 3.1.1. analyze hanger arrengements based on the linear variation of the slopes. It is found that it is not recommendable to use configurations with small initial angles and large angle increments or large initial angles and small angle increments. This is because while the first case presents small stresses in the deck and the arch but high stresses in the hangers, the second case presents small stresses in the hangers, but high stresses in the deck and the arch. In addition, configurations with small initial angles and small angle increments present relaxed hangers. Hence, the best solutions are obtained with large initial angles and large angle increments.

The Section 3.1.2. examine radial arrangements, as proposed for Brunn and Schanack in their diploma thesis [BSC]. It is found that the best results are obtained for cross angles between 40° and 50°.

In the Section 3.2. the variation of the shape of the arch is analyzed. It is found that a slightly change in the form of the arch could be a solution for the problem of the relaxation of the hangers. However, it also causes the stresses in the elements to increase drastically.

The Section 3.3. examine the effects of the rise of the arch. As expected, an increment in the ratio between the rise and the span reduce the stresses in the arch, the deck and the hangers. Nevertheless, due to aestethic reasons the rise of the arch should be between 14% and 17%.

In the Section 3.4. the influence of the number of hangers is analyzed. An increment in the number of hangers implies a decrease of the stresses in arch, deck and hangers. It is not recommendable to use more than 40 hangers, as at this point relaxation occur.

Considering the conclusions of Chapter 3, three alternatives are proposed in Chapter 4: The Alternative A presents an arrangement based on the linear variation of the slopes with an initial angle of 81° and increment angle of 3.4°, t he Alternative B presents a radial arrangement with a cross angle of 41.5°, and the Alternative C proposes a circular arch with a parabolic shape in the extremes, maintaining the original hanger arrangement. Prestressing is only considered in the original configuration.

Comparing the stresses obtained for the alternatives with the original configuration, the best results are obtained for the Alternatives A and B. The Alternative C presents high values for the stresses in the deck, the arch, and the hangers near the left support. None of the alternatives present relaxed hangers. Alternatives A and B presents similar results.

However, more practical issues should be considered, as total length of the hangers and number of intersection between them, in order to find the most adequate solution.

# Appendix A

# Sections of the Lužnice Bridge

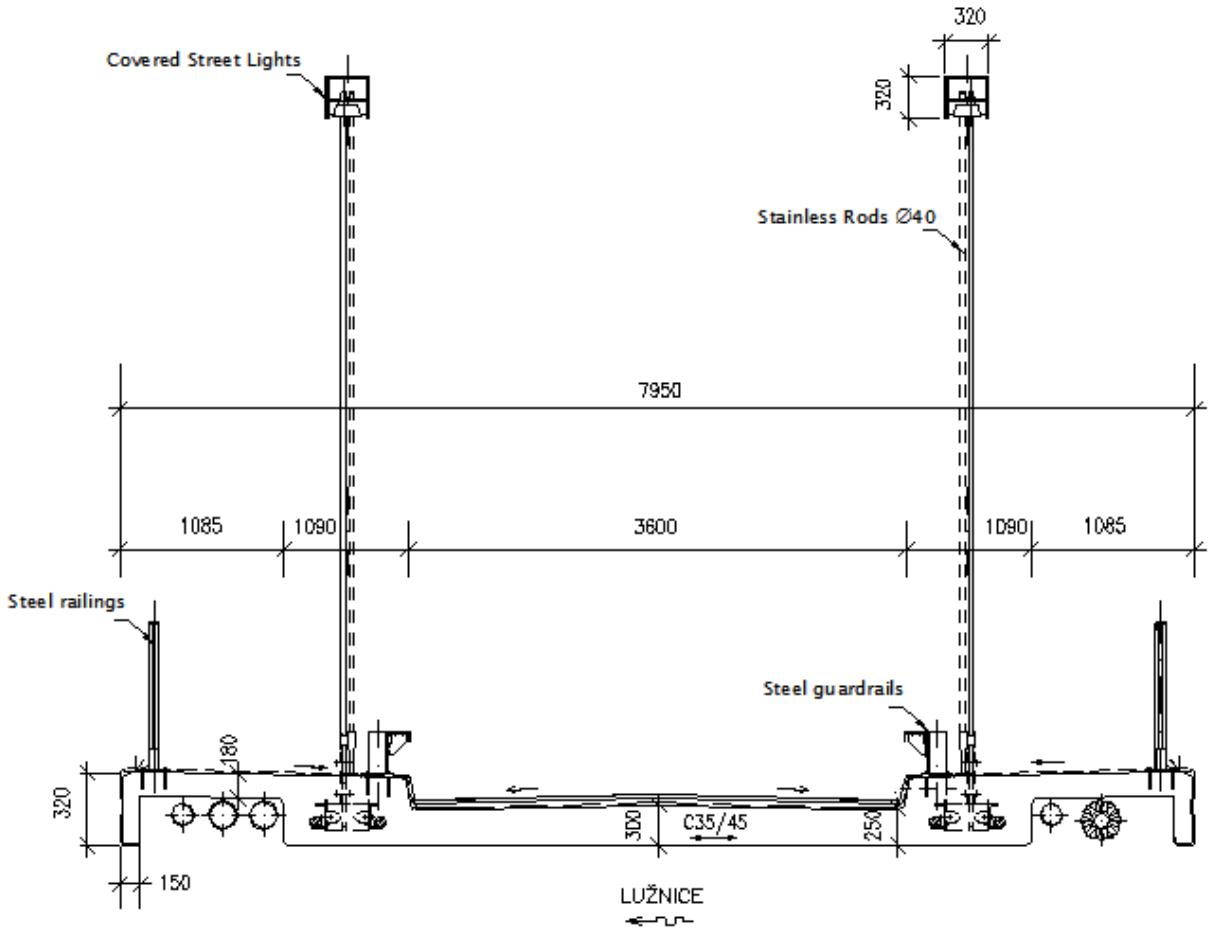


**Figure A.1** Cross section of the Lužnice Bridge [DSL]

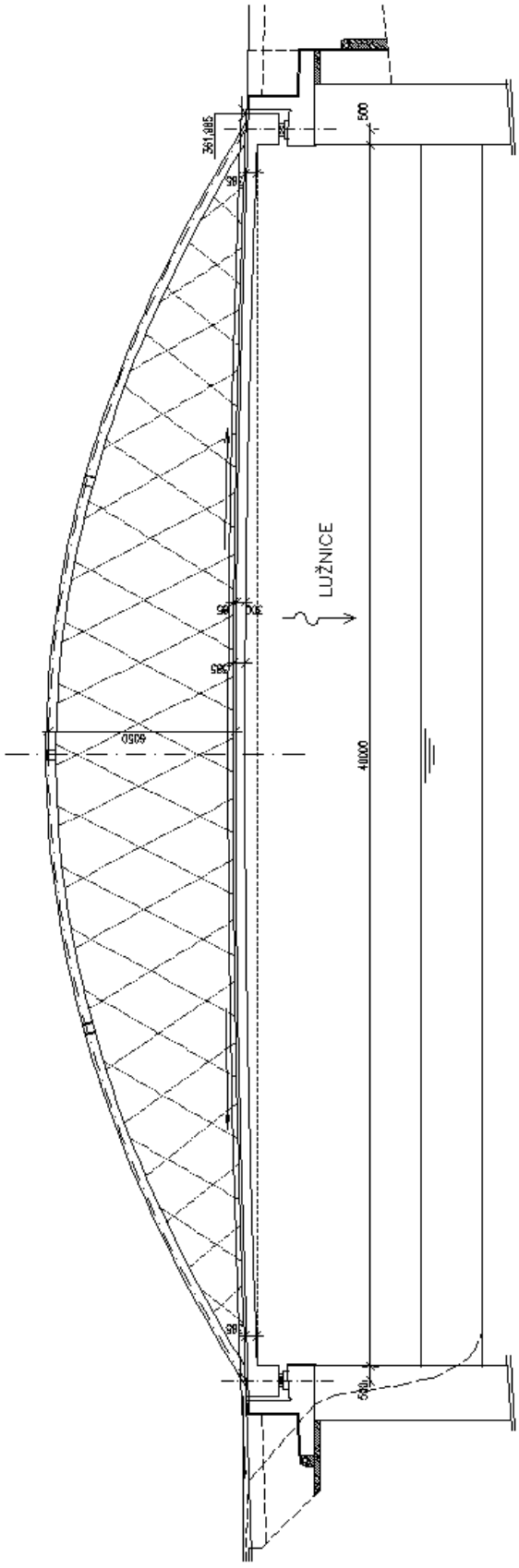


**Figure A.2.** Longitudinal section of the Lužnice Bridge [DSL]

# Appendix B

# Results for the Lužnice Bridge

| Element | Max N | | Min N | | Max M | | Min M | |
|---|---|---|---|---|---|---|---|---|
| | Load Case | Value | Load Case | Value | Load Case | Value | Load Case | Value |
| 2001 | 1.12 | 3496.99 | 2.42 | 2150.3 | 1.02 | 341.47 | 3 | 39.35 |
| 2002 | 1.12 | 3496.98 | 2.42 | 2150.3 | 1.03 | 457.72 | 1.28 | 50.8 |
| 2003 | 1.12 | 3381.62 | 2.42 | 2091.98 | 1.03 | 507.47 | 1.28 | 50.79 |
| 2004 | 1.12 | 3381.61 | 2.42 | 2091.98 | 1.04 | 684.99 | 1.28 | 67.4 |
| 2005 | 1.12 | 3418.59 | 2.42 | 2123.44 | 1.05 | 771.28 | 2.29 | 88.79 |
| 2006 | 1.13 | 3395.21 | 2.42 | 2112.49 | 1.05 | 803.13 | 2.29 | 98.33 |
| 2007 | 1.13 | 3395.21 | 2.42 | 2112.49 | 1.06 | 841.61 | 2.3 | 75.89 |
| 2008 | 1.13 | 3449.54 | 2.42 | 2153.18 | 1.06 | 854.07 | 1.29 | 60.89 |
| 2009 | 1.14 | 3421.96 | 2.42 | 2134.24 | 1.07 | 864.91 | 1.29 | 54.04 |
| 2010 | 1.14 | 3421.96 | 2.42 | 2134.24 | 1.07 | 864.94 | 1.29 | 6 |
| 2011 | 1.13 | 3472.28 | 2.42 | 2164.78 | 1.07 | 845.08 | 1.29 | -3.63 |
| 2012 | 1.13 | 3472.28 | 2.42 | 2164.79 | 1.08 | 830.37 | 1.29 | -41.51 |
| 2013 | 1.15 | 3426.69 | 2.42 | 2137.41 | 1.08 | 801.4 | 1.29 | -54.11 |
| 2014 | 1.15 | 3426.69 | 2.42 | 2137.41 | 1.09 | 789.12 | 1.3 | -101.7 |
| 2015 | 1.15 | 3496.2 | 2.42 | 2174.81 | 1.09 | 760.83 | 1.3 | -109.26 |
| 2016 | 1.15 | 3496.2 | 2.42 | 2174.81 | 1.1 | 731.68 | 1.3 | -132.87 |
| 2017 | 1.16 | 3447.28 | 2.42 | 2146.24 | 1.1 | 706.59 | 1.3 | -136.85 |
| 2018 | 1.16 | 3447.28 | 2.42 | 2146.24 | 1.11 | 695.02 | 1.3 | -165.6 |
| 2019 | 1.15 | 3506.49 | 2.42 | 2177.78 | 1.11 | 678.18 | 1.3 | -172.43 |
| 2020 | 1.15 | 3506.49 | 2.42 | 2177.78 | 1.12 | 645.91 | 1.31 | -189.03 |
| 2021 | 1.17 | 3461.11 | 2.42 | 2152.9 | 1.12 | 630.81 | 1.31 | -192.63 |
| 2022 | 1.17 | 3461.1 | 2.42 | 2152.9 | 1.13 | 612.54 | 1.31 | -209.95 |
| 2023 | 1.16 | 3522.31 | 2.42 | 2183.97 | 1.13 | 603.26 | 1.31 | -209.95 |
| 2024 | 1.16 | 3522.3 | 2.42 | 2183.97 | 1.14 | 566.5 | 1.31 | -214.11 |
| 2025 | 1.18 | 3480.04 | 2.42 | 2161.53 | 1.14 | 555.64 | 1.31 | -214.11 |
| 2026 | 1.18 | 3480.04 | 2.42 | 2161.53 | 1.15 | 530.83 | 1.31 | -220.66 |
| 2027 | 1.18 | 3538.13 | 2.42 | 2190.51 | 1.15 | 519.48 | 1.31 | -220.66 |
| 2028 | 1.19 | 3493.04 | 2.42 | 2167.03 | 1.16 | 481.01 | 1.32 | -210.04 |
| 2029 | 1.19 | 3493.02 | 2.42 | 2167.03 | 1.17 | 474.26 | 1.32 | -188.44 |
| 2030 | 1.19 | 3542.71 | 2.42 | 2191.52 | 1.17 | 468.7 | 1.32 | -188.44 |
| 2031 | 1.2 | 3496.81 | 2.42 | 2168.94 | 1.18 | 427.68 | 1.32 | -169.16 |
| 2032 | 1.2 | 3542.59 | 2.42 | 2190.98 | 1.19 | 420.62 | 1.33 | -138.81 |
| 2033 | 1.2 | 3495.5 | 2.42 | 2168.64 | 1.22 | 402.62 | 1.08 | -112.35 |
| 2034 | 1.22 | 3543 | 2.42 | 2191.58 | 1.23 | 418.64 | 1.09 | -138.56 |
| 2035 | 1.22 | 3497.53 | 2.42 | 2169.24 | 1.24 | 432.73 | 1.09 | -168.91 |
| 2036 | 1.23 | 3543.54 | 2.42 | 2191.79 | 1.25 | 459.31 | 1.1 | -193.39 |
| 2037 | 1.23 | 3492.45 | 2.42 | 2167.07 | 1.25 | 472.97 | 1.1 | -1.93E+002 |
| 2038 | 1.23 | 3492.46 | 2.42 | 2167.07 | 1.26 | 490.37 | 1.1 | -206 |
| 2039 | 1.24 | 3536.49 | 2.42 | 2189.69 | 1.27 | 520.36 | 1.1 | -215.15 |
| 2040 | 1.24 | 3481.27 | 2.42 | 2162.15 | 1.27 | 538.76 | 1.1 | -215.15 |
| 2041 | 1.24 | 3481.27 | 2.42 | 2162.15 | 1.28 | 556.76 | 1.11 | -211.96 |
| 2042 | 1.25 | 3524.53 | 2.42 | 2185.39 | 1.28 | 566 | 1.11 | -211.96 |
| 2043 | 1.25 | 3524.53 | 2.42 | 2185.39 | 1.29 | 599.43 | 1.11 | -214.12 |
| 2044 | 1.25 | 3466.54 | 2.42 | 2155.72 | 1.29 | 608.2 | 1.11 | -214.12 |
| 2045 | 1.25 | 3466.54 | 2.42 | 2155.72 | 1.3 | 627.85 | 1.11 | -200.45 |
| 2046 | 1.26 | 3513.24 | 2.42 | 2181.51 | 1.3 | 641.79 | 1.11 | -200.45 |
| 2047 | 1.26 | 3513.24 | 2.42 | 2181.51 | 1.31 | 663.54 | 1.11 | -185.94 |
| 2048 | 1.26 | 3450.7 | 2.42 | 2148.59 | 1.31 | 693.3 | 1.12 | -182.16 |
| 2049 | 1.26 | 3450.7 | 2.42 | 2148.59 | 1.32 | 709.99 | 1.12 | -148.38 |
| 2050 | 1.27 | 3499.22 | 2.42 | 2176.46 | 1.32 | 731.87 | 1.12 | -139.32 |
| 2051 | 1.27 | 3499.22 | 2.42 | 2176.46 | 1.33 | 748.15 | 1.12 | -112.65 |
| 2052 | 1.27 | 3438.36 | 2.42 | 2143.21 | 1.33 | 788.65 | 1.12 | -102.72 |
| 2053 | 1.27 | 3438.36 | 2.42 | 2143.21 | 1.34 | 802.02 | 1.12 | -53.78 |
| 2054 | 1.28 | 3481.34 | 2.42 | 2169.8 | 1.34 | 829.29 | 1.12 | -40.2 |
| 2055 | 1.28 | 3481.34 | 2.42 | 2169.8 | 1.34 | 834.08 | 1.13 | -6.16 |
| 2056 | 1.28 | 3424.02 | 2.42 | 2134.3 | 1.35 | 872 | 1.13 | 1.71 |
| 2057 | 1.28 | 3424.02 | 2.42 | 2134.3 | 1.35 | 871.97 | 1.13 | 56.01 |
| 2058 | 1.29 | 3447.33 | 2.42 | 2151.37 | 1.35 | 868.48 | 1.13 | 65.87 |
| 2059 | 1.29 | 3411.35 | 2.42 | 2122.13 | 1.36 | 860.23 | 2.13 | 80.08 |
| 2060 | 1.29 | 3411.36 | 2.42 | 2122.14 | 1.37 | 796.39 | 2.14 | 83.95 |
| 2061 | 1.3 | 3430.86 | 2.42 | 2132.76 | 1.37 | 766.75 | 2.14 | 60.23 |
| 2062 | 1.3 | 3369.54 | 2.42 | 2084.99 | 1.38 | 644.63 | 1.13 | 20.43 |
| 2063 | 1.3 | 3369.54 | 2.42 | 2085 | 1.39 | 451.64 | 1.14 | 2.92 |
| 2064 | 1.3 | 3504.89 | 2.42 | 2152.03 | 1.39 | 412.6 | 1.14 | 2.93 |
| 2065 | 1.3 | 3504.89 | 2.42 | 2152.03 | 1.4 | 292.14 | 3 | 21.04 |

**Table B.1.** Maximum and minimum bending moments and axial forces for the deck elements (Even Load)

| Element | Max Stress | | Min Stress | |
|---|---|---|---|---|
| | Load Case | Value | Load Case | Value |
| 2001 | 1.02 | 8166.28 | 1.02 | -590.59 |
| 2002 | 1.03 | 9705.19 | 1.03 | -2032.78 |
| 2003 | 1.03 | 10207.53 | 1.03 | -2806.31 |
| 2004 | 1.04 | 12529.18 | 1.04 | -5037.19 |
| 2005 | 1.05 | 13721.69 | 1.05 | -6057.47 |
| 2006 | 1.05 | 14092.27 | 1.05 | -6503.68 |
| 2007 | 1.06 | 14625.94 | 1.06 | -6956.95 |
| 2008 | 1.06 | 14849.72 | 1.06 | -7052.48 |
| 2009 | 1.07 | 14986.7 | 1.07 | -7193.57 |
| 2010 | 1.07 | 14987.03 | 1.07 | -7193.91 |
| 2011 | 1.07 | 14783.7 | 1.07 | -6888 |
| 2012 | 1.08 | 14629.99 | 1.08 | -6664.6 |
| 2013 | 1.08 | 14195.07 | 1.08 | -6356.42 |
| 2014 | 1.09 | 14068.8 | 1.09 | -6167.76 |
| 2015 | 1.09 | 13771.87 | 1.09 | -5739.34 |
| 2016 | 1.1 | 13427.37 | 1.1 | -5336.27 |
| 2017 | 1.1 | 13032.78 | 1.1 | -5087.48 |
| 2018 | 1.11 | 12911.41 | 1.11 | -4912 |
| 2019 | 1.11 | 12751.3 | 1.11 | -4640.42 |
| 2020 | 1.12 | 12363.27 | 1.12 | -4200.77 |
| 2021 | 1.12 | 12110.63 | 1.12 | -4066.31 |
| 2022 | 1.13 | 11899.26 | 1.13 | -3809.05 |
| 2023 | 1.13 | 11834.79 | 1.13 | -3635.57 |
| 2024 | 1.14 | 11385.23 | 1.14 | -3142.34 |
| 2025 | 1.14 | 11193.78 | 1.14 | -3055.51 |
| 2026 | 1.15 | 10894.3 | 1.15 | -2718.51 |
| 2027 | 1.15 | 10799.23 | 1.15 | -2522.52 |
| 2028 | 1.16 | 10265.17 | 1.16 | -2070.13 |
| 2029 | 1.17 | 10196.25 | 1.17 | -1966.05 |
| 2030 | 1.17 | 10166.57 | 1.17 | -1853.13 |
| 2031 | 1.18 | 9601.45 | 1.18 | -1366.22 |
| 2032 | 1.19 | 9563.21 | 1.19 | -1223.31 |
| 2033 | 1.22 | 9287.85 | 1.22 | -1037.19 |
| 2034 | 1.23 | 9535.78 | 1.23 | -1200.1 |
| 2035 | 1.24 | 9664.03 | 1.24 | -1433.12 |
| 2036 | 1.25 | 10043.91 | 1.25 | -1734.85 |
| 2037 | 1.25 | 10176.45 | 1.25 | -1952.8 |
| 2038 | 1.26 | 10382.21 | 1.26 | -2193.24 |
| 2039 | 1.27 | 10802 | 1.27 | -2542.35 |
| 2040 | 1.27 | 10990 | 1.27 | -2826.31 |
| 2041 | 1.28 | 11201.03 | 1.28 | -3076.83 |
| 2042 | 1.28 | 11378.59 | 1.28 | -3136.39 |
| 2043 | 1.29 | 11785.6 | 1.29 | -3586.63 |
| 2044 | 1.29 | 11845.96 | 1.29 | -3750.97 |
| 2045 | 1.3 | 12075.24 | 1.3 | -4025.83 |
| 2046 | 1.3 | 12314.19 | 1.3 | -4144.35 |
| 2047 | 1.31 | 12567.15 | 1.31 | -4449.12 |
| 2048 | 1.31 | 12890.46 | 1.31 | -4889.03 |
| 2049 | 1.32 | 13077.31 | 1.32 | -5130.07 |
| 2050 | 1.32 | 13425.72 | 1.32 | -5342.88 |
| 2051 | 1.33 | 13603.98 | 1.33 | -5582.05 |
| 2052 | 1.33 | 14064.55 | 1.33 | -6160.06 |
| 2053 | 1.34 | 14204.08 | 1.34 | -6363.47 |
| 2054 | 1.34 | 14621.37 | 1.34 | -6645.51 |
| 2055 | 1.34 | 14682.8 | 1.35 | -6719.9 |
| 2056 | 1.35 | 15073.77 | 1.35 | -7288.32 |
| 2057 | 1.35 | 15073.44 | 1.35 | -7287.98 |
| 2058 | 1.35 | 15063.46 | 1.36 | -7232.1 |
| 2059 | 1.36 | 14876.62 | 1.36 | -7183.66 |
| 2060 | 1.37 | 14017.3 | 1.37 | -6405.71 |
| 2061 | 1.37 | 13669.02 | 1.37 | -5994.06 |
| 2062 | 1.38 | 11987.07 | 1.38 | -4544.29 |
| 2063 | 1.39 | 9466.31 | 1.39 | -2115.71 |
| 2064 | 1.39 | 9125.56 | 1.39 | -1455.39 |
| 2065 | 1.39 | 7557.63 | 2.41 | 15.52 |

**Table B.2.** Maximum and minimum stresses for the deck elements (Even Load)

| Element | Max N | | Min N | | Max M | | Min M | |
|---|---|---|---|---|---|---|---|---|
| | Load Case | Value | Load Case | Value | Load Case | Value | Load Case | Value |
| 2001 | 1.01 | 2865.54 | 2.21 | 2025.57 | 2.01 | 62.24 | 1.06 | -116.24 |
| 2002 | 1.01 | 2865.51 | 2.21 | 2025.56 | 2.21 | -5.78 | 1.07 | -271.8 |
| 2003 | 1.01 | 2774.02 | 2.21 | 1968.87 | 2.21 | -77.83 | 1.07 | -285.99 |
| 2004 | 1.01 | 2773.99 | 2.21 | 1968.84 | 2.21 | -81.6 | 1.08 | -379.17 |
| 2005 | 1.01 | 2802.72 | 2.21 | 1997.58 | 2.21 | -122.97 | 1.08 | -451.38 |
| 2006 | 1.01 | 2770.69 | 2.21 | 1965.56 | 2.21 | -154.32 | 1.09 | -467.71 |
| 2007 | 1.01 | 2770.65 | 2.21 | 1965.52 | 2.21 | -155.5 | 1.09 | -538.16 |
| 2008 | 1.01 | 2801.08 | 2.21 | 1994.03 | 2.21 | -178.94 | 1.09 | -594.7 |
| 2009 | 1.01 | 2771.54 | 2.21 | 1964.5 | 2.21 | -187.26 | 1.09 | -606.77 |
| 2010 | 1.01 | 2771.5 | 2.21 | 1964.46 | 2.21 | -187.26 | 1.09 | -649.22 |
| 2011 | 1.01 | 2777.34 | 2.21 | 1967.98 | 2.21 | -189.61 | 1.09 | -666.79 |
| 2012 | 1.01 | 2777.32 | 2.21 | 1967.96 | 2.21 | -194.25 | 1.09 | -713.85 |
| 2013 | 1.01 | 2747.7 | 2.21 | 1938.34 | 2.21 | -209.82 | 1.09 | -735.41 |
| 2014 | 1.01 | 2747.65 | 2.21 | 1938.3 | 2.21 | -209.82 | 1.09 | -781.22 |
| 2015 | 1.01 | 2815.94 | 2.21 | 1975.11 | 2.21 | -216.02 | 1.09 | -781.58 |
| 2016 | 1.01 | 2815.94 | 2.21 | 1975.1 | 2.21 | -216.02 | 1.09 | -789.18 |
| 2017 | 1.01 | 2785.61 | 2.21 | 1944.77 | 2.21 | -195.73 | 1.09 | -789.18 |
| 2018 | 1.01 | 2785.6 | 2.21 | 1944.75 | 2.21 | -186.84 | 1.1 | -776.17 |
| 2019 | 1.01 | 2793.63 | 2.21 | 1947.23 | 2.21 | -186.84 | 1.1 | -783.43 |
| 2020 | 1.01 | 2793.63 | 2.21 | 1947.23 | 2.21 | -187.46 | 1.1 | -794.74 |
| 2021 | 1.01 | 2772.95 | 2.21 | 1926.54 | 2.21 | -188.1 | 1.1 | -799.54 |
| 2022 | 1.01 | 2772.96 | 2.21 | 1926.54 | 2.21 | -188.1 | 1.1 | -810.06 |
| 2023 | 1.01 | 2837.58 | 2.21 | 1962.1 | 2.21 | -178.22 | 1.1 | -810.07 |
| 2024 | 1.01 | 2837.62 | 2.21 | 1962.13 | 2.21 | -176.94 | 1.11 | -777.29 |
| 2025 | 1.01 | 2822.3 | 2.21 | 1946.79 | 2.21 | -161.87 | 1.11 | -769.09 |
| 2026 | 1.01 | 2822.34 | 2.21 | 1946.83 | 2.21 | -161.86 | 1.11 | -734.09 |
| 2027 | 1.01 | 2870.51 | 2.21 | 1973.23 | 2.21 | -146.1 | 1.11 | -725.73 |
| 2028 | 1.01 | 2845.75 | 2.21 | 1948.45 | 2.02 | -75.71 | 1.11 | -667.41 |
| 2029 | 1.01 | 2845.8 | 2.21 | 1948.51 | 2.02 | -63.91 | 1.12 | -557.04 |
| 2030 | 1.01 | 2886.81 | 2.21 | 1971.4 | 2.02 | -0.58 | 1.12 | -537.3 |
| 2031 | 1.01 | 2869.42 | 2.21 | 1954.03 | 1.01 | 112.3 | 1.12 | -429.62 |
| 2032 | 1.01 | 2895.16 | 2.21 | 1964.75 | 1.01 | 312.81 | 1.12 | -283.74 |
| 2033 | 1.01 | 2872.19 | 2.21 | 1947.37 | 1.01 | 467.83 | 1.13 | -150.32 |
| 2034 | 1.01 | 2925.49 | 2.21 | 1973.83 | 1.02 | 583.08 | 1.13 | -14.22 |
| 2035 | 1.01 | 2903.4 | 2.21 | 1965.46 | 1.03 | 658.44 | 2.15 | 57.06 |
| 2036 | 1.02 | 2954.78 | 2.21 | 1992.52 | 1.04 | 757.97 | 2.16 | 85.11 |
| 2037 | 1.02 | 2922.69 | 2.21 | 1974.59 | 1.04 | 772.44 | 2.16 | 1.17E+002 |
| 2038 | 1.02 | 2922.64 | 2.21 | 1974.55 | 1.05 | 815.76 | 2.17 | 127.6 |
| 2039 | 1.04 | 2966.76 | 2.21 | 1998.01 | 1.06 | 887.6 | 2.18 | 138.83 |
| 2040 | 1.03 | 2939.63 | 2.21 | 1984.33 | 1.07 | 902 | 2.2 | 153.05 |
| 2041 | 1.03 | 2939.61 | 2.21 | 1984.3 | 1.07 | 902.03 | 2.21 | 135.45 |
| 2042 | 1.05 | 2996.53 | 2.21 | 2018.41 | 1.08 | 925.74 | 2.21 | 135.44 |
| 2043 | 1.05 | 2996.51 | 2.21 | 2018.38 | 1.08 | 952.55 | 2.02 | 122.75 |
| 2044 | 1.04 | 2961.27 | 2.21 | 1996.52 | 1.09 | 973.53 | 2.02 | 120.2 |
| 2045 | 1.04 | 2961.27 | 2.21 | 1996.52 | 1.09 | 973.55 | 2.02 | 97.4 |
| 2046 | 1.06 | 3011.94 | 2.21 | 2026.42 | 1.1 | 991.07 | 2.02 | 97.39 |
| 2047 | 1.06 | 3011.95 | 2.21 | 2026.41 | 1.1 | 992.83 | 2.02 | 88.2 |
| 2048 | 1.05 | 2982.05 | 2.21 | 2009.97 | 1.11 | 1001.49 | 2.02 | 80.78 |
| 2049 | 1.05 | 2982.09 | 2.21 | 2010 | 1.11 | 1001.49 | 2.02 | 56.25 |
| 2050 | 1.07 | 3045.99 | 2.21 | 2047.83 | 1.12 | 985.07 | 2.02 | 56.24 |
| 2051 | 1.07 | 3046 | 2.21 | 2047.84 | 1.12 | 985.07 | 2.02 | 54.36 |
| 2052 | 1.06 | 3028.86 | 2.21 | 2042.08 | 1.12 | 975.39 | 2.02 | 34.24 |
| 2053 | 1.06 | 3028.9 | 2.21 | 2042.12 | 1.13 | 953.16 | 2.02 | 5.81 |
| 2054 | 1.08 | 3100.4 | 2.21 | 2086.95 | 1.14 | 909.59 | 2.02 | 5.49 |
| 2055 | 1.08 | 3100.42 | 2.21 | 2086.97 | 1.14 | 909.58 | 2.02 | 8.15E-002 |
| 2056 | 1.07 | 3081.11 | 2.21 | 2074.29 | 1.14 | 898.35 | 2.02 | -23.38 |
| 2057 | 1.07 | 3081.17 | 2.21 | 2074.34 | 1.15 | 848.31 | 2.02 | -45.82 |
| 2058 | 1.09 | 3142.13 | 2.21 | 2116 | 1.15 | 799.99 | 2.02 | -45.82 |
| 2059 | 1.09 | 3119.48 | 2.21 | 2093.34 | 1.15 | 774.41 | 2.02 | -61.51 |
| 2060 | 1.09 | 3119.53 | 2.21 | 2093.39 | 1.16 | 662.38 | 2.02 | -75.64 |
| 2061 | 1.09 | 3185.04 | 2.21 | 2136.06 | 1.17 | 598.27 | 2.02 | -75.88 |
| 2062 | 1.09 | 3136.88 | 2.21 | 2092.42 | 1.17 | 523.69 | 2.01 | -77.86 |
| 2063 | 1.09 | 3136.91 | 2.21 | 2092.45 | 1.18 | 354.03 | 2.01 | -90.57 |
| 2064 | 1.1 | 3292.61 | 2.21 | 2172.25 | 1.18 | 294.4 | 2.01 | -90.56 |
| 2065 | 1.1 | 3292.62 | 2.21 | 2172.27 | 1.19 | 240.83 | 2.02 | -9.92 |

**Table B.3.** Maximum and minimum bending moments and axial forces for the deck elements (Partial Load)

| Element | Max Stress | | Min Stress | |
|---|---|---|---|---|
| | Load Case | Value | Load Case | Value |
| 2001 | 1.05 | 4829.13 | 2.21 | 1785.63 |
| 2002 | 1.05 | 6812.9 | 1.09 | -180.79 |
| 2003 | 1.06 | 6884.55 | 1.09 | -469.75 |
| 2004 | 1.07 | 8064.28 | 1.09 | -1672.11 |
| 2005 | 1.08 | 9020.18 | 1.09 | -2568.61 |
| 2006 | 1.08 | 9191.31 | 1.09 | -2817.04 |
| 2007 | 1.08 | 10089.43 | 1.09 | -3720.42 |
| 2008 | 1.08 | 10845.66 | 1.09 | -4409.49 |
| 2009 | 1.08 | 10963.41 | 1.09 | -4599.15 |
| 2010 | 1.09 | 11505.48 | 1.09 | -5143.49 |
| 2011 | 1.09 | 11735.55 | 1.09 | -5363.91 |
| 2012 | 1.09 | 12338.95 | 1.09 | -5967.37 |
| 2013 | 1.09 | 12580.49 | 1.09 | -6278.86 |
| 2014 | 1.09 | 13167.83 | 1.09 | -6866.32 |
| 2015 | 1.09 | 13250.52 | 1.1 | -6796.12 |
| 2016 | 1.09 | 13347.86 | 1.1 | -6901.54 |
| 2017 | 1.09 | 13312.09 | 1.1 | -6937.41 |
| 2018 | 1.09 | 13139.07 | 1.1 | -6776.28 |
| 2019 | 1.1 | 13225.73 | 1.1 | -6864.94 |
| 2020 | 1.1 | 13370.82 | 1.1 | -7010.04 |
| 2021 | 1.1 | 13407.89 | 1.11 | -7097.22 |
| 2022 | 1.1 | 13542.85 | 1.11 | -7237.37 |
| 2023 | 1.1 | 13618.51 | 1.11 | -7162.71 |
| 2024 | 1.1 | 13192.79 | 1.11 | -6753.88 |
| 2025 | 1.1 | 13062.76 | 1.11 | -6666.87 |
| 2026 | 1.11 | 12607.47 | 1.11 | -6217.99 |
| 2027 | 1.11 | 12555.26 | 1.11 | -6055.74 |
| 2028 | 1.11 | 11778.24 | 1.11 | -5337.18 |
| 2029 | 1.11 | 10361.34 | 1.12 | -3943.05 |
| 2030 | 1.11 | 10145.83 | 1.12 | -3644.48 |
| 2031 | 1.12 | 8733.22 | 1.12 | -2284.3 |
| 2032 | 1.01 | 7428.86 | 1.01 | -593.05 |
| 2033 | 1.01 | 9389.5 | 1.01 | -2607.91 |
| 2034 | 1.02 | 10922.38 | 1.02 | -4030.37 |
| 2035 | 1.03 | 11863.2 | 1.03 | -5022.17 |
| 2036 | 1.04 | 13186.59 | 1.04 | -6251.37 |
| 2037 | 1.04 | 13350.33 | 1.05 | -6466.53 |
| 2038 | 1.05 | 13889.83 | 1.05 | -7030.11 |
| 2039 | 1.06 | 14848.62 | 1.06 | -7913.5 |
| 2040 | 1.07 | 14997.3 | 1.07 | -8134.17 |
| 2041 | 1.07 | 14997.58 | 1.07 | -8134.59 |
| 2042 | 1.08 | 15357.26 | 1.08 | -8382.93 |
| 2043 | 1.08 | 15700.96 | 1.08 | -8726.77 |
| 2044 | 1.09 | 15921.9 | 1.09 | -9043.91 |
| 2045 | 1.09 | 15922.11 | 1.09 | -9044.19 |
| 2046 | 1.1 | 16188.34 | 1.1 | -9227.24 |
| 2047 | 1.1 | 16210.87 | 1.1 | -9249.84 |
| 2048 | 1.11 | 16276.01 | 1.11 | -9406.71 |
| 2049 | 1.11 | 16276 | 1.11 | -9406.71 |
| 2050 | 1.12 | 16122.63 | 1.12 | -9139.14 |
| 2051 | 1.12 | 16122.57 | 1.12 | -9139.04 |
| 2052 | 1.12 | 15991.76 | 1.12 | -9021.83 |
| 2053 | 1.13 | 15675.41 | 1.13 | -8768.13 |
| 2054 | 1.14 | 15183.84 | 1.14 | -8142.29 |
| 2055 | 1.14 | 15183.67 | 1.14 | -8142.07 |
| 2056 | 1.14 | 15024.69 | 1.14 | -8013.02 |
| 2057 | 1.14 | 14368.67 | 1.15 | -7407.36 |
| 2058 | 1.15 | 13805.76 | 1.15 | -6709.7 |
| 2059 | 1.15 | 13451.14 | 1.15 | -6408.41 |
| 2060 | 1.16 | 11974.71 | 1.16 | -5011.69 |
| 2061 | 1.17 | 11197.3 | 1.17 | -4145.14 |
| 2062 | 1.17 | 10184.29 | 1.17 | -3245.47 |
| 2063 | 1.18 | 7963.5 | 1.18 | -1115.41 |
| 2064 | 1.18 | 7381.31 | 1.18 | -168.49 |
| 2065 | 1.19 | 6646.29 | 1.19 | 470.33 |

**Table B.4.** Maximum and minimum stresses for the deck elements (Partial Load)

| Element | Max N | | Min N | | Max M | | Min M | |
|---|---|---|---|---|---|---|---|---|
| | Load Case | Value | Load Case | Value | Load Case | Value | Load Case | Value |
| 4001 | 2.42 | -2469.33 | 1.12 | -4011.44 | 1.03 | 16.47 | 2.01 | -83.98 |
| 4002 | 2.42 | -2463.53 | 1.12 | -4003.39 | 1.03 | 84.87 | 2.01 | -6.82 |
| 4003 | 2.42 | -2462.3 | 1.12 | -3995.34 | 1.03 | 97.32 | 2.29 | 40.37 |
| 4004 | 2.42 | -2466.98 | 1.12 | -4004.45 | 1.03 | 97.27 | 1.28 | 25.05 |
| 4005 | 2.42 | -2370.04 | 1.12 | -3812.02 | 1.03 | 85.54 | 1.27 | -48.69 |
| 4006 | 2.42 | -2367.74 | 1.12 | -3807.76 | 1.04 | 64.1 | 1.27 | -48.69 |
| 4007 | 2.42 | -2380.51 | 1.12 | -3824.73 | 1.04 | 76.59 | 1.27 | -4.76 |
| 4008 | 2.42 | -2375.55 | 1.12 | -3823.14 | 1.05 | 120.31 | 1.28 | 6.65 |
| 4009 | 2.42 | -2374.02 | 1.12 | -3816.24 | 1.05 | 130.89 | 2.29 | 39.75 |
| 4010 | 2.42 | -2382.5 | 1.12 | -3830.01 | 1.05 | 130.89 | 2.3 | 31.91 |
| 4011 | 2.42 | -2362.16 | 1.13 | -3792.25 | 1.05 | 117.36 | 1.3 | -5.09 |
| 4012 | 2.42 | -2358.95 | 1.13 | -3789.17 | 1.05 | 70.67 | 1.31 | -72.52 |
| 4013 | 2.42 | -2371.51 | 1.14 | -3814.73 | 1.07 | 85.51 | 1.31 | -72.5 |
| 4014 | 2.42 | -2339 | 1.14 | -3766.64 | 1.07 | 89.95 | 1.3 | 5.76 |
| 4015 | 2.42 | -2336.79 | 1.14 | -3764.94 | 1.07 | 93.68 | 1.3 | 10.34 |
| 4016 | 2.42 | -2347.5 | 1.14 | -3783.17 | 1.07 | 93.69 | 1.3 | -31.05 |
| 4017 | 2.42 | -2345.38 | 1.14 | -3780.54 | 1.07 | 47.76 | 1.3 | -86.31 |
| 4018 | 2.42 | -2342.48 | 1.14 | -3775.11 | 1.08 | 86.78 | 1.3 | -86.32 |
| 4019 | 2.42 | -2314.73 | 1.16 | -3740.79 | 1.08 | 86.73 | 1.31 | -10.08 |
| 4020 | 2.42 | -2311.51 | 1.16 | -3736.32 | 1.09 | 73.46 | 1.31 | -43.79 |
| 4021 | 2.42 | -2326.22 | 1.16 | -3754.55 | 1.1 | 44.08 | 1.31 | -55.82 |
| 4022 | 2.42 | -2283.62 | 1.17 | -3692.94 | 1.11 | 72.92 | 1.31 | -55.81 |
| 4023 | 2.42 | -2281.38 | 1.17 | -3690.37 | 1.12 | 107.33 | 1.32 | -14.19 |
| 4024 | 2.42 | -2258.77 | 1.18 | -3654.92 | 1.12 | 107.39 | 1.32 | -103.1 |
| 4025 | 2.42 | -2259.15 | 1.18 | -3654.11 | 1.13 | 16.29 | 1.32 | -103.11 |
| 4026 | 2.42 | -2258.05 | 1.18 | -3653.55 | 1.14 | 116.65 | 1.32 | -65.28 |
| 4027 | 2.42 | -2245.58 | 1.19 | -3632.89 | 1.14 | 116.69 | 1.33 | 17.71 |
| 4028 | 2.42 | -2244.21 | 1.19 | -3632.53 | 1.14 | 101.85 | 1.33 | -57.58 |
| 4029 | 2.42 | -2243.88 | 1.19 | -3630.64 | 1.15 | 13.85 | 1.33 | -78.84 |
| 4030 | 2.42 | -2241.44 | 1.19 | -3626.29 | 1.15 | 68.62 | 1.33 | -78.84 |
| 4031 | 2.42 | -2237 | 1.2 | -3619.68 | 1.15 | 68.61 | 1.34 | -1.05 |
| 4032 | 2.42 | -2236.58 | 1.2 | -3619.46 | 1.16 | 65.47 | 1.35 | -7.02 |
| 4033 | 2.42 | -2236.39 | 1.2 | -3618.88 | 1.17 | 46.56 | 1.35 | -1.68E+001 |
| 4034 | 2.42 | -2236.24 | 1.22 | -3618.4 | 1.17 | 34.3 | 1.07 | -26.08 |
| 4035 | 2.42 | -2236.16 | 1.22 | -3618.94 | 1.26 | 78.81 | 1.07 | -26.09 |
| 4036 | 2.42 | -2236.65 | 1.22 | -3619.12 | 1.26 | 90.59 | 2.08 | 13.87 |
| 4037 | 2.42 | -2241.4 | 1.23 | -3626.43 | 1.26 | 90.59 | 1.09 | -89.61 |
| 4038 | 2.42 | -2242.61 | 1.23 | -3630.37 | 1.28 | 119.05 | 1.09 | -89.6 |
| 4039 | 2.42 | -2257.46 | 1.24 | -3652.81 | 1.28 | 119.03 | 1.1 | -50.51 |
| 4040 | 2.42 | -2258.89 | 1.24 | -3653.76 | 1.29 | 32.66 | 1.1 | -95.61 |
| 4041 | 2.42 | -2257.38 | 1.24 | -3651.54 | 1.3 | 84.31 | 1.1 | -95.62 |
| 4042 | 2.42 | -2281.19 | 1.25 | -3689.81 | 1.3 | 84.24 | 1.1 | -9.53 |
| 4043 | 2.42 | -2283.7 | 1.25 | -3692.47 | 1.31 | 77.17 | 1.11 | -29.82 |
| 4044 | 2.42 | -2307.87 | 1.26 | -3726.41 | 1.32 | 62.53 | 1.11 | -73.54 |
| 4045 | 2.42 | -2311.8 | 1.26 | -3736.25 | 1.33 | 72.72 | 1.11 | -73.51 |
| 4046 | 2.42 | -2314.93 | 1.26 | -3739.82 | 1.34 | 121.04 | 1.11 | -13.99 |
| 4047 | 2.42 | -2342.58 | 1.27 | -3778.58 | 1.34 | 121.06 | 1.12 | -109.33 |
| 4048 | 2.42 | -2345.13 | 1.27 | -3780.13 | 1.35 | 64.17 | 1.12 | -109.35 |
| 4049 | 2.42 | -2335.29 | 1.28 | -3762.19 | 1.35 | 91.84 | 1.11 | -6.38 |
| 4050 | 2.42 | -2337.57 | 1.28 | -3763.99 | 1.35 | 105.22 | 2.11 | 16.29 |
| 4051 | 2.42 | -2367.46 | 1.28 | -3806.11 | 1.35 | 105.18 | 2.14 | 17.97 |
| 4052 | 2.42 | -2358 | 1.29 | -3789.13 | 1.36 | 93.65 | 1.13 | -108.43 |
| 4053 | 2.42 | -2360.87 | 1.29 | -3791.14 | 1.37 | 61.1 | 1.13 | -108.45 |
| 4054 | 2.42 | -2381.22 | 1.3 | -3822.22 | 1.37 | 97.5 | 1.12 | -19.56 |
| 4055 | 2.42 | -2372.29 | 1.3 | -3808.04 | 1.37 | 108.62 | 1.11 | 19.96 |
| 4056 | 2.42 | -2373.88 | 1.3 | -3815.2 | 1.38 | 133.09 | 2.15 | 32.71 |
| 4057 | 2.42 | -2379.03 | 1.3 | -3816.83 | 1.38 | 136.79 | 2.15 | 57.83 |
| 4058 | 2.42 | -2369.41 | 1.3 | -3808.53 | 1.38 | 136.75 | 2.14 | 33.8 |
| 4059 | 2.42 | -2475.41 | 1.3 | -4018.18 | 1.38 | 98.35 | 1.15 | -39.04 |
| 4060 | 2.42 | -2479.34 | 1.3 | -4025.23 | 1.39 | 54.49 | 1.15 | -39.04 |
| 4061 | 2.42 | -2467.64 | 1.3 | -4008.4 | 1.39 | 54.51 | 1.15 | 9.71 |
| 4062 | 2.42 | -2468.88 | 1.3 | -4016.59 | 1.39 | 48.08 | 2.01 | -17.02 |
| 4063 | 2.42 | -2474.78 | 1.3 | -4024.77 | 3 | 8.74 | 2.01 | -69.25 |

**Table B.5.** Maximum and minimum bending moments and axial forces for the arch elements (Even Load).

| Element | Max Stress | | Min Stress | |
|---|---|---|---|---|
| | Load Case | Value | Load Case | Value |
| 4001 | 2.42 | -50974.7 | 1.12 | -154391.81 |
| 4002 | 2.03 | -55733.79 | 1.11 | -157980.92 |
| 4003 | 2.03 | -51400.86 | 1.05 | -162844.14 |
| 4004 | 2.03 | -51715.29 | 1.05 | -163168.3 |
| 4005 | 2.04 | -52847.45 | 1.04 | -152039.52 |
| 4006 | 2.04 | -58337.04 | 1.05 | -142628.14 |
| 4007 | 2.04 | -55632.02 | 1.05 | -148930.73 |
| 4008 | 2.05 | -44967.16 | 1.05 | -168625.11 |
| 4009 | 2.05 | -42649.89 | 1.05 | -173146.47 |
| 4010 | 2.05 | -42959.73 | 1.05 | -173591.86 |
| 4011 | 2.05 | -46961.41 | 1.05 | -165982 |
| 4012 | 2.34 | -58349.74 | 1.28 | -148898.82 |
| 4013 | 2.07 | -58761.87 | 1.07 | -154899.94 |
| 4014 | 2.07 | -56472.56 | 1.07 | -154989.65 |
| 4015 | 2.07 | -55739.94 | 1.08 | -156572.03 |
| 4016 | 2.07 | -56140.67 | 1.08 | -157183.93 |
| 4017 | 2.33 | -55440.05 | 1.28 | -154654.1 |
| 4018 | 2.33 | -55378.93 | 1.09 | -154892.2 |
| 4019 | 2.08 | -58091.18 | 1.09 | -153043.91 |
| 4020 | 2.09 | -61855.33 | 1.09 | -147999.49 |
| 4021 | 2.34 | -63774.41 | 1.29 | -140398.79 |
| 4022 | 2.11 | -60869.57 | 1.11 | -147051.25 |
| 4023 | 2.12 | -51082.15 | 1.12 | -162632.06 |
| 4024 | 2.34 | -48414.77 | 1.12 | -161052.35 |
| 4025 | 2.34 | -48443.57 | 1.3 | -157427.85 |
| 4026 | 2.14 | -47291.37 | 1.14 | -166259.89 |
| 4027 | 2.14 | -46658.4 | 1.14 | -165224.3 |
| 4028 | 2.14 | -50964.74 | 1.14 | -158774.73 |
| 4029 | 2.35 | -54004.07 | 1.32 | -145467.48 |
| 4030 | 2.35 | -53920.91 | 1.32 | -145332.38 |
| 4031 | 2.16 | -60315.68 | 1.16 | -144298.46 |
| 4032 | 2.16 | -61105.04 | 1.16 | -143056.37 |
| 4033 | 2.17 | -66567.41 | 1.17 | -135315.47 |
| 4034 | 2.06 | -67887.43 | 1.24 | -130137.13 |
| 4035 | 2.27 | -57221.84 | 1.26 | -148752.45 |
| 4036 | 2.27 | -53911.18 | 1.26 | -153869.67 |
| 4037 | 2.08 | -51059.48 | 1.26 | -154559.04 |
| 4038 | 2.29 | -46136.86 | 1.28 | -165933.29 |
| 4039 | 2.29 | -46906.84 | 1.28 | -167208.18 |
| 4040 | 2.09 | -50370.22 | 1.11 | -154192.97 |
| 4041 | 2.09 | -50287.35 | 1.11 | -154073.8 |
| 4042 | 2.31 | -57969.87 | 1.3 | -152533.1 |
| 4043 | 2.32 | -59640.71 | 1.31 | -148824.78 |
| 4044 | 2.1 | -58190.66 | 1.13 | -147220.27 |
| 4045 | 2.1 | -58317.6 | 1.33 | -147429.02 |
| 4046 | 2.35 | -48070.41 | 1.33 | -168024.59 |
| 4047 | 2.09 | -47809.3 | 1.33 | -170075.4 |
| 4048 | 2.09 | -47784.58 | 1.14 | -164904.08 |
| 4049 | 2.36 | -55820.54 | 1.35 | -155658.99 |
| 4050 | 2.36 | -51719.12 | 1.35 | -161519.66 |
| 4051 | 2.36 | -52762.49 | 1.35 | -163085.28 |
| 4052 | 2.13 | -51226.2 | 1.15 | -165289.23 |
| 4053 | 2.13 | -51182.03 | 1.15 | -165252.54 |
| 4054 | 2.38 | -52469.79 | 1.37 | -158597.6 |
| 4055 | 2.38 | -48075.86 | 1.37 | -163016.02 |
| 4056 | 2.39 | -38347.24 | 1.37 | -173656.9 |
| 4057 | 2.39 | -36842.1 | 1.37 | -175017.42 |
| 4058 | 2.39 | -36507.36 | 1.37 | -174577.28 |
| 4059 | 2.39 | -53277.35 | 1.38 | -163849.25 |
| 4060 | 2.39 | -65378.89 | 1.38 | -144986.45 |
| 4061 | 2.39 | -64908.8 | 1.38 | -144392.46 |
| 4062 | 2.39 | -67564.17 | 1.37 | -141755.84 |
| 4063 | 2.42 | -55471.82 | 1.36 | -144878.61 |

**Table B.6.** Maximum and minimum stresses for the arch elements (Even Load)

| Element | Max N | | Min N | | Max M | | Min M | |
|---|---|---|---|---|---|---|---|---|
| | Load Case | Value | Load Case | Value | Load Case | Value | Load Case | Value |
| 4001 | 2.21 | -2315 | 1.01 | -3271.83 | 2.02 | -10.38 | 2.01 | -62.22 |
| 4002 | 2.21 | -2309.19 | 1.01 | -3263.75 | 2.2 | 6.34 | 1.2 | -24.47 |
| 4003 | 2.21 | -2307.94 | 1.01 | -3255.66 | 2.21 | 9.23 | 1.08 | -20.16 |
| 4004 | 2.21 | -2311.83 | 1.01 | -3262.33 | 2.21 | 9.23 | 1.07 | -71.33 |
| 4005 | 2.21 | -2217.51 | 1.01 | -3108.37 | 2.21 | -23.96 | 1.06 | -150.04 |
| 4006 | 2.21 | -2217.06 | 1.01 | -3106.91 | 2.21 | -52.77 | 1.06 | -150.04 |
| 4007 | 2.21 | -2225.63 | 1.01 | -3115.26 | 2.21 | -47.66 | 1.07 | -124.49 |
| 4008 | 2.21 | -2220.65 | 1.01 | -3113.66 | 2.21 | -32.92 | 1.07 | -117.77 |
| 4009 | 2.21 | -2219.12 | 1.01 | -3106.74 | 2.21 | -30.83 | 1.08 | -99.41 |
| 4010 | 2.21 | -2218.78 | 1.01 | -3106.13 | 2.21 | -30.83 | 1.09 | -98.65 |
| 4011 | 2.21 | -2164.13 | 1.01 | -3051.9 | 2.21 | -31.8 | 1.09 | -123.37 |
| 4012 | 2.21 | -2160.93 | 1.01 | -3048.82 | 2.21 | -54.6 | 1.1 | -165.05 |
| 4013 | 2.21 | -2172.75 | 1.01 | -3074.13 | 2.21 | -36.97 | 1.1 | -164.99 |
| 4014 | 2.21 | -2123 | 1.01 | -3019.47 | 2.21 | -37.02 | 1.1 | -105.9 |
| 4015 | 2.21 | -2120.8 | 1.01 | -3017.76 | 2.21 | -39.95 | 1.1 | -113.52 |
| 4016 | 2.21 | -2119.59 | 1.01 | -3017.53 | 2.21 | -48.01 | 1.1 | -128.14 |
| 4017 | 2.21 | -2117.47 | 1.01 | -3014.9 | 2.21 | -60.62 | 1.1 | -148.7 |
| 4018 | 2.21 | -2112.3 | 1.01 | -3006.61 | 2.02 | -10.16 | 1.1 | -148.71 |
| 4019 | 2.21 | -2083.9 | 1.01 | -2995.17 | 2.02 | -7.66 | 1.11 | -54.05 |
| 4020 | 2.21 | -2080.69 | 1.01 | -2990.72 | 2.02 | -7.66 | 1.11 | -72.11 |
| 4021 | 2.21 | -2093.91 | 1.01 | -3011.6 | 2.02 | -18.25 | 1.11 | -82.74 |
| 4022 | 2.21 | -2048.75 | 1.01 | -2967.62 | 2.02 | 4.96 | 1.11 | -82.72 |
| 4023 | 2.21 | -2046.52 | 1.01 | -2965.06 | 2.02 | 27.8 | 1.11 | -49.52 |
| 4024 | 2.21 | -2029.02 | 1.01 | -2956.72 | 2.02 | 27.82 | 1.11 | -123.17 |
| 4025 | 2.21 | -2029.39 | 1.01 | -2954.92 | 2.02 | -19.87 | 1.11 | -123.19 |
| 4026 | 2.21 | -2028.29 | 1.01 | -2954.36 | 2.02 | 43.54 | 1.11 | -92.34 |
| 4027 | 2.21 | -2016.41 | 1.01 | -2952.2 | 2.02 | 43.55 | 1.12 | -16.87 |
| 4028 | 2.21 | -2015.05 | 1.01 | -2951.84 | 2.02 | 41.97 | 1.12 | -27.61 |
| 4029 | 2.21 | -2014.71 | 1.01 | -2949.96 | 2.02 | 25.6 | 1.12 | -33.11 |
| 4030 | 2.21 | -2010.27 | 1.01 | -2943.17 | 1.02 | 101.22 | 1.12 | -33.12 |
| 4031 | 2.21 | -2007.67 | 1.01 | -2965.21 | 1.03 | 107.04 | 1.13 | 47.27 |
| 4032 | 2.21 | -2007.26 | 1.01 | -2964.99 | 1.04 | 117.15 | 1.13 | 56.61 |
| 4033 | 2.21 | -2007.07 | 1.01 | -2964.42 | 1.04 | 117.67 | 2.15 | 5.66E+001 |
| 4034 | 2.21 | -2016.56 | 1.01 | -2989.86 | 1.04 | 117.66 | 2.15 | 51.21 |
| 4035 | 2.21 | -2016.59 | 1.01 | -2990.23 | 1.05 | 154.88 | 2.15 | 51.17 |
| 4036 | 2.21 | -2017.09 | 1.01 | -2990.42 | 1.06 | 164.05 | 2.17 | 75.57 |
| 4037 | 2.21 | -2027.23 | 1.02 | -3012.21 | 1.06 | 164.01 | 2.03 | 10.94 |
| 4038 | 2.21 | -2028.85 | 1.03 | -3016.05 | 1.08 | 185.72 | 2.03 | 10.91 |
| 4039 | 2.21 | -2067.19 | 1.04 | -3073.55 | 1.08 | 185.72 | 2.04 | 24.03 |
| 4040 | 2.21 | -2068.61 | 1.04 | -3074.48 | 1.09 | 107.66 | 2.05 | -9.94 |
| 4041 | 2.21 | -2067.74 | 1.04 | -3074.34 | 1.09 | 141.78 | 2.05 | -9.94 |
| 4042 | 2.21 | -2100.95 | 1.05 | -3128.62 | 1.09 | 141.68 | 2.21 | 31.87 |
| 4043 | 2.21 | -2103.45 | 1.05 | -3131.27 | 1.11 | 128.22 | 2.06 | 10.35 |
| 4044 | 2.21 | -2149.46 | 1.06 | -3200.84 | 1.11 | 108.04 | 2.06 | -18.09 |
| 4045 | 2.21 | -2153.44 | 1.06 | -3210.84 | 1.13 | 107.03 | 2.06 | -18.1 |
| 4046 | 2.21 | -2156.59 | 1.06 | -3214.49 | 1.13 | 139.95 | 2.21 | 15.18 |
| 4047 | 2.21 | -2214.98 | 1.07 | -3306.03 | 1.13 | 139.97 | 1.01 | -93.41 |
| 4048 | 2.21 | -2219.6 | 1.07 | -3310.99 | 1.14 | 23.59 | 1.01 | -93.4 |
| 4049 | 2.21 | -2216.06 | 1.07 | -3304.19 | 1.15 | 53.55 | 2.01 | -32.83 |
| 4050 | 2.21 | -2218.34 | 1.07 | -3306 | 1.15 | 68.61 | 2.02 | -14.48 |
| 4051 | 2.21 | -2288.86 | 1.08 | -3411.55 | 1.15 | 68.6 | 2.02 | -45.32 |
| 4052 | 2.21 | -2289.89 | 1.08 | -3410.43 | 1.15 | 15.17 | 1.01 | -144.95 |
| 4053 | 2.21 | -2291.95 | 1.08 | -3411.69 | 1.16 | 8.56 | 1.01 | -145 |
| 4054 | 2.21 | -2365.12 | 1.09 | -3520.8 | 1.17 | 28.35 | 1.01 | -57.35 |
| 4055 | 2.21 | -2362.94 | 1.09 | -3516.96 | 1.17 | 42.97 | 2.02 | -38.76 |
| 4056 | 2.21 | -2364.52 | 1.09 | -3524.11 | 1.17 | 79.06 | 2.02 | -25.81 |
| 4057 | 2.21 | -2369.68 | 1.09 | -3525.74 | 1.17 | 84.88 | 2.02 | 8.28 |
| 4058 | 2.21 | -2362.52 | 1.09 | -3522.44 | 1.17 | 84.86 | 2.02 | 1.17 |
| 4059 | 2.21 | -2488.03 | 1.1 | -3762.05 | 1.18 | 70.46 | 1.01 | -56.66 |
| 4060 | 2.21 | -2491.25 | 1.1 | -3768.74 | 1.18 | 31.33 | 1.01 | -56.66 |
| 4061 | 2.21 | -2480.79 | 1.1 | -3755.93 | 1.18 | 31.35 | 1.01 | -9.41 |
| 4062 | 2.21 | -2482.03 | 1.1 | -3764.11 | 1.18 | 28.74 | 2.01 | -14.15 |
| 4063 | 2.21 | -2487.92 | 1.1 | -3772.3 | 3 | 7.86 | 2.01 | -43.11 |

**Table B.7.** Maximum and minimum bending moments and axial forces for the arch elements (Partial Load)

| Element | Max Stress | | Min Stress | |
|---|---|---|---|---|
| | Load Case | Value | Load Case | Value |
| 4001 | 2.21 | -54017.96 | 1.01 | -122336.79 |
| 4002 | 2.21 | -68033.17 | 1.01 | -113112.02 |
| 4003 | 2.21 | -70088.17 | 1.03 | -111748.33 |
| 4004 | 3 | -60006.07 | 1.04 | -133936.57 |
| 4005 | 3 | -29618.74 | 1.04 | -163533.58 |
| 4006 | 3 | -29664.06 | 1.04 | -163620.01 |
| 4007 | 3 | -40353.84 | 1.05 | -152694.27 |
| 4008 | 3 | -42813.38 | 1.05 | -149648.83 |
| 4009 | 3 | -50171.45 | 1.05 | -141030.12 |
| 4010 | 3 | -51183.37 | 1.06 | -140381.27 |
| 4011 | 3 | -39887.02 | 1.07 | -149098.73 |
| 4012 | 1.13 | -22055.67 | 1.07 | -166689.56 |
| 4013 | 1.13 | -22947.6 | 1.07 | -167612.94 |
| 4014 | 2.13 | -46355.84 | 1.08 | -140058.4 |
| 4015 | 2.13 | -43535.19 | 1.08 | -143235.05 |
| 4016 | 1.12 | -37364.33 | 1.08 | -149628.51 |
| 4017 | 1.12 | -28408.66 | 1.08 | -158557.7 |
| 4018 | 1.12 | -28234.97 | 1.08 | -158387.76 |
| 4019 | 2.19 | -61527.64 | 1.08 | -116410.34 |
| 4020 | 2.14 | -57549.48 | 1.09 | -123850.91 |
| 4021 | 2.13 | -55714.55 | 1.09 | -129310.3 |
| 4022 | 2.13 | -54331.03 | 1.09 | -127926.41 |
| 4023 | 2.21 | -56283.18 | 1.09 | -113082.78 |
| 4024 | 1.13 | -36970.78 | 1.1 | -144545.35 |
| 4025 | 1.13 | -37002.76 | 1.1 | -144589.69 |
| 4026 | 2.13 | -50035.79 | 1.1 | -131046.57 |
| 4027 | 2.02 | -51436.92 | 1.01 | -113658.47 |
| 4028 | 2.02 | -52114.57 | 1.01 | -112807.99 |
| 4029 | 2.21 | -58374.74 | 1.11 | -104425.77 |
| 4030 | 2.03 | -34664.21 | 1.02 | -138028.28 |
| 4031 | 2.03 | -33473.49 | 1.02 | -141019.64 |
| 4032 | 2.04 | -32764.76 | 1.03 | -145087.56 |
| 4033 | 2.04 | -32739.3 | 1.03 | -145118.03 |
| 4034 | 2.05 | -34683.36 | 1.04 | -146105.93 |
| 4035 | 2.06 | -25852.1 | 1.05 | -161815.48 |
| 4036 | 1.06 | -23003.18 | 1.05 | -165549.26 |
| 4037 | 1.06 | -24141.04 | 1.05 | -166708.47 |
| 4038 | 1.08 | -13718.19 | 1.07 | -175141.8 |
| 4039 | 1.08 | -16103.17 | 1.07 | -177556.84 |
| 4040 | 2.1 | -49082.8 | 1.08 | -142873.63 |
| 4041 | 1.1 | -34202.46 | 1.09 | -157602.53 |
| 4042 | 1.1 | -36388.75 | 1.09 | -159790.77 |
| 4043 | 1.11 | -41316.21 | 1.1 | -153053.85 |
| 4044 | 1.12 | -52494.1 | 1.11 | -146869.66 |
| 4045 | 1.13 | -52142.02 | 1.12 | -145661.54 |
| 4046 | 1.14 | -37900.38 | 1.13 | -159401.34 |
| 4047 | 2.21 | -38923.83 | 1.13 | -163129.94 |
| 4048 | 2.21 | -38963.06 | 1.01 | -145629.42 |
| 4049 | 2.21 | -59452.4 | 1.14 | -124685.77 |
| 4050 | 2.16 | -66120.34 | 1.14 | -131009.83 |
| 4051 | 2.02 | -59176.79 | 1.14 | -134584.37 |
| 4052 | 2.02 | -26189.99 | 1.01 | -171335.46 |
| 4053 | 2.02 | -26115.51 | 1.01 | -171285.61 |
| 4054 | 2.02 | -56397.37 | 1.01 | -136707.5 |
| 4055 | 2.02 | -64294.97 | 1.01 | -126463.7 |
| 4056 | 2.18 | -61097.27 | 1.16 | -140516.98 |
| 4057 | 2.18 | -58634.22 | 1.17 | -142984.93 |
| 4058 | 2.18 | -58371.33 | 1.17 | -142714.33 |
| 4059 | 2.02 | -66038.37 | 1.01 | -143710.03 |
| 4060 | 2.02 | -66070.32 | 1.01 | -143782.14 |
| 4061 | 2.19 | -75707.03 | 1.17 | -126205.09 |
| 4062 | 2.21 | -75695.8 | 1.17 | -125200.56 |
| 4063 | 2.21 | -65751.37 | 1.15 | -128971.05 |

**Table B.8.** Maximum and minimum stresses for the arch elements (Partial Load)

| Element | Max Stress | | Min Stress | |
|---|---|---|---|---|
| | Load Case | Value | Load Case | Value |
| 3001 | 3 | 46612.57 | 2.42 | 39477.81 |
| 3002 | 1.12 | 75250.54 | 2.42 | 55377.99 |
| 3003 | 1.13 | 72973.47 | 2.42 | 42562.41 |
| 3004 | 1.14 | 93046.7 | 2.42 | 48976.84 |
| 3005 | 1.15 | 91805.41 | 2.42 | 46918.2 |
| 3006 | 1.16 | 91585.68 | 2.42 | 45660.97 |
| 3007 | 1.18 | 95024.76 | 2.42 | 47407.39 |
| 3008 | 1.19 | 90470.84 | 2.17 | 43809.52 |
| 3009 | 1.2 | 91775.02 | 2.19 | 43174.59 |
| 3010 | 1.22 | 96978.96 | 2.2 | 45058.12 |
| 3011 | 1.23 | 95174.24 | 2.21 | 44509.7 |
| 3012 | 1.25 | 93764.34 | 2.22 | 44494.35 |
| 3013 | 1.28 | 94385.04 | 2.24 | 43827.14 |
| 3014 | 1.29 | 98216.37 | 2.42 | 48702.97 |
| 3015 | 1.31 | 103470.41 | 2.42 | 49851.37 |
| 3016 | 1.33 | 98227.49 | 2.42 | 45478.16 |
| 3017 | 1.31 | 56804.39 | 2.42 | 31139.35 |
| 3018 | 1.37 | 43036.96 | 2.42 | 17073.1 |
| 3019 | 1.31 | 194047.12 | 2.42 | 94630.6 |
| 3020 | 3 | 75598.54 | 2.42 | 58669.51 |
| 3021 | 3 | 46055.71 | 2.42 | 37280.86 |
| 3022 | 1.29 | 83036.68 | 2.42 | 49465.86 |
| 3023 | 1.28 | 94868.14 | 2.42 | 49775.76 |
| 3024 | 1.27 | 95561.28 | 2.42 | 48972.91 |
| 3025 | 1.25 | 90002.56 | 2.42 | 46064.11 |
| 3026 | 1.24 | 96569.22 | 2.42 | 48156.36 |
| 3027 | 1.23 | 95992.65 | 2.41 | 46205.32 |
| 3028 | 1.22 | 93374.3 | 2.41 | 44716.41 |
| 3029 | 1.2 | 96183.79 | 2.41 | 44879.62 |
| 3030 | 1.18 | 96629.3 | 2.41 | 45498.89 |
| 3031 | 1.16 | 96912.8 | 2.41 | 45536.36 |
| 3032 | 1.15 | 90775.11 | 2.41 | 45106.78 |
| 3033 | 1.13 | 97909.12 | 2.42 | 48239.8 |
| 3034 | 1.1 | 110303.87 | 2.42 | 51108.89 |
| 3035 | 1.09 | 98173.69 | 2.42 | 49567.24 |
| 3036 | 1.11 | 61626.41 | 2.42 | 34547.07 |
| 3037 | 1.05 | 51384.82 | 2.42 | 17593.47 |
| 3038 | 1.11 | 173091.23 | 2.42 | 85045.45 |

**Table B.9.** Maximum and minimum stresses for the hanger elements (Even Load)

| Element | Max N | | Min N | |
|---|---|---|---|---|
| | Load Case | Value | Load Case | Value |
| 3001 | 3 | 45.37 | 3 | 45.37 |
| 3002 | 3 | 52.34 | 2.21 | 48.81 |
| 3003 | 1.01 | 10.28 | 2.21 | 6.21 |
| 3004 | 1.04 | 112.67 | 2.21 | 60.38 |
| 3005 | 1.01 | 14.96 | 2.21 | 4.63 |
| 3006 | 1.05 | 119.88 | 2.21 | 65.13 |
| 3007 | 1.04 | 98.59 | 2.21 | 53.59 |
| 3008 | 1.01 | 92.8 | 2.21 | 51.53 |
| 3009 | 1.01 | 64.13 | 2.19 | 26.02 |
| 3010 | 1.01 | 132.4 | 2.21 | 65.3 |
| 3011 | 1.03 | 134.96 | 2.21 | 67.07 |
| 3012 | 1.04 | 119.3 | 2.02 | 56.55 |
| 3013 | 1.07 | 153.13 | 2.03 | 77.99 |
| 3014 | 1.08 | 133.81 | 2.04 | 67.61 |
| 3015 | 1.11 | 163.73 | 2.05 | 84.61 |
| 3016 | 1.13 | 183.24 | 2.21 | 96.08 |
| 3017 | 1.1 | 157.97 | 2.21 | 95.34 |
| 3018 | 1.16 | 147.41 | 2.21 | 86.18 |
| 3019 | 1.1 | 277.79 | 2.21 | 141.59 |
| 3020 | 3 | 74.71 | 2.21 | 67.41 |
| 3021 | 3 | 36.35 | 3 | 36.35 |
| 3022 | 1.09 | 37.69 | 3 | 22.19 |
| 3023 | 1.08 | 34.66 | 3 | 10.83 |
| 3024 | 1.06 | 56.98 | 3 | 30.55 |
| 3025 | 1.05 | 71.55 | 3 | 42.23 |
| 3026 | 1.04 | 64.46 | 3 | 29.59 |
| 3027 | 1.02 | 74.98 | 3 | 41.56 |
| 3028 | 1.01 | 56.55 | 3 | 21.04 |
| 3029 | 2.01 | 60.72 | 3 | 43.91 |
| 3030 | 3 | 43.94 | 3 | 43.94 |
| 3031 | 3 | 60.4 | 3 | 60.4 |
| 3032 | 3 | 38.48 | 3 | 38.48 |
| 3033 | 3 | 49.99 | 3 | 49.99 |
| 3034 | 3 | 67.85 | 3 | 67.85 |
| 3035 | 3 | 67.14 | 3 | 67.14 |
| 3036 | 3 | 67.54 | 3 | 67.54 |
| 3037 | 3 | 64.64 | 3 | 64.64 |
| 3038 | 2.01 | 169.21 | 2.21 | 103.89 |

**Table B.10.** Maximum and minimum stresses for the hanger elements (Partial Load)

# Appendix C

# Numbers assigned to hanger elements

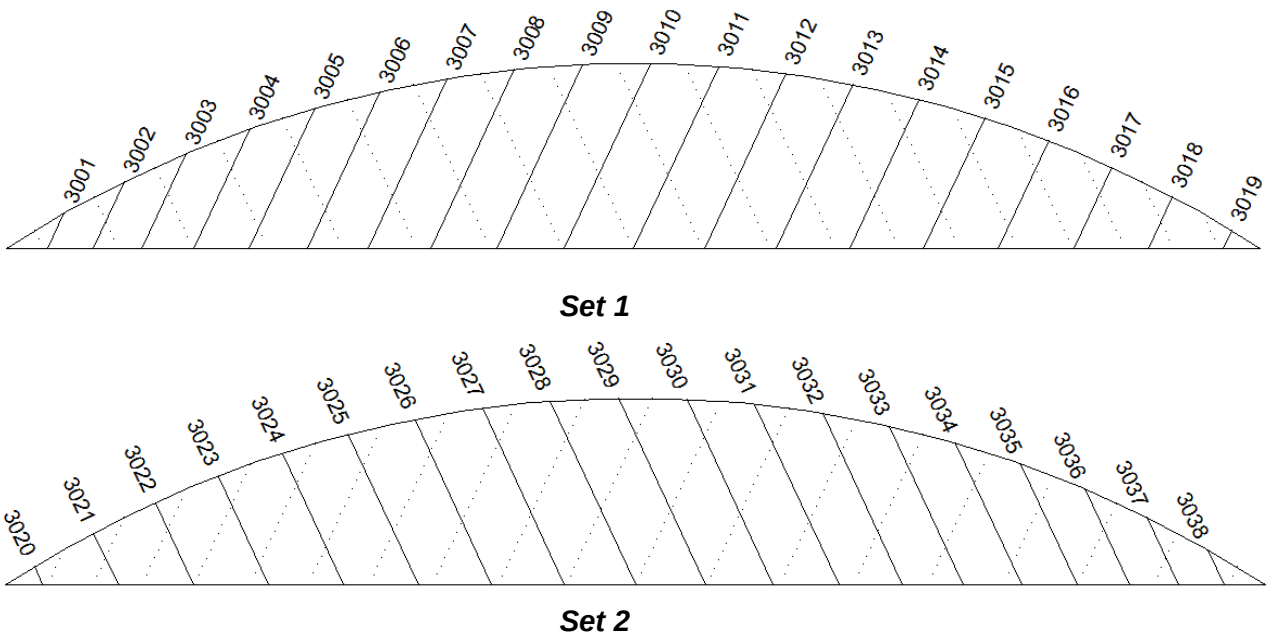


**Figure C.1.** Numbers assigned to hanger elements (Original hanger arrangement and hanger arrangements based on the linear variation of the slopes)

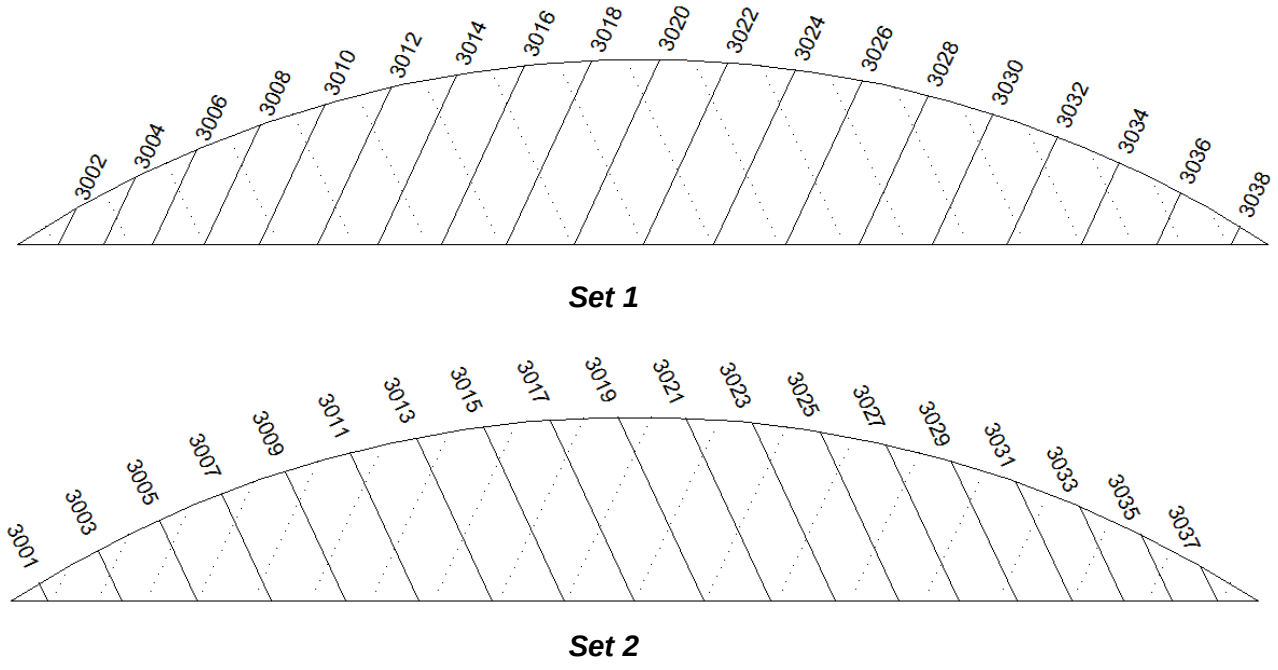


**Figure C.2.** Numbers assigned to hanger elements (Radial arrangements)

# Appendix D

# Input File

The input file for the radial arrangement of Section 3.1.2. can be found here. This is presented as an example of the codes used in this thesis. The definitions of the commands are obtained from [Ahlp].

## D.1. Preliminary Definitions

Commands for clearing the database and entering the model creation preprocesor.

```
FINISH
/CLEAR
/PREP7
```

## D.2. Definition of Parameters

## D.2.1. Geometry and dimensions

- Span of the bridge

```
span=41
```

- Rise of the bridge, expressed as percentage of the span

```
w=6.05/span
```

- Number of hangers

```
nh = 38
```

- *lsmall* limits the minimum length of an element in the deck and the arch, as explain in Section D.3.3.

```
lsmall=0.2
```

- Geometry of the circular arch

```
r=span*w
c=span/2
d=r/2-span**2/(8*r)
Ra=sqrt(c**2+d**2)
```

### D.2.1.1. Deck

- Parameters for the effective cross section

```
db=1.090
dh=0.56

db1=1.085*0.2+0.1*(1.5*1.085)
dh1=0.18

db2=1.8*0.2+0.1*(0.7*1.8*2)
```

*dh2=0.275*

- Parameters for the real cross section
*dbreal=1.090*
*dhreal=0.56*
*db1real=1.085*
*dh1real=0.18*

*db2real=1.8*
*dh2real=0.275*

- Areas and moment of inertia
*Aread=db*dh+db1*dh1+db2*dh2*
*Id=1/12*db*dh**3*
*Id=Id+db1*dh1*(dh/2-dh1/2)**2*
*Id=Id+db2*dh2*(dh/2-dh2/2)**2*
*Areadreal=dbreal*dhreal+db1real*dh1real+db2real*dh2real*

### D.2.1.2. Arch

- Parameters for the cross section
*ah=0.32*
*at=0.035*

- Area and moment of inertia
*Areaa=ah*at+2*at*(ah-at)*
*Ia=2*1/12*at*ah**3+(ah-2*at)*at*(ah/2-at/2)**2*

### D.2.1.3. Hangers

- Parameters for the cross section
*hd=0.04*

- Area and moment of inertia
*Areah=3.14159*hd**2/4*
*Ih=3.14159*hd**4/64*

## D.2.2. Material and Loading properties

- Elastic modulus
*Esteel=2e8*
*Econcr=2.99e7*

- Self weight
*Gsteel=7.8*
*Gconcr=2.5*

- Limit coordinates of the portion of the span where the live load is applied.
*LongLL1=0.5*
*longLL2=1*
*l1=span*longLL1*
*l2=span*longLL2*

- Distance between two consecutives positions of the moving load.
*lstep=1*

- Partial factors:
*gammaSteel=1.20*
*gammaConcr=1.35*

- Parameters for load combination LM1
*qLM1=15.38*
*pLM1=87.35*

- Dead load
*qDL=5.06+Areadreal*Gconcr*9.8*

## D.2.3. Cross angles for the Radial Arrangement

*Radang1 = 0*
*Radang2 = 57*
*Radangstep = 0.5*

## D.2.4. Definition of Matrices

These matrices are used to store the results obtained for each bridge.

- Deck
**DIM,Matrixd,ARRAY,(Radang2-Radang1)/Radangstep+1,10*
**vfill,Matrixd(1,1),ramp,radang1,radangstep*

- Arch
**DIM,Matrixa,ARRAY,(Radang2-Radang1)/Radangstep+1,10*
**vfill,Matrixa(1,1),ramp,radang1,radangstep*

- Hangers
**DIM,Matrixh,ARRAY,(Radang2-Radang1)/Radangstep+1,10*
**vfill,Matrixh(1,1),ramp,radang1,radangstep*

## D.3. Geometry of the bridge

### D.3.1. Loop

**do,Radang,Radang1, Radang2,Radangstep*

In the beginning of each loop, the model creation preprocesor is accessed and all the elements of the previous bridges are erased.

```
/prep7

lsdele,all
lclear,all
ldele,all
kdele,all
```

### D.3.2. Geometry of arch and deck

Several lines are defined following the geometry of the arch. Using the command *LCOMB* the lines are combined into one. This line is divided in equal parts according to the number of hangers *nh.*

In the same way, the deck is divided according to the number of hangers *nh.*

```
k,1000,0,0
numstr,line,1000

*do,i,1,m
        x = span/m*i
        y = sqrt(Ra**2-(x-c)**2)+d

        k,1000+i,x,y
        l,999+i,1000+i
*enddo

kmodif,1000+m,,0
LCOMB,all
l,1000,1000+m
```

- Division of the arch

```
numstr,line,501
numstr,kp,501
Larch=2*Ra*ACOS((Ra-r)/Ra)
narch=(nh+1)*nint(Larch/(nh+1))
LDIV,1000,,,narch,1
```

- Division of the deck

```
numstr,line,702
numstr,kp,701
ndeck=(nh+1)*nint(span/(nh+1))
LDIV,1001,,,ndeck,0
ldele,1001
numstr,line,701
l,1000,701
```

### D.3.3. Hanger arrangement

The number of hangers for the Set1 *nh1* and for the Set 2 *nh2* are obtained.

```
nh2=nint(nh/2)
*if,nh2,eq,nh/2,then
        nh1=nh2
*else
        nh1=nh2-1
*endif
```

The hanger arrangement is created with a loop. In each step, the coordinate *xo* from where the hanger starts is obtained and the angle of the radial direction of the arch in this point is calculated as *alfa*. The cross angle *Radang* is consecutively added and subtracted from *alfa*, and the final point *x1* of the hanger is found. Finally, the line element is created.

```
numstr,line,801
numstr,kp,800
RadangAux=Radang/180*3.14

        *do,l,1,nh
                xo=kx(500+(l*nint(Larch/(nh+1))))
                alfa=3.14/2-ATAN(-(xo-c)/sqrt(Ra**2-(xo-c)**2))
                rot=(-1)**l

                y1=ky(500+(l*nint(Larch/(nh+1))))
                x1=xo+y1/tan(alfa+RadangAux*rot)
                k,800+l,x1,0
                l,800+l,500+(l*nint(Larch/(nh+1)))

        *enddo

numstr,line,701
lsel,s,line,,801,800+nh,2,0
lsel,a,line,,701,799,1,0
lglue,all

lsel,s,line,,802,800+nh,2,0
lsel,a,line,,701,799,1,0
lglue,all
```

```
lsel,all
ldele,1000
```

## D.3.4. Enhancement of the model

After running the precedent codes, the model obtained could present some inconvenients: lines too large, different directions of the normals between adjacent elements, or disordered numbering. The following codes correct these problems.

### D.3.4.1. Deck

The first and last keypoints of the deck are renamed, as well as the numbering of the lines that belong to the deck. The maximum number assign to the lines is obtained as *lmaxd*.

```
numstr,kp,1
k,1,0,0
k,2,span,0

numstr,line,2501
lgen,2,701,799,1,0,0,0,0,0,0
ldele,701,799,1,0

lsel,s,line,,2501,2599
*get,lmaxd,line,0,num,max
```

Using the command *lreverse,* the normals of the lines are modified in a way that the X-coordinate of the first keypoint is smaller than the X-coordinate of the second keypoint.

```
*do,j,2501,lmaxd
        *if,lx(j,0),ge,lx(j,1),then
                lreverse,j
        *endif
*enddo
nummrg,kp
```

The lines which length is smaller than the parameter *lsmall* defined in Section D.2.1. are eliminated. The new maximum number assign to the lines is obtained as *lmaxd*.

```
allsel
*do,k,2501,lmaxd
        *get,ltemp,line,k,leng
        *if,ltemp,le,lsmall,then
                ktemp1=lx(k,0)
                *get,ktemp2,line,k,kp,2
                kmodif,ktemp2,ktemp1+1.0e-10
                ldele,k
                nummrg,kp
        *endif
```

```
*enddo

numstr,line,2801
lgen,2,2501,2599,1,0,0,0,0,0,0
ldele,2501,2599,1,0

numstr,line,2501
lgen,2,2801,2899,1,0,0,0,0,0,0
ldele,2801,2899,1,0

lsel,s,line,,2501,2599
*get,lmaxd,line,0,num,max
```

Finally, the lines are ordered from left to right, assigning the number 2001 to the first line.

```
coord=0
*do,j,1,(lmaxd-2500)
        *do,i,2501,lmaxd
                *if,i,le,lmaxd,then
                        *if,lx(i,0),eq,coord,then
                                numstr,line,2000+j
                                coord=lx(i,1)
                                lmaxd=lmaxd-1
                                lgen,2,i,
                                ldele,i

                                numstr,line,2801
                                lgen,2,2501,2599,1,0,0,0,0,0,0
                                ldele,2501,2599,1,0

                                numstr,line,2501
                                lgen,2,2801,2899,1,0,0,0,0,0,0
                                ldele,2801,2899,1,0
                        *endif
                *endif
        *enddo
*enddo
nummrg,kp
allsel
```

## D.3.4.2. Arch

The same procedure applied for the deck is applied for the arch.

The numbering of the lines that belong to the arch is renamed. The maximum number assign to the lines is obtained as *lmaxa*.

```
numstr,line,4501
lgen,2,501,699,1,0,0,0,0,0,0
ldele,501,699,1,0

lsel,s,line,,4501,4699
*get,lmaxa,line,0,num,max
```

Using the command *lreverse* the normals of the lines are modified in a way that the X-coordinate of the first keypoint is smaller than the X-coordinate of the second keypoint.

```
*do,j,4501,lmaxa
        *if,lx(j,0),ge,lx(j,1),then
                lreverse,j
        *endif
*enddo
nummrg,kp
```

The lines which length is smaller than the parameter *lsmall* defined in Section D.2.1. are eliminated. The new maximum number assign to the lines is obtained as *lmaxa*.

```
allsel
*do,k,4501,lmaxa
        *get,ltemp,line,k,leng
        *if,ltemp,le,lsmall,then
                kxtemp1=lx(k,0)
                kytemp1=ly(k,0)
                *get,ktemp2,line,k,kp,2
                kmodif,ktemp2,kxtemp1+1.0e-10,kytemp1
                ldele,k
                nummrg,kp

        *endif
*enddo

numstr,line,4801
lgen,2,4501,4699,1,0,0,0,0,0,0
ldele,4501,4699,1,0

numstr,line,4501
lgen,2,4801,4999,1,0,0,0,0,0,0
ldele,4801,4999,1,0

lsel,s,line,,4501,4699
```

```
*get,lmaxa,line,0,num,max
nummrg,kp
```

Finally, the lines are ordered from left to right, assigning the number 4001 to the first line.

```
coord1=1

*do,j,1,(lmaxa-4500)
        aux2=0

        *do,i,4501,lmaxa
                *if,i,le,lmaxa,and,aux2,eq,0,then
                        *get,coord2,line,i,kp,1
                        *if,coord2,eq,coord1,then
                                numstr,line,4000+j
                                lmaxa=lmaxa-1
                                aux2=1
                                lgen,2,i
                                ldele,i

                                numstr,line,4801
                                lgen,2,4501,4699,1,0,0,0,0,0,0
                                ldele,4501,4699,1,0

                                numstr,line,4501
                                lgen,2,4801,4999,1,0,0,0,0,0,0
                                ldele,4801,4999,1,0

                                nummrg,kp
                                *get,coord1,line,4000+j,kp,2
                        *endif
                *endif
        *enddo
*enddo
nummrg,kp
allsel
```

### D.3.4.3. Hangers

The numbering of the lines that belong to the hangers is renamed.

```
numstr,line,3001
lgen,2,801,899,1,0,0,0,0,0,0
ldele,801,899,1,0
```

## D.4. Boundary conditions

The degrees of freedom constraints at the keypoints are defined with the command *kd*.

```
dk,1,ux,,,uy
dk,2,uy
```

## D.5. Elements and sections

The material and geometrical properties are assigned to the elements.

- Deck

```
et,1,beam3
r,1,Aread,Id,dh
mp,ex,1,Econcr
mp,dens,1,0
```

- Arch

```
et,2,beam3
r,2,Areaa,Ia,ah
mp,ex,2,Esteel
mp,dens,2,Gsteel*gammaSteel
```

- Hangers

```
et,3,link10
r,3,Areah,0.1e-10
mp,ex,3,Esteel
mp,dens,3,Gsteel*gammaSteel
```

The element attributes are associated with the lines.

- Deck

```
lsel,s,line,,2001,2999
latt,1,1,1
```

- Arch

```
lsel,s,line,,4001,4999
latt,2,2,2
```

- Hanger

```
lsel,s,line,,3001,3999
latt,3,3,3
```

The maximum numbers assign to the lines is obtained for deck, arch and hangers. The number of line divisions is specified with the command *esize*. Finally the lines are meshed.

```
lsel,s,line,,2001,2099
*get,lmaxd,line,0,num,max

lsel,s,line,,3001,3999
*get,lmaxh,line,0,num,max

lsel,s,line,,4001,4999
*get,lmaxa,line,0,num,max

esize,20
allsel
numstr,elem,2001
lmesh,2001,lmaxd
numstr,elem,3001
lmesh,3001,lmaxh
numstr,elem,4001
lmesh,4001,lmaxa
```

The gravity acceleration is defined.

```
acel,,9.8
```

## D.6. Loads

### D.6.1. Preliminary Definitions

The following commands are defined.
- Enter the solution processor.

```
/solu
```

- Specify a static analysis.

```
antype,0
```

- Include large deflection effects.

```
nlgeom,on
```

-Specify the use of automatic time stepping. This allows ANSYS to determine appropriate size to break the load steps into. [UA-AT]

```
autots,on
```

- Specify the number of substeps to be taken at this load step.

```
nsubst,10
```

## D.6.2. Load steps

### D.6.2.1. LM1. Distributed load

The distributed load *qLM1* is applied as a surface load with *sfbeam,* according to the limit coordinates of the portion of the span where the live load is applied: *l1* and *l2*, defined in Section C2.2. *Lswrite* writes load and load step option data to a file. *Lssolve* reads and solve the load step.

Finally, the loads applied to the model are deleted with *sfldele*.

```
*do,i,2001,lmaxd
        esel,s,,,i
        *if,lx(i,0),lt,l1,AND,lx(i,1),gt,l1,then
                temp1=lx(i,1)-l1
                sfbeam,all,1,pres,qLM1,,,,temp1
        *elseif,lx(i,0),ge,l1,AND,lx(i,1),le,l2,then
                sfbeam,all,1,pres,qLM1
        *elseif,lx(i,0),lt,l2,AND,lx(i,1),gt,l2,then
                temp1=lx(i,1)-l2
                sfbeam,all,1,pres,qLM1,,,,,temp1
        *endif
*enddo
allsel

/title, Load Case 1.1
lswrite,11
lssolve,11

sfldele,all,all
```

### D.6.2.2. LM1. Punctual loads

Two punctual loads of value pLM1, separated 1.20, are applied every a certain distance, defined by the parameter *lstep* (Section C2.2.).

At each step of the loop, a load case is defined with the current position of the movil load. The load and load step option data are written to a file, and the load step is solved. Afterwards, the loads applied to the model are deleted, and a new position of the punctual load is considered.

```
number1=0

*do,i,l1,(l2-1.20),lstep
        number1=number1+1
        *do,j,2001,lmaxd
                esel,s,,,j
                *if,lx(j,0),lt,i,AND,lx(j,1),gt,i,then
                        temp2=i-lx(j,0)
                        sfbeam,all,1,pres,pLM1,,,,temp2,-1
                *endif
        *enddo

        *do,k,2001,lmaxd
                esel,s,,,k
                *if,lx(k,0),lt,(i+1.2),AND,lx(k,1),gt,(i+1.2),then
                        temp2=(i+1.2)-lx(k,0)
                        sfbeam,all,1,pres,pLM1,,,,temp2,-1
                *endif
        *enddo
allsel

/Title, Load Case 1.2.%number1%
lswrite,number1
lssolve,number1
sfldele,all,all

*enddo
```

### D.6.2.3. Dead Load

The dead loads are separated in two load cases, as to each case corresponds a different partial factor. First, the dead load in the portion of the span where the live load is applied is considered as unfavourable. Second, the dead load in the portion of the span where the live load is not applied is considered favourable.

#### D.6.2.3.1. Dead Load. Unfavourable

The dead load *qDL* (unfavourable) is applied as a surface load with *sfbeam,* in the portion where the live load is applied. *Lswrite* writes load and load step option data to a file. *Lssolve* reads and solve the load step.

Finally, the loads applied to the model are deleted with *sfldele*.

```
*do,i,2001,lmaxd
        esel,s,,,i
        *if,lx(i,0),lt,l1,AND,lx(i,1),gt,l1,then
                temp1=lx(i,1)-l1
                sfbeam,all,1,pres,qDL,,,,temp1
        *elseif,lx(i,0),ge,l1,AND,lx(i,1),le,l2,then
                sfbeam,all,1,pres,qDL
        *elseif,lx(i,0),lt,l2,AND,lx(i,1),gt,l2,then
                temp1=lx(i,1)-l2
                sfbeam,all,1,pres,qDL,,,,,temp1
        *endif
*enddo
allsel

/title, Load Case 4
lswrite,4
lssolve,4

sfldele,all,all
```

### D.6.2.3.2. Dead Load. Favourable

The dead load *qDL* (favourable) is applied as a surface load with *sfbeam,* in the portion where the live load is not applied. *Lswrite* writes load and load step option data to a file. *Lssolve* reads and solve the load step.

Finally, the loads applied to the model are deleted with *sfldele*.

```
*do,i,2001,lmaxd
        esel,s,,,i
        *if,lx(i,0),lt,l1,AND,lx(i,1),gt,l1,then
                temp1=lx(i,1)-l1
                sfbeam,all,1,pres,qDL,,,,,temp1
        *elseif,lx(i,0),le,l1,AND,lx(i,1),le,l1,then
                sfbeam,all,1,pres,qDL
        *elseif,lx(i,0),lt,l2,AND,lx(i,1),gt,l2,then
                temp1=lx(i,1)-l2
                sfbeam,all,1,pres,qDL,,,,temp1
        *elseif,lx(i,0),ge,l2,AND,lx(i,1),ge,l2,then
                sfbeam,all,1,pres,qDL
        *endif
*enddo
allsel

/title, Load Case 5
lswrite,5
lssolve,5

sfldele,all,all
```

## D.7. Solution

### D.7.1. Preliminary Definitions

Commands for entering the database results postprocessor.

```
finish
/post1
```

### D.7.2. Elements Output definitions

The command ETABLE defines a table of values to be used in the processing.

- Element BEAM3 for arch and deck.

```
ETABLE,SDIR-I,LS,1
ETABLE,SDIR-J,LS,4

ETABLE,SBYT-I,LS,2
ETABLE,SBYT-J,LS,5

ETABLE,SBYB-I,LS,3
ETABLE,SBYB-J,LS,6

ETABLE,MFORX-I,SMISC,1
ETABLE,MFORX-J,SMISC,7

ETABLE,MFORMZ-I,SMISC,6
ETABLE,MFORMZ-J,SMISC,12
```

- Element LINK10 for the hangers.

```
ETABLE,MFORX,SMISC,1
ETABLE,SAXL,LS,1
```

## D.7.3. Definition of load cases

The load steps of Section D.6.2.1. and D.6.2.3. are defined as load cases and the scale factors are applied.

```
lczero
lcdef,number1+1,1
lcdef,number1+2,2
lcdef,number1+3,3

lcfact,number1+1,1.5
lcfact,number1+2,1.35
lcfact,number1+3,1
```

This load cases must be combinated with the punctual loads defined in D.6.2.2. in order to obtain the definitive load cases.

A loop is defined. In each step of the loop a load case that corresponds to a position of the punctual load of LM1 (Section D.6.2.2.) is created and a scale factor is applied. Later, a final load case is defined combining the dead loads with the punctual and distributed loads of LM1.

*Lcwrite* creates the load case by writing the results to a load case file.

Finally, *lcase* reads the load case into the database, and *ETABLE,REFL* refills the tables previously defined with the ETABLE commands.

```
*do,i,1,number1
        loadname=1

        lcdef,i,i+3
        lcfact,i,1.5

        lczero
        lcoper,add,i
        lcoper,add, number1+1
        lcoper,add, number1+2
        lcoper,add, number1+3

        /Title, Load Case %(loadname+i/100)%
        lcfact,i,1
        lcwrite,i
        Lcase,i
        ETABLE,REFL
```

## D.7.4. Storage of the results

### D.7.4.1. Hangers

```
RelhAux=0
*do,j,1,lmaxh-3000
        Nelem=j+3000
```

The axial force *MFORX* is obtained for each element and compared with the stored value. If the current axial force is bigger, the value is stored, as well as the current load case and element.

```
        *GET,Aux1,ELEM,Nelem,ETAB,MFORX

        *if,Aux1,ge,Matrixh((Radang-Radang1)/Radangstep+1,2),then
                Matrixh((Radang-Radang1)/Radangstep+1,2)=Aux1
                Matrixh((Radang-Radang1)/Radangstep+1,3)= loadname+i/100
                Matrixh((Radang-Radang1)/Radangstep+1,4)= Nelem
        *endif
```

The axial stress *SAXL* is obtained for each element and compared with the stored value. If the current axial stress is bigger, the value is stored, as well as the current load case and element.

```
        *GET,Aux1,ELEM,Nelem,ETAB,SAXL

        *if,Aux1,ge,Matrixh((Radang-Radang1)/Radangstep+1,8),then
                Matrixh((Radang-Radang1)/Radangstep+1,8)=Aux1
                Matrixh((Radang-Radang1)/Radangstep+1,9)= loadname+i/100
                Matrixh((Radang-Radang1)/Radangstep+1,10)= Nelem
        *endif
```

*RelhAux* counts how many hangers relax for every load case. This number is compared with the stored value. If it is bigger, the value is stored, as well as the current load case and element.

```
        *if,Aux1,lt,1,then
                RelhAux=RelhAux+1
        *endif

        *if,RelhAux,gt,Matrixh((Radang-Radang1)/Radangstep+1,5),then
                 Matrixh((Radang-Radang1)/Radangstep+1,5)= RelhAux
                Matrixh((Radang-Radang1)/Radangstep+1,6) = loadname+i/100
                Matrixh((Radang-Radang1)/Radangstep+1,7) = Nelem
        *endif
*enddo
```

### D.7.4.2. Arch

The command *centrx(Nelem)* returns the X-coordinate of the centroid of the element.

```
*do,j,1,lmaxa-4000
        Nelem=j+4000
        Centr=centrx(Nelem)
```

The axial forces *MFORX* in the extremes of the element are obtained for each element and compared with the stored value. If the current negative axial force is bigger, the value is stored, as well as the current load case and coordinate.

```
        *GET,Aux1a,ELEM,Nelem,ETAB,MFORX-I
        *GET,Aux1b,ELEM,Nelem,ETAB,MFORX-J

        *if,min(Aux1a,aux1b),le,Matrixa((Radang-Radang1)/Radangstep+1,5),then
                Matrixa((Radang-Radang1)/Radangstep+1,5)=min(Aux1a,Aux1b)
                Matrixa((Radang-Radang1)/Radangstep+1,6)= loadname+i/100
                Matrixa((Radang-Radang1)/Radangstep+1,7)= Centr
        *endif
```

The bending moments *MFORMZ* in the extremes of the element are obtained for each element and its absolute values are compared with the stored value. If the current bending moment is bigger, the value is stored, as well as the current load case and coordinate.

```
        *GET,Aux1c,ELEM,Nelem,ETAB,MFORMZ-I
        *GET,Aux1d,ELEM,Nelem,ETAB,MFORMZ-J

*if,max(abs(Aux1c),abs(aux1d)),ge,abs(Matrixa((Radang-Radang1)/Radangstep+1,2)),then
        *if,abs(Aux1c),gt,abs(Aux1d),then
                Matrixa((Radang-Radang1)/Radangstep+1,2)=Aux1c
        *else
                Matrixa((Radang-Radang1)/Radangstep+1,2)=Aux1d
        *endif
        Matrixa((Radang-Radang1)/Radangstep+1,3)= loadname+i/100
        Matrixa((Radang-Radang1)/Radangstep+1,4)= Centr
*endif
```

The axial direct stress *SDIR*, as well as the bending stress on the element +Y and -Y side of the beam, *SBYT* and *SBYB*, are obtained for the extremes of each element. The Figure D.1 shows these parameters.

The maximum and minimum stresses are obtained adding the bending stress and the direct axial stress. The values obtained are compared with the stored value. If the current stresses are bigger, the value is stored, as well as the current load case and coordinate.

```
*GET,Aux1c,ELEM,Nelem,ETAB,SDIR-I
*GET,Aux1d,ELEM,Nelem,ETAB,SDIR-J

*GET,Aux1e,ELEM,Nelem,ETAB,SBYT-I
*GET,Aux1f,ELEM,Nelem,ETAB,SBYT-J

*GET,Aux1g,ELEM,Nelem,ETAB,SBYB-I
*GET,Aux1h,ELEM,Nelem,ETAB,SBYB-J

Aux2a=Aux1c+Aux1e
Aux2b=Aux1c+Aux1g
Aux2c=Aux1d+Aux1f
Aux2d=Aux1d+Aux1h

*if,max(abs(Aux2a),abs(aux2b),abs(aux2c),abs(aux2d)),ge,abs(Matrixa((Radang-
Radang1)/Radangstep+1,8)),then
    *if,abs(max(Aux2a,Aux2b,Aux2c,Aux2d)),ge,abs(min(Aux2a,Aux2b,Aux2c,Aux2d)),then
        Matrixa((Radang-Radang1)/Radangstep+1,8)=max(Aux2a,Aux2b,Aux2c,Aux2d)
    *else
        Matrixa((Radang-Radang1)/Radangstep+1,8)=min(Aux2a,Aux2b,Aux2c,Aux2d)
    *endif

    Matrixa((Radang-Radang1)/Radangstep+1,9)= loadname+i/100
    Matrixa((Radang-Radang1)/Radangstep+1,10)= Centr
    *endif
        *enddo
```

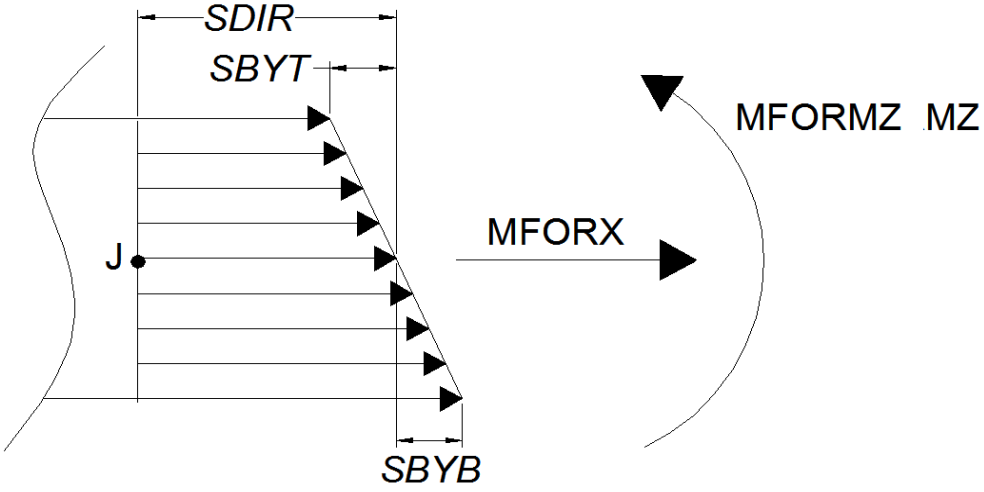


**Figure D.1.** Parameters SDIR, SBYT and SBYB

### D.7.4.3. Deck

The same procedure applied for the arch is applied for the deck.
The command *centrx(Nelem)* returns the X-coordinate of the centroid of the element.

```
*do,j,1,lmaxd-2000
        Nelem=j+2000
        Centr=centrx(Nelem)
```

The axial forces MFORX in the extremes of the element are obtained for each element and compared with the stored value. If the current axial force is bigger, the value is stored, as well as the current load case and coordinate.

```
        *GET,Aux1a,ELEM,Nelem,ETAB,MFORX-I
        *GET,Aux1b,ELEM,Nelem,ETAB,MFORX-J

        *if,max(Aux1a,aux1b),ge,Matrixd((Radang-Radang1)/Radangstep+1,5),then
                Matrixd((Radang-Radang1)/Radangstep+1,5)=max(Aux1a,Aux1b)
                Matrixd((Radang-Radang1)/Radangstep+1,6)= loadname+i/100
                 Matrixd((Radang-Radang1)/Radangstep+1,7)= Centr
        *endif
```

The bending moments *MFORMZ* in the extremes of the element are obtained for each element and its absolute values are compared with the stored value. If the current bending moment is bigger, the value is stored, as well as the current load case and coordinate.

```
        *GET,Aux1c,ELEM,Nelem,ETAB,MFORMZ-I
        *GET,Aux1d,ELEM,Nelem,ETAB,MFORMZ-J

*if,max(abs(Aux1c),abs(aux1d)),ge,abs(Matrixd((Radang-Radang1)/Radangstep+1,2)),then
        *if,abs(Aux1c),gt,abs(Aux1d),then
                Matrixd((Radang-Radang1)/Radangstep+1,2)=Aux1c
        *else
                Matrixd((Radang-Radang1)/Radangstep+1,2)=Aux1d
        *endif

        Matrixd((Radang-Radang1)/Radangstep+1,3)= loadname+i/100
        Matrixd((Radang-Radang1)/Radangstep+1,4)= Centr
*endif
```

The axial direct stress SDIR, as well as the bending stress on the element +Y and -Y side of the beam, SBYT and SBYB, are obtained in the extremes of each element. The Figure D.1 shows this parameters.

The maximum and minimum stresses are obtained adding the bending stress and the direct axial stress. The values obtained are compared with the stored value. If the current stresses are bigger, the value is stored, as well as the current load case and coordinate.

```
            *GET,Aux1c,ELEM,Nelem,ETAB,SDIR-I
            *GET,Aux1d,ELEM,Nelem,ETAB,SDIR-J

            *GET,Aux1e,ELEM,Nelem,ETAB,SBYT-I
            *GET,Aux1f,ELEM,Nelem,ETAB,SBYT-J

            *GET,Aux1g,ELEM,Nelem,ETAB,SBYB-I
            *GET,Aux1h,ELEM,Nelem,ETAB,SBYB-J

            Aux2a=Aux1c+Aux1e
            Aux2b=Aux1c+Aux1g
            Aux2c=Aux1d+Aux1f
            Aux2d=Aux1d+Aux1h

*if,max(abs(Aux2a),abs(aux2b),abs(aux2c),abs(aux2d)),ge,abs(Matrixd((Radang-
Radang1)/Radangstep+1,8)),then
        *if,abs(max(Aux2a,Aux2b,Aux2c,Aux2d)),ge,abs(min(Aux2a,Aux2b,Aux2c,Aux2d)),then
            Matrixd((Radang-Radang1)/Radangstep+1,8)=max(Aux2a,Aux2b,Aux2c,Aux2d)
        *else
            Matrixd((Radang-Radang1)/Radangstep+1,8)=min(Aux2a,Aux2b,Aux2c,Aux2d)
        *endif

        Matrixd((Radang-Radang1)/Radangstep+1,9)= loadname+i/100
        Matrixd((Radang-Radang1)/Radangstep+1,10)= Centr
*endif

            *enddo

        *enddo
```

Finally, the databare is cleared and the load cases are erased in order to prepare the database for the next load case.

```
            lczero
            lcdef,erase
        *enddo
```

### D.7.5. Matrices

The matrices are written to a file using the command *MWRITE.

- Arch

```
*CREATE,Matrixa
*MWRITE,Matrixa,'Matrixa','dat','..\..\Alejandro\MasterMecComp\The
sis\Code\Results\RadArr\Circ'
(F8.1,'   ',F12.2,' ',F12.2,' ',F12.2,' ',F12.2,' ',F12.2,' ',F12.2
,'   ',F12.2,' ',F12.2,' ',F12.2)
*END
/INPUT,Matrixa
```

- Deck

```
*CREATE,Matrixd
*MWRITE,Matrixd,'Matrixd','dat','..\..\Alejandro\MasterMecComp\The
sis\Code\Results\RadArr\Circ'
(F8.1,'   ',F12.2,' ',F12.2,' ',F12.2,' ',F12.2,' ',F12.2,' ',F12.2
,'   ',F12.2,' ',F12.2,' ',F12.2)
*END
/INPUT,Matrixd
```

- Hangers

```
*CREATE,Matrixh
*MWRITE,Matrixh,'Matrixh','dat','..\..\Alejandro\MasterMecComp\The
sis\Code\Results\RadArr\Circ'
(F8.1,'   ',F12.2,' ',F12.2,' ',F12.2,' ',F12.2,' ',F12.2,' ',F12.2
,'   ',F12.2,' ',F12.2,' ',F12.2)
*END
/INPUT,Matrixh
```

# Bibliography

[TNA] TVEIT P., (2008) "*The Network Arch – Bits of Manuscript in Septmeber 2008 after Lectures in 50 Countries*", Internet edition. http://pchome.grm.hia.no/~ptveit/

[AHlp] ANSYS version 12.0.1. (2009) *Mechanical APDL Documentation Descriptions.*

[DIN] DIN 1045-1:2001-07 (2001) *Tragwerke aus Beton, Stahlbeton und Spannbeton - Teil 1: Bemessung und Konstruktion*.

[E2-1] DD ENV 1992-1-1:1992. (1992) *Eurocode 2: Design of concrete structures. Part 1: General rules and rules for buildings*.

[E1-2] prEN 1991-2:2002. (2002) *Eurocode 1: Action on structures – Part 2: Traffic Loads on bridges.*

[E1-3] DD ENV 1991-3:2000. (2000) *Eurocode 1: Basic of designs and action on structures – Part 3: Traffic loads on bridges.*

[E3-1.1] DD ENV 1993-1-1:1992. (1992) *Eurocode 3: Design of steel structures – Part 1.1: General structural rules.*

[GST] GRAF W., STRANSKY W., (2000) "*Optimierung – Optimaler Entwurf von Tragwerken*", Lehrstuhl für Statik, Technische. Universität Dresden, Germany.

[BSC] BRUNN, B. and SCHANACK, F. (2003). *Calculation of a double track railway network arch bridge applying the european standards*, Diploma Thesis, Grimstad, Norway.

[UA-AT] UNIVERSITY OF ALBERTA (2001) *Ansys Tutorials* http://www.mece.ualberta.ca/tutorials/ansys/index.html.

[LIM] ŠAŠEK, LADISLAV. (2006) *Less is More*. American Society of Civil Engineerings.

[BDE] THE STEEL CONSTRUCTION INSTITUTE. (2007) *Bridge design to the Eurocodes. Simplified rules for use in student projects.* Document RT1156

[YW] YIDONG WANG (2009) *Statische Untersuchung einer Netzwerk-Bogenbrücke.* Master thesis

[DSL] CAD drawings provided by ŠAŠEK, LADISLAV. Mott MacDonald Prague.